The University Of Sheffield.

Scottish Water
Trusted to serve Scotland

Understanding the Impact of Assimilable Organic Carbon on Biological Stability and Biofilm Development within Drinking Water

Frances Catherine Pick

Department of Civil and Structural Engineering

University of Sheffield

Thesis submitted as part of STREAM EngD Programme

Submitted: July 2019

I dedicate this thesis to my Dad, David

Abstract

Assimilable organic carbon (AOC) is the fraction of carbon utilised by heterotrophic organisms, potentially leading to (re)growth, loss of biological stability and deterioration of water quality within drinking water distribution system (DWDS). This study developed a novel AOC method that combines the standardisation of using known strains of bacteria, with the speed of flow cytometric enumeration, enabling AOC to be routinely and extensively sampled within operational DWDS. The new AOC method was applied to both water treatment works (WTW) and DWDS to successfully validate the method and determine how AOC fluctuates on a spatial and temporal basis. AOC analyses provide first time evidence of pipes and service reservoirs (SR) exhibiting different AOC and (re)growth behaviour, with AOC being found to increase within the majority of pipe only sections of the DWDS, but decrease within SR.

To ensure a uniquely holistic view of the impact of AOC within DWDS, both the bulk water and, critically, the attached biofilm phase were studied. Biofilms were developed for 12 months in three purpose-built, full-scale pipe loop test facilities, each supplied by post-treated water containing very different AOC concentrations. Each system replicated the hydraulic retention time, water chemistry and microbiology of operational DWDS, whilst enabling laboratory level control of bulk water and biofilm sampling, thus overcoming limitations of bench scale studies. By following the 12 month growth period with a series of flushing steps, it was possible to assess the mobilisation of material and its correlation to the AOC concentration. AOC concentration was found to impact the cell count, community composition and physical structure of the biofilm during growth, and the amount of material mobilised (and therefore discolouration risk) following flushing. This thesis presents original evidence of AOC cycling within the biofilm, advancing our understanding of how and why AOC concentration varies within DWDS and the impacts this has on microbial (re)growth. A unifying conceptual model is presented that describes the complex AOC processes in DWDS, capturing both bulk water and previously overlooked, biofilm processes. Ultimately, the information gained in this study will enable better management of DWDS environments to maintain the quality of drinking water from source to tap, essential in the future management of biological stability.

Acknowledgments

FCP was funded by the STREAM Industrial Doctoral Centre (IDC) (http://www.stream-idc.net/) Engineering Doctorate (EngD) studentship. The project is jointly funded by the EPSRC (Engineering and Physical Sciences Research Council) and Scottish Water.

My EngD project has provided me with the opportunity to work with both staff and students at The University of Sheffield and within Scottish Water. I would firstly like to thank my supervisors Prof. Joby Boxall, Dr. Katherine Fish and Prof. Catherine Biggs for their academic guidance and personal support throughout my EngD. Thank you to Joby for your guidance during our many meetings, for being patient and encouraging during our discussions, and giving me the freedom to decide the scope of my EngD project. A special thank you to Kat Fish for showing me how to operate the test pipe loop facility at the University of Sheffield and offering me extensive microbiological guidance. Thank you to Kat for your great editing skills and your constant words of encouragement throughout my EngD.

I would also like to thank Jon Moses and Graeme Moore at Scottish Water. A special thank you to Jon for showing me around the Scottish Water laboratory facilities, introducing me to staff, and always being just a phone call away. Thank you to Jon for also helping me find suitable WTW for AOC sampling and pipe loop installations, for offering me lifts to sites/offices and offering your support whenever I needed it. Thank you to Jon, Graeme, Paul Weir, Scott Lambie, Simon Gillespie, David Main, Claire Thome and Elise Cartmel for providing constructive feedback and encourage at project steering and Process Science Meetings. Thank you to other Scottish Water staff including David Kaylor, Ryan Cheswick, Andy Upton, Laura Murray, Kristen Helmes and Paul Hastie.

Thank you to the staff working with the STREAM programme, including Lindsay Hopcroft, Tania Rice, Justine Easten, James Shucksmith and Vanessa Speight for your organisational skills and making the TSEL and Challenge Weeks so enjoyable! Thank you to

my fellow STREAM EngD / PhD students including Matthew Mahoney, Fiona Calder and Sally Jones for their friendship and support throughout my EngD. Thank you to all the members of the Water Distribution Research Group for being so welcoming and offering help whenever I needed it.

I would also like thank my friends and family, particularly my Mum and sister for offering me support throughout my EngD and always believing in me. Thank you to my partner Joe Slater for your kind, motivational words and bringing me many cups of tea when I was writing my thesis! Finally, a special mention to my Dad, who sadly passed away during the first year of my EngD. Thank you for your years of encouragement, giving me the self-belief to apply for this EngD – this thesis is dedicated to you.

Contents

Table of Figures

Table of Tables

Abbreviations and Nomenclature

%	percentage
°C	degrees Celsius
µg	microgram
A	aeration
AC	activated carbon filtration
AOB	ammonia oxidising bacteria
AOC	assimilable organic carbon
ANOSIM	analysis of similarity, used for multivariate data
ANOVA	analysis of variance
AMP	asset management plan
APHA	American Public Health Association
ATCC	American Type Culture Collection
ATP	adenosine triphosphate
BAC	biological activated carbon
BAR	biofilm annual reactor
BF	bank filtration
BFP	biofilm forming potential
BFR	biofilm formatting rate
BIO	bio-filtration
BRP	bacterial (re)growth potential
BDOC	biodegradable organic carbon
BOM	biodegradable organic matter
C	carbon
CC	chemical coagulation
CDSC	Communicable Disease Surveillance Centre
CFU	colony forming unit
CIWEM	Chartered Institution of Water and Environmental Management
Cl_2	chlorine
ClO_2	chlorine dioxide
CT	function of disinfectant concentration & contact time
DAF	dissolved air flotation
DAPI	diamidino-2-pheny-lindole
DBP	disinfection by-product
DE	decantation
df	degrees of freedom
DF	dune filtration
DOC	dissolved organic carbon
DOM	dissolved organic matter
DMA	district metered area
DNA	deoxyribonucleic acid
DWDS	drinking water distribution system
DWI	Drinking Water Inspectorate

DWQR	Drinking Water Quality Regulator for Scotland
E. coli	*Escherichia coli*
EngD	Engineering doctorate
EPA	Environment Protection Agency
EPS	extracellular polymeric substances
EU	European Union
F	fluoridation
Fe	Iron
$FeSO_4$	Iron (II) sulphate
FI	filtration
FL	flocculation
FLO	flotation
g	gram
G	Gradient
GAC	granular activated carbon
GRP	glass reinforced plastic
global R	statistic from ANOSIM analysis
h	hour(s)
HAA	haloacetic acids
HCI	hydrochloric acid
HDPE	high-density polyethylene
HRT	hydraulic retention time
HPC	heterotrophic plate count
HPLC	high performance liquid chromatography
IC	inorganic carbon
ICC	intact cell count
IDC	industrial doctorate centre
K_2HP0_4	potassium phosphate dibasic
KH_2PO_4	Monopotassium phosphate
L	litre
m	metre
M	molar
MAC	*Mycobacterium avium complex*
MAP	microbially available phosphorous
MF	multi-media filtration;
Mg	milligram
MgSO4 7H₂O	magnesium sulphate heptahydrate
MIC	microbially induced corrosion
MIC-F	micro-filtration
min	minute(s)
Mn	manganese
mm	millimetre
MRWA	Minnesota Rural Water Association
N	Nitrogen
NaCl	sodium chloride
NF	nanofiltration
NH_2Cl	chloramination
NH_4SO_4	ammonium sulphate
nMDS	non-metric multi-dimensional scaling

NOX	*Spirillum sp.* strain NOX
NPOC	non-purgeable organic carbon
NTU	nephelometric turbidity unit
NF	Nanofiltration
NOB	Nitrite-oxidising bacteria
NOM	natural organic matter
NOX	*Spirillum* strain NOX
O_3	ozonation
OCT	optical coherence tomography
ORP	oxidising reduction potential
OTU	operational taxonomic unit
OX	oxidation
p-value	probability value
P-17	*Pseudomonas fluorescens* P-17
PAC	powdered activated carbon
PaOC	particulate organic carbon
PBS	phosphate buffer solution
PE	polyethylene
PES	polyethylene sulphone
PL	pipe loop
PODDS	Prediction Of Discoloration in Distribution Systems (model)
Pre-OX	pre-oxidation
PTFE	polytetrafluoroethylene
PuOC	purgeable organic carbon
PVC	polyvinyl chloride
PWG	Pennine Water Group
R^2	linear regression – co-efficient of determination
RBMR	rotating biofilm membrane reactor
RCF	relative centrifugal force
RGF	rapid gravity filter
RO	reverse osmosis
RSF	rapid sand filtration
SDS	sodium dodecyl sulfate
SDWF	Safe Drinking Water Foundation
SED	sedimentation
SEM	scanning electron microscope
SF	sand filtration
SIMPER	similarity percentages, statistical test used with multivariate data
SIMPROF	similarity profile test, used with multivariate data
SSF	slow-sand filtration
StDev	standard deviation
SUVA	specific ultraviolet absorbance
TCC	total cell count
THM	trihalomethanes
TOC	total organic carbon
UF	ultrafiltration

UNICEF	United Nations Children's Fund
UK	United Kingdom
UV	ultraviolet
v/v	volume/volume
WHO	World Health Organisation
WTW	water treatment works

Chapter 1: Introduction

1.1 Microbial Water Quality and Biological Stability

Drinking water is a fundamental human resource. In 2015, 91% of the global population had access to an 'improved' (free from faecal and priority chemical contamination) drinking water source, compared to 86% in 2010 and 76% in 1990 (United Nations Children's Fund (UNICEF) and World Health Organisation (WHO), 2015). Despite this progress, the threat of inadequate quality of drinking water remains an issue of global concern, with waterborne disease being estimated to cause more than 2.2 million deaths pear year due to diarrhoea, gastrointestinal diseases and systematic illnesses (World Health Organisation, 2015). Waterborne illnesses also generate an economic loss of approximately $12 billion per year (Alhamlan *et al*. 2015).

Drinking water suppliers are required to produce a sufficient supply of safe drinking water to consumers. This means that drinking water should be "*free from any microorganisms and parasites and from any substances which, in numbers or concentrations, constitute a potential danger to human health*" (European Council, 1998). Failure to do so will not only result in economic sanctions and loss of customer confidence for the water utility, but also potentially pose as a risk to public health. To ensure the continuous supply of high quality, safe drinking water, water utilities not only have to provide extensive water treatment, but also maintain and monitor drinking water quality within the drinking water distribution system (DWDS). Between 2000 and 2015, the number of people with access to drinking water supplied by distribution pipes increased from 3.5 billion to 4.7 billion (WHO and UNICEF, 2017). Although the number is increasing, access to safe and clean drinking water from household taps is not universal and is often taken for granted, especially in developed nations. In countries such as the UK, drinking water utilities are reliant on ageing infrastructure systems with piecemeal design and construction. DWDS are highly complex systems comprising of different

pipe materials, dimensions, ages and being subject to variations in source water quality and customer demand. In addition, the surface-area-to- volume-ratio of the DWDS is not inert as DWDS surfaces interact with the water they supply. Therefore, whilst modern water treatment works (WTW) and DWDS have drastically improved water quality, degradation does still occur.

To regulate water quality, a number of international and national quality controls are in place. WHO guidelines state that *'water entering the distribution system must be microbially safe and ideally should also be biologically stable'* (WHO, 2006). Biologically stable water is defined as water in which the microbial quality is maintained throughout the DWDS (Prest *et al.* 2016). Uncontrolled growth of microorganisms within DWDS can cause the microbial water quality to exceed guideline values. The term (re)growth has previously been used to describe the recovery of disinfectant injured cells, whereas aftergrowth has been used to describe microbial growth in a distribution system (Characklis, 1988; van der Kooij, 2003). In this document (re)growth will be used to include both the recovery of disinfection damaged cells which have passed through the treatment works and the multiplication of organisms within the DWDS itself.

Until recently the majority of research regarding the impact of microorganisms on water quality, and vice versa, has focused upon planktonic organisms. However, 95% of the overall biomass within DWDS is found attached to pipe walls, whilst only 5% resides in the water itself (Flemming *et al.* 2002). Microorganisms are known to exist in microbial communities attached to the inner surface of the pipe by self-producing extracellular polymeric substance (EPS), forming a biofilm. Microbial assemblages residing in a biofilm have a selective advantage over their planktonic counterparts as the biofilm provides protection from environmental stress including disinfectants (Schwering, *et al*. 2013) and the influence of shear forces (Flemming and Wingender, 2010). Biofilms are a concern to drinking water utilities, as

they can increase the occurrence of biofouling and biocorrosion and act as the transient or long-term habitat of faecal indicator organisms and potentially pathogenic bacteria, thereby posing a threat to human health when they detach (Wingender & Flemming, 2011; Ashbolt, 2015). In addition, biofilms act as a source of organics and inorganics which can cause water quality concerns if mobilised. The mobilisation of biofilm microorganisms and associated material into the bulk water, can lead to aesthetic deterioration such as taste, colour, and odour issues. Vreeburg and Boxall, (2007) found that 41% of complaints made by customers to English and Welsh drinking water utilities were reporting issues with drinking water aesthetics.

The determination of biostability or (re)growth potential of water is useful in evaluating water quality during treatment and through the distribution system. A number of different indicator methods can be used assess the degree of biological stability, including the assimilable organic carbon concentration (AOC). Microbial re-growth can also be used to assess the degree of organic matter removal during treatment and the efficiency of disinfection during distribution. Microorganisms can be classed as either heterotrophic:- utilise organic compounds as a source of energy and carbon, or autotrophc:- capable of generating energy from inorganic substances. The majority of the microorganisms in drinking water are heterotrophic and therefore require organic compounds for energy and growth (Miettnen *et al.* 1997). The molar ratio of carbon, nitrogen and phosphorus required for bacterial growth is 100C:10N:1P (LeChevallier *et al.* 1991; Chandy & Angles, 2001). The ratio infers that in most DWDS carbon is regarded as the main limiting nutrient, being required in the greatest quantity for growth.

Limiting growth supporting substrates in post-treated water is a common technique employed to restrict microbial (re)growth within DWDS, especially in the absence of a disinfection residual. Although modern treatment systems produce drinking water containing low nutrient concentrations, trace amounts remain in the treated water which can concentrate

in biofilms, where lysed cells act as a further nutrient source and nutrient cycling is thought to occur. AOC is one of the most important fractions of carbon in drinking water as it is easily assimilated by microorganisms. If AOC is not removed during the treatment process, AOC in post-treated water can be regarded as one of the main contributors towards microbial re-growth in DWDS. The AOC concentration within drinking water can therefore be used as an indicator of drinking water biostability. It should be noted that there is currently no universal AOC concentration threshold for drinking water stability.

DWDS are complex systems consisting of pipes and service reservoirs, with varying hydraulic retention times (HRT). It is therefore important to understand how the AOC concentration varies on a spatial and temporal basis in DWDS. Additionally, it is not known how biofilms are influenced by the concentration of AOC, and how these attached microorganisms themselves contribute to the nutrient load. This literature review will highlight the biotic and abiotic factors (particularly AOC) that govern the growth of microbiota in the DWDS, and the management strategies that can be employed by water utilities to produce and maintain biologically stable drinking water. Throughout this review key gaps in the literature will be highlighted and future research needs suggested.

Chapter 2: Literature Review

2.1 Drinking Water Treatment and Distribution

Drinking water networks are composed of four main components (a) water source (b) water treatment (c) storage of treated water and (d) distribution to the consumer (Figure 2.1). To ensure the production and distribution of safe drinking water, water utilities apply a multi-barrier approach including source water protection, appropriate and well-operated treatment steps and management of DWDS. Steps employed to control microbial growth at the WTW will lead to better water quality in the DWDS and ultimately at the consumers tap.

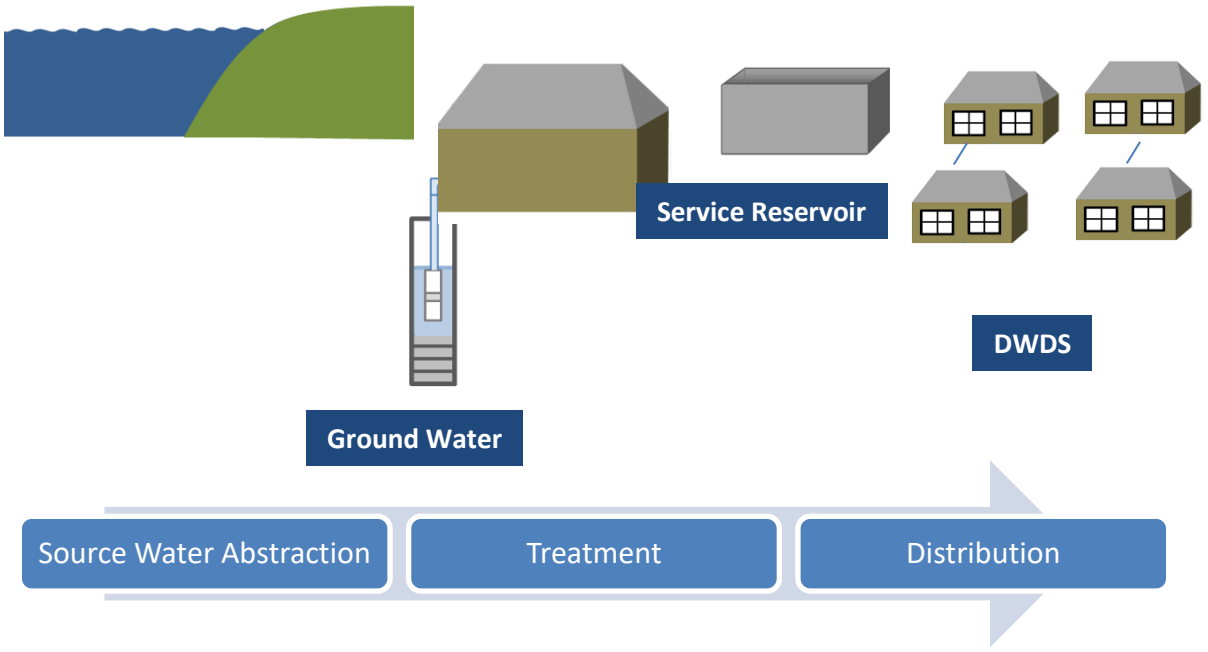

Figure 2.1: An example of a drinking water system from source to tap. Source water may be surface water (reservoir or river abstraction) or groundwater. Water is pumped to a water treatment works, where specific treatment processes vary depending on source water quality. Treated water in the UK is disinfected (in most cases with chlorine or chloramine) before being distributed via the DWDS network consisting of pipes and service reservoirs (SR).

2.1.1 Drinking Water Treatment

Conventional drinking water treatment usually has a similar sequence of processes, though the source and hence quality of incoming water will dictate the exact treatment process. Compared

to surface water, groundwater sources generally have higher initial water quality and therefore usually require fewer treatment steps than surface water sources. Treatment generally includes coagulation, flocculation, sedimentation, filtration and disinfection, although some WTW may include additional steps to remove contaminants. Water treatment is designed to remove any undesirable chemicals, (micro) biological contaminants and suspended particles prior to distribution (Table 2.1). Generally, coagulation, flocculation and sedimentation steps are employed to improve the turbidity, taste, odour and colour of the water. Ion exchange or activated carbon can also be used during this process to remove inorganic or organic contaminants. The treatment steps employed at the WTW can considerably influence a) the characteristics of the bacteria (and other microorganisms) in the post-treated water, and b) the chemical composition of the post-treated water, including organic matter concentration. The AOC removal efficiencies of each treatment step are discussed in detail in Section 2.3.3.5.

Subsequently, the water is disinfected in a contact tank which aims to inactivate (pathogenic) organisms, commonly using a chlorine based agent. The 'CT' method is often employed to assess the disinfection dosage, using the chlorine residual (mg/L) and contact time (mins) to give a CT value (mg.min /L) (a minimum CT of 15 mg.min /L is recommended (WHO, 2008)). Ultimately, the treatment steps employed at the WTW can ultimately influence the degree of microbial (re)growth within the DWDS, thus affecting the biological stability of the water.

Natural organic matter (NOM) not only created problems with taste, colour and odour of drinking water but it also reacts with disinfectants, increasing the amount of disinfection by-products. Removal of NOM to reach compliance with drinking water quality regulations is a challenge for many drinking water treatment works (WTW). NOM can be present in a particulate or dissolved form, with dissolved organic matter being the most difficult to remove from drinking water. NOM is often removed from drinking water using coagulation and

flocculation followed by sedimentation/flotation and sand filtration. Most of the NOM can be removed by coagulation, although, the hydrophobic fraction and high molar mass compounds of NOM are removed more efficiently than hydrophilic fraction and the low molar mass compounds (Matilainen, *et al*. (2010). As a result, total organic carbon (TOC) still remains within the mg/L concentration in final treated water.

Table 2.1: Water treatment works methods applied to control a number of water constituents (data collated from Crittenden *et al.* 2005; Drinking Water Inspectorate (DWI), 2016).

Parameter / Contaminant	Treatment Approach	Associated UK Regulations
Bacteria, viruses, protozoa	Disinfection Membrane filtration (UF, NF, RO) Coagulation Sedimentation Filtration	*Escherichia coli* (E. coli): 0 per 100 ml Total Coliforms 0/100 ml[A] Colonies/ml at 22°C: no abnormal change[B] Colonies/ml at 37°C: no abnormal change[B]
Organic carbon	Coagulation Biological filtration Membrane filtration (RO, NF)	Total organic carbon (TOC): no abnormal change
Particles / turbidity	Flocculation Sedimentation Sand filtration Membrane filtration (MIC-F, UF)	Turbidity: 1-4 NTU[C]
Metals	Aeration, oxidation	Iron (Fe): 200µg / L Manganese: 50µg/ L Lead: 25µg / L Copper: 2 mg / L
Chemical micro-pollutants	Coagulation Adsorption Oxidative treatment	Arsenic: 5 µg / L Ammonia: 0.50 mg / L Nitrate: 50 mg / L as NO_3 Nitrite: 0.5 mg / L as NO_2 Sodium: 200 mg / L Sulphate 250 mg / L

A: 95% of the last 50 samples taken must meet the standard; B: Indicator parameter; C: Max values, water leaving a treatment plant must be ≤ 1 nephelometric turbidity units (NTU), end point water ≤ 4 NTU. UF = ultrafilration; NF = nanofiltration; RO = reverse osmosis; MIC-F = microfiltration.

2.1.2 Drinking Water Distribution Systems (DWDS)

Treated water is transported to the consumer via a series of trunk mains, district metered areas (DMA), disinfection booster stations and service reservoirs. Despite drinking water leaving water treatment works (WTW) being of a high standard, the quality of the water deteriorates

as it travels through the DWDS. DWDS in England and Wales alone consist of 4,430 service reservoirs and over 347,000 km of mains (DWI, 2015). DWDS are a complex system of ageing pipes and service reservoirs, varying in hydraulic retention time, surface to volume ratio, material, water chemistry, disinfection regime and flow regime. All of these abiotic factors have the potential to influence the growth rate and community composition of microorganisms in DWDS. Microorganisms can enter the DWDS either by surviving the treatment process or through ingress via the pipe network. Bacteria have been found to exist in both the bulk water and within biofilms attached to pipe walls, in systems with and without a residual disinfection. As DWDS are such complex environments, the management of drinking water microbiology throughout DWDS presents a series of challenges.

DWDS are subject to continuous changes in water demand and water source quality, a trend which will be amplified by future pressures including population growth and climate change. A growing population will likely significantly increase water demand. Furthermore, future variation in climate will not only impact water availability but also accelerate the deterioration of water quality due to changes in source water quality and the impact of changing temperatures on biological (re)growth and biofilm formation. Understanding the parameters that influence (re)growth of bacteria in drinking water supply systems is critical to maintaining DWDS water quality now and in the future.

2.2 The Importance of Biostability within Drinking Water

2.2.1 Public Health Concerns

Although modern treatment systems generally provide safe, high quality drinking water, microbial failures and waterborne illness outbreaks still occur. This is either a result of mismanagement/contamination of fresh water resources, technical failure at the WTW, inadequate detection regimes or ingress into the DWDS (WHO, 2003). The microbial content of drinking water within DWDS can vary temporally and spatially throughout a network due

to largely unknown, complex interactions with environmental parameters such as nutrients, disinfection residual, hydraulic regime, temperature, turbidity (Lehtola *et al.* 2007) and oxygen (Vaerewijck *et al.* 2005). Although considerable efforts have been made to improve or maintain the quality of water supplies, bacterial pathogens within drinking water are believed to be an increasing threat to human health due to a reduction in the quality and availability of source water (Brettar & Höfle, 2008). Even within modern treatment systems, pathogens have been identified as the most likely cause of a number of disease outbreaks in recent years. In the USA, 833 drinking water borne disease outbreaks caused illness among 577,991 persons and were linked to 106 deaths during 1971 to 2006 (Craun *et al*. 2010). In England and Wales, although the Communicable Disease Surveillance Centre (CDSC) was established in 1992 to create improved reporting of infectious intestinal diseases, there is no obligation to report any outbreaks under investigation. Of those reported between 1992 and 2003 *Cryptosporidium* was reported to be responsible for 69% of outbreaks, *Campylobacter sp*. for 14%, *E. coli* O157 for 3%, *Giardia* for 2%, and *Astrovirus* for 1% (Smith *et al*. 2006). The recent *Cryptosporidium* outbreak during August 2015, affected 300,000 homes in Lancashire costing United Utilities approximately £25 million as listed in their trading update for the six months ending 30 September 2015 (Water Briefing, 2015). Utilities also face increasing pressure from emerging waterborne pathogens including *E. coli O157:H7, Helicobacter sp*. and *Mycobacterium avium complex (MAC)* (Medema *et al*. 2003).

A large number of waterborne disease outbreaks have been linked to chemical and biological contaminants entering the distribution systems (Craun & Calderon, 2001). Ingress into the DWDS may have a delayed impact if the intruding organisms seek refuge in the biofilm, and are then later released back into the bulk water. Microbial contamination remains a universal issue, with over 500 waterborne pathogens having been identified as potential concern in drinking waters (US EPA, 2017). In addition, a significant proportion of

microorganisms are often in such low concentrations within a DWDS that they may go undetected. Whether from contaminant ingress or biofilm mobilisation, these microorganisms can potentially cause endemic disease transmission, depending on the number and species of microorganisms. Although smaller events may not cause regulatory failures for water utilities, they can cause gastrointestinal illness for consumers potentially leading generating a significant economic cost if consumers are forced to take leave from their employment (Payment, 1997).

Public health concerns within drinking water are not due to bacterial pathogens alone. Microorganisms within drinking water often consist of prokaryotes (bacteria and archaea), eukaryotes (fungi and protozoa) and viruses (Vaerewijck *et al.* 2005; Denkhaus *et al.* 2007; White *et al.*, 2011; Gall *et al.* (2015). Water-transmitted viral pathogens that are classified as having a moderate to high health significance by the World Health Organization (WHO) include adenovirus, astrovirus, hepatitis A and E viruses, rotavirus, norovirus and other caliciviruses, and enteroviruses (WHO, 2011).

2.2.2 Aesthetic Water Quality

Discoloured water is one of the most common incidents reported to the Drinking Water Inspectorate (DWI), being responsible for 33% of incidents in England and Wales (Husband & Boxall, 2011). Discoloration events generally occur when material such as clay, silt, microorganisms, organics and inorganics accumulate on the pipe wall in the DWDS and subsequently become mobilised, creating a reduction in water clarity. The European Union (EU) Drinking Water Directive (98/83/EC) states that that the levels of turbidity at the tap must be "a*cceptable to consumers and no abnormal change*". In the UK, water quality regulations specify a numeric standard of 1 nephelometric turbidity unit (NTU) in water leaving the treatment works and 4 NTU of water at consumers taps (DWI, 2017). The mobilisation of microorganisms and associated particles from biofilms can cause discolouration events (Husband & Boxall, 2010) and/or microbial regulatory failures depending on the amount and

composition of the detached material. Furthermore, suspended particles have the ability to transport both nutrients and microorganisms within the DWDS, and to generate a disinfection demand resulting in a loss of disinfectant residual. Gauthier *et al.* (1999) found that bacterial biomass represented 1-12% of the organic matter within deposits in a DWDS, acting as both a food source for bacteria and creating a reduction in residual disinfectant.

Although the number of suspended particles within treated drinking water is generally low (Brazos & O'Connor, 1996), turbidity has been reported to increase with distance from WTW (Capellier *et al*. 1996). Turbidity was previously thought to be a result of gravity driven sedimentation at low flows and subsequent remobilisation when the flow rate increased (Wu *et al.* 2003). However, the particulates responsible for discolouration have been demonstrated to remain in suspension even at very low flows (Boxall *et al*. 2001). Instead it is suggested that discolouration is a result of particulate mobilisation from pipe walls in which the shear force generated by water flow is greater than the cohesive and adhesive strength with which the particles are bound, thus causing the particles to detach (Boxall *et al*. 2001; Prince *et al.* 2003; Husband and Boxall, 2010; Cook and Boxall, 2011). The behaviour of particulates within the DWDS has been highlighted as being analogous to biofilm behaviour, in which both will detach from the pipe wall when the adhesive strength exceeds the self-weight (Husband & Boxall, 2016). This is known as shear stress driven mobilisation (Husband & Boxall, 2016).

2.2.3 Drinking Water Regulations

Drinking water utilities are required by national (e.g. Drinking Water Inspectorate (DWI) (England and Wales) & Drinking Water Quality Regulator (DWQR) (Scotland)), and international governing bodies (e.g. European Drinking Water Directive) to undertake regulatory drinking water sampling to monitor a range of chemical and microbiological parameters at WTW, service reservoirs (SR), and at randomised point-of-use locations (customer tap). The EU provided the European Drinking Water Directive with specific methods

for the enumeration of microbiological parameters in drinking water. According to the Council Directive 98/83/EC of 3 November 1998 on the quality of water intended for human consumption, only culturable, non-pathogenic bacteria are required to be sampled. Microbiological standards require 0 per 100 ml of *Escherichia coli* and 'no abnormal change' in indicator organisms including coliform bacteria and colony counts at 22°C (European Council, 1998). Although compliance with the regulations by drinking water utilities is consistently high (average of 99.96% in 2017 (DWI, 2017)), regulatory sampling includes spatially unrepresentative, discrete samples which only sample a minute percentage of the volume of real systems. Furthermore, events such as discoloration are sporadic and short lived and are therefore not captured by discrete sampling. Water utilities are required to use traditional microbiological enumeration techniques, such as heterotrophic plate counts (HPC) that underestimate the actual number of microorganisms within drinking water. Culturable bacteria within bulk water represent only a small fraction of the total microbial community in drinking water (Hammes *et al*. 2008; Siebel *et al.* 2008; Prest, 2015). Regulatory samples exclude other microorganisms such as fungi and archaea, as well as microorganisms existing at the pipe wall within drinking water biofilms. Improved management of DWDS is required to ensure water quality does not decline through the network and that the regulations are adhered.

2.2.4 Biofilm Formation

The majority of new microbial growth in DWDS occurs on the pipe wall, in comparison to the bulk water (Lehtola *et al.* 2004; Moritz *et al.* 2010). Biofilm formation in the DWDS is a one of the main causes of a loss in biostability of distributed water (Manuel *et al*. 2010). Biofilms, originally coined as such in 1978 (Costerton *et al*. 1978), are defined as a complex arrangement of microorganisms bound together in a microbially derived extracellular polymeric substances (EPS) adhered to a surface, which may be organic or inorganic. Biofilms mature as more

microorganisms attach and replicate, increasing the density and diversity of the biofilm cells and expanding the EPS matrix. Biofilm growth and subsequent mobilisation is a successional process (Martiny *et al.* 2003) consisting of 1) primary adhesion to the surface; 2) secondary adhesion; 3) growth (maturation and micro-colony formation); and 4) mobilisation (Vaerewijck *et al*. 2005). The community composition will vary throughout the biofilm cycle, with initial colonisers being determined by the selection pressures of attachment (Martiny *et al.* 2003). The rate of biofilm maturation is dependent on a host of factors including hydrodynamics, rate of oxygen perfusion and nutrient availability (Dunne, 2002). Even when nutrient levels are extremely low within DWDS, non-ologotrophs are to survive in this environment by residing within biofilms where nutrients are elevated (Volk & LeChevallier 1999). As the biofilm EPS matrix is often negatively charged a number of nutrients will accumulate on the biofilm surface. Water channels can facilitate the mass transfer of nutrients to microorganisms residing within the biofilm (de Beer & Stoodley, 1995, de Beer *et al.* 1996). Microorganisms are also able to corrode pipe materials such as iron and steel which may provide nutrients for (re)growth including carbon, nitrogen and phosphorus (Morton *et al*. 2005). Biofilms can affect water quality by processes they mediate during growth (bio-corrosion), and from ongoing exchange and mobilisation into the bulk water. Biofilms within DWDS can generate a decline in water quality, disinfection residual and pipe infrastructure condition, and pose a discolouration risk when they mobilise and release materials, such as inorganics, into the bulk water. Therefore, understanding biofilms and how they may impact drinking water quality (and similarly how the environmental conditions of the DWDS impacts the biofilm), is critical to water biostability and water quality management.

Due to the difficulty of removing biofilms from operational DWDS, the majority of research investigating the various biotic or abiotic parameters that act upon biofilm are based in laboratory scale experiments. These include bench-top reactor systems or flow through cells

(e.g. Deines *et al.* 2010; Ginige *et al*. 2011; Abe *et al*. 2012). Although these systems offer fine scale control of environmental parameters, they do not accurately represent the ever-changing conditions in an operational DWDS, including fluctuations in nutrient supply, hydraulic conditions and disinfection residual. Furthermore, the majority of studies researching DWDS biofilms often focus solely on bacteria, despite other microbial taxa being known to exist in drinking water biofilms (Wingender and Flemming, 2011; Fish *et al*. 2015; Douterelo *et al*. 2016). It is therefore important to consider other microbial taxa in addition to bacteria to gain a holistic understanding of DWDS microbiology.

2.2.4.1 Biofilm EPS Matrix

The EPS matrix has been reported to provide protection from multiple environmental stresses in the water column included changes in disinfection, pH, osmotic shock and desiccation (Kokare *et al.* 2009). The EPS is also able to provide structure and mechanical stability through a variety of processes including hydrophobic, electrostatic and dispersive interactions (Flemming *et al*. 2007; Neu and Lawrence, 2009). The amount of EPS produced is dependent on the species of organism, biofilm age (Kokare *et al.* 2009) and hydraulic regime (Fish *et al.* 2017). Biofilms are universal in nature due to the ability of microorganisms to develop biofilms on the majority of surfaces and in challenging environmental conditions whereby the necessary substrates for growth and metabolism are limited (Wingender & Flemming, 2011). Carbon and nutrients concentrate at the pipe wall due to the turbulence of the bulk water. Organic and inorganic particles become incorporated within the EPS matrix providing a nutrient source (Denkhaus *et al.* 2007) and therefore selective advantage for biofilm microorganisms over their planktonic counterparts (Volk & LeChevallier, 1999). This results in the biofilm environment being able to support non-oligotrophic microorganisms (Volk and LeChevallier, 1999). Microorganisms within biofilm can obtain organic carbon from the bulk water, disinfection degradation or from cells within the biofilm itself. These particles will become mobilised into

the bulk water if the biofilm is released from the pipe wall (Section 2.3.2.1 for hydraulic and biofilm interactions), potentially leading to a loss of biological stability in the bulk water.

2.3 Parameters Governing Biological Stability & Biofilms

2.3.1 Disinfection Regime

Many drinking water utilities rely on the addition of a chemical disinfection, either free chlorine (Cl_2) or monochloramine (NH_2Cl), to act as a biocide agent to manage planktonic microorganisms and drinking water biostability. Chlorination can be performed during the treatment process or to disinfect the post-treated water and maintain a chlorine residual in the DWDS. Pre-chlorination (when chlorine is applied at the beginning of the treatment process) is used to remove taste and odour, control biological growth (including algal growth) in subsequent steps such as sedimentation and filtration, and to oxidise any iron, manganese and/or hydrogen sulphide, so they can be removed during sedimentation and filtration (Safe Drinking Water Foundation (SDWF), 2016). WHO guidelines state that terminal disinfection must produce a residual concentration ≤0.5 mg L−1 (after at least 30 min of contact time at pH less than 8.0) (WHO, 1993). A free chlorine residual range of 0.2–0.5 mg/L is recommended to be maintained throughout the DWDS, with higher concentrations being close to the disinfection point, and the lower concentration at the far extremities of networks (WHO, 1997). Chlorine has been suggested to be a stronger biocide agent than chloramines against planktonic bacteria (Menaia & Mesquita, 2004; De Beer *et al.* 1994). Previous research has demonstrated that the presence of free chlorine reduces biofilm accumulation compared to non-chlorinated systems (Butterfield *et al.* 2002; Van der Wende *et al.* 2006). However, both studies used bench top scale reactors (rotating annual reactors (BAR) and plug flow reactor) and also quantified the cellular component of the biofilm, with no quantification of the EPS. It is important to quantify the EPS as well as number of cells as the EPS determines the point at which the biofilm

will detach into the bulk water, therefore impacting water quality (Abe *et al.* 2012) and biological stability.

Increasing the disinfection residual beyond a certain concentration can also create a trade-off between reducing (re)growth and generating potentially harmful disinfection by-products (DBPs). DBPs are generated when a disinfectant, such as chlorine, reacts with natural organic matter (NOM) and/or inorganic substances within the water (Sadiq & Rodriguez, 2004). In systems containing high organic loads, chlorine has been shown to readily react with organic carbon leading to loss of a disinfection residual in the network (Chandy & Angles, 2001) and production of DBPs (Richardson *et al.* 2007). DBPs provide a source of AOC (LeChevallier *et al.* 1991; van der Kooij, 1992; Escobar *et al.* 2001) leading to microbial growth and loss of biological stability. DBPs also pose as a potential health risk to consumers (Wei *et al*. 2010), with some epidemiologic studies (International Agency for Research on Cancer (IARC), 1991; WHO, 1996; Nieuwenhuijsen *et al.* 2008) presenting an association between long-term exposure to disinfection by-products and increased risk of cancer and potential adverse reproductive effects.

Some water utilities in the UK are opting to use chloramines (rather than chlorine) as a residual because chloramines are considered to be more stable and only generate trace amounts of trihalomethanes (THM) and haloacetic acid (HAAs) (Bougeard *et al*. 2010), therefore lowering the water quality risk to public health. Chloramine is typically found in drinking water supplies at a concentration of 0.5-2 mg/l (WHO, 2008), whether it is used as either a primary disinfectant or as a disinfection residual in the DWDS. Chloramination has been demonstrated to be more efficient at suppressing planktonic intact cells or (re)growth more efficiently than free chlorine even at low residual concentrations (LeChevallier *et al*. 1996; Gillespie *et al.* 2014). This is thought to be a result of chloramines being more effective at being able to penetrate biofilms (De Beer, Srinivasan & Stewart, 1994; Chandy & Angles, 2001;

LeChevallier *et al.* 2007). However, these benefits are often counteracted by the ability of monochlorines to act as a source of ammonia, providing a nutrient source for ammonia-oxidising bacteria (AOB). AOB have previously been demonstrated to produce nitrites from ammonia (Pryor *et al*. 2004).

2.3.1.1 Disinfection and Biofilms

Although disinfection residuals are able to slow biological growth (Hallam *et al*. 2011), disinfection does not completely prevent biofilm development (White *et al.* 2011). Disinfection has been shown in numerous studies to be more effective on bulk water bacteria than on biofilm bacteria (Costerton *et al.* 1995; Wingender *et al.* 1999; Gagnon *et al*. 2004; Hageskal *et al.* 2012), however the exact mechanisms of achieving this are unclear. Disinfection molecules are thought to bind to the EPS and become neutralised (Menaia & Mesquita, 2004), or enzymes found within the EPS matrix degrade the residuals (Mah & O'Toole, 2001). Other proposed mechanisms of resistance include increased cell density, slower growth and physiological changes to the cell including a activating quorum sensing systems and changing profiles of outer membrane proteins (Mah & O'Toole, 2001; Menaia & Mesquita, 2004). Disinfection regime (type and dose) also influences microbial community composition and the occurrence or persistence of opportunist pathogens (Wang *et al.* 2012). When subjected to either a chlorine or chloramine residual, differences in the bacterial community diversity of biofilms have been demonstrated suggesting that biofilm communities can respond to changes in disinfection regimes (Williams *et al.* 2005, Revetta *et al.* 2007; Mi *et al*. 2015). Different bacterial groups have greater sensitivity to chlorine (McCoy *et al.* 2012), with *Alphaproteobacteria* being predominant in the bulk water due to their higher resistance to chlorine, and *Betaproteobacteria* being dominant within biofilms (Douterelo *et al.* 2013). However, when considering the impact of disinfection on drinking water biofilms, it is important to understand that other abiotic and

biotic factors, such as nutrient concentration, may act in tandem with disinfection in the DWDS and therefore influence the response of the biofilm.

2.3.1.2 Disinfectant Free Drinking Water

A small number of countries, including The Netherlands, Germany and Switzerland choose not to use a disinfectant residual, either due to alternative treatment options (such as filtration, UV disinfection or ozone to reduce the organic content of the water) being used, unnecessity or customer preference (Smeets *et al*, 2009). In the Netherlands, a large proportion of the water supply originates from deep groundwater aquifers which are generally absent from faecal contamination, whilst surface water is filtered in dune systems via artificial recharge or bank filtration to remove the pathogen load. Furthermore, in European countries such as Germany, consumers would rather receive water free of chlorine due to taste/odour preferences and concerns over disinfection by-product formation (Uhl & Schaule, 2004). In the absence of a disinfectant, the most commonly employed method used to limit planktonic (re)growth and hence reduce biofilm formation within the DWDS is to limit growth supporting nutrients prior to distribution. Physical processes such as sedimentation, filtration and UV-disinfection, which are primarily used to control growth limiting substances, are favoured over chemical disinfection to produce biologically stable water (Hammes *et al.* 2008; Smeets *et al*. 2009). The absence of a disinfection residual or use of UV-radiation are only possible in well maintained distribution systems in which microbial growth is reduced by the production of high quality oligotrophic water, the use of biologically stable materials, low temperatures, minimal ingress into the system and short hydraulic retention times (HRT) within the system (Smeets *et al*. 2009). Such processes have no residual effect within DWDS (Lehtola *et al*. 2005) generating potential problems such as (re)growth and a reduction in drinking water biostability and water quality.

2.3.2 Carbon

Uncontrolled levels of organic matter create significant problems including degradation of aesthetic water quality, an increase in microbial growth rate and increased disinfection demand potentially forming disinfection by-products (Sadiq & Rodriguez, 2004). The majority of natural organic matter (NOM) is removed during treatment (Table 2.1). Organic carbon in water supplies is predominantly a function of the water source, seasonality, treatment combinations, and operational practices through the DWDS (Sharp *et al.* 2006). The availability organic carbon has the potential to either limit or promote bacterial (re)growth and biofilm formation in DWDS, dependent on the concentration and availability.

NOM consists of a complex mixture of organic matter that varies in molecular size, structure, and chemical composition. Organic matter, in terms of weight, is: 45–55% carbon, 35–45% oxygen, 3–5% hydrogen, 1–4% nitrogen (Cabaniss *et al*. 2007). NOM is commonly measured as total organic carbon (TOC) or dissolved organic carbon (DOC), as carbon is the most abundant element in dissolved organic matter (DOM). Other measures of organic carbon include the concentration of assimilable organic carbon (AOC), biodegradable organic carbon (BDOC), specific ultraviolet absorbance (SUVA), and bacterial (re)growth potential (BRP). SUVA is defined as the UV absorbance of a water sample normalised with respect to the DOC concentration. The BRP is a bioassay using a natural microbial inoculum to take into account other possibly limiting nutrients (Sathasivan & Ohgaki, 1999). The dissolved organic carbon (DOC) fraction of TOC can be divided into two subsets; biodegradable dissolved organic carbon (BDOC) and AOC (Figure 2.2). AOC and BDOC are considered as two of the main nutrient and energy sources for heterotrophic bacteria. However, it has previously been found that BDOC, generally used to quantify higher molecular weight (MW) organics, is not significantly correlated with AOC (Charnock and Kjønnø, 2000) or counts of heterotrophic

bacteria (Van der Kooij, 1992). More recently, BDOC has instead been used as an indicator of chlorine demand and disinfection by-product formation (Escobar and Randall, 2001).

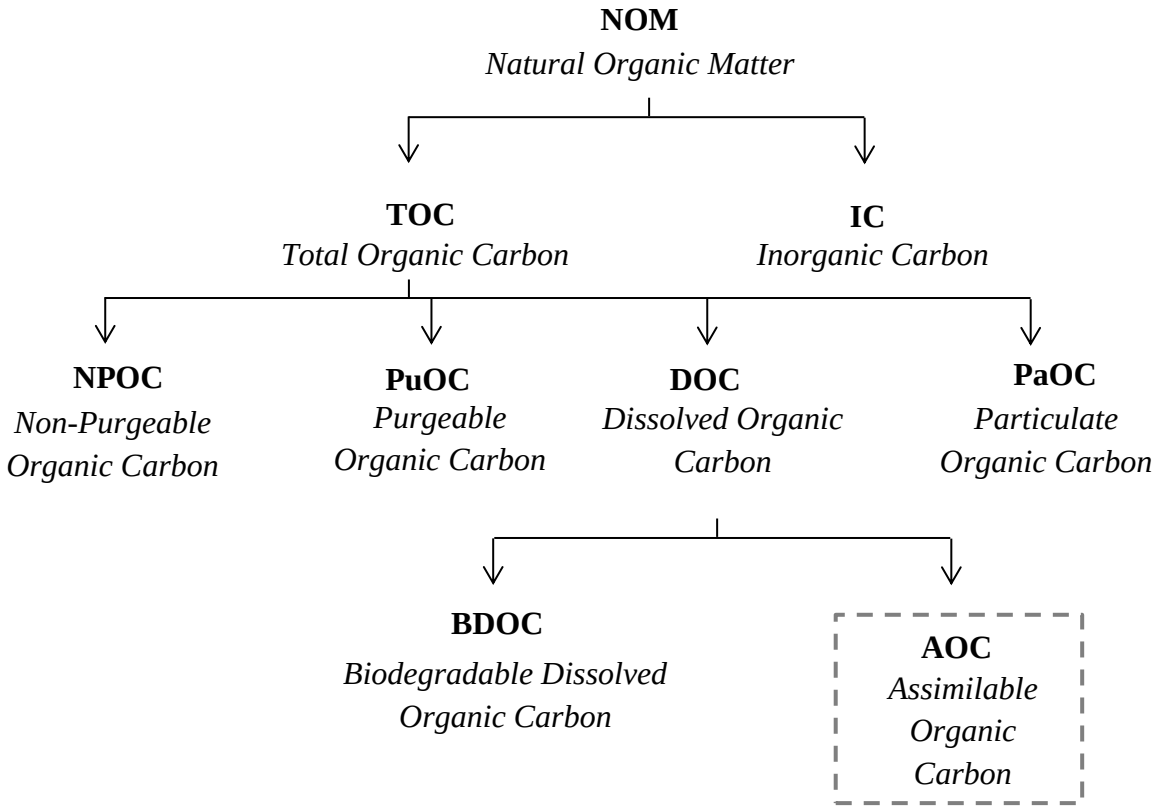

Figure 2.2: Fractions of carbon found within drinking water, including their universal acronyms. AOC (dashed box) is investigated in this study as it is the portion available for bacterial (re)growth.

2.3.2.1 Assimilable Organic Carbon

AOC is generated either via lysis of bacterial cells or biological and chemical hydrolysis of organic matter. AOC is made up of low molecular weight organic molecules (Escobar *et al.* 2000), including acaetate, formate and oxalate (Hammes *et al*. 2006). The exact composition of AOC within drinking water is not constant, and will depend on source water quality, the treatment process and the disinfection residual applied. It is only the low molecular weight fraction of organic carbon that can be assimilated by heterotrphic bacteria (Van der Kooij & Hijen, 1984; Polanska *et al.* 2005). Therefore, AOC is often used as a surrogate to assess the

(re)growth potential of heterotrophic organisms within drinking water. It is important to note that as no direct chemical test exists to determine AOC concentrations, AOC must be measured indirectly by utilising the linear relationship between the maximum growth of bacteria in a water sample and the AOC concentration (American Public Health Association (APHA), 2005). Given that different organisms, even those used in AOC test, consume different amounts of carbon, the AOC test is only an estimate of the (re)growth potential of drinking water, and should be used in tandem with other regrowth potential indicators such as flow cytometry.

2.3.2.2 Assimilable Organic Carbon Measurements

As the AOC fraction of organics represents a small fraction (<10 %) of the TOC in water (Hammes and Egli, 2005), the assay must be sensitive to detect low concentrations. In the AOC assay, bacteria are grown in a water sample and enumerated over time to determine the maximum cell density. The maximum growth of bacteria is divided by a yield factor, which is obtained from growth of the organism on a defined substrate, usually acetate. The principle behind AOC analyses assumes that organic carbon is the limiting nutrient within the water sample (Escobar *et al.* 2001; Liu *et al*. 2002). This is normally assessed using control samples to check that other nutrients such as nitrogen and phosphorous are not growth limiting. The individual steps involved in the method include: pasteurisation / filtration of the collected water sample, inoculation with a known cell density, incubation until maximum cell density is reached, enumeration and conversion of cell counts to carbon concentration. Existing AOC methodologies can be broadly divided into those that use known bacterial strains known bacterial strains (such as *Pseudomonas fluorescens* strain P-17 and *Spirillum* strain NOX) as an inoculum (proposed by Van der Kooij *et al.* 1982; van der Kooij and Hijnen, 1984), and those that incorporate a natural microbial inoculum (proposed by Hammes & Egli, 2005) (Table 2.2). These methods are further divided into those that use different samples preparation steps, inoculum volumes, incubation time and temperatures, and enumeration methods.

2.3.2.3 AOC Method Using Known Bacterial Strains, P-17 and NOX

Van der Kooij *et al.* (1982) presented the original AOC bioassay which included the use of a known bacterial strain: *Pseudomonas fluorescens* strain P-17, hereafter referred to as P-17. P-17 is used for AOC analysis as it is ubiquitous in the DWDS and able to cope with low organic carbon concentrations by metabolising a range of biodegradable compounds such as amino acids, carboxylic acids, hydrocarboxylic acids, alcohols and carbohydrates (excluding polysaccharides) (Stanier *et al.* 1966). More recently, *Spirillum* strain NOX, hereafter referred to as NOX, has been used in tandem with P-17 as it was found that NOX, unlike P-17, can degrade ozonation products (Van der Kooij, 2002). Full details of the standardised method can be found in APHA, (2005). In summary: once a water sample is collected, the sample is pasteurised to inactivate the indigenous bacteria population, before inoculating the sample with P-17. Subsequently, samples are incubated at 15 °C for 7-9 days before the maximum growth rate (stationary phase) is recorded. This is done using the standard plate count method on R2A agar. Plates are incubated at 25 °C for 3 to 5 days before the number of colonies of each strain is counted. It is this maximum growth value which is then converted to an AOC value (expressed as an acetate carbon concentration), assuming that cell numbers in the stationary phase of the two bacteria are linearly correlated to AOC concentration in the water sample. Previously derived yield values of 4.1×10^6 CFU P-17 / µg acetate carbon and 1.2×10^7 CFU NOX / µg acetate carbon can be used (Van der Kooij, 1992). The lengthy incubation period required for bacteria in the water sample to reach their maximum growth, followed by the incubation of plate counts (3-5 days), can create a sample processing period of up to 14 days for one sample. This is often deemed too long for routine industrial analyses.

Alternative methods used to enumerate the bacteria in a sample have been proposed including the use of Adenosine triphosphate (ATP) luminescence (LeChevallier *et al*. 1993a) and bioluminescence (Haddix *et al.* 2004, Weinrich *et al.* 2009, 2011). LeChevallier *et al.*

(1993a) were able to convert ATP luminescence to AOC concentration using the linear relationship between viable cell counts and ATP luminescence units, and the yield factor for acetate carbon. The method was able to detect a greater number of bacteria than the plate count procedure and was a substantially faster enumeration method. However, it was also evident that the different test organisms did not contain the same amount of ATP per cell, consequently showing bias towards different strains and therefore not suited for the use of indigenous bacterial populations. Aggarwal *et al.* (2015) assessed the use of flow cytometry, with and without SYTO9 staining, to enumerate P-17 and NOX. Aggarwal *et al.* 2015 found that flow cytometry was a rapid and accurate enumeration method of both P-17 and NOX. However, when using flow cytometric enumeration, Aggarwal *et al.* (2015) found the yield of P-17 and NOX to be lower than HPC yield factors. The lower yield factor produced when using flow cytometric enumeration could have been due to the relatively high incubation temperature of 23 °C. It is known that the optimum incubation temperature for NOX and P-17 is 15°C (LeChevallier *et al*. 1993). The use of flow cytometric enumeration and an optimum incubation temperature of 15 °C in the AOC assay is a knowledge gap that will be addressed in this thesis.

2.3.2.4 Natural Microbial Community Inoculum

Modifications to the Van der Kooij AOC bioassay include the use of a natural microbial community inoculum in which the bacteria are indigenous to the water sample in question. Samples are enumerated using flow cytometry (Hammes & Egli, 2005, Hammes *et al.* 2010) or turbidity measurements (Werner & Hambsch, 1986; Hambsch & Werner, 1990). The use of a natural microbial inoculum instead of P-17 and NOX has been demonstrated to result in a higher final cell count (Ross *et al.* 2013), suggesting that a more diverse inoculum is able to utilise a wider array for organic compounds. A higher incubation temperature (30 °C) reduces the incubation time of the assay, and the use of flow cytometry enables rapid enumeration of all cells, including those that are unculturable on conventional media. However, a natural

microbial inoculum necessitates the use of a theoretical conversion value (1 μg AOC = 1 x 10^7 cells) (Hammes & Egli, 2005) to convert cell concentrations to AOC concentrations. 1 x 10^7 cells was determined by assessing the growth of a natural microbial inoculum on acetate carbon (Hammes & Egli, 2005). Furthermore, the use a natural microbial inoculum instead of a pure culture creates additional complexity in the form of quantifying the microorganisms present and understanding the interactions between the various bacterial strains. This can potentially create deviations in AOC cell counts and difficulties in standardising the assay

Table 2.2: AOC methodologies incorporating either known strains of bacteria or a natural microbial inoculum.

Inoculum Type	Sample Preparation	Inoculum	Incubation	Enumeration	Yield Factors	Reference
Known strains of bacteria	Pasteurisation 60 °C for 30 mins	500 CFU P-17 only	15 °C no shaking	HPC 25 °C 40-48 hours	$4.1x10^6$ P-17	Van der *Kooij et al.* 1982
		100-300 CFU/mL of strains PI 7 and NOX			4.1 x 10^6 P-17, 1.2 x 10^7 NOX	Vander Kooij, 1992
		Either strain P-17 or strain NOX	Room temp for 1-3 days	ATP	*	LeChevallier *et al,* 1993a
	Pasteurisation 70 °C for 1 hour		Room temp 3-5 days	HPC 25 °C for 7 days	4.1 x 10^6 P-17, 1.2 x 10^7 NOX	Escobar and Randall, 1999
	Pasteurisation 70 °C for 30 min					Escobar and Randall, 2000
		Inoculate with P-17, incubate & enumerate, pasteurise again, inoculate NOX, incubate & enumerate	25 °C for 2 days for P-17 and 3 days for NOX	HPC 25 °C 3 days		Liu *et al.* 2002
	Pasteurisation 70 °C for 30 min followed by 15 min at 70 °C in heating cabinet	P17, PF-1 or a combined inoculum of P17/NOX to final concentration 50–500 CFU/mL	20 °C with shaking		*	Charnock & Kjønnø, 2000
	Pasteurisation 30 min at 60 °C, rapidly cooled in ice bath to 15 °C	Inoculated with P17 and NOX simultaneously, to reach 300 cfu/mL of each strain	15 °C	HPC every 2 days	4.6 x 10^6 P-17, 1.3 x 10^7 NOX	Polanksa *et al.* 2005

	Pasteurisation 70 °C for 30 min	500 CFU/mL each of P-17 and NOX		25 °C for 3 to 5 days	4.1 x 10^6 P-17, 1.2 x 10^7 NOX	American Public Health Association (APHA), 2005
	Samples filtered through a baked 0.3-µm GF-75 glass filter, pasteurisation 70 °C for 30 min			HPC R2A agar 7, 8, and 9 days		Thayanukul *et al*. 2013
	Pasteurisation 70 °C for 40 min	P-17 and NOX	25 °C 1-8 days	HPC on nutrient agar	*	Lou *et al*. 2011; Han *et al*. 2012; Lou et al. 2014
	Pasteurisation 75 °C for 30 min	Samples inoculated simultaneously with P-17 and NOX	20 °C	Pour plating on R2A agar 14–20 days at 20 °C	4.53 x 10^6 P-17, 1.56 x 10^7 NOX	Ohkouchi *et al.* 2011; Ohkouchi *et al.* 2013
	*	*	22 °C–25 °C	HPC 1–5 days 25 °C	*	Zhao et al. 2013
	Pasteurisation 70 °C for 30 min	1 mL of either P17 or NOX	23 °C for 5 days	Flow Cytometry	4.33 x 10^6 P-17, 1.03 x 10^7	Aggarwal *et al.* 2015
Natural microbial inoculum	Filtered 0.22 µm (not pasteurised)	Triplicate vials inoculated with 100 µL giving a final concentration of 5x 10^3 (±2 x 10^2) cells mL^{-1}	30 °C until stationary phase	Flow cytometry	1 x 10^7 cells µg C	Hammes & Egli, 2005
	Filtered 0.22 µm (not pasteurised) Autoclaved (20 min 12 °C), filtered 0.22 µm	Cell concentration of 1 x 10^4 cell / mL	30 °C until stationary phase *	Flow cytometry Turbidity (NTU)	1 x 10^7 cells µg C *	Hammes *et al.* 2006
		Cell concentration of 1 x 10^4 cell / mL *				Hammes & Egli, 2007
						Bazri & Mohseni, 2013
						Vital *et al*. 2007

	Sample pasteurised, filtered 0.22 µm					Hammes *et al.* 2010; Vital *et al*. 2012; Liu *et al.* 2015
	Filtered 0.2 µm, pasteurised 60 °C for 30 min					Elhadidy *et al.* 2016
	*					Werner & Hambsch, 1986; Hambsch & Werner, & 1990

*Details not included in reference

A yield factor is generated by monitoring the growth of the test organisms on pure solutions of acetate-carbon or oxalate-carbon which are used as reference standards. Each of these methods uses a different yield factor to convert cell counts to nutrient concentration (Table 2.3), potentially leading to large difference in the final AOC concentration. This therefore creates difficulties in comparing between studies that employ different AOC methods.

Table 2.3: Comparison of Yield Factors used in the AOC Bioassay.

Yield Coefficient P-17 (cells/µg acetate-carbon)	Yield Coefficient NOX (cells/µg acetate-carbon)	Yield Coefficient Natural Inoculum (cells/µg acetate-carbon)	Study
4.1×10^6	-	-	Van der Kooij *et al*. 1982
	1.2×10^7		Van der Kooij, 1990; Van der Kooij, 1992; Escobar & Randall, 1999; APHA, 2005
		1×10^7	Ross *et al*. 2013
	-	1×10^6	Hammes & Egli, 2005
1.4×10^7	1.8×10^7	-	Thayanukul *et al*. 2013
			Liu *et al*. 2002
			Escobar & Randall, 2000
2.56×10^6	1.17×10^7		Aggarwal *et al*. 2015
4.08×10^6	9.6×10^6		Chang *et al*. 2002
4.33×10^6	1.03×10^7		Aggarwal *et al*. 2015 (using flow cytometry)
4.53×10^6	1.56×10^7		Ohkouchi *et al*. 2011; Ohkouchi *et al*. 2013
4.6×10^6	1.3×10^7		Polanska *et al*. 2005
$6.4 \times 10^6 – 8.3 \times 10^6$	-		Wang *et al*. 2014
-	-	1×10^7	Vital *et al*. 2012; Bazri & Mohseni, 2013; Liu *et al*. 2015

2.3.2.5 AOC within Water Treatment Works

The amount of AOC in raw water is reduced during treatment to avoid bacterial (re)growth through nutrient limitation in the DWDS (Van der Kooij *et al.* 1992; Ramseier *et al.* 2011). The treatment process can help manage microbial (re)growth in DWDS by limiting nutrient availability in post-treated water. Due to the limitations of the current AOC methodology (section 2.3.3.2), AOC is not regularly monitored through the WTW, despite AOC measures being useful assessments of WTW performance and to help predict the degree of biostability in the DWDS. The WTW process is designed to reduce the AOC concentration (see Table 2.4) and produce biologically stable water, which contains approximately <100 µg C/L (LeChevallier *et al.* 1996) in DWDS that apply a disinfectant residual, or <10 µg C/L (van der Kooij, 1992) in systems without a residual. It should be noted that <100 µg C/L is only an estimate and this value is likely to vary of a system by system basis, depending on the DWDS conditions (particularly presence and type of disinfectant).

Treatment processes reported to reduce AOC in drinking water include granular activated carbon (GAC) (LeChevallier *et al.* 1992; Volk & LeChevallier, 2002; Polanska *et al.* 2005), slow / rapid sand filtration (SSF / RSF) (Hammes *et al.* 2006, 2010; Ohkouchi *et al.* 2011), biological activated carbon (BAC) (Van der Kooij *et al,* 1989; Volk & LeChevallier, 2002), and to a lesser extent conventional treatment processes (including chemical coagulation & sedimentation) (Liu *et al.* 2002). The AOC removal efficiencies of each treatment step are listed in Table 2.5. As highlighted in Table 2.5, the AOC removal efficiency has a large range and is dependent on the raw water quality and the treatment processes used. Due to the complexity of organic carbon, the removal rate of AOC during coagulation & sedimentation is thought to vary with the organic molecular weight and hydrophobicity of the source water (Volk & Lechevallier, 2002; Klimenko *et al.* 2012). In contrast, Escobar & Randell, (2001) found that nanofiltration (NF) was not effective as reducing the AOC concentration as AOC

compounds are small enough to pass through NF membranes. Furthermore, ozonation has been found to create a significant increase in AOC concentrations most likely as a result of the breakdown of larger-molecular weight compounds into smaller compounds that are measurable as AOC (Hu *et al.* 1999; Escobar & Randall 2001; Lehtola *et al*. 2001; Hammes *et al.* 2006; Wen *et al*. 2017).

The efficiency of AOC removal during the treatment process is not only determined by the choice of individual treatment steps, but is also dependent on the incoming raw water quality. Ohkouchi *et al.* (2011) found that the seasonal difference in AOC levels detected in the finished water were consistent with the results of AOC in raw water. Therefore, these seasonal changes of organic constituents in raw water could directly affect the AOC levels in post-treated water. The treatment efficiency of AOC removal is also thought to be dependent on seasonality / temperature. Hammes *et al.* (2010) and Müller *et al.* (2003) reported higher AOC concentrations after ozonation in winter months, as a result of temperature or seasonal changes in the raw water composition. Following on from treatment, the AOC concentration in final water is also dependent on the type of disinfection. Post-chlorination has been widely shown to increase the AOC concentration in final water (Volk & Lechevallier, 2002; Chen *et al*. 2007). However, AOC analysis is often used to assess the efficiency of AOC removal at the treatment works, rather than reporting concentrations within the DWDS. Despite WTW producing high quality drinking water, microbial growth can occur in the DWDS if there are sufficient nutrients to support their growth.

Table 2.4 Assimilable organic carbon concentrations found in drinking water.

WTW / DWDS	Treatment / Disinfection	AOC Concentration (µg C/L)	AOC Method	Length of Study	Location	Study
WTW	NF membrane; Cl_2; O_3	Raw: 23-120 Post-treated: 65 - 278	Van der Kooij *et al*. 1982; LeChevallier *et al*. 1993a	12 month sampling	USA	Escobar & Randell, 2001
WTW	Pre-O_3; RSF; O_3; AC; SSF	Pre-ozonation: ~171 Post-treated: ~50	Hammes & Egli	March - June	Switzerland	Hammes, 2006
WTW	CC; MF; UV; O_3; BAC; ClO_2; PAC; FLO	Raw: 200 ± 242* BAC effluent: 5 ± 2.8*	Van der Kooij *et al*. 1982; Sack *et al*. 2011	3 years	The Netherlands	Hijnen *et al*. 2018
WTW	Biological pre-treatment; O_3; GAC	Raw: 265 – 1193 Post-treated: 15 - 62	Van der Kooij *et al.* 1982; LeChevallier *et al*. 1993a	March and May sampling	China	Hu *et al*. 1999
WTW	AC; BF; CC; SSF UV; O_3; Cl_2	Pre-ozonation: ~106 Post-treated: ~ >200	Van der Kooij *et al.* 1982; Miettinen *et al*. 1999	Spot samples	Finland	Lehtola *et al*. 2001
WTW	FL; SED; MF; post-O_3; BAC; Cl_2	Raw: 83 – 188 Post-treated: 14 - 48	Van der Kooij, 1999; Polanska *et al.* 2005	March - Oct	Taiwan	Lou *et al.* 2009
WTW	FL; RSF; SSF; AC; OX; Cl_2; UV; DE; A; NaClO	15 - 255	Van der Kooij *et al*. 1982	1 year	Belgium	Polanska *et al*. 2005
WTW	MF; GAC; CC; Cl_2; NH_2Cl_2	Raw: 92-250 Post-treated: 90 – 224	LeChevallier *et al*. 1993	10 month sampling	USA	Volk & Lechevallier, 2002
WTW & DWDS	Pre-O3; RSF; O_3; GAC; SSF	WTW: 32 DWDS: 28 - 30	Hammes & Egli, 2005	18 months	Switzerland	Hammes *et al.* 2010
WTW & DWDS	CC; SED; RSF; Cl_2; O_3; BAC	Raw: 32.2 – 148 Post-treated: 53 – 151	Japan Water Works	May, June & Jan	Japan	Ohkouchi *et al.* 2011

		DWDS: 60 – 174	Association (JWWA), 2001			
WTW & DWDS	Pre-Cl_2; CC; SED; SF; GAC; Cl_2	Raw: 69 – 350 Post-treated: 69 – 342 DWDS: 92 – 482	Van der Kooij *et al.* 1982	~ 1 year	China	Liu *et al.* 2002
WTW & DWDS	Pre-OX; pre-Cl_2; CC; SED; SF; O_3; BAC; Cl_2	WTW: 62 – 80 DWDS: 33-149	Van der Kooij *et al.* 1982; Liu *et al.* 2002	4 months (Aug, Nov, Jan, Mar)	China	Lu *et al.* 2014
WTW & DWDS	SED; A; CC; Pre-Cl_2; SF; Pre O_3; BIO; BAC; O_3; MIC-F; RO; GAC; UV; Cl_2	Post-treated: 36 - 446	APHA, 2005	Nov & Apr	Japan	Thayanukul *et al.* 2013
WTW & DWDS	A; BF; Cl_2; CC; DF; GAC; NSF; O_3; PAC; RSF; SSF	1.1 - 57	Van der Kooij *et al.* 1982	2 summer & autumn periods	The Netherlands	Van der Kooij *et al.* 1992
WTW & DWDS	CC; SED; SF; F-	WTW: 110 ±60 120 ±50 DWDS: <50 - >200	APHA, 2005	14 months	USA	Zhang *et al.* 2002
WTW & DWDS	FL; SED; FI; NH_2Cl	WTW: 117 – 195 DWDS: 117 - 227	Lechevallier *et al.* 1993a	July – Dec; Jan - Apr	USA	Zhang & *DiGiano,* 2002
WTW & DWDS	Pre-O3; CC; FL; FI; O3; BAC; Cl_2	41 - 308	Liu et al. 2002	1 year	China	Zhang *et al.* 2016
DWDS	Pre-Cl_2; CC, SED; RGF; AC; NH_2Cl	73 – 995	Stanfield & Jago, 1989	3 years	UK	Gibbs *et al.* 1993
DWDS	MF; GAC; O3; Cl_2, NH_2Cl	18 – 189	LeChevallier *et al.* 1993a	18 months	USA & Canada	LeChevallier et al. 1996
DWDS	Cl_2, NH_2Cl, O_3; BAC	26 - 430	Hammes *et al.* 2007	2 years	China	Li *et al*, 2018

Key: A, aeration; AC, activated carbon filtration; BAC, biological activated carbon; BF, bank filtration; BIO, bio-filtration; CC, chemical coagulation; Cl_2, chlorination; ClO2; chlorine dioxide; DE; decantation; DF, dune filtration; F-, fluoridation; FL, flocculation; FLO, flotation; FI, filtration; GAC, Granular activated carbon; MF, multi-media filtration; MIC-F, micro-filtration; NaClO, sodium hypochlorite; NH2Cl, chloramination; NF, nano-filtration membrane; OX, oxidation; O_3, ozonation; PAC, powdered activated carbon; Pre-OX, pre-oxidation; RO, reverse osmosis; RSF, rapid sand filtration; SF, sand filtration; SSF, slow-sand filtration; SED, sedimentation; UV, ultraviolet radiation; *standard deviation

Table 2.5 Assimilable organic carbon removal efficiencies following individual drinking water treatment processes.

Raw Water AOC Concentration (µg C/L)	Treated Water AOC Concentration (µg C/L)	Change AOC (µg C/L)	Treatment Process	Notes	Study
141	147 NF	↑ 6%	NF	Addition of antiscalant & low purity acid may ↑ AOC. AOC compounds are small enough to pass through NF membranes.	Escobar & Randall, 2001
-	70 (2 – 100) (prior ozonation installation)	↑ 112% following introduction ozonation	O_3	↑ AOC following ozonation is due to significant breakdown of larger carbon compounds into AOC compounds (Block *et al*. 1993; Volk *et al*. 1993, 1997; Servais *et al.* 1993).	
-	148 (65 – 27) (after ozonation installation)				
-	171 ±57 post ozonation	3 fold ↑ post ozonation 3 fold ↓ after rapid sand filtration	O_3 / RSF	3-fold ↑ corresponds to values reported for ozonation (Escobar and Randall, 2001; Lehtola *et al*. 2001). ↓ in AOC during RSF reveals good efficiency for AOC removal, and it suggests the presence of high biological activity on the filters.	Hammes *et al*. 2006
23 ±17	113 pre-O_3 46 RSF 58 Intermediate O_3 - GAC 32 SSF	- ↓ 59% total AOC - ↓ 31% remaining AOC ↓ 6% remaining AOC	O_3, RSF, GAC, SSF	Pre-O_3 ↑ AOC. Amount of AOC formed during O_3 varied seasonally (range: 50–311), with typically more AOC formed during colder raw water temperature periods (Muller *et al*. 2003).	Hammes *et al.* 2010
301 243 165	248 conventional 165 GAC 198 chlorination	17.6% removed 33.5% removed +20%	Conventional treatment (CC, SED & FI). GAC, Cl_2.	Low removal efficiencies suggested that AOC could only be partially removed in a	Liu *et al*. 2002

329 275 205 270 247 195	275 conventional 205 GAC 342 chlorination 247 conventional 195 GAC 247 chlorination	16.4% removed 25.5% removed +66.9 8.5% removed 21.1% removed +26.7	(Only April, 1998 values).	conventional treatment process. GAC could attain a much higher AOC removal efficiency. The removal mechanisms of AOC by GAC could be attributed to GAC adsorption and biodegradation by microorganisms grown onto the GAC. AOC ↑ dramatically from GAC effluent to finished water, which might be attributed to post-chlorination.	
148 winter 32.2 summer	151 winter 52.7 summer	BAC did not remove AOC at all during winter but removed 50% of AOC in the summer.	BAC, CC, SED, O_3, RSF	CC–SED was effective for AOC reduction. O_3 ↑ NOX component of AOC significantly. AOC removed during rapid sand filtration (RSF) process. Low efficiency of the BAC process during winter could be an immature bacterial community on the surface of activated carbon because of lower water temperature.	Ohkouchi *et al.* 2011
92 (53-148) 122 (43-300) 95 (53-254) 250 (48-869) 132 (82-937) 119 (72-208)	224 (153-337) MF 156 (110-218) MF 110 (66-193) MF 158 (114-245) GAC 156 (68-260) GAC 90 (58-163) GAC	↑ 164 (16 to 535) ↑ 46 (-48 to 74) 0 (-25 to 42) ↑ 7 (-86 to 222) ↓ 6 (-177 to 78) ↓ 11 (-104 to 67)	MF GAC	AOC were not removed by mixed-media filtration, probably because a continuous chlorine residual was maintained through the filters. AOC ↑ during pre-oxidation but ↓ by 40% by GAC. Post disinfection ↑ AOC by 20%	Volk & Lechevallier, 2002

AOC, assimilable organic carbon; BAC, biological activated carbon; CC, chemical coagulation; Cl_2, chlorination; FI, filtration; GAC, granular activated carbon; MF, multimedia filtration; NF, nanofiltration; O_3, ozonation; RSF, rapid sand filtration; SED, sedimentation; SSF, slow sand filtration.

2.3.2.6 AOC & HRT within DWDS

With regards to AOC values reported in distribution, LeChevallier *et al.* (1987) and Van der Kooij *et al.* (1989) demonstrated that the AOC concentration decreased with distance through the DWDS. However, studies that analyse spatial variation in AOC in the DWDS do not analyse the impact of DWDS infrastructure on AOC concentration. Where service reservoir (SR) inlet and outlet sampling is not undertaken, it is not clear if the DWDS pipes or SR are acting as sources or sinks of AOC. LeChevallier *et al.* (1987) concludes that AOC was consumed by heterotrophic organisms within the DWDS. However, Gibbs *et al*. (1993) did not find a statistically significant relationship between the concentration of AOC and hydraulic retention time, or AOC and microbial counts in the examined distribution system. This could be a result of this study a natural microbial inoculum and adenosine triphosphate (ATP) in the AOC test (Gibbs *et al.* 1993). Different organisms contain a different amount of ATP per cell, consequently showing bias towards different strains of bacteria. AOC concentration was found to fluctuate throughout the DWDS with no evident decline in the AOC concentration through the distribution system. Gibbs *et al.* (1993) also found no seasonal peaks in AOC concentrations in reservoir water, raw water or final treated water. Gibbs *et al.* (1993) acknowledged that a natural inoculum used in this study may not have been representative of the bacteria found within the DWDS. Furthermore, it is difficult to compare AOC values between studies as they incorporate different steps in the AOC methodology.

2.3.2.7 AOC & Biological Stability

Attempts have been made to monitor AOC concentrations within either treatment works or DWDS and to correlate this with the degree of (re)growth within these systems. Such information is used to assess the degree of biostability within drinking water, where biological stability is defined as:

"no changes occurring in the concentrations and composition of the microbial community in the water during distribution" (Lautenschlager et al. 2013).

As AOC is easily assimilated by heterotrophic bacteria, it is a significant contributor to biological instability within DWDS (Nescerecka *et al.* 2014). A significant positive correlation has been found to exist between the AOC concentration and the density of heterotrophic bacteria (van der Kooij *et al.* 1982; LeChevallier *et al.* 1987). The AOC concentration within raw or post-treated drinking water has been reported at concentrations between 1 – 995 µg C/ L, depending on water source and treatment steps (Table 2.4). AOC has been demonstrated to limit microbial growth, and therefore constitute biostable water, at concentrations spanning (≤10 – 120 µg/L) (Van der Kooij, 1992; LeChevallier *et al.* 1996; Ohkouchi *et al.* 2013; Wang, Tao & Xin, 2014; LeChevallier *et al*. 2015) (Table 2.6). These concentrations are thought to differ due to the presence or choice of disinfection residual and other (a)biotic parameters in the DWDS. There is no global consensus as to the AOC concentration that constitutes biostable water. Comparisons between studies is often made difficult as each study applies a different AOC method protocol and therefore employs different yield factors to convert cell counts to AOC equivalents. Furthermore, water biostability is also dependent on whether a disinfectant is applied. Van der Kooij, (1992) reported an AOC range of 1.1 and 57 µg/L, with biostable water containing ≤10 µg/L in the absence of a secondary disinfectant. In contrast, Gibbs *et al.* (1993) found the concentration of AOC to be much higher in disinfected water within a UK DWDS, ranging from 73 – 995 µg/L. None of the AOC values reported by Gibbs *et al.* (1993) would therefore fall into the biostable water category as defined by Van der Kooij (1992). In this study, we conduct an AOC analysis of raw, treated and distributed drinking water to quantify AOC within and between different systems. This study will assess if the reported threshold of <100 µg/L (Van der Kooij, 1992; LeChevallier *et al.* 1993a; LeChevallier *et al*.

1996; Wang, Tao & Xin, 2014; Ohkouchi *et al*. 2013) constitutes biostable water within these systems.

Table 2.6: Comparison of acceptable assimilable organic carbon levels for biological stability.

AOC Concentration (µg C/L)	Parameter used to reflect water biostability	Disinfection	Sample Point	Length of Study	Study
<10	HPC Counts	None	20 supplies: Post-treatment & 9 / 10 locations in DWDS	2 summer & autumn periods	van der Kooij, 1992
<100	Coliforms	Chlorine residual above 0.1 mg/L	31 supplies: Post-treatment & DWDS	18 months	LeChevallier *et al*. 1996
≤32	HPC and flow cytometry TCC	None	1 WTW & 2 points in DWDS	18 months	Hammes *et al*. 2010
≤10.9	HPC counts	Chlorine residual of 0.05 mg/L	Bench test	-	Ohkouchi *et al*. 2013
≤27.58 – 111.4	ATP	-	Bench test	-	Wang, Tao & Xin, 2014
<135	HPC Counts	Chlorine < 0.15 mg/L	Bench test	-	Zhang *et al.* 2016

AOC, assimilable organic carbon; HPC, heterotrophic plate counts; DWDS, drinking water distribution systems; TCC, total cell count; ATP, adenosine triphosphate.

A significant positive correlation has been found to exist between the AOC concentration in post-treated water (essentially free from chlorine (<0.1 mg/L) and the density of heterotrophic bacteria within the DWDS (Van der Kooij *et al.* 1992). Similarly, Escobar *et al.* (2001) found a strong positive correlation between HPC and AOC ($r = 0.85–0.98$) within distributed water containing a disinfection residual. This trend is not observed within all systems; with no clear correlation being found between AOC and bacterial concentration (as HPC) within DWDS

(Carter *et al.* 2000; Zhang and DiGiano, 2002). However, the weak negative correlation between HPC bacteria and AOC observed by Zhang and DiGiano, (2002) may be due to much lower levels of AOC in water, which might have provided limited support for microbial (re)growth in chlorinated water (LeChevallier 2003; Van der kooij 2003). Furthermore, HPC's are not representative of all the bacteria in a water sample. Hammes *et al.* (2010) used flow cytometry to obtain total cell counts (TCC) to assess the biological stability of drinking water without a disinfectant residual. A direct correlation was found between changes in TCC and the AOC concentration, in which an increase in cell concentration (biomass increase) was always associated with a decrease in organic carbon (substrate decrease).

The relationship between AOC and microbial (re)growth is influenced by the choice of disinfectant. Liu *et al*. (2015) demonstrated that AOC and free chlorine can have contrasting effects on bacterial growth. Although free chlorine was able to inhibit the consumption of AOC by reducing the microbial growth, chlorination was also found to increase the AOC concentration by damaging the structures of organic matters macromolecules and transforming them into AOC molecules (Thayanukul *et al.* 2013). This is similar to Weinrich *et al.* (2010) who found that chlorination of reclaimed water in a distribution system significantly increased the level of biodegradable organic matters, including AOC, subsequently increasing the microbial (re)growth potential of the water.

2.3.2.8 AOC & Biofilms

Although AOC has been demonstrated to contribute towards microbial (re)growth within DWDS, the majority of these studies have analysed the effects of AOC on heterotrophic bacteria and/or coliforms within the bulk water, and not bacteria within biofilms. It has been demonstrated that AOC concentration can impact the bulk water and biofilm differently. Despite drinking water containing a disinfect residual and an AOC concentration <50 µg C/l being defined as biologically stable (LeChevallier *et al.* 1993), the formation of biofilms has

been observed on pipe surfaces exposed to drinking water containing an AOC concentration of 39 µg C/L (Okabe *et al.* 2004). The degree of biofilm formation in drinking water has been shown to be sensitive to changes in AOC concentration. Sharp *et al*. (2001) assessed the influence of AOC concentration on biofilm protein production and biofilm HPC counts within a biofilm annual reactor (BAR). The BAR was fed by various treated waters, including anthracite filtered, GAC and ozonated / GAC water. The relationship between biofilm HPC and influent AOC was found to be significant for all water types (Sharp *et al.* 2001). This infers that the numbers of cells within biofilms are higher at elevated AOC concentrations. Okabe *et al.* (2002) assessed the biofilm formation rate (BFR) of drinking water four different advanced water treatment processes, including rotating biofilm membrane reactor (RBMR), biological activated carbon (BAC) filter, ultrafiltration (UF) and conventional treatment (multi-media filtration; MF). The RBMR and BAC filter reduced the AOC concentration by 50% resulting in the BFR being reduced by a factor of 5 to 10 (from 3,200–5,100 to 490–710 pg ATP cm^{-2}). Similarly the BFR fell from 362 pg ATP/cm^2 to 3.9 ATP/cm^2 when the AOC concentration in drinking water was reduced from 10 µg C/L to 3.2 µg/L C/l (Van der Kooij *et al.* 1995). Consequently, when considering the impact of AOC concentration on biologically stability within drinking water it is important to consider both microorganisms in the bulk water and within biofilms.

However, studies that assess the effect of AOC concentration on BFR typically use BAR (Van der Kooij *et al*. 1995; Sharp *et al.* 2001; Okabe *et al.* 2002) that typically do not accurately represent the conditions within DWDS systems but do allow laboratory scale control. Whilst lab based experimental set-ups go some way to understand the impact of AOC on biofilms within drinking water, bench scale reactors do not accurately reflect the changes in AOC concentration within the DWDS environment. This study will therefore analyse the

relationship between AOC and biofilm formation within fully operational drinking water supply systems.

Biofilm structure / architecture and community composition are thought to be determined by environmental conditions such as carbon availability (Karthikeyan *et al.* 2001). However, the impact of AOC on bacterial or fungal community composition within drinking water (bulk water or biofilm) have largely been overlooked. The few studies that have analysed the impact of AOC on the community structure and composition of microorganisms within drinking water environments have done so to analyse the efficiency of individual treatment processes such as bio-filtration (Pang *et al.* 2006; Soonglerdsongpha *et al.* 2011; Yang *et al.* 2011; Liao *et al.* 2013). Liao *et al.* (2013) suggested that the concentrations of AOC in influent water to the biological activated carbon (BAC) could impact microbial community composition (at class level) in biofilters.

2.3.3 Nutrients (Non-Carbon)

2.3.3.1 Phosphorous

Approximately >95% of UK drinking water supplies are dosed with phosphate (CIWEM, 2012) to reduce the formation of iron and manganese precipitates which can cause deterioration in the aesthetic water quality (Kohl and Medlar, 2006). In addition, water can be dosed with phosphate or lime to increase the water pH (to 8 – 8.5) and thereby reducing the extent to which lead dissolves in water. Inorganic phosphates (including phosphoric acid, zinc phosphate and sodium phosphate) can be added to water to form orthophosphate which forms an insoluble coating DWDS pipes to limit lead corrosion (EPA, 2018). Phosphorous is required by microorganisms for cellular metabolism, particularly for the formation of high-energy compounds such as ATP. In countries where drinking water contains a high concentration of organic matter, such as boreal regions, phosphorous limits bacterial growth (Miettinen *et al.* 1997; Lehtola *et al*. 2002, 2004). In such situations, an increase in phosphorous has been

correlated with an increase in biofilm biomass (Lehtola *et al.* 2002, Chu *et al*. 2005). Interestingly, bacteria can store phosphorous for future use when the nutrient concentration becomes limited, therefore bacterial growth is not directly linked to phosphorous intake. As a result it is not conclusive that phosphorus removal from drinking water would ultimately control biofilm development within a DWDS (Lehtola *et al.* 2004). Although heterotrophic organisms require inorganic nutrients such as phosphorus, nitrogen or trace elements (iron, magnesium, copper, potassium etc.), they are required in much smaller amounts than organic carbon (Ihssen and Egli, 2004).

Phosphorus has not only been found to impact biofilm biomass but also the microbial communities within the biofilm (Keinänen *et al.* 2002) and biofilm structure (Fang *et al.* 2009). Juhna *et al*. (2007) found that elevated phosphorus concentrations prolonged the survival of culturable *E. coli* in water and biofilms. This therefore poses a public health risk if *E. coli* strains such as O157:H7 (which is an emerging cause of waterborne illnesses), are released into the bulk water. Fang *et al*. (2009) found that whilst phosphorous addition promoted bacterial growth within the biofilm, elevated phosphorous levels reduced EPS production and homogeneity of the biofilm structure. Fang *et al.* (2009) concluded that this may reduce the stability of the biofilm and its ability to be resistant to disinfectants. Conclusively phosphorous availability may affect drinking water biostability indirectly by influencing the biofilm stability and subsequently vulnerability to be mobilised into the bulk water.

2.3.3.2 Nitrogen

Autotrophic nitrifying bacteria or nitrifiers use nitrogen-based compounds (e.g. ammonia, and nitrite) found in DWDS for growth, and are found within both bulk water and biofilms (van der Wielen *et al.* 2009). Ammonia is found in untreated water, released during chloramine decay (Vikesland *et al.* 2001) and generated during reactions between nitrate and metal surfaces in DWDS (Alowitz *et al.* 2002). During the nitrification process, ammonia is oxidisied

to nitrite by ammonia oxidising bacteria (AOB), before nitrite is oxidised to nitrate by nitrite-oxidising bacteria (NOB). Increased nitrite levels not only promote the growth of NOB but can also cause the deterioration of water taste and odour, and might increase heterotrophic bacteria, including opportunistic pathogens (Wilczak *et al*. 1996). The concentration of available nitrogen also shapes the microbial composition within DWDS, with high nitrogen-to-carbon ratios favouring autotrophic bacteria, whereas low nitrogen-to-carbon ratios promote growth of heterotrophic bacteria (Ohashi *et al.* 1995). It is therefore important to consider nitrogen availability when quantifying the degree of biological stability within DWDS, particularly in drinking water with highly elevated organic carbon concentrations (no carbon limitation).

2.3.4 Iron and Manganese

The concentration and bioavailability of metals is dependent on the source of drinking water, pipe material, treatment processes and disinfection. The accumulation of metals in the DWDS can lead to discoloration when they become mobilised by changes in the hydraulic regime, resulting in exceedance of regulatory standards (DWI, 2014). Iron and manganese have been identified to be the dominant materials mobilised, irrespective of pipe material (Boxall *et al.* 2003; Seth *et al.* 2004; Boxall & Saul, 2005). Drinking water treatment technologies employed to control iron and manganese include ion exchange, filtration, oxidation and the addition of phosphate to the water to keep iron and manganese in solution (Minnesota Rural Water Association (MRWA), 2009). Two of the main sources of inorganic matter in DWDS include carryover from water treatment (Vreeburg and Boxall, 2007; Vreeburg *et al*. 2008) and corrosion by-products within pipes (Peng and Korshin, 2011; Prasad and Danso-Amoako, 2014).

The presence of iron and manganese, commonly associated with discoloured water events within DWDS (Husband *et al*. 2008), have also been observed to be positively correlated with biofilm activity (Ginige *et al*. 2011). Ginige *et al*. (2011) found that during late summer

and early autumn increased biofilm activity was associated with increased deposition of iron and manganese. Consequently when biofilms detach, due to a change in abiotic conditions (e.g. hydraulics), it is likely that the entrapped iron and manganese will be released and cause discolouration. Iron and manganese have also been demonstrated to influence microbial community composition within bulk water and biofilms (Li *et al.* 2010, Löhrig *et al.* 2015). Li *et al.* (2010) found a high percentage of iron-oxidising bacteria (*Gallionella*) within red water. Similarly, Löhrig *et al*. (2015) identified *Pedomicrobium* (manganese-oxidising) within water containing iron and manganese. Iron-oxidising gram-negative bacteria such as members of the genus *Pseudomonas* are likely to increase in abundance when iron concentrations are elevated (LeChevallier *et al.* 1993b). However, although there exists a large amount of research regarding the impact of nutrients on the bacterial community composition of drinking water biofilms, there is a lack of research regarding other taxa.

Although required in a smaller amount than organic carbon, inorganics trace elements, including iron, manganese, copper and potassium are required for heterotrophic growth (Ihssen and Egli, 2004). In drinking water containing high levels of organic carbon, very low levels of inorganic compounds can limit bacterial growth (Miettinen *et al*. 1997). Furthermore, drinking water contains autotrophic organisms such as iron-oxisding bacteria that are able to synthesize organic substances from inorganic materials (Rittmann and Snoeyink, 1984; Pepper *et al*. 2004). It is therefore important to consider inorganic nutrients, as well as organic carbon, when understanding microbial dynamics in operational DWDS.

2.3.5 Hydraulic Conditions

DWDS are characterised by variable hydraulic conditions due to variations in customer demand, operational changes, and occasional pipe bursts. The varying hydraulic conditions are thought to influence the adhesive/cohesive strength of the biofilm, the accumulation or

mobilisation of biofilms (Stoianov & Aisopou, 2014) and rate of mass-transfer (including nutrients (organic and inorganic), planktonic cells and disinfectant residual) at the pipe wall (Fish *et al.* 2017). The hydraulic residence time (HRT) can also impact water quality, as a long HRT can lead to a loss of disinfection residual as the water age increases (Machell *et al.* 2009). A higher HRT has been found to correlate with higher bacterial abundances within the DWDS (Uhl and Schaule, 2004; Nescerecka *et al.* 2014). The HRT also dictates the time that water can potentially come into contact with the pipe surface, therefore influencing processes occurring at the boundary layer interface. Ellis *et al*. (2013) analysed the number of bacterial failures by sample point at a UK water utility and found that the highest percentage of non-compliance occurred at customer taps (in comparison to post-treatment or service reservoir water), suggesting that water quality had declined with HRT.

2.3.5.1 Hydraulic and Biofilm Interactions

Biofilm formation has been found to be limited by elevated flow rates, with the number of bacteria negatively correlating with the flow rate of the water (Ragazzo & Nardo, 2002). Cloete *et al.* (2003) found that a flow velocity in the range of 3 m/s and 4 m/s resulted in biofilm mobilisation. However, it is established that even when subjected to high shear stresses, a biofilm base layer is always present (Park *et al.* 2002, Abe *et al.* 2012).The ability of the biofilm to resist mobilisation is thought to be a result of the adhesive forces of the EPS matrix (Stoodley *et al.* 2002). It is only when the shear stresses acting upon the biofilm exceed the internal forces of the EPS that the biofilm (cells, EPS and associated material) will mobilise into the bulk water, therefore impacting water quality (Abe *et al.* 2012; Mathieu *et al.* 2014). Biofilm mobilisation is thought to be directly analogous to the cohesive-layer theory of discolouration (Husband and Boxall, 2016). Material is thought to accumulate at the pipe wall in cohesive-layers that form at different strengths influenced by the boundary layer hydraulic conditions (Boxall and Saul, 2005; Husband *et al.* 2008; Van Thienen *et al.* 2011). Disinfection processes

and temperature (Ginige *et al.* 2011) or chemical process such as nutrient availability (Ginige *et al.* 2011) change the adhesive properties of the biofilm. Mobilisation is mainly thought to be a physical process caused by changes in hydraulic shear stress (Stoodley *et al.* 2001b). Mobilisation events can also cause a deterioration in water biostability, generate microbiological regulatory failures, pose a discolouration risk and even be detrimental to human health (Vaerewijck *et al.* 2005).

Biofilm morphology has been demonstrated to be a function of hydraulic conditions, with shear forces impacting the thickness, density, strength and structure of the biofilm (Liu & Tay, 2002; Laspidou & Rittmann, 2004; Menaia & Mesquita, 2004; Abe *et al*. 2012). When subject to elevated shear stress the density of the biofilm has been demonstrated to increase whilst the biofilm thickness decreased. This is thought to be a result of increased compression of the biofilm (Paul *et al.* 2012), potentially generating a more stable structure (Manuel *et al.* 2007). In contrast, Rochex *et al*. (2008) found that thicker biofilms developed under higher shear stresses, which they argue could be a result of increased biomass due to increased mass transfer or an increase in the cohesive strength of the biofilm (Stoodley *et al*. 1999, Horn *et al*. 2003). The shear stress required to generate mobilisation is also a function of biofilm volume. Larger sized biofilm clusters have been demonstrated to both be able to resist mobilisation due to their adhesive properties (Lehtola *et al.* 2006) and more readily detach than their smaller counterparts (Abe *et al*. 2012). The hydraulic regime is therefore able to influence biofilm stability, and potential to be mobilised into the bulk water, by indirectly dictating biofilm morphology.

Although biofilm development has been shown to be limited by high water velocities due to the shear stress at the interface (Ragazzo & Nardo, 2002), the velocity can also impact the nutrient available for the biofilm (Ollos *et al*. 2003; Lehtola *et al*. 2006; Torvinen *et al.* 2007). Ollos *et al*. (2003) found that higher flow velocity of water increased the mass transfer

of growth limiting nutrients to the biofilm. Fish *et al*. (2017) used a full-scale, experimental DWDS facility to analyse the impact of flow variation on biofilm growth and subsequent mobilisation. The study found that biofilms subjected to high flow variation during growth had the largest biomass. The accumulation of greatest biofilm biomass at high varied flow was attributed to greater mass-transfer of trace nutrient to the pipe wall during times of greater turbulence (Reynolds number >4000 for turbulent flow) (Fish *et al.* 2017). Therefore, high flow rates can lead to greater nutrient uptake by the biofilm, acting as a net sink of nutrients.

Douterelo *et al.* 2013 assessed the influence hydrological regime on bacterial community structure and composition within biofilms in an experimental DWDS. Bacterial community composition was found to differ between biofilms and bulk water samples, with *Gammaproteobacteria* and *Betaproteobacteria* being the most abundant phyla in biofilms. It has previously been demonstrated that particular bacterial species have selective advantage in being able to attach to surfaces and form biofilms due to their ability to express cell surface polymers that can increase cell hydrophobicity and promote processes such as co-aggregation (Rickard *et al.* 2003; 2004).

An increasing amount of research has been conducted aiming to understand hydraulic and biofilm interactions (Lehtola *et al.* 2005; 2006; Fish *et al*. 2017). However, the majority of which use idealised laboratory studies that incorporate bench top reactors that do not accurately replicate the conditions in operational DWDS (Murga *et al*. 2001; Simoes *et al.* 2005). Drinking water demands not only vary spatially due to different environmental and socio-economic climates, but also temporarily due to diurnal and seasonal changes in customer behaviour. The domestic pattern in demand for water for example includes two peak periods at approximately 7:00-10:00am and 5:00-8:00pm (Beal *et al*. 2011), and low night time flow. Although it is important to replicate diurnal flow within DWDS test facilities, this study chose to adopt a

steady state flow to ensure that AOC was the dominant factor influencing biofilm formation, rather than changes in hydraulic regime.

2.3.5.2 Discolouration

A change in hydraulic conditions, such as a pipe burst or increase in demand, that raises the boundary shear stress above the conditioned value, is recognised as the trigger for discolouration events (Husband *et al.* 2008). As the material responsible for generating discolouration consists of small particulates approximately ~10μm in size (Gauthier *et al.* 2001; Seth *et al.* 2004; Verberk *et al.* 2006), unless DWDS exhibit very low flows for extended periods of time, gravitational sedimentation is not the dominant force controlling material behaviour (Boxall *et al.* 2001). Similarly, Fish *et al.* (2013) found no statistical difference between attached microbial assemblages found on high-density polyethylene (HDPE) coupons within a pipe loop test facility positioned on the bottom, middle and top of the pipe. This suggests that gravitational processes are not the dominant force acting upon biofilms. Greater flow rates and shear stresses can re-suspend particles (often containing a high organic matter content) (Gauthier *et al*. 1999, Camper *et al*. 2003) resulting in a greater degree of chlorine residual decay. This can promote microbial growth downstream and lead to a loss of biological stability in the DWDS.

2.3.5.3 Network Cleaning

Network cleaning programmes are used to remove material from the pipe walls of the DWDS. Cleaning programmes include the use of water flushing, water/air scouring, pigging, swabbing or scraping. Although methods such as swabbing and pigging are able to remove the greatest amount of attached material from the pipe wall, these methods are disruptive and comparatively expensive (Vreeburg & Boxall, 2007). Sunny *et al.* (2017) found that although trunk main cleaning using pigging substantially improved the hydraulic capacity and reduced headloss, relatively loose material had not been fully removed from the pipe wall and therefore the water

quality risk still remained. In general, water flushing programmes are more cost effective (Vreeburg and Boxall, 2007), however large volumes of water are required. Furthermore, all of the above listed cleaning methods can potentially generate customer complaints due to inconvenience or potentially produce a large quantity of mobilised material which can generate turbid water. Particularly abrasive cleaning methods can expose underlying ferrous material of the pipe surface which was previously protected accumulated deposits (Vreeburg and Boxall, 2007). Flushing cannot completely remove biofilms from pipe walls due to the cohesive properties of the system and their ability to recolonise the pipe wall once detached (Abe *et al*. 2012, Paul *et al.* 2012).

Prediction of Discolouration in Distribution Systems (PODDS) (Husband & Boxall, 2010) is an empirically validated model, based upon a 'cohesive layer theory', which proposes that flows above peak daily demands can lead to mobilisation of material from the pipe walls. In this way it is possible to increase the flow rate during standard operation to incrementally remove accumulated material layers and hence reduce discolouration risk pro-actively. This has been demonstrated for distribution pipes with diameters less than 150 mm (Boxall and Saul, 2005; Husband *et al*. 2008; Husband and Boxall, 2010) and trunk mains (Husband and Boxall, 2016). Consequently, hydraulics can be used to manage biofilms within DWDS. In the Netherlands, a velocity at which shear stresses reduce the rate of material accumulation has been established, termed the self-cleaning velocity (Van den Boomen *et al.* 2004). At a velocity of at least 0.4 m/s material within the DWDS is re-suspended preventing accumulation on pipe surfaces. Countries such as the Netherlands are also reliant on very low concentrations of AOC (<10 µg / L) to limit microbial (re)growth within drinking water. It has not yet been determined if AOC limitation in drinking water can help prevent biofilm accumulation and be used in tandem with other DWDS management strategies such as network cleaning.

2.3.6 Temperature / Seasonality

Seasonality can significantly affect the quantity and quality of available raw drinking water, and the quantity of water used by consumers. Water companies can experience seasonality in customer contacts. For example periods of freezing temperatures followed by a rapid thaw can lead to burst pipes in the DWDS, and an increase in customer contacts due to discolouration as the supply is recharged (DWI, 2018). Similarly a significant increase in temperature can lead to unprecedented levels of customer demand, which can cause a decline in source water levels, potentially causes interruptions in supply.

Increased temperatures within the DWDS has frequently been associated with an increase in bacterial abundance (Francisque *et al*. 2009; Henne *et al.* 2012; Liu *et al.* 2013), and an increase in indicator organisms such as coliforms (LeChevallier *et al.* 1996) within bulk water samples. Francisque *et al.* (2009) found that growth of heterotrophic bacterial was limited at lower water temperatures, with no HPC in 75% of collected samples at water temperatures ≤4°C. Temperature has also been found to have a significant influence on biofilm activity, with an increase in temperature often resulting in elevated bacterial numbers and biomass in biofilms due to increased growth and replication (Hallam *et al.* 2001; Lehtola *et al*. 2004). Hallam *et al*. (2001) reported that biofilm activity decreased by approximately half at a temperature of 7°C compared to 17°C. Not only is temperature thought to influence bacterial abundance, but also affect bacterial community composition (Prest *et al.* 2016). Water temperature may provide a selective advantage to microorganisms, including pathogenic species, which are better adapted to specific temperature ranges (Vital *et al.* 2007, 2012). Torvinen *et al.* (2007) found that water temperature had the greatest influence on the survival of *Mycobacterium avium* (assessed using culture and fluorescence in situ hybridization methods) in biofilms, in comparison to changes in flow velocity or phosphorous.

Elevated temperatures can also generate increased bacteriological activity (LeChevallier *et al*. 1996; Silhan *et al*. 2006) and accelerate the rate of reactions, such as the formation of disinfection by-products (therefore providing a food source for heterotrophic organisms) (Toroz & Uyak, 2005; Roccaro *et al*. 2008). Furthermore, temperature can influence the kinetics of chlorine demand in the system. Ndiongue *et al.* (2005) found that a temperature of 12 to 18°C caused the chlorine demand in an annual reactor to almost triple, therefore leading to a potential loss of biological stability within the system. Temperature has also been found to influence the amount and rate of biofilm mobilisation into the bulk water (Sharpe *et al.* 2012). In a temperature controlled pipe loop facility, Sharpe *et al.* (2012) found that larger quantities of material were mobilised at 16°C, than at 8°C. The biofilm mobilisation rate was also influenced by the hydraulic regime, with temperature having the greatest effect on turbidity, iron and manganese release at the lowest flow rate with a steady shear stress of 0.1 (N/m^2). Sunny *et al.* (2018) found a correlation between seasonal temperature, TOC concentration and microbial growth within UK DWDS trunk mains. The authors suggest that higher temperatures resulted greater accumulation of material on boundary surfaces should it be mobilised. Temperature is therefore potential a major influence on biological stability within DWDS, particularly when temperatures are elevated.

2.3.7 DWDS Infrastructure: Pipe material, Diameter and Roughness

DWDS infrastructure can affect water quality in a number ways through corrosion, ingress potential and biofilm forming potential (BFP). Pipe material, diameter and roughness are all components that can ultimately impact water quality due to their BFP. The DWI lists a number of approved pipe materials for use in public supply in the UK, including polyethylene (PE), polyvinyl chloride (PVC), glass reinforced plastic (GRP), cement mortar lined and stainless steel (DWI, 2019), although a large number of historical pipes are made of cast iron. Pipe materials are able to able to modify biofilm formation through two mechanisms: (1) release of

organic and inorganic compounds such as iron or copper which subsequently influence microbial (re)growth (Lehtola *et al*. 2004); (2) affect the decay rate of disinfection residuals, in some cases resulting in elevated microbial (re)growth (Hallam *et al.* 2001).

Recently, plastic materials have been favoured over traditional metal materials as they are more cost-effective (Yu *et al*. 2010) and provide a smoother surface that can potentially reduce biofilm (re)growth (Chang *et al*. 2003). Distribution pipes with a high surface roughness, such as unlined cast iron, can have a high BFP as corroded iron pipes may offer numerous bacterial attachment sites (LeChevallier *et al.* 1993b). Microbially influenced corrosion of the pipe surface can also release nutrients from the pipe material and form by-products that affect surface roughness (Niquette *et al*. 2000). A large number of studies have found that pipes consisting of plastic materials are able to reduce bacteria density and diversity in comparison to those made of iron (Kerr *et al.* 1998; Niquette *et al.* 2000), steel (Yu *et al*. 2010) or cement (Niquette *et al*. 2000, Camper *et al.* 2003). Niquette *et al.* (2000) demonstrated the density of fixed bacterial biomass to be lower on PVC and PE in comparison to those consisting of iron (bacterial biomass was 10-45 times higher on grey iron than plastic-cased materials) or cement-based materials. Furthermore, the quickest rate of biofilm development has been demonstrated to occur on iron pipes than other materials (Camper, 1996). Pipe material also impacts the microbial diversity of biofilms. In a study of faucet biofilms, Liu *et al.* (2010) used pyrosequencing to find that the bacterial composition was substantially influenced by the pipe materials (PVC and cast iron). Similarly, Yu *et al*. (2010) demonstrated that the DGGE profile of bacteria 16S rDNA fragments presented differences between different pipe materials. Plastic material can also have affects beyond reducing biofilm formation. Particulate material can also accumulate at a slower rate upon plastics than on cast iron pipes due to in-situ corrosion of cast iron pipes. However, in some scenarios, biofilm activity has

been demonstrated to be more strongly influenced by abiotic factors, such as chlorine (Hallam *et al.* 2001), than pipe material.

Whilst plastic pipes may have demonstrated to reduce the BFP, they can release biodegradable organic compounds and phosphorus potentially trigger microbial (re)growth and biofilm formation (Yu *et al.* 2010). Furthermore, some metals such as copper, have been demonstrated to reduce the BFP and bacterial diversity in comparison to plastics (Yu *et al.* 2010). Using a pilot DWDS, Lehtola *et al*. (2004) found that biofilm formation was slower in copper pipes than PE pipes, and that pipe material also influenced the bacterial community structure within both biofilms and the bulk water. Copper produces corrosion products that affect bacterial attachment on the surface by creating an environment that is toxic to most microorganisms e.g. *Legionella* (Kim *et al.* 2002).

However, bacteria, such as *Pseudomonas aeruginosa*, have demonstrated greater resistance to the toxic effects of copper when residing within in biofilm than when in the planktonic phase (Teitzel & Parsek 2003). Not only does pipe material influence the degree of biofilm formation, but the establishment of biofilms also impacts the condition of the pipe material via biocorrosion. Biocorrosion (or microbially influenced corrosion - MIC) consists of a number of complex interactions between the substrate, corrosion products, bacterial cells and the substances generated during metabolism (Beech & Sunner, 2004). The result of biocorrosion is twofold, with an increase in nutrient concentration in the area immediate to the pipe wall, and an increase in pipe surface roughness as metabolic by-products form (Norton & LeChevallier, 2000).

Volk *et al*. (2000) found that iron-oxidising bacteria can precipitate iron oxides where iron is converted to ferric iron. It is this increase in surface roughness due to bio-corrosion that can subsequently concentrate organic nutrients and promote biofilm development (LeChevallier *et al.* 1993b) by creating an environment more suitable for colonisation e.g. a

greater surface area for adhesion. Corrosion has also been demonstrated to generate increased protection from free chlorine disinfection (LeChevallier *et al*. 1993b). During corrosion, the released ferrous iron can remove reduce chlorine (Li *et al.* 2010), subsequently decreasing the rate of biofilm mobilisation. It is therefore important to consider pipe material when designing experimental pipe loop facilities and ensure it is representative of operational DWDS (Section 4.5.1 DWDS Pipe Loop Test Facilities).

2.4 Summary

One of the main goals of water utilities is to provide the consumer with microbially safe, high quality drinking water. In order to achieve this, drinking water in the DWDS should be biologically stable and therefore the concentration of bacterial cells and composition of the microbial community should not deteriorate from the point of leaving the treatment works to reaching the customers tap. The (re)growth of microorganisms within the DWDS is influenced by a host of parameters including hydraulic regime, disinfection residual or nutrient availability. A disinfectant residual is applied to limit (re)growth of microorganisms within the network. However, the maintenance of a chlorine residual alone cannot be relied upon to completely eliminate bacterial growth within DWDS as bacteria have been found to grow when residual disinfectants are depleted, at remote locations and/or during warm periods (LeChevallier *et al.* 1996; Uhl and Schaule, 2004; Nescerecka *et al.* 2014). Alternatively, few European countries, including the Netherlands, Switzerland, Austria and Germany use extensive treatment strategies to limit nutrients in water that can serve as food source for bacteria to grow. As AOC is the fraction of carbon most easily consumed by bacteria for growth, it is considered one of the most important parameters governing biological stability in drinking water systems. Despite this, water utilities do not conduct routine AOC measurements due the time required to complete the assay and its lack of reproducibility. Furthermore, studies which analyse AOC variation within DWDS do not undertake service reservoir (SR) inlet and

outlet sampling, and therefore it is not clear if the DWDS pipes or SR are acting as sources or sinks of AOC. The majority of microorganisms found within the DWDS are known to exist in communities attached to the inner surface of the pipe forming a biofilm. Although it has been demonstrated that microbial communities occur ubiquitously at the DWDS pipe interface, we lack understanding of their relationship with AOC and biological stability. To fully understand the impact of AOC within DWDS, research into drinking water at the pipeline level is essential. Understanding the relationship between drinking water microbiology and AOC will allow water utilities to better quantify biological stability, and limit biofilm formation and (re)growth within operational DWDS.

Chapter 3: Aims & Objectives

3.1 Introduction

There is a need to better understand the concentration of AOC within operational DWDS and its relationship to biological stability and (re)growth. DWDS are complex environments consisting of pipes and SR, varying in hydraulic retention time (HRT), surface to volume ratio, material, water chemistry, disinfection regime and flow regime. All of these parameters can potentially impact the AOC concentration and subsequently the growth rate and community composition of microorganisms, both in the bulk water and within biofilms in DWDS.

This thesis chapter will set out the aims and objective of this thesis. This research aimed to develop a refined AOC method, which could be used to determine AOC removal efficiencies at WTW and determine a wide range of AOC concentrations. Furthermore, this study will determine the impact of spatial and temporal variation in AOC concentration on the biostability of post-treated water, and identify any sources or sinks of AOC within the DWDS. Purpose built DWDS pipe loop test facilities will be used to understand the impact of AOC concentration on biofilm growth and subsequent mobilisation within the DWDS. This research will provide a new understanding of the role that AOC plays within drinking water systems, in particularly how AOC impacts biofilm growth, development and mobilisation.

3.2 Aims & Objectives

The objectives of this research were:

i) To develop a rapid, robust AOC method that can be routinely applied to operational WTW to gain an insight into AOC removal efficiencies during treatment.

ii) To quantify AOC concentrations from DWDS supplied by different source waters and WTW, ranging from clean borehole to surface water site and different disinfection residuals (chlorinated and chloraminated). This work will determine if

and how AOC varies within and between different systems, and how AOC is impacted upon by the choice and concentration of disinfection residual.

iii) To quantify the degree of 'biological stability' within DWDS by comparing the AOC concentration with routine bulk water quality parameters to provide a greater insight the relationship between AOC concentration, microbial cell counts and disinfectant within DWDS.

iv) To understand spatial and temporal fluctuations in AOC within DWDS by conducting service reservoir (SR) inlet and outlet sampling. This piece of work aims to identify which areas of the DWDS (pipes or service reservoirs) were acting as sources and sinks of AOC.

v) To determine the relationship between AOC concentration and biofilm volume, community composition and stability within a DWDS.

vi) To characterise the effect of elevated shear stress (flushing) upon the biofilms that has accumulated under different AOC concentrations, and to quantify how easily the material mobilised into the bulk water. The released material will be assessed in terms of AOC concentration, cell counts, turbidity and inorganic material. Ultimately this research will determine if an elevated AOC concentration in the bulk water will affect the microbial and discolouration risk of the biofilm.

Chapter 4: Methodology & Methods

4.1 Introduction

AOC is considered one of the key parameters governing biological stability within DWDS. Understanding the AOC concentration within drinking water and the impact it has on planktonic and attached biofilm microbiology, is critical to achieving effective drinking water management. This chapter will set out the methods used to answer the aims set out in Chapter 3, and set out how they will be integrated together. The experimental plan will be divided into laboratory method development, fieldwork sampling and finally experimental work (Figure 4.1).

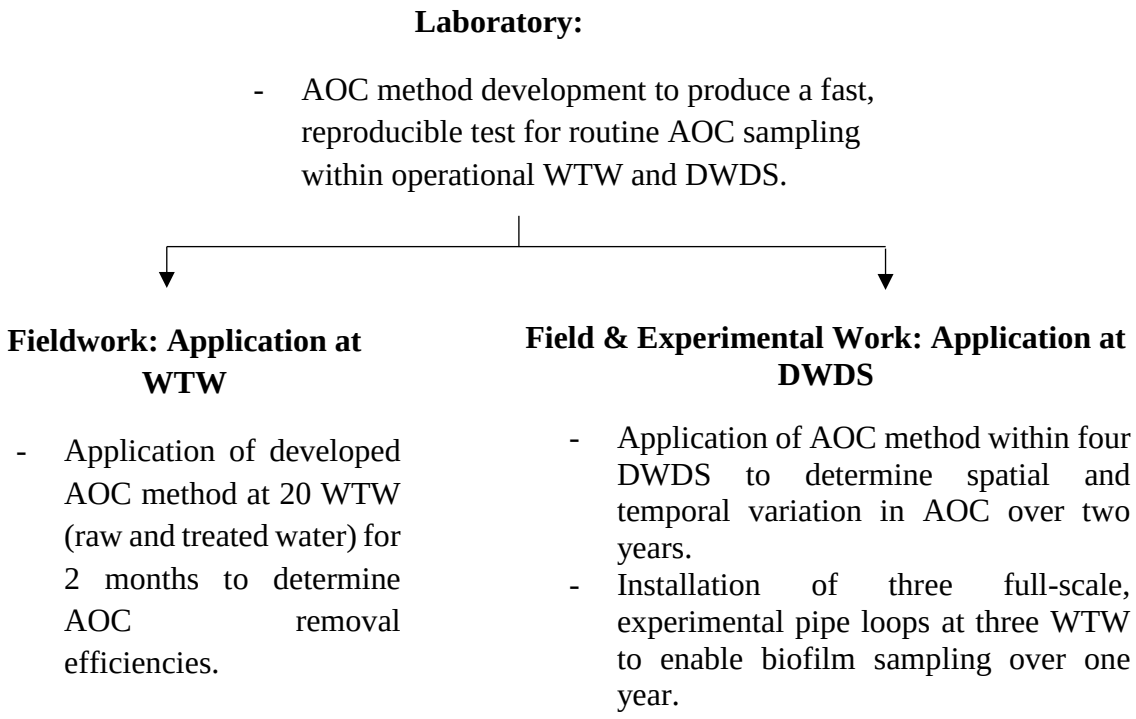

Figure 4.1: Overview of experimental plan, including laboratory, field and experimental work.

4.2 Aims, Objectives & Experimental Overview

AOC is not currently routinely sampled in drinking water due to the time-consuming nature of the method, and lack of reproducibility between measurements. A series of lab trials were conducted to develop novel advancements in the AOC method to improve the speed and robustness of the protocol. By developing a quick, standardised AOC method, this study aimed to conduct detailed AOC sampling of WTW and DWDS water to reveal new understandings of AOC within operational drinking water systems. The developed AOC method was applied to raw and post-treated water at twenty Scottish Water WTW to assess the AOC removal efficiencies across a range of source water and treatment types. Four of the WTW were then selected for further AOC sampling at a number of service reservoirs in their DWDS to reveal how AOC varies on both a temporal 0nad spatial scale within the DWDS.

Current field application of AOC is often limited to laboratory scale systems (Aggarwal *et al.* 2015; Hammes & Egli, 2015; Ross *et al*. 2013; Wen *et al*. 2017) or application at WTW without consideration of AOC concentrations and behaviour within the DWDS. Although the impact of AOC on bulk water microbiology has been studied (Escobar *et al.* 2001; Zhang and DiGiano, 2002), there is a paucity of information regarding the impact of AOC on biofilm communities residing on the pipe walls of DWDS. This thesis will determine if AOC varies within different components of the DWDS (such as pipes and service reservoirs), which are characterised by different surface-area-to-water-volume ratios, thereby impacting the time water comes into contact with the infrastructure surface. The successfully validated AOC method developed in this study was used to determine the AOC concentration within four DWDS (downstream of four Scottish Water WTW) for two years. The second year of bulk water sampling corresponded with the one-year experimental pipe loop programme outlined in the following section. Unique sampling was conducted at service reservoir (SR) inlets and outlets to determine if the AOC concentration changes in service reservoir or pipe dominated

areas of the network. Each of the four WTW / DWDS were characterised by different source water qualities, treatment practices and choice of secondary disinfectant.

AOC has previously been shown to contribute towards microbial (re)growth within DWDS but the majority of research has focused upon effects of AOC on heterotrophic bacteria and/or coliforms within the bulk water, rather than considering bacteria within biofilms. To explore the impact of AOC on DWDS biofilms as well as bulk water quality, whilst maintaining full-scale hydraulic conditions, three unique pipe loop test facilities were designed and installed for the first time at fully operational WTW. Previous biofilm investigations at the University of Sheffield pipe loop experimental facility have analysed accumulated material at 7 days (Husband, *et al.* 2008), 28 days (Sharpe *et al.* 2010; Douterelo, *et al.* 2013, Fish *et al.* 2017) and three months (Douterelo *et al.* 2018). Although short times scales enable weekly biofilm sampling, this timeframe only allows insight into the initial development of biofilms and not biofilm maturation. The experimental programme consisted of a one year-long study, in which biofilm samples were collected every three months during the growth phase, whilst the AOC concentration was monitored in the bulk water. The impact of AOC concentration on the cell count, community composition and total volume of the biofilm (including organic and inorganic components) was assessed. The experimental programme was designed to run for 12 months to capture biofilm maturation over a long-term timescale and to capture the seasonal impacts on AOC concentration and biofilm growth. Following on from the one year-long growth period, the pipe loops were flushed to provide an insight into the impact of AOC concentration on biofilm mobilisation into the bulk water at different AOC concentrations.

The pipe loop test facilities were installed at the exit of three WTW, each being fed with post-treated water containing contrasting AOC concentrations (high, medium and low). The three test pipe loop facilities were purpose built for this study, based on the successful designed used by Sharpe *et al*. (2010), Fish *et al.* (2017) and Douterelo *et al.* (2018). This thesis

presents the first use of the pipe loops at the outlet of WTW to study the impact of different AOC concentrations on biofilm and bulk water quality in down-stream pipes. These unique pipe loops accurately represent the real environmental conditions of an operating DWDS, whilst enabling quick and controlled biofilm sampling, with laboratory level control. The design of the pipe loop is such that it is able to accurately represent biofilm accumulations in the networks during the 12 month 'growth phase', but also biofilm mobilisation during the 'flushing / mobilisation phase'.

4.3 AOC Method Development

To develop a quicker but robust AOC method, established methods by van der Kooij *et al.* (1982), LeChevallier *et al.* (1993a) and Hammes & Egli (2005) were assessed in combination with different variations of these protocols and incorporating alternative cell quantification approaches (Figure 4.2)**.**

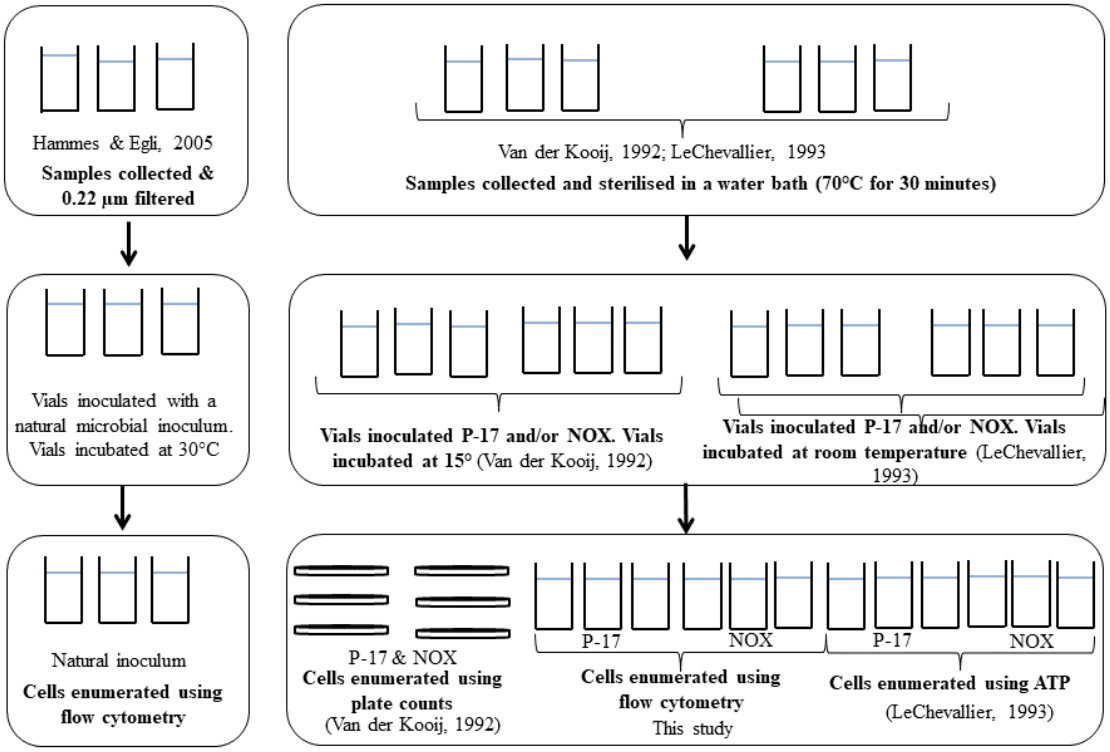

Figure 4.2: Overview of AOC methods evaluated in this study. This included AOC methods from van der Kooij *et al.* (1982), LeChevallier *et al.* (1993a) and Hammes & Egli (2005).

Assessment of the methods included protocols that incorporated different inoculum strains, incubation temperatures and enumeration techniques that were varied beyond the variations listed in Table 2.2 (Chapter 2). An initial laboratory trial analysed differences in the yield values and AOC results obtained when using two known bacterial strains (*Pseudomonas fluorescens* strain P-17 and *Spirillum* strain NOX), in comparison to using a natural inoculum. The results from this test were used to inform further trials to determine the possible options for reducing the time and resources required to complete an AOC assay by modifying the: incubation temperature, inoculation volume and enumeration technique. The use of an indigenous bacterial inoculum assumes that, due to the bacterial community being diverse, the organisms would be able to grow on any AOC combination within a water sample. To

investigate this, different microbial inoculums were collected from post-treated water and used to measure AOC in a number of drinking water and sodium acetate samples.

4.3.1 Overview of AOC Trials

The ability of the AOC methods described van der Kooij *et al*. (1982), LeChevallier *et al.* (1993a) and Hammes & Egli (2005) to quantify AOC within 40 ml sodium acetate standards containing 0 (n=3), 100 (n=3), 250 (n=3), 500 (n=3), 750 (n=3) and 1000 µg C / L (n=3) was first assessed. In the Van der Kooij *et al*. (1982) method, sodium acetate standards were first sterilised before being inoculated with 500 CFU/mL of each of the pure cultures P-17 and NOX. The sodium acetate standards were then incubated at 15 °C for 9 days, with samples being removed on days 7, 8 and 9 for enumeration using heterotrophic plate counts (HPC) (Section 4.3.5.1). The LeChevallier *et al.* (1993a) method was performed as listed except samples were enumerated using the adenosine triphosphate (ATP) method, instead of HPC. Furthermore, 500 CFU/mL of each of the cultures of P-17 and NOX were inoculated into separate vials.

When using the Hammes & Egli (2005) method, a natural microbial inoculum was used instead of known bacterial strains. As the inoculum used in this assay was autochonous to the water sample in question, pasteurisation was not required. Instead the water samples were filtered (0.22 µm pore, Millex-GP, Millipore) to remove bacteria and interfering particles, and re-inoculated within 100 µL of the natural microbial inoculum (Section 4.3.4). Samples were enumerated at 30 °C until stationary phase is reached (after 2-3 days) and then enumerated using flow cytometry (Section 4.3.5.2).

Although flow cytometry has been demonstrated to be a successful enumeration method when using a natural inoculum, it has not yet been used to count P-17 and NOX incubated at 15 °C. Using sodium acetate standards containing 0 or 100 µg C/L, samples were inoculated with either 500 CFU/mL of either P-17 or NOX, before being incubated at three

different temperatures; 15 °C, 23 °C and 30 °C, to determine the effect of incubation temperature on the maximum cell yield. To determine the effect of inoculum density in the assay the inoculum volume was increased from 500 CFU/mL of each P-17 and NOX to 20,000 CFU/mL, whilst maintaining the incubation temperature at 15 °C. When using a natural microbial inoculum in the AOC method, the exact microbial composition of the inoculum is not known, and it is unclear if this can affect the final AOC concentration. To test the influence of different natural microbial inoculums, inoculums were collected from four different post-treatment locations at Scottish Water WTW. The four inoculums were subsequently used to calculate the AOC concentration within sodium acetate samples containing 100 µg C /L (n=3).

4.3.2 Glassware Preparation

For all AOC analysis protocols, all glassware was rendered organic-carbon free using the following series of washes and sterilisation. Wash common detergent (30 mins), rinse distilled water, soak in 0.2 M hydrochloric acid (HCl) (Fisher Scientific, UK) overnight, rinse distilled water, cap in foil and heat in a muffle furnace at 550 °C for 6 h. A Polytetrafluoroethylene (PTFE) lined silicone septa was used to cap the carbon-free 45 mL borosilicate glass vials.

4.3.3 Preparation of *Pseudomonas fluorescens* strain P-17 and *Spirillum* strain NOX Inoculum

When using the two known strains, cultures of P-17 (ATCC 49642) and NOX (ATCC 49643) were acquired from the American Type Culture Collection (ATCC). The cultures were rehydrated using Nutrient Broth (made up of 3.0 g/L beef extract (Sigma-Aldrich, UK), 5.0g peptone (Sigma-Aldrich, UK)) for P-17 (26 °C for 24 hours) and Trypticase Soy Broth (Sigma-Aldrich, UK) (30 g/L) for NOX (28 °C for 72-96 hours). The cultures were stored in cryovials using 20 % glycerol at -70 °C. Frozen cultures were thawed and streaked out on R2A agar (Sigma-Aldrich, UK) (18.1 g/L) and incubated at room temperature for 3-5 days. The

preparation of the stock cultures was performed as described in LeChevallier *et al*. (1993) and Aggarwal *et al.* (2015).

4.3.4 Preparation of Natural Microbial Inoculum

The natural microbial inoculum was prepared according to the protocol described by Hammes & Egli (2005). In short, 40 mL of water was collected from a WTW and filtered using a 0.22 µm pore filter (Millex-GP, Millipore). The filtered water sample was then inoculated with 100 µL of unfiltered water and incubated at 30 °C for 14 days. Microbial cells were harvested from the water sample by centrifugation (10 min, 3000g (relative centrifugal force)) and re-suspended in mineral buffer. Mineral buffer consisted of 7.0 mg/L K_2HP0_4 (potassium phosphate dibasic)) (Sigma-Aldrich, UK); 3.0 mg/L KH_2PO_4 (Monopotassium phosphate (monobasic potassium phosphate) (Sigma-Aldrich, UK); 0.1mg/L $MgSO^4$ $7H_2O$ (Magnesium sulphate heptahydrate) (Sigma-Aldrich, UK); 1.0 mg/L NH_4SO_4 (Ammonium Sulphate) (Sigma-Aldrich, UK); 0.1 mg/L NaCl (Sodium chloride) (VWR International, UK); 1.0 µg/L $FeSO_4$ (Iron(II) sulphate)) (Sigma-Aldrich, UK) and 1 L HPLC (high performance liquid chromatography) water. The resulting solution was incubated for an additional seven days to ensure that all residual organic carbon had been degraded.

4.3.5 Enumeration

4.3.5.1 Heterotrophic plate counts (HPC)

Water samples were inoculated with P-17 and NOX and incubated at 15°C for 7-9 days, before being enumerated using HPC, flow cytometry (Section 4.3.5.2) and ATP (Section 4.3.5.3). HPC were performed by generating a dilution series before plating on nutrient or R2A agar and incubating at 25 °C for 3 to 5 days. Samples enumerated using HPC counts were plated at 10^2, 10^3 and 10^4 dilutions in duplicate. The average net growth of the 3 days was then used to

generate a final AOC concentration in acetate-C equivalents using a pre-derived yield value of 4.1 x10^6 CFU P-17/µg acetate-C and 1.2 x10^7 CFU-NOX/µg acetate-C.

4.3.5.2 Flow Cytometry

A 500 µL volume of samples are stained with 5 µg/mL of SYBR Green (Life Sciences) and enumerated with flow cytometry (Section 4.6.1). Where necessary, samples were diluted after staining in filtered (0.22 µm) mineral water, so that counts measured were always less than 3 x 10^5 cells/mL. To convert the cell counts to AOC concentrations, a theoretical conversion value of 1x10^7 cells was used:

AOC (µg/L) = ((netgrowncells) / L)) / ((1 x 10^7 cells) / (µg/C)) (Hammes & Egli, 2005).

Equation 1

4.3.5.3 Adenosine triphosphate (ATP)

Samples were enumerated using ATP as described in LeChevallier *et al.* 1993a. Measurements were made using the BacTiter-GloTM Microbial Cell Viability Assay (Promega, UK). Total ATP was established using the BacTiter-Glo reagent (G8231; Promega Corporation) and a luminometer (Tecan). ATP analysis introduces an additional conversion factor to convert ATP to cell concentrations. Relative light units (RLU) were first converted to cell concentrations using a calibration curve (LeChevallier *et al.* (1993a) proposed values of 1.85 fg/cell (P17) and 0.213 fg/cell (NOX)). The estimated cell concentrations were further converted to AOC concentrations using the proposed conversion values of van der Kooij *et al.* (1982).

4.3.6 Controls

Controls were included for growth, yield and negative controls for carbon contamination in all cases. The blank control consisted of inoculating a carbon free mineral salts solution (inorganics) with P-17 and NOX to check for any carbon contamination from glassware. The growth control, consisting of a water sample containing diluted mineral salts (inorganics) and diluted acetate (carbon) and was used to determine if samples were limited by nutrients other

than carbon. The yield control was used to check the yield of the organisms by monitoring their growth in high-performance liquid chromatography (HPLC) water containing diluted mineral salts (inorganics) and diluted acetate (carbon).

4.3.7 Summary

The developed AOC methodology combined the known strain inoculum approach (using P-17 and NOX), with a larger inoculum volume (10,000 cells/mL) and flow cytometric enumeration.

4.4 Validation of AOC Method at Water Treatment Works (WTW)

The developed AOC method was validated via application to water samples collected from 20 drinking WTW, with water samples being taken from raw (pre-treatment) and treated (post-treatment) water (Table 4.1); between which an AOC decrease was expected. WTW were selected with contrasting source waters, treatment processes and disinfectant types to confirm the application of the method to a large array of AOC concentrations. 40 mL water samples were collected in 45 ml carbon free glass vials weekly for 2 months (n=3) and analysed for AOC in the lab within 24 hours. In addition to AOC, various other water quality parameters were also analysed to help correlate expected trends and help assess the degree of drinking water biostability.

Table 4.1: Twenty WTW selected for AOC method validation, including sampling within raw (pre-treatment) and final (post-treatment) water. The twenty WTW were selected to represent a range of water sources, treatment stages and disinfectant types.

Source Water	Treatment Type	WTW ID	Disinfectant Residual	DWDS ID	Pipe Loop ID
Reservoir	RGF	1, 2, 3, 4, 5	Cl_2	1	A
	DAF	6		-	-
	GAC	7		-	-
	Membrane	8		-	-
		9	NH_2Cl	-	-
River	Clarification	10		-	-
	RGF	11, 12, 13		2	-
	DAF	14	Cl_2	-	-
	Membrane	15		-	-
		16	NH_2Cl	3	B
Groundwater	Conditioning only	17, 18, 19	Cl_2	-	-
	Membrane	20	NH_2Cl	4	C

WTW = water treatment works; DWDS = drinking water distribution system, ID = identification number / letter. Table includes water source, treatment type (RGF: rapid gravity filter, DAF: dissolved air flotation, GAC: granular activated carbon, or membrane), choice of disinfectant (Cl_2: chlorine, NH_2Cl: monochloramine) and number of WTW with each treatment type. The final column represents the 4 DWDS selected for further AOC sampling at service reservoirs inlet and outlets. *DWDS 1-4 were selected for investigation as they contain different AOC concentrations in post-treated water.

4.5 Quantifying AOC Concentration within DWDS

4.5.1 Four DWDS: Source to Tap Details

To understand variations in AOC concentration with increasing distance into the distribution system, and compare the behaviour of pipes and SR as sources or sinks of AOC, four DWDS were selected for in-depth AOC sampling. Each supply system comprised of a WTW and three downstream SR at increasing distances into the DWDS. The supply systems were selected from the 20 WTW (as highlighted in Table 4.1), included WTW 2 (DWDS 1), WTW 12 (DWDS 2), WTW 16 (DWDS 3) and WTW 20 (DWDS 4). The supply systems were characterised by three main source water types (groundwater, surface water (river) and surface water (reservoir)), differing treatment processes (see Table 4.2) and disinfection residuals (chlorine and

chloramine), enabling comparisons of the impact of AOC across different water matrices. An outline of the treatment processes applied at each of the four WTW are found in Table 4.2.

Table 4.2: Treatment processes within the four supply systems

WTW ID	WTW 4	WTW 12	WTW 16	WTW 20
Water Source	Surface: Reservoir	Surface: River	Surface: River	Borehole
Full Treatment Process	pH Adjustment	pH Adjustment	pH Adjustment	pH Adjustment
	Coagulation	Coagulation	Coagulation	Coagulation
	Clarification (DAF)	Clarification (DAF)	Ultrafiltration	Clarification
	Gravity Filtration	Gravity Filtration	Chlorine Gas Disinfection	Hollow Fibre Membrane
		pH adjustment	pH adjustment	
Disinfectant Residual	Chlorination	Chloramination	Chloramination	Chloramination
DWDS ID	DWDS 1	DWDS 2	DWDS 3	DWDS 4
Pipe Loop	A		B	C

WTW = water treatment works; DWDS = drinking water distribution system; DAF = dissolved air flotation

The SR within the DWDS were positioned up to 53 km into the network, with both service reservoir inlets and outlets being sampled. The four DWDS were each characterised by different size of distribution zones and pipe / SR configurations. The aim of this analysis was to detect any spatial or temporal trends in AOC concentration within these DWDS by collecting samples every two weeks, over a two year period (the second year of sampling was conducted simultaneously with the 12 month pipe loop experimental programme – Section 4.6). Water samples (n=3) were collected using AOC-free glassware from raw and post-treated water at the works, and from each of the three SR inlets and outlets as indicated in Figure 4.1. All water samples were transported to the laboratory within 24 hours, and subsequently analysed for AOC. Separate water samples were also collected from raw and post-treated water at the works, and SR outlets for total (TCC) and intact cell counts (ICC), temperature, turbidity, free and total chlorine, HPC and ATP (Section 4.7). Bulk water parameters collected by Scottish Water

(including TCC, ICC, temperature, turbidity, free and total chlorine, HPC and ATP) only include one biological replicate (n=1) as part of their routine analyses. It should be noted that ATP and cell count data were unavailable for DWDS 1 as these parameters were not collected as part of routine analyses conducted by Scottish Water.

4.5.1.1 DWDS 1 (Supplied by WTW 4)

WTW 4 is supplied by a surface water reservoir. Source water quality is expected to show little variability due to the buffering effect of a large reservoir source. After abstraction, raw water is dosed with chlorine and sulphuric acid, before entering an ash mixer where it is dosed with poly aluminium chloride (PAC) and polymer. Clarification is performed using dissolved air flotation (DAF). The treated water then enters a mixer where it is treated with ozone before again being dosed with polymer. The water passes into a rapid gravity filter (RGF) before entering a chlorine contact tank. In the tank chlorine, orthophosphoric acid and lime are added, prior to distribution. The maximum hydraulic retention time (HRT) of the sampled SR within DWDS 1 is 371 hrs (SR 1.3) (Table 4.3).

4.5.1.2 DWDS 2 (Supplied by WTW 12)

WTW 12 is supplied by a river water source, which is therefore expected to show flashy changes in water quality. Raw water in WTW 12 flows into a baffled contact tank in which the water is dosed with lime, ferric sulphate (coagulation aid) and polyelectrolyte (flocculation aid) before the water travels out of the tank and into six upward flow clarifiers. The effluent then passes into four RGF before reaching the disinfection stage. Disinfection is undertaken using chlorine gas as a disinfecting agent, along with ammonium sulphate for chloramination. The water is finally dosed with lime before entering the DWDS. DWDS 2 consists is heavily SR dominated; water passes through a clear water tank (CWT) and six other SR before reaching SR 2.2.The outlet of SR 2.3 had the longest hydraulic retention time of the SR (510 hrs) (Table 4.3).

4.5.1.3 DWDS 3 (Supplied by WTW 16)

The pH of raw water is first adjusted using lime, before being dosed with poly aluminium chloride (PAC) coagulant. The treated water is pumped through ultra-filtration stacks. The water is again disinfected using a combination of chlorine gas and ammonium sulphate. Lime is does for final pH correction.

4.5.1.4 DWDS 4 (Supplied by WTW 20)

DWDS 4 is supplied by high quality post-treated water, containing a low concentration of organic nutrients. The incoming water to WTW 20 is abstracted from boreholes, before being combined in two raw water conditioning tanks in which sodium hypochlorite is injected. The water is then filtered using a number of hollow fibre membranes, before being treated with orthophosphoric acid and sodium hypochlorite. The water then passes into the chlorine tank after which it is dosed with lime (for pH adjustment) and transported to the CWT for distribution. DWDS 4 contains a small number of SR with a short HRT (to 126 hours) (Table 4.3). The SR within DWDS 4 that were selected for sampling in this study consist of SR subject to the pipe only effect, as water has not previously passed through a SR (Figure 4.3).

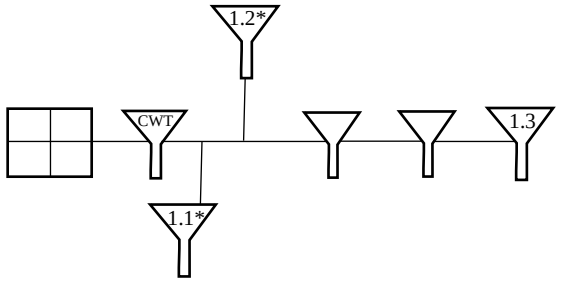

DWDS 1: reservoir; gravity filtration; chlorination

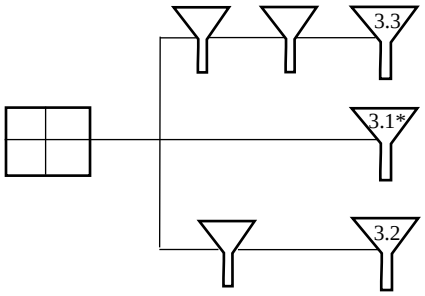

DWDS 3: river; membrane; chloramination

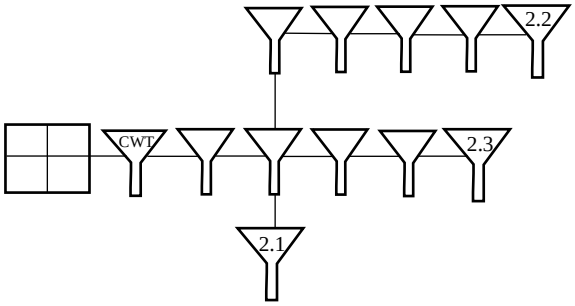

DWDS 2: river; gravity filtration; chloramination

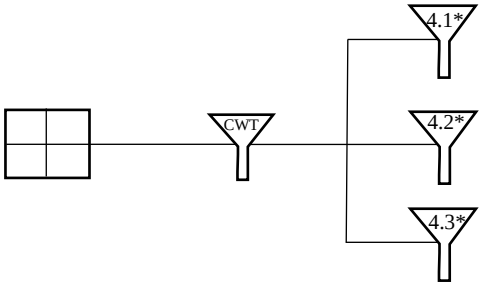

DWDS 4; groundwater; chloramination

Key:

= WTW **= SR** **= Pipeline** CWT **= Clear Water Tank**

Figure 4.3: Schematic of the arrangement of service reservoirs (SR) within the four DWDS selected for further sampling (not to scale). The SRs sampled for AOC are numbered from one to three in each distribution system, as indicated by the second number in each case, with the first number denoting the DWDS to which the SR belongs. Unlabelled SRs are not sampled as part of this study and are only drawn to show the pathway of the water. SRs labelled with a * are subject to the pipe only effect, as water has not previously passed through a SR. Samples analysed included: WTW (raw): AOC, TCC & ICC; WTW (post-treatment): AOC, TCC, ICC & total chlorine; SR inlets: AOC; SR outlets: AOC, TCC, ICC & total chlorine.

Table 4.3: Hydraulic retention time of service reservoirs within DWDS 1, DWDS 2, DWDS 3 and DWDS 4.

Site	Location	Hydraulic Retention Time (Hours)
DWDS 1 (Supplied by WTW 4)	SR 1.1 Inlet	63.77
	SR 1.1 Outlet	76.36
	SR 1.2 Inlet	212.26
	SR 1.2 Outlet	249.70
	SR 1.3 Inlet	338.39
	SR 1.3 Outlet	371.21
DWDS 2 (Supplied by WTW 6)	SR 2.1 Inlet	135.73
	SR 2.1 Outlet	138.41
	SR 2.2 Inlet	357.59
	SR 2.2 Outlet	359.65
	SR 2.3 Inlet	484.79
	SR 2.3 Outlet	510.45
DWDS 3 (Supplied by WTW 16)	SR 3.1 Inlet	22.96
	SR 3.1 Outlet	49.62
	SR 3.2 Inlet	72.52
	SR 3.2 Outlet	113.73
	SR 3.3 Inlet	193.94
	SR 3.3 Outlet	243.94
DWDS 4 (Supplied by WTW 20)	SR 4.1 Inlet	65.97
	SR 4.1 Outlet	119.54
	SR 4.2 Inlet	76.24
	SR 4.2 Outlet	121.96
	SR 4.3 Inlet	76.32
	SR 4.3 Outlet	126.32

4.6 The Impact of AOC on Biofilm Growth and Mobilisation

In order to explore the impact of AOC on biofilms as well as bulk water quality within DWDS, whilst maintaining full-scale hydraulic conditions, biofilm investigations were undertaken within three test pipe loop facilities at fully operational WTW. Specifically, this research was conducted to determine the relationship between AOC concentration and biofilm volume, community composition and stability within a DWDS, and to characterise the effect of elevated

shear stress (flushing) upon the biofilms that remain attached, and to quantify the material mobilised into the bulk water.

The pipe loop test facility locations were selected to cover a broad range of AOC concentrations, to help determine the effect of AOC concentration on biofilm accumulation and potentially mobilisation. The pipe loop test facilities (A, B & C) were installed at the outlet of WTW 2 (surface, reservoir water, chlorinated) (start of DWDS 1) (PL A), WTW 16 (surface, river water, chloraminated) (start of DWDS 3) (PL B) and WTW 20 (ground water, chloraminated) (start of DWDS 4) (PL C) (PL = pipe loop) and supplied with post-treated drinking water. These three WTW sites were selected to enable comparisons between sites with post-treated water containing different AOC concentrations (high, medium and low), to enable comparison between sites supplied by ground-water, surface water (reservoir) and surface water (river) sites and also sites with different disinfectant (1 site was chlorinated, 2 sites were chloraminated). WTW 12 (supplying DWDS 2) was not selected for pipe loop installation due to space restrictions at the site.

Post-treated water supplying PL A generally contained the highest concentration of AOC (~300 µg C/L), PL B had a medium range AOC concentration and finally PL C contained a generally low concentration of AOC (<100 µg C/L). The bulk water quality within the pipe loop was compared to that of post-treated water to check if any changes in water quality occurred in the pipe loop. The design of the pipe loop is such that it is able to accurately represent biofilm accumulations in the networks during the study 'growth phase', but also biofilm mobilisation during the 'flushing / mobilisation phase'.

4.6.1 DWDS Pipe Loop Test Facilities

This section will give an overview of the pipe loop test facility; including the pipe loop test facility and coupon design, running schedule and sampling procedures. The DWDS test loops installed at each of the three sites met the same exact design specifications. Each pipe loop

consisted of a 10 m long length of high-density polyethylene (HDPE) PE100 pipe with a 79.3 mm internal diameter. HDPE was selected as it is frequently used in modern DWDS (Husband *et al*. 2008) and is a high grade plastic with a smooth surface that is stated to have a low biofilm forming potential (BFP). Each pipe loop was fed with post-treated water supplied directly from the WTW (see Table 4.1 for details of selected field sites).

Drinking water was re-circulated around the system from an enclosed, 30 L (0.03 m^3) tank, via a variable speed pump. A system residence time of 24 hours was set using a trickle-feed and drain to provide representative water quality of each DWDS, and preserve a baseline nutrient supply and disinfection residual, among other water quality parameters. Pipe loop retention time was a function of the chosen flow regime. During growth phase, the pipe loop was run at conditioning flow rate of 0.4 l/s (shear stress 0.03 Nm^{-2}). This flow rate was selected as this was the average flow rate in 75-100 mm diameter pipes within UK DWDS, as stated by Husband *et al*. (2008). This flow rate has also been used in previous studies (Fish *et al.* 2013) and so using the same flow rate will allow comparisons with data from previous research.

The flow rate was monitored using a Siemens Sitrans F M Mag 6000 flow meter. Shear stress was calculated theoretically using Equation 2 (Section 4.6.4.1). A Darcy–Weisbach roughness (k_s) value of 0.075 mm was used, which is representative of the roughness of HDPE pipe (Husband *et al*. 2008) (Appendix 5 for full details). Flow was controlled by adjusting the controlled valves at the end of each loop and/or the pump speed. The straight section (~1m long) (four in each loop) contained 12 apertures (positioned 75 mm apart) into which removable coupons were inserted (Figure 4.4 & Figure 4.5). The coupons were positioned at least 10x internal diameter away from a pipe bend to minimise any effect of turbulence generated by the pipe bends. A 1 m section of clear polyvinyl chloride (PVC) pipe was also included in each loop to enable a visual, qualitative comparison of biofilm development within the pipe loops. The water was trickle fed into the tank with a system retention time of 24 hours,

preserving a baseline nutrient supply and disinfection residual, among other water quality parameters.

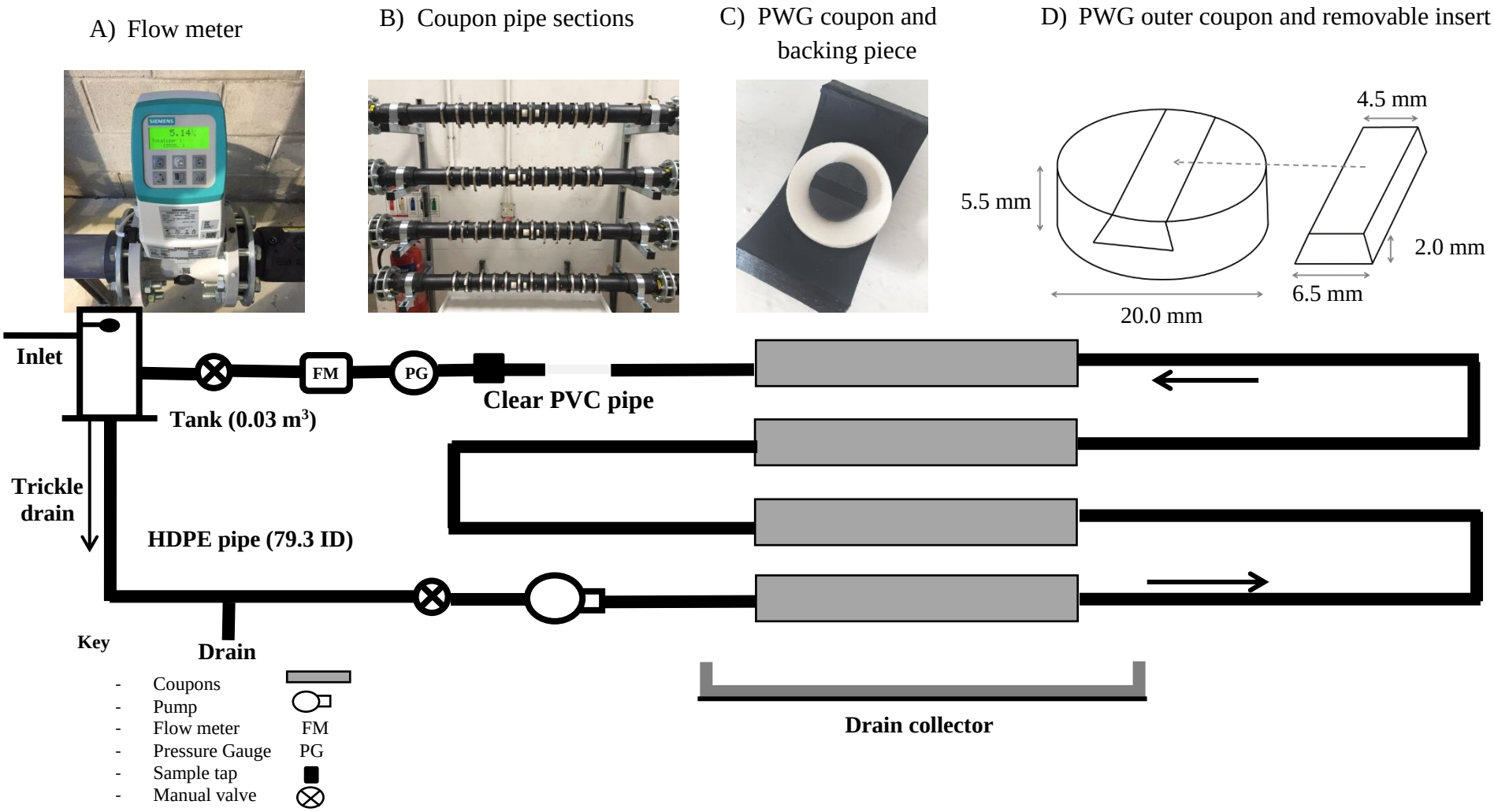

Figure 4.4: Schematic diagram of DWDS pipe loop facilities including dimensions. The pipe loop contained 4 horizontal coupons sections, with each section containing 12 HDPE PWG coupons (48 in total). Online turbidity meters were connected to the sample tap during the mobilisation 'flushing' phase. A) Siemens FM Mag 6000 flow meter was used to control the hydraulics of the system throughout the growth and mobilisation phases; B) Coupons inserted into the pipe were secured with brackets; C) HDPE PWG coupon, rubber seal and HDPE backing piece; D) Coupon schematic consisting of a curved outer coupon section and flat insert piece. A tipping bucket mechanism was installed on the trickle drain to monitor flow and system residence time.

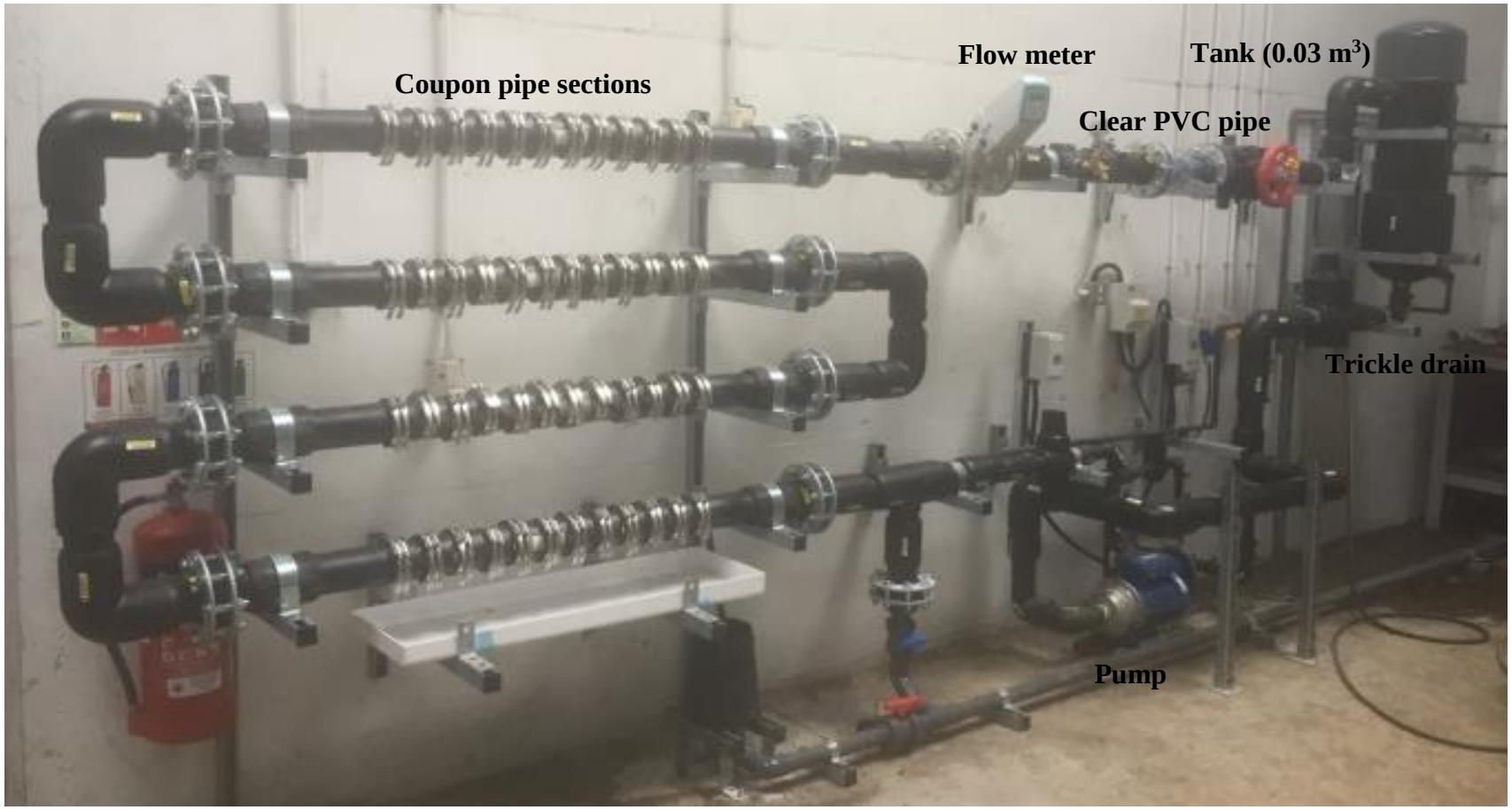

Figure 4.5: DWDS pipe loop facility (see Figure 4.3 for schematic). The pipe loops consist 4 horizontal coupons sections, with each section containing 12 HDPE PWG coupons (48 in total). Coupons inserted into the pipe were secured with jubilee clips.

To monitor flow remotely when not on site, three Wi-Fi enabled micro-controllers were designed at the University of Sheffield and installed at each of the three pipe loop sites (Figure 4.6). As the three sites locations were considerable distances from each other, with a wide spread across Scotland, flow was used as the main indicator to check if the systems were running optimally during the 12 month experiment. The Wi-Fi enabled micro-controller could log to Google drive every 10 seconds. The Wi-Fi enabled micro-controller either used existing site Wi-Fi, or in cases where Wi-Fi was absent a portable Wi-Fi hotspot was installed.

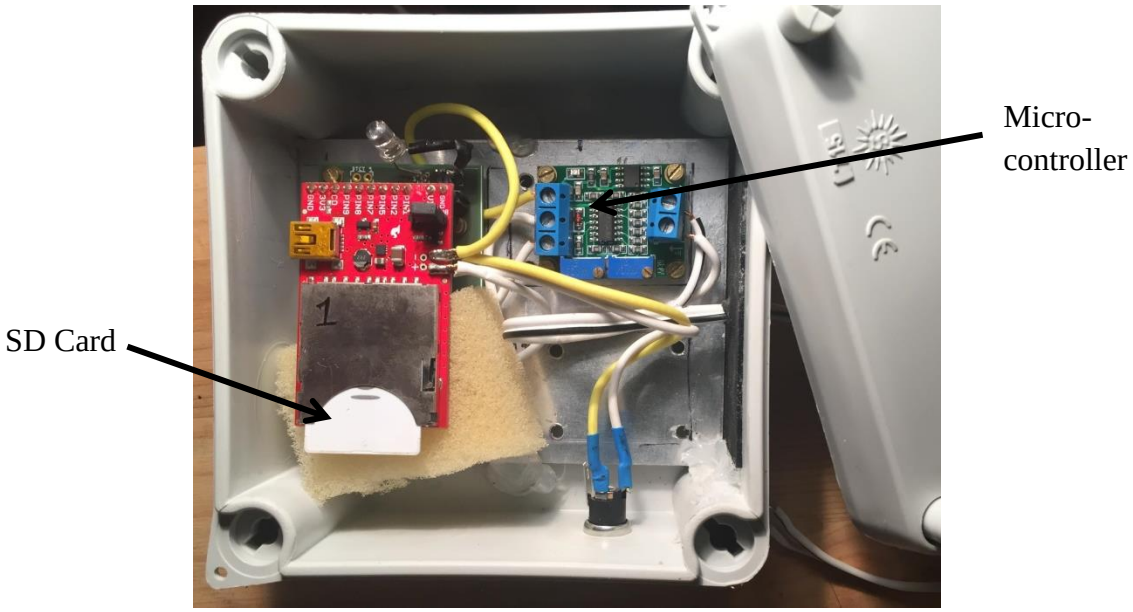

Figure 4.6: Wi-Fi enabled micro-controller designed by the University of Sheffield. The micro-controller was connected to the Siemens Sitars FM mag 6000 flow meter. The flow meter had a 4-20mA analogue signal.

4.6.2 Coupon Design

Pennine Water Group (PWG) coupons (Deines *et al.* 2010) were installed in each DWDS test loop to provide a removable surface for biofilm sampling. The PWG coupon consists of an outer curved coupon and a removable flat 'insert', which enables dual analysis of the same sample (Figure 4.4 (D)). The PWG coupon has a curved structure that is designed to mimic the pipe curvature,

therefore reducing boundary layer flow distortion. Although the PWG has been used within an DWDS experimental facility (Sheffield University) (Fish *et al.* 2013; Douterelo *et al.* 2013) and within operational DWDS (Douterelo *et al*. 2017), this presents the first use within field-based pipe loop test facilities at the outlet of WTW.

The insert piece had a maximum width of 6.5 mm, minimal width of 4.5 mm and flat surface designed for microscopy analyses (Deines *et al.* 2010). The insert was specially manufactured using a dovetail cutter so that the surface finish closely matched that of the main pipeline and the outer coupon (Sharpe, 2012). Each coupon was secured to a backing piece with a circular rubber gasket in between to ensure a watertight fit. The majority of coupons were side-positioned to enable efficient coupon sampling. Coupons were positioned along either side of the pipe length (described as left' and 'right' in Table 4.4), with the exception of nine top or bottom positioned coupons. Three top and three bottom positioned coupons were used to assess any difference in biofilm accumulated at either position, following on from 12 months growth (Section 2.3.5.2). A further three bottom coupons were installed to enable a comparison between biofilm accumulated after 12 months on bottom coupons and biofilm remaining on bottom coupons following the mobilisation phase (post-flush).

Table 4.4: Coupon layout in each pipe loop. Each pipe loop contains 48 removable coupons (numbered 1-48), with 12 coupons in each row (1-4). Coupons are positioned on the left or right side of the pipe, with the exception of the top and bottom coupons. R = row; Tp = top; Btm = bottom; yellow = coupon present.

R1	1	2	3	4	5	6	7	8	9	10	11	12
											Btm	Btm
R2	13	14	15	16	17	18	19	20	21	22	23	24
											Tp	Btm
R3	25	26	27	28	29	30	31	32	33	34	35	36
											Btm	Tp
R4	37	38	39	40	41	42	43	44	45	46	47	48
										Btm	Tp	Btm

4.6.3 Growth Phase & Sampling

4.6.3.1 Growth Conditions

At the start of each experiment, each pipe loop was disinfected for 24 hours with a 20 mgl-1 concentration of a sodium hypochlorite solution (VWR International Ltd, UK) (11-14 % free chlorine), which was re-circulated within the system at a maximum flow rate of 5.0 l/s. After 24 hours, each pipe loop was flushed repeatedly at the maximum flow rate with post-treated water from each WTW. This was continued until chlorine levels decreased to those of the inlet water. Before use, the PWG coupons were sterilised via sonication with a 2% (w/v) sodium dodecyl sulfate (SDS) solution for 45 minutes, then sonicated in distilled deionised water for a further 15 minutes before being autoclaved (Appendix A2.1) (Fish *et al.* 2013).

At the beginning of the 12 month growth phase, each of the three pipe loops (A, B & C) had a staggered start time so that all three experiments had the same number of days. Each loop start time was staggered by two days, which was deemed to be insignificant as the total length of the experiment was 12 months. It was not possible to sample all 3 sites on the same due to the distances between site locations. Although all three pipe loops were operated indoors, room temperature was subject to seasonal variation.

4.6.3.2 Sampling

Biofilm samples were collected in triplicate at Day 0 (n=3), 3 month (n=3), 6 month (n=3), 9 month (n=3) and 12 month (n=3) time periods. Each triplicate consisted of at least one 'right' and one 'left' positioned coupon (Table 4.4). Day 0 samples were defined as coupons which were in the pipe loop for ≤ 90 minutes (Fish *et al*. 2015). The outer coupons were used to establish any variations in community composition by using Ilumina sequencing (Section 4.7.3), and to determine the number of intact and damaged cells within the biofilm using flow cytometry (Section 4.7.4). The coupon insert pieces were used to assess biofilm volume using scanning electron microscopy (SEM) (4.6.5). During biofilm sampling the pump was stopped and the relevant manual valves closed (Figure 4.4). The system was not drained during this time, so that the biofilms were not allowed to dry out in the loop. The coupons collected were immediately replaced with sterile coupon, the location of which was recorded so that no further samples were taken from that location.

In order to compare the planktonic and biofilm communities, bulk water samples were also collected from each pipe loop (Table 4.5). Three replicates of bulk water were taken directly from the sample tap of each loop at Day 0, 6 Months and 12 Months. A total of 27 bulk water samples were collected from the three loops (9 samples from each loop) and filtered through 0.22 μm pore

nitrocellulose filter (Millipore, MA, USA) using a Microstat membrane filtration unit (Sartorius, UK). Filters were then stored in sterile bags at -80 °C ready for DNA extraction.

Throughout the 12 month growth phase, bulk water quality (including AOC (n=3), TOC (n=3), total chlorine (n=3), turbidity (n=3), iron (n=3) manganese (n=3), temperature (n=3) and pH (n=3)) was measured every two weeks from the tapping point in the pipe loop (Figure 4.4), to assess any changes throughout the period (Section 4.6.1). Online flow was logged every 10 seconds throughout the growth and mobilisation phases via the online instrumentation (Figure 4.6).

Table 4.5: Dates of coupon sampling in each of the three pipe loops. Bulk water quality samples were also collected on a fortnightly basis during the 'growth' phase, and during every flushing step during the 'flushing' phase. PF = Post-flush.

	Biofilm Samples Collected	Bulk water Samples Collected	Months
Growth Phase	Day 0	↓	May
	3 month		August
	6 month		November
	9 month		February
	12 month		May
Flushing 'mobilisation' Phase	12 month PF		May

4.6.4 Mobilisation 'Flushing' Phase & Sampling

4.6.4.1 Mobilisation Conditions

Following on from the 12 month period, the pipe loops were 'flushed' and the amount of material mobilised recorded. The aim of the mobilisation phase was primarily to assess if the biofilm strength differs between the three sites (due to differences in AOC concentration), and if the biofilm strength was linear or non-linear. A flushing sequence was performed wherein the flow rate, and subsequently the shear stress was incrementally increased to the rates described in Table 4.6.

Table 4.6: Details of five flushing steps including flow, velocity, shear stress and turnover time.

Flushing Step	Flow Rate (l/s)	Velocity (m/s)	Hydraulic Gradient	Shear Stress (N/m^2)	Time 5 Turnovers (Mins)
Mixing	0.4	0.08	0.00016	0.03	10.16
1	1.5	0.30	0.00170	0.33	2.44
2	2.5	0.51	0.00429	0.83	1.39
3	3.5	0.71	0.00799	1.55	1.10
4	5	1.01	0.01553	3.02	0.49

The shear stress for each flushing step was calculated using:

$$\tau = \rho g R S \quad \text{(see table 4.7 for definitions and units)} \qquad \textbf{Equation 2}$$

Table 4.7: Shear stress calculations.

Component	Equation	Symbol	Units	Value
Diameter	-	Ø	mm	792
Hydraulic radius	D/4	R	mm	19.8
Length	-	L	m	10
Acceleration due to gravity	-	g	m/s^2	9.81
Density	ρ=m/V	ρ	g/cm^3	1

The hydraulic gradient (S) was calculated using the Colebrook-White and Darcy-Weisbach equations.

$$\text{Colebrook-White } \lambda = \left[-1.52 log_{10}\left(\left(\frac{k_s}{7.21 D_i}\right)^{1.042} + \left(\frac{2.731}{Re}\right)^{0.9152}\right)\right]^{-2.169} \qquad \textbf{Equation 3}$$

In which, λ = lamda, k_s = roughness height (mm) , Di = pipe diameter (mm) , Re = Reynolds number.

Darcy-Weisbach: Hydraulic gradient: $\frac{h_f}{L} = \frac{\lambda}{D}\frac{v^2}{2g}$ **Equation 4**

In which, h_f = frictional head loss (m), L = length (m), λ = lamda, D = pipe diameter (m), V = velocity (m/s) and g = gravity (m/s^2). See section 7.3.4.1 for details regarding how head loss within the pipe loop was empirically generated.

At the start of the mobilisation phase, the pipe loops were isolated by the closing the entry valve into the tank and the exit valve on the trickle drain. The two valves remained shut so that that the same volume of water was maintained throughout the mobilisation phase, ensuring that any water quality changes were due to the mobilisation of material from the pipe wall and not incoming water.

When elevating the shear stress, care was taken to slowly open the valve so as to not create any transients within the systems, which could influence the rate of removal of the attached material and therefore the discolouration response. Water was then circulated around the pipe loops at each of the flow rates shown in Table 4.6, for five turnovers. As the time needed to complete one turnover was relatively short, five turnovers were conducted to enable time for the bulk water to be thoroughly mixed and for the turbidity to stabilise before the next step up in flow. Furthermore, five turnovers were selected to allow enough time for sample collection. Following an increase in the flow rate, the peak increase in turbidity would be expected after one turnover, following the patterns as described by PODDS (Boxall *et al.* 2001).

The flushing sequence and time of biofilm and bulk water sampling are shown in Figure 4.7.

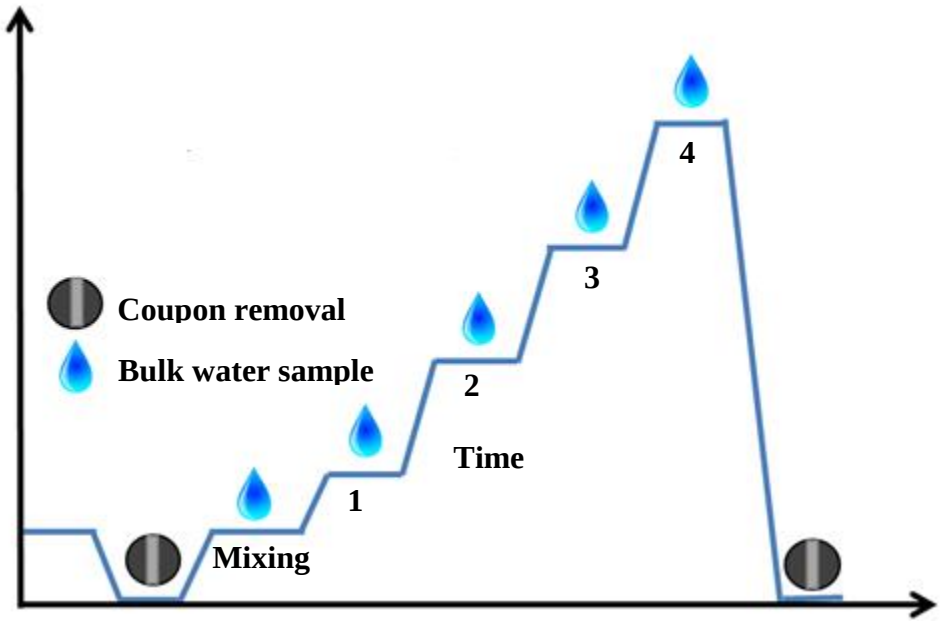

Figure 4.7: Flushing sequence during the flushing phase. The number indicates the flushing step (see Table 4.6 for flow rate and shear stress). Coupon removal and bulk water sample collection points are illustrated.

4.6.4.2 Sampling

During the mobilisation phase, bulk water quality parameters including AOC (n=3), TOC (n=3), total chlorine (n=3), turbidity (n=3), iron (n=3) manganese (n=3), temperature (n=3), pH (n=3) were measured after five turnovers (Table 4.6) from the tapping point in the pipe loop (Figure 4.4), to assess initial mobilisation of material into the water column before dilution. Turbidity was also measured continuously throughout the entire mobilisation phase. Biofilm samples (coupons) were taken post-flush (after the final flushing step) (Figure 4.7). This process was then repeated for the other two pipe loops.

4.7 Sample Analysis

4.7.1 Water Quality Analysis

A summary of the instruments and methods used for measuring discrete bulk water parameters during both the growth and the mobilisation experimental phases is provided in Table 4.8. AOC measurements were conducted using the AOC method developed in Chapter 5**.** In summary, dechlorinated water samples were collected and pasteurised by heating in a water bath at 70°C for 30 minutes. Water samples are then inoculated with 10^4 cells / mL of each bacterial strain (P-17 and NOX) into separate vials. Samples are then incubated at 15°C for 6 days before being enumeration using flow cytometry.

Planktonic TCC and ICC (cells/mL) were measured using the flow cytometry method detailed in Gillespie *et al.* (2014). In summary, 500 µl dechlorinated water samples were stained with 5 µl SYBR Green (Life Sciences, California, USA) for TCC. 500 µl dechlorinated water samples were stained with 6 µl SYBR Green/ Propidium Iodine mixture (Life Sciences, California, USA) (with a final concentration of 1x SYBR Green and 3µM PI) for ICC. Samples were analysed using BD Accuri C6 Flow Cytometer with autosampler (BD Accuri, UK). The proportion of intact cell counts (%) is defined as intact cell count / total cell count * 100. HPC were performed by combining a 1 mL water sample mixed with 18 mL molten YEA (Yeast Extract Agar, cat. No. CM0019B, Oxoid Ltd., ThermoFisher Scientific, Loughborough, U.K.). Plates were incubated at 37 °C for 48 h or at 22 °C for 72 h, then counted. ATP Measurements were made using the BacTiter-GloTM Microbial Cell Viability Assay (Promega, UK). Total ATP was established using the BacTiter-Glo reagent (G8231; Promega Corporation) and a luminometer (Tecan).

Table 4.8: Discrete bulk water parameters (n=3) and online turbidity collected during the growth and flushing phases.

Water Quality Parameter	Instrument / Analysis Method	Range	Resolution	Accuracy
AOC	C6 Flow Cytometer with autosampler (BD Accuri, UK).	The EawagA method works well for bacterial concentrations ranging from about 102–107 cells/mL.	10,000 events / second and a sample concentration over 5 x 106cells / mL	-
TCC & ICC	C6 Flow Cytometer with autosampler (BD Accuri, UK).	The Eawag[A] method works well for bacterial concentrations ranging from about 10^2–10^7 cells/mL.	10,000 events / second and a sample concentration over 5 x 10^6cells / mL	-
TOC[B]	Formacs high temperature catalytic combustion system (Skalar Analytical B.V., Breda, Netherlands).	100 ppb[C] -5000 ppm[D] carbon	-	-
Total and Free Chlorine	Pocket colorimeter (Hach-Lange, Salford, U.K.)	0.00 to 5.00 mg/L	0.01 mg/L	± 0.02 mg/L
Turbidity	Hach handheld 2100Q formazine calibrated turbidity meter	0–1000 NTU	±1% of reading or 0.01 NTU	±2%
Online Turbidity	ATI A15/76 (Analytical Technology Inc, UK)	0.001 NTU - 4000 NTU	0.001 NTU	± 5% of reading or ± 0.02 NTU
Iron, Manganese	PerkinElmer Nexion 300X ICPMS Spectrometer	-	-	-
Temperature	Sealey THC100 Thermometer	-50°C to +70°C	-	±1°C
pH	ROSS Ultra pH electrode (Thermo Fisher Scientific Ltd., Loughborough, U.K.)	0-14	-	± 0.01
Flow	Siemens Sitrans fm mag 6000 flow meter	-	-	± 0.2% of the flow rate

[A] The Swiss Federal Institute of Aquatic Science and Technology; [BTOC] = total organic carbon; [C]ppb – parts per billion; [D]ppm – parts per million

4.7.1.1 Data Analysis of Discrete Water Quality Samples

The mean, median, range and standard deviation were calculated for each of the parameters listed in Table 4.8 during the growth phase. The normality of the data was analysed using the Shapiro-Wilks test and parametric (ANOVA and Tukey) or non-parametric tests (Kruskal Wallis and two-sample Wilcoxon), as appropriate, to identify any differences in water quality parameters between experiments. Data collected during the mobilisation phase was plotted against shear stress and a linear model and regression analysis was performed to identify relative changes (each loop was analysed separately). The R_2 and p values were used to assess the fit of the linear model to the data and the significance of the gradient, so as to determine which parameters responded significantly to the elevation in shear stress. All statistical analysis and graphical plots were generated in R v3.5.2 (R Foundation for Statistical Computing Platform, 2018) with a significance level of <0.05. A self-organsising map (SOM) analysis was run in MATLAB and used to analyse water quality data in Chapter 6. SOM analysis allows data to be arranged so that similar data points are clustered together, enabling non-linear relationships to be visualised. The cell shading denotes the numerical value of the vectors and the colour bar shows the mapping between shading and numerical value.

4.7.2 Biofilm Analysis

This study set out to investigate the biofilm volume (cells, EPS and organic / inorganic particles), cell number and community (bacterial and fungal) composition of the developed biofilms (during the growth phase) and those that remained attached (following on from the mobilisation phase). The outer coupons were used to establish any variations in community composition and determine

the number of intact and damaged cells within the biofilm. The inserts were also used to quantify the biofilm volume.

4.7.2.1 Biofilm Preparation

During biofilm sampling, coupons were carefully removed from each pipe rig and the outer coupon and insert separated using sterilised forceps. The outer coupons to be used for analysis of the microbial community composition were processed as described in Section 4.7.3 and the outer coupons to be used for TCC and ICC analysis were processed as described in Section 4.7.4. The inserts, to be used for biofilm volume quantification, were fixed in 5% formaldehyde solution (Fisher Scientific, UK) (Fish *et al.* 2013).

4.7.2.2 Biofilm Suspension Preparation

Outer coupon samples were collected on Day 0, Month 3, Month 6, Month 9, Month 12 and Post-flush (for each n=3), therefore 18 samples were collected per loop, 54 in total. The biofilm was first removed from the coupon by placing the coupon in a petri dish with 30 ml of sterile phosphate buffer (Appendix A3.1) (as described by Fish, 2013) and repeatedly brushed using a sterile toothbrush (Appendix A2.2). All tooth brushes were sterilised using the same protocol as for the coupons (sonication with 2% SDS and distilled deionised water and autoclaving) (see Appendix A2.1). The same number of strokes and motion were used per coupon (30 horizontal and 30 vertical, rinsing the tooth brush in the solution after every 10 strokes). This 30 ml volume of biofilm suspension was transferred to a sterile falcon tube and stored at 4 °C for ≤ 30 minutes before filtering through a 47 mm diameter, 0.22 μm pore nitrocellulose filter (Millipore, MA, USA) using a Microstat membrane filtration unit (Sartorius, UK). Filters were then stored in sterile bags at -80 °C ready for DNA extraction. Negative controls were carried out in triplicate during

each sample collection, at each site. The process as above was performed for negative controls, but sterile coupons were used.

4.7.3 16s rRNA Sequencing

Biofilm samples were sent to MR DNA (Molecular Research LP), Texas, USA for DNA extraction and sequencing using Illumina MiSeq technology.

4.7.3.1 DNA Extractions

DNA was extracted from the nitrocellulose filters using the CTAB (hexadecyltmethyl ammonium bromide) and Proteinase K chemical lysis method (Zhou et al., 1996). Each filter was transferred into a sterile 15 ml tube to which 720 µl of SET buffer (see Appendix A3.2) and 90 µl of lysozyme 10 mgml-1 (Sigma Aldrich Co.,UK) were added. Samples were incubated at 37 °C for 30 minutes with rotation in a hybridization oven (Thermoscientific, UK). A 90 µl volume of 10% SDS (w/v) and 25 µl volume of Proteinase K (Applied Biosystems, Life Technologies Ltd., UK) were then added and the samples incubated for a further 2 hours (with rotation) at 55 °C. The lysate was transferred to a sterile tube to which 137 µl of 5 M NaCl and 115 µl of CTAB solution (Appendix A3) were added before incubation at 65 °C for 30 minutes (with rotation). Subsequently the top aqueous layer of the sample was removed and the supernatant extracted with an equal volume of chloroform, centrifuged at 13,000 RPM for 5 minutes. DNA was precipitated at -20 °C, over a 12-14 hour period with 815 µl of 100% isopropanol before centrifugation at 13,000 RPM for 30 minutes. The supernatant was discarded and the DNA pellet washed twice in 1 ml of 70% ethanol (centrifuge at 13,000 RPM for 10 minutes), dried and then eluted in 30 µl of sterile nuclease free water (Ambion, Warrington, UK). DNA was visualised via gel electrophoresis and the quantity and quality of DNA was assessed with a Nanodrop ND-1000 spectrophotometer (Nanodrop, Wilminton, USA). In addition to the samples, "biofilm control" filters were also exposed to the

DNA extraction process and "DNA controls" were run: empty sterile tubes to which all the solutions were added and all the processes applied. Aliquots of the application ready stock DNA solution were made to limit the effects of freeze-thawing on DNA quality and were stored at -20 °C.4.7.3.2 Polymerase chain reaction (PCR) amplification and purification

PCR amplifications were carried out, using the DNA extract, to amplify specific genes from bacteria and fungi. For each gene, a standard was generated by running PCRs using the primers in Table 4.9 then purifying via gel-purification (Qiagen Gel-Extraction Kit) and combining the purified amplicons into one "DWDS biofilm" standard per gene.

Table 4.9: Primer pairs used for PCR amplifications.

Gene Target (organisms)	Primer Pair	Primer Sequences (5'-3')	Primer References
16S rRNA (bacteria)	Eub338	ACTCCTACGGGAGGCAGCAG.	Lane, 1991
	Eub518	ATTACCGCGGCTGCTGG	Muyzer et al., 1993
ITS (fungi)	ITS1F	TCCGTAGGTGAACCTGCGG	Gardes and Bruns, 1993
	5.8S	CGCTGCGTTCTTCATCG	Vilgalys and Hester 1990

A 28 cycle PCR was performed using the HotStarTaq Plus Master Mix Kit (Qiagen, USA). The following conditions were used: 94°C for 3 minutes, followed by 28 cycles of 94°C for 30 seconds, 53°C for 40 seconds and 72°C for 1 minute, after which a final elongation step at 72°C for 5 minutes was performed. After amplification, PCR products are checked in 2% agarose gel to determine the success of amplification and the relative intensity of bands. Multiple samples are pooled together (e.g., 100 samples) in equal proportions based on their molecular weight and DNA concentrations. Pooled samples are purified using calibrated Ampure XP beads.

4.7.3.3 Illumina sequencing

Sequencing was performed by Illumina MiSeq technology with the paired-end protocol by Mr DNA Laboratory (TX, USA). The bacterial 16s region was amplified using primers 28F (GAGTTTGATCNTGGCTCAG) and 519 (RGTNTTACNGCGGCKGCTG), and the fungal 18S rRNA gene was amplified using SSUfungiF (TGGAGGGCAAGTCTGGTG)/SSUFungiR (TCGGCATAGTTTATGGTTAAG) (Hume *et al.* 2012). Firstly, paired-end reads were merged and de-noised to remove short sequences, singletons, and noisy reads, before chimeras were detected using UCHIME and subsequently removed. Sequences were then clustered in operational taxonomic units (OTUs) and selected using UPARSE (Edgar, 2013). Taxonomic assignments were made with USEARCH global alignment program (Edgar, 2013). Biofilm samples for taxonomic analysis are labelled in which the first letter / number indicates time point, the second letter indicates the pipe loop, and the third number indicates the triplicate number.

4.7.3.4 Microbial Community Analysis: Data Analysis

Bacteria and Fungi presence / absence and relative abundance data were analysed using PRIMER-6 (v6.1.13, PRIMER-E Ltd, UK). Data was first normalised using a square root transformation before a Bray Curtis analysis was performed to generate similarity matrices. The similarity of datasets was assessed first using an analysis of similarities (ANOSIM), before non-metric multi-dimensional scaling (nMDS) plots were generated. All nMDS plots were generated using 400 iterations of the data and the stress values for 2D plots noted (stress <0.05 = excellent representation of data, <0.1 = good representation, > 0.3 = weak representation). Cluster analysis was run for 20,000 permutations and a dendrogram plotted.

ANOSIM analyses (one-way and two-way both run with a maximum of 400,000 permutations) detected the similarity between samples, providing a global R value: 0 = same, 1 =

completely different; and the significance level (P value) (<0.05 significant; >0.05 weak evidence). The p-value percentage produced in the ANOSIM analysis will be expressed as a decimal in this thesis. The global-R statistic values represent the strength of the impact that the factors analysed had on the samples, in this case it was the impact due to AOC concentration. The 2D stress value of each NMDS plot was noted (stress < 0.05 = excellent representation of data, < 0.1 = good ordination, < 0.2 = potentially useful but check with cluster analysis, > 0.3 = weak representation, misleading, discard plot) (Fish, 2013). Similarity percentage analysis (SIMPER) was used to evaluate the similarity and dissimilarity between sample groups (expressed as %).

4.7.3.5 Ecological indices

Ecological indices were used to assess the relative richness , the relative diversity (determined using the Shannon index as calculated using Equation 5), and relative evenness (generated using the Pielou index as calculated using Equation 6). The relative diversity indices were exported from PRIMER 6 and analysed using R v3.5.2 (R Foundation for Statistical Computing Platform, 2018) to determine similarities/differences (via T-tests or analysis of variance (ANOVA)).

$$H' = -\sum_{I=1}^{S} \rho_i ln_{\rho i} \qquad \textbf{Equation 5}$$

Where H' is the Shannon diversity index value, s is the total number of T-RFs/fragments and is the relative abundance of each T-RF (i).

$$J' = \frac{H'}{ln_s} \qquad \textbf{Equation 6}$$

Where J' is Pielou's evenness index value; H' is diversity according to the Shannon index and s is the total number of T-RFs/fragments.

4.7.4 Flow Cytometry

Biofilm samples were collected on Day 0, Month 3, Month 6, Month 9, Month 12 and Post-Flush (for each n=3 (triplicate samples) (18 samples per loop, 54 in total). Biofilm suspensions were prepared using the same method as described in Section 4.6.2.2 and Appendix A2.2. 0.5 ml of the biofilm suspension was stained and analysed in accordance with the flow cytometry protocol (Section 4.6.1). To convert the cell counts into cell concentrations (ICC / mm^2 or TCC / mm^2), Equation 7 was used:

$$ICC\ or\ TCC = \frac{\left(\frac{Count}{Volume\ analysed}\ x\ Total\ volume\ of\ sample\right)}{SA} \qquad \textbf{Equation 7}$$

Where the count is the total or intact cell count, volume analysed is the volume of sample that was processed in the flow cytometer (50 µl), the total volume of samples in this case was 30 ml (30,000 µl) and SA is the surface area from which the biofilm was removed. All the raw biofilm data were converted into ICC mm^2 or TCC mm^2. Both the planktonic (ICC / mL) and biofilm ICC (TCC mm^2) were also expressed as a percentage of the TCC (i.e. as an ICC proportionally relative to the TCC). Preliminary tests of technical replication showed no difference so only biological reps were undertaken (n=3).

4.7.5 Microscope Methods

To determine the total volume of biofilm (including cells, EPS and (in)organics) accumulated on each of the coupons, a number of potentially suitable methods were explored including; optical coherence tomography (OCT), reflective light microscopy and confocal microscopy (without the use of stains). Both reflective light microscopy (100x magnitude) and confocal microscopy were found to be unsuitable as the biofilm was not visible.

4.7.5.1 Optical Coherence Tomography

OCT was used to image biofilms on three 12 month HDPE insert samples taken from PWG coupons installed within the three pipe loops (PL A, PLA B and PLC), and one negative control blank sample. The Magnetomotive (MM) OCT was made in-house at The University of Sheffield and uses light of wavelength 890nm. The samples were tilted to reduce reflections at the surface of the insert, which would interfere with viewing the biofilm. To quantitatively analyse these structural images, the software ImageJ was used to obtain the reflectivity profile of each image. For each image, the surface of the plastic insert was first straightened. The average intensity of the pixels in the horizontal direction was then calculated.

4.7.5.2 Biofilm Visualisation

Scanning Electron Microscopy (SEM) is able to provide a qualitative assessment of biofilm accumulation, giving an indication surface coverage and the physical structure. In this study SEM was used to assess biofilm accumulation between different time points at the same site and compare biofilm accumulation between the three sites.

4.7.5.3 Biofilm Samples Used for SEM

The samples analysed using SEM included six HDPE insert samples, taken from PWG coupons installed within the three pipe loops (PL), named PL A, PL B and PL C. One 6 month and one 12 month sample were analysed from each loop. Each biofilm sample was imaged at 500x, 1000x and 5000x magnification, with a total of 50 images being taken per sample.

4.7.5.4 SEM Protocol

All SEM sample preparation and imaging was undertaken at the Biomedical Science Electron Microscopy Unit, The University of Sheffield. Biofilm samples were first fixed with 5% (volume

/ volume (v/v)) formaldehyde, before being washed 0.1M phosphate buffer, twice with 10min intervals at 4°C. Biofilm samples then underwent a secondary fixation step in 1% aqueous osmium tetroxide for 1 hour at room temperature, before being washed again using 0.1m phosphate buffer, twice with 10min intervals at 4°C. Samples were then dehydrated using the following ethanol series: 75% ethanol (15 mins); 95% ethanol (15 mins); 100% ethanol (15 mins); 100% ethanol (15 mins); 100% ethanol dried over anhydrous copper sulphate (15 mins). All of the above steps were carried out at room temperature. Samples were placed in 50/50 mixture of 100% ethanol/100% Hexamethyldisilazane for 30 mins followed by 30 mins in 100% Hexamethyldisilazane. Biofilm samples were air-dried overnight. When dry, HDPE inserts were mounted on aluminium stubs, attached with carbon sticky adhesive tape, and coated with approximately 25nm of gold in an Edwards S150B sputter coater. Biofilm samples were examined in a TESCAN Vega 3 LMU scanning electron microscope at an accelerating voltage of 15Kv.

4.8 Summary Table of Samples

This section presents a summary of all samples collected during the AOC validation trials (Table 4.0), AOC and biological stability DWDS sampling (Table 4.11 and Table 4.12) and samples obtained from the pipe loop test facility (Table 4.13). Both the biofilm samples obtained from coupons, and bulk water quality data from the pipe loop test facility, are presented in Table 4.12. The replication undertaken at each sample point is indicated by the “n” value listed in each table.

Table 4.10: Summary of samples collected per WTW site during the AOC method validation (for total number of samples analysed across all experiments multiply each value by 20).

Sampling Duration	Sampling Frequency	AOC	
		Raw Water	Post-treated Water
2 months	Weekly	n=3	n=3

[A]AOC – assimilable organic carbon

Table 4.11: Summary of samples collected per water supply system site during the AOC sampling within the network during Year 1 of the sampling regime. Four drinking water supply systems WTW 4 DWDS 1; WTW 6 DWDS 2; WTW 16 DWDS 3 and WTW 20 DWDS 4 (for total number of samples analysed across all experiments multiply each value by 4 (sites)).

Parameter	Sampling Duration	Sampling Frequency	Sample Location							
			Raw Water	Post-treated Water	SR 1 Inlet	SR 2 Outlet	SR 2 Inlet	SR 2 Outlet	SR 3 Inlet	SR 3 Outlet
Total chlorine[B]	**1 year**	2 days	-	n = 1	n = 1	n = 1	n = 1	n = 1	n = 1	n = 1
Iron[B]		Bi-monthly	n = 1	n = 1	n = 1	n = 1	n = 1	n = 1	n = 1	n = 1
Manganese[B]		Bi-monthly	n = 1	n = 1	n = 1	n = 1	n = 1	n = 1	n = 1	n = 1
ATP[BCD]		Bi-monthly	n = 1	n = 1	n = 1	n = 1	n = 1	n = 1	n = 1	n = 1
Colony counts[B]		Bi-monthly	n = 1	n = 1	n = 1	n = 1	n = 1	n = 1	n = 1	n = 1
Temperature[B]		2 days	n = 1	n = 1	n = 1	n = 1	n = 1	n = 1	n = 1	n = 1
TOC[B]		Bi-monthly	n = 1	n = 1	n = 1	n = 1	n = 1	n = 1	n = 1	n = 1
AOC[A]		Bi-monthly[E]	n=3	n = 3	n = 3	n = 3	n = 3	n = 3	n = 3	n = 3
TCC[BC]		2 days	n = 1	n = 1	n = 1	n = 1	n = 1	n = 1	n = 1	n = 1

ICC[BC]	2 days	n = 1	n = 1	n = 1	n = 1	n = 1	n = 1	n = 1	n = 1

[A]AOC – assimilable organic carbon; [B]analysed by Scottish Water not FP; [C]no raw water data for WTW 4, DWDS 1; [D]no post-treated or service reservoir data for WTW 4, DWDS 1; [E]samples analysed in triplicate.

Table 4.12: Summary of samples collected per water supply system site during the AOC sampling within the network during Year 2 of the sampling regime. Three drinking water supply systems WTW 4 DWDS 1; WTW 6 DWDS 2 and WTW 20 DWDS 4 (for total number of samples analysed across all experiments multiply each value by 3 (sites)).Year 2 of network sampling corresponds with the 12 month sampling programme in each of the pipe loops.

Parameter	**Sampling Duration**	**Sampling Frequency**	**Sample Location**							
			Raw Water	**Post-treated Water**	**SR 1 Inlet**	**SR 2 Outlet**	**SR 2 Inlet**	**SR 2 Outlet**	**SR 3 Inlet**	**SR 3 Outlet**
Total chlorine[B]	**1 year**	2 days	-	n = 1	n = 1	n = 1	n = 1	n = 1	n = 1	n = 1
Iron[B]		Bi-monthly	n = 1	n = 1	n = 1	n = 1	n = 1	n = 1	n = 1	n = 1
Manganese[B]		Bi-monthly	n = 1	n = 1	n = 1	n = 1	n = 1	n = 1	n = 1	n = 1
ATP[BCD]		Bi-monthly	n = 1	n = 1	n = 1	n = 1	n = 1	n = 1	n = 1	n = 1
Colony counts[B]		Bi-monthly	n = 1	n = 1	n = 1	n = 1	n = 1	n = 1	n = 1	n = 1
Temperature[B]		2 days	n = 1	n = 1	n = 1	n = 1	n = 1	n = 1	n = 1	n = 1
TOC[B]		Bi-monthly	n = 1	n = 1	n = 1	n = 1	n = 1	n = 1	n = 1	n = 1
AOC[A]		Bi-monthly[E]	n=3	n = 3	n = 3	n = 3	n = 3	n = 3	n = 3	n = 3
TCC[BC]		2 days	n = 1	n = 1	n = 1	n = 1	n = 1	n = 1	n = 1	n = 1
ICC[BC]		2 days	n = 1	n = 1	n = 1	n = 1	n = 1	n = 1	n = 1	n = 1

[A]AOC – assimilable organic carbon; [B]analysed by Scottish Water not FP; [C]no raw water data for WTW 4, DWDS 1; [D]no post-treated or service reservoir data for WTW 4, DWDS 1; samples analysed in triplicate

Table 4.13 : Summary of samples collected per site during the growth and mobilisation phases of biofilm growth (for total number of samples analysed across all experiments multiply each value by 3). The 12 month sampling programme in each of the pipe loops corresponds with Year 2 of network sampling.

Phase	Time	Inserts		Outer Coupons	
		Microscopy	Spare	Flow Cytometry	DNA Analysis
Growth	Day 0	n=3	n=3	n=3	n=3
	3 month	n=3	n=3	n=3	n=3
	6 month	n=3	n=3	n=3	n=3
	9 month	n=3	n=3	n=3	n=3
	12 month	n=3	n=3	n=3	n=3
	12 month bottom	n=3	-	n=3	-
	12 month top	n=3	-	n=3	-
Mobilisation	Post-flush[A]	n=3	n=3	n=3	n=3
	Post-flush bottom[A]	n=3	-	n=3	-

Phase	Time Period	Water Quality Samples							
		AOC[B]	TOC[C]	Chlorine	Turbidity[D]	Manganese	pH	ORP[E]	Temperature[F]
Growth[E]	Day 0 – 3 Month	n=3	n=3	n=3	n=3	n=3	n=3	n=3	n=3
	3 Month – 6 Month	n=3	n=3	n=3	n=3	n=3	n=3	n=3	n=3
	6 Month – 9 Month	n=3	n=3	n=3	n=3	n=3	n=3	n=3	n=3
	9 Month – 12 Months	n=3	n=3	n=3	n=3	n=3	n=3	n=3	n=3

Mobilisation	Flush Step 1	n=3	n=3	n=3	n=3	n=3	n=3	n=3	n=3
	Flush Step 2	n=3	n=3	n=3	n=3	n=3	n=3	n=3	n=3
	Flush Step 3	n=3	n=3	n=3	n=3	n=3	n=3	n=3	n=3
	Flush Step 4	n=3	n=3	n=3	n=3	n=3	n=3	n=3	n=3
	Flush Step 5	n=3	n=3	n=3	n=3	n=3	n=3	n=3	n=3

[A]Post-flush samples taken at the end of the mobilisation phase (after flush step 5); [B] AOC – assimilable organic carbon; [C]TOC – total organic carbon; [D]Discrete turbidity; [E]ORP – oxidising reduction potential; F Temperature – room temperature.

4.9 Summary

This chapter gave an overview of the methods used to develop the bespoke AOC method developed and applied in this study. The new AOC method was validated within 20 WTW, before being used to monitor the AOC concentration within bulk water at service reservoir inlets and outlets of four DWDS, for two years. Details of AOC sampling within the network were provided, along with an overview of the other bulk water samples collected. The second year of AOC sampling in the bulk water of the DWDS was conducted simultaneously with the operation of three state-of the-art pipe loops facilities. The pipe loop facilities were purpose-built to enable a long-term biofilm sampling programme, in which the impact of AOC concentration on biofilm accumulation and subsequent mobilisation could be assessed. An experimental overview of the 12 month sampling programme in each pipe loop was provided.

Chapter 5: Assimilable Organic Carbon Method Development, Validation and Application

5.1 Aims and Objectives

This chapter will first evaluate existing AOC methods (Section 5.2) before developing of a rapid, robust AOC method that can be used for routine analyses within drinking water systems (Section 5.3). Current AOC method application is limited due to the time and resources required to complete the assay, and the variation in available AOC methods making it difficult to compare between applications (as outlined in Table 2.4). The developed AOC method will be validated to ensure its reproducibility and test the ability of the method to capture a wide range of AOC concentrations in drinking water pre- and post-treatment (Section 5.4).

5.2 Evaluation of Existing AOC Methods

To develop a quicker but robust AOC method, established methods by Van der Kooij *et al.* (1982), LeChevallier *et al.* 1993a and Hammes & Egli (2005) were first evaluated. Assessment of the methods included protocols that incorporated different inoculum strains, incubation temperatures and enumeration techniques. A comparison of the yield curves produced by using bacterial strains *Pseudomonas fluorescens* P-17 (P-17) and *Spirillum sp.* strain NOX (NOX) enumerated with plate counts (Van der Kooij *et al*. (1982) and ATP (LeChevallier *et al*. 1993a), compared to a natural microbial inoculum enumerated using flow cytometry (Hammes & Egli, 2005), can be seen in Figure 5.1. Triplicate sodium acetate standards containing 0 – 1000 µg/L were used to assess the ability of both methods to enumerate different carbon concentrations. Flow cytometry and HPC enumeration methods showed good reproducibility between triplicate measurements. The ATP method generated a higher degree of standard error (approximately two-fold) between measurements than flow cytometry and HPC, and consistently underestimated cell counts. Using a natural microbial inoculum resulted in a higher

final cell count per mL than using known strains, when the NOX and P-17 counts per sample were averaged as required in the Van der Kooij *et al.* (1982) protocol. Additionally, the yield curve of the natural microbial inoculum was very different from that of P-17 (Figure 5.1). Ultimately the time consuming nature of enumerating known strains with HPC, along with the results of the two AOC protocols being statistically different (ANOVA: degrees of freedom (df)=2, p = 0.01), demonstrated the need for an improved AOC method.

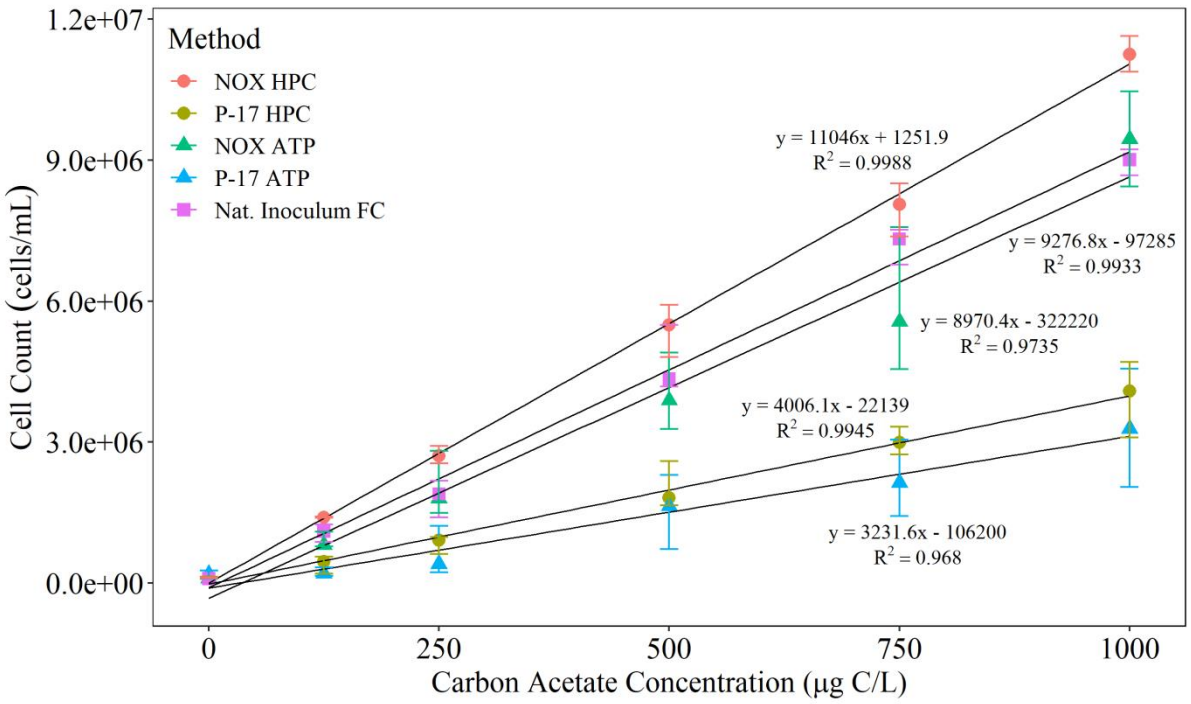

Figure 5.1: Comparison of cell counts enumerated using bacterial strains NOX (NOX HPC) and P-17 (P-17 HPC) with heterotrophic plate counts or ATP, or using a natural microbial inoculum with flow cytometry (Nat Inoculum FC). The average (n=3) cell counts (± standard deviation) at each acetate carbon concentration are plotted. The flow cytometry count refers to the total cell count.

5.3 Development of AOC Method

5.3.1 Inoculum Enumeration

In order to develop a quick standardised AOC method, each individual step in the AOC protocol, including the incubation temperature, inoculum density, inoculum type (known

strains or natural microbial inoculum) and enumeration method, were analysed in series of laboratory trials. To assess the repeatability and accuracy of two enumeration methods, a comparison of flow cytometric enumeration, HPC and ATP to enumerate P-17 was first assessed. As demonstrated in Figure 5.2, flow cytometry results showed equal or smaller variance between triplicate measurements, with greater consistency than HPC counts. The same experiment was performed using NOX (not plotted).

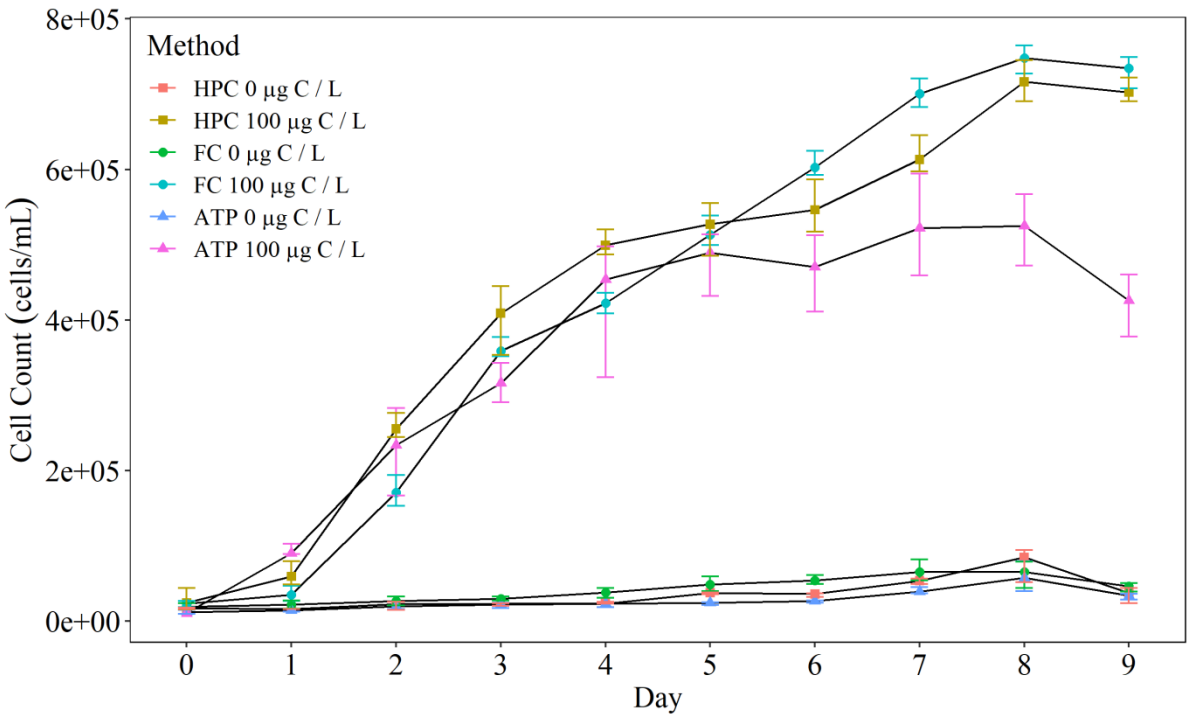

Figure 5.2: Comparison of P-17 cell concentrations when enumerated using heterotrophic plate counts (HPC) or flow cytometry (FC) over a nine day period (Pick *et al.* 2018). Cells are grown on in solutions containing 0 µg acetate carbon / L (control), and 100 µg acetate carbon / L. HPCs are recorded as CFU / mL and total cell counts (TCC) are recorded as cells / mL. The average (n=3) cell counts (± one standard deviation) are plotted.

5.3.2 Incubation Temperature and Inoculum Density

To investigate the effect of incubation temperature on cell growth rate, P-17 cells were grown in solutions containing 100 µg acetate carbon / L and enumerated using flow cytometry. When using different incubation temperatures for P-17, the stationary phase of growth was reached

more quickly with increasing temperature, but the peak number of cells (N-max) was lower at 23 or 30 °C than that achieved at 15 °C (Figure 5.3A). This demonstrates that each temperature will generate a different yield factor, and secondly, confirms that 15 °C is the optimal temperature for P-17 growth.

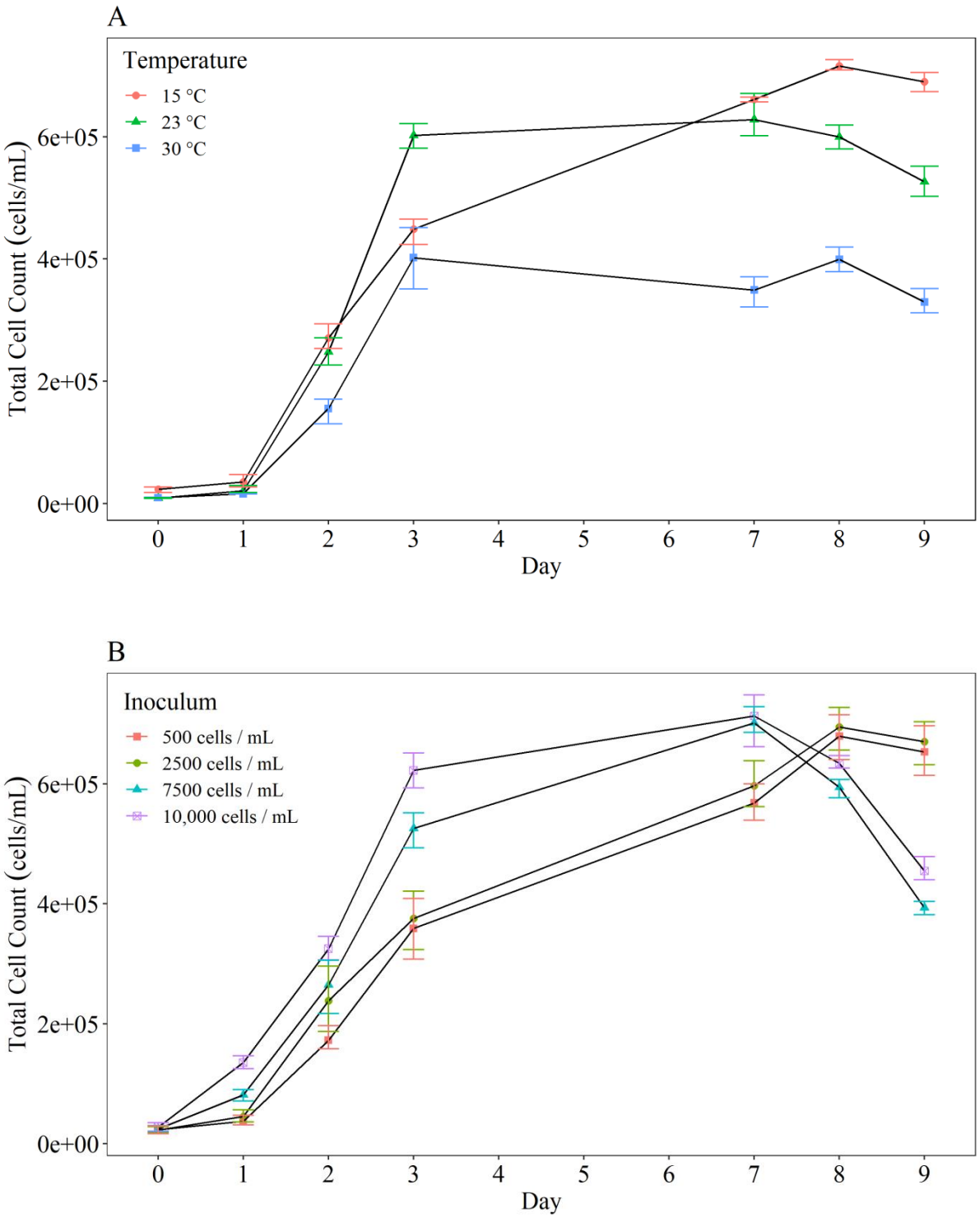

Figure 5.3: Comparison of P-17 cell growth when incubated at different temperatures (A) and with different inoculum densities (B) during a nine day incubation period. All samples were enumerated using flow cytometry and recorded as cells / mL. Cells were grown in solutions containing 100 µg acetate carbon/L. (A) Inoculum density was 500 CFU/mL, temperature as indicated by the key. (B) Temperature was 15 °C, inoculum density as indicated by the key. The average (n=3) cell counts (± one standard deviation) are plotted.

When the incubation temperature was kept constant (15 °C) but the inoculum density changed, a more concentrated inoculum resulted in the stationary phase of growth (maximum number of cells / mL) being reached in a shorter amount of time. This did not affect the maximum growth value (Figure 5.3B). A higher inoculum volume of 10,000 CFU/mL will therefore be used for subsequent tests.

5.3.3 Natural Microbial Inoculum

A further test was conducted to assess the reproducibility of using a natural inoculum in the AOC method. As alternate strains of bacteria have different growth rates, it is important to assess the consistency of growth rates resulting from different inoculums. Natural inoculums were obtained from three separate drinking water sources characterised by different conventional treatment processes to obtain a diverse natural inoculum (post-treated / filtered water from WTW 6, 13 and 14; see Table 4.1 for site details).

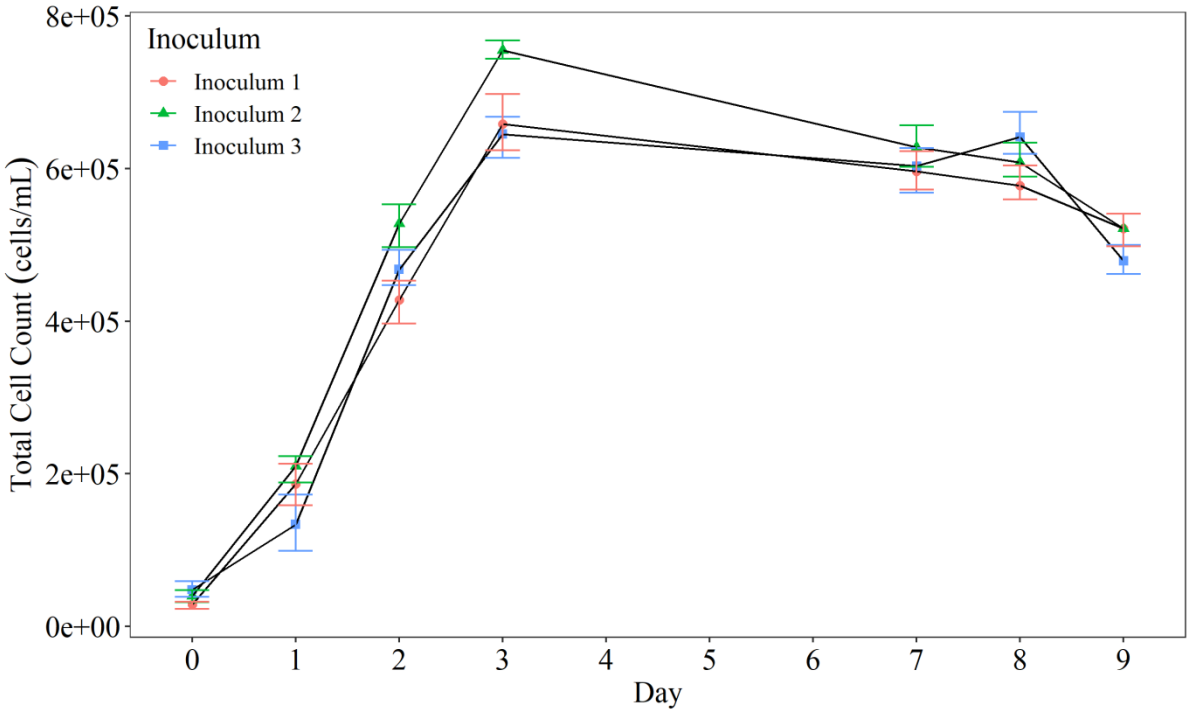

Figure 5.4: The effect of sample location on natural inoculum growth rate. The three inoculums were collected from three separate treated (post-treatment) water locations and prepared according to Hammes & Egli, 2005. Inoculums were added to separate solutions containing 100 µg acetate carbon/L and incubated at 30 °C for 9 days. Cell enumeration was via flow cytometry. The average (n=3) cell counts (± one standard deviation) are plotted.

Comparison of the three natural microbial inoculum, demonstrated that the growth rate of inoculum 1 was statistically significant different (p=0.0015) from inoculums 2 and 3, most likely due to differences in their microbial community composition. Using a natural microbial inoculum for the AOC assay requires that the inoculum is changed at least every month, this would make standardising the method difficult given the variability in the natural microbial inoculum. Consequently, it was desirable to create an adapted method that incorporates the use of bacterial strains P-17 and NOX to increase the reproducibility of the test, coupled together with flow cytometric enumeration to increase the speed and accuracy of the method.

5.3.4 Optimised AOC Protocol

To generate a quicker, robust method for AOC sampling, an optimised AOC protocol was developed which combines strains P-17 and NOX, a higher inoculum volume (10^4 cells / mL) and enumeration using flow cytometry. By utilising known bacterial strains it is possible to use standardised yield curves to convert the cell count to AOC concentration. The yield factors generated by monitoring the growth of the test organisms on pure solutions of acetate-carbon (P-17) or oxalate-carbon (NOX) are exhibited in Figure 5.5. These were subsequently used as reference standards to convert cell counts to AOC.

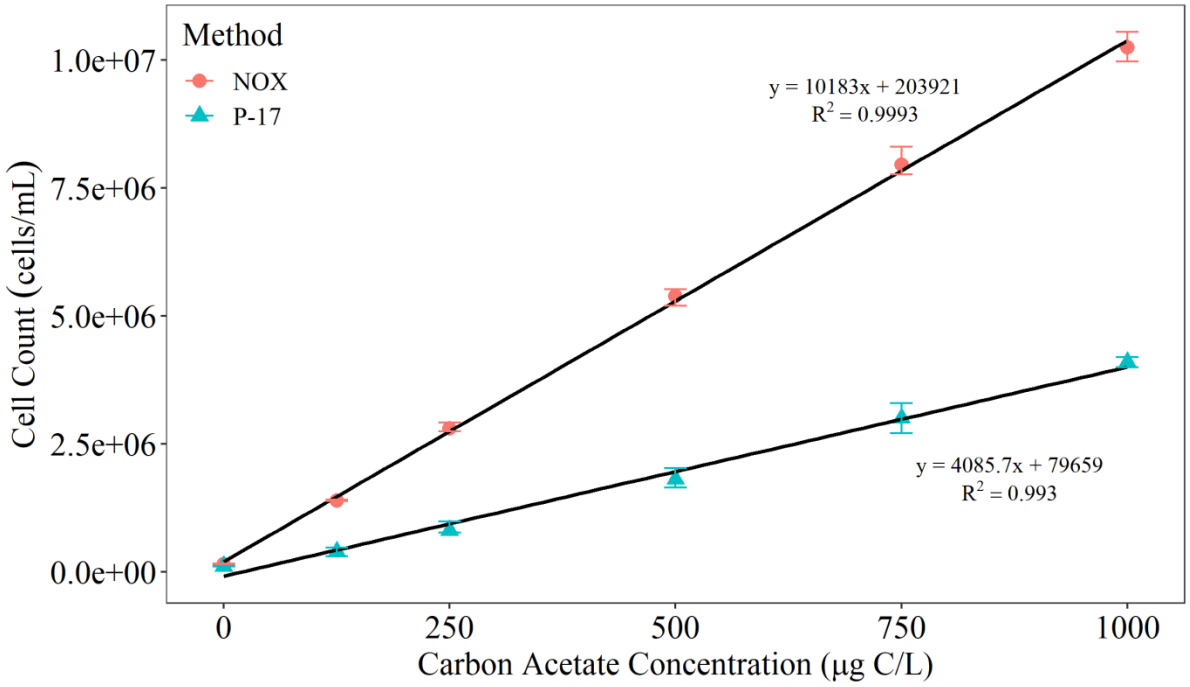

Figure 5.5: Yield factors produced when using NOX and P-17 grown in 0 – 1000 µg/L sodium acetate solutions. Samples were inoculated with 1000 cells ml^{-1}, incubated at 15 °C until maximum cell growth was achieved and enumerated using flow cytometry. Total cell counts are presented as averages ± standard deviation. The average (n=3) cell counts (± one standard deviation) are plotted.

5.4 Assessment of AOC Removal at the WTW

5.4.1 AOC at the Treatment Works: Raw vs. Treated Water

To confirm the ability of the optimised AOC method to capture a wide range of AOC concentrations, and quantify treatment efficacy, the developed AOC method was used to quantify AOC removal at 20 WTW (Table 4.1), by measuring AOC in raw (pre-treated) and post-treated water (Figure 5.6). Application of the method yielded informative, repeatable results, confirming the AOC method was able to capture AOC reduction at the WTW. The AOC concentration was found to decrease post-treatment at every WTW during the treatment process with an average of 45% removal of AOC across the twenty WTW sampled (Figure 5.6).

The AOC concentration in post-treated water was found to be more dependent on incoming water quality than the specific treatment process employed at the WTW. It was found that WTW supplied from groundwater sources (WTW 1-4) contained, on average, 50% less organic carbon in both raw and post-treated water than their surface water counterparts (WTW 5-20). The AOC concentration within raw surface water (234-403 µg/L) was much higher than raw groundwater (117-190 µg/L). Among the water treatment works supplied by groundwater water, the AOC concentration in post-treated water ranged from 61-96 µg/L, with all of the groundwater WTW having an AOC concentration in treated water below the threshold for biostable water (<100 µg/L).

TCC and ICC were also measured within raw and post-treated water for the same 20 WTW to determine the degree of cell removal / inactivation during treatment. When comparing the quality of post-treated water to the raw water quality, the post-treated water contained 93.41-99.73 % fewer TCC and 99.73-99.92 % fewer ICC. A comparison of cells counts and AOC concentrations indicate that the WTW containing a large number of total cells in which

the proportion of intact cells was small within raw water, exhibited the highest concentration of AOC in post-treated water**.**

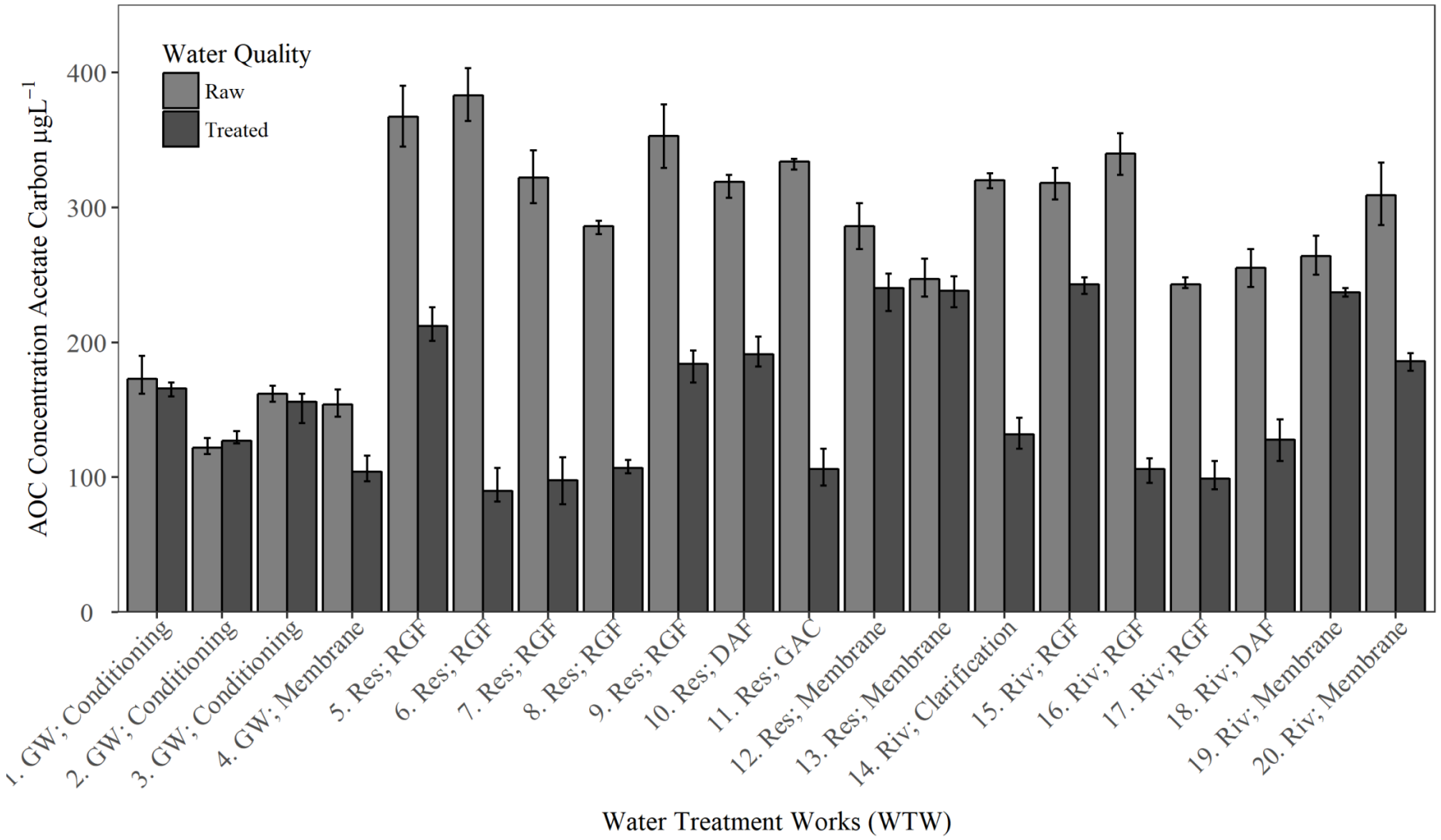

Figure 5.6: AOC concentration in raw (light bar) and post-treated (dark bar) water at 20 WTW (See Table 4.1 for details of source water, treatment type and disinfectant). Data collected weekly over a two month period (samples collected in triplicate) (n=24 at each WTW). Average ± standard deviation is plotted.

5.5 Discussion

This chapter developed a novel AOC methodology which combined the use of two known strains of bacteria, a larger inoculum volume and flow cytometric enumeration to increase the speed and reproducibility of AOC concentration. By using P-17 and NOX instead of a natural microbial inoculum, there is greater consistency between measurements. Unlike using known strains, the diversity of a natural inoculum was shown to depend upon the location and time in which the sample is taken. Hammes and Egli, (2005) use a fixed yield value of 1×10^6 bacteria (µg of AOC) to convert the maximum growth of the natural microbial consortium to an AOC value, but this does not accurately reflect the changing bacterial composition of each water sample. This can therefore create difficulties in standardising the AOC method. In contrast, using P-17 and NOX facilitated robust replication and repeatability. The analysis presented herein showed that increasing the density of P-17 and NOX decreased the time taken for the bacteria to reach stationary phase, whilst ensuring the growth yield values will be unaffected. Conversely, temperature changes decreased the peak in the bacterial growth rate, therefore requiring a different growth yield to be utilised. As the aim of this study was to create a standardised AOC it was deemed more suitable to use standardised yield values.

Comparison of enumeration methods used in the AOC protocol highlighted that flow cytometry had equal or better reproducibility between triplicate measurements than standard plate counts, and therefore offers a suitable alternative to HCP's in the AOC method. This is possibly a result of the selectivity of HCPs only culturing <1% of the population. Conversely, flow cytometry counts all cells present in the sample. ATP showed the most variability between measurements, potentially due to the two conversions needed to convert ATP (expressed as RLU) to cell counts, and finally cell counts to AOC concentration. The time and resources required to complete the assay were reduced significantly (from 14 to 8 days) by using flow cytometric enumeration of the water samples, which removes the need for incubation of

standard plate counts, hence is a more rapid method (2 minutes per sample compared to 3-4 days for HPC). Moreover, flow cytometry can detect a greater number of cells per sample (6×10^4 events per analysis (the total volume analysed is 200 µL) before sample dilution is required (Hammes & Egli, 2005). It is only possible to detect up to 300 CFU per plate when using HPC. By combining the reproducibility of using two strains of bacteria with known growth rates, together with an increased inoculum density and cell enumeration using flow cytometry, this study presents a novel, fast and standardised AOC method suitable for application within urban water systems.

The AOC concentration in treated water was predominantly influenced by source water quality. Groundwater systems contained a much lower concentration of AOC and produced treated water that could be classed as bio-stable (<150 µg/L). The final water AOC concentration at the majority of the treatment works supplied by surface water sources was found to contain AOC concentrations that exceed the existing criteria for bio-stable drinking water (Van der Kooij, 1992). In general, drinking water containing a disinfectant is classed as biologically stable when it contains AOC concentrations of <100 µg/L with appropriate level of chlorine residual (LeChevallier *et al.* 1993a). Taking this into account, the majority of the treated waters sampled are not classed as biologically stable.

AOC is made up of small molecular weight particles, which are removed to different extents by different treatment processes. In this study an average of 40% AOC removal was found. Greatest AOC removal was achieved at WTW's using rapid gravity filtration (RGF) or granular activated carbon (GAC). GAC or biological activated carbon (BAC) is able to remove small easily biodegradable compounds. Easton (1993) found coagulation and sedimentation (clarification) was able to achieve good removals (up to 57%) of AOC. The degree of AOC removal via membrane processes is dependent on the type of membrane. However, Escobar & Randall, (1999) found that Nanofiltration had no effect on AOC removal.

5.6 Summary

The AOC assay developed in this chapter incorporates known strains P-17 and NOX, a higher inoculum volume and enumeration using flow cytometry to generate a quicker (total test time reduced from 14 to 8 days), robust method. By utilising known bacterial strains it is possible to use standardised yield curves to convert the cell count to AOC concentration. First application of the developed assay has confirmed its suitability for use in the field, capturing an extensive range of AOC loading in raw and post-treated water at 20 WTW. In order to assess how AOC concentration changes from leaving the WTW to the customers tap, the optimised AOC method was applied to fully operational DWDS.

Chapter 6: AOC Concentration Variation within DWDS and the Impact on Drinking Water Biostability

6.1 Aims and Objectives

The AOC method developed and validated in Chapter 5 was used to explore the behaviour and fate of AOC across four DWDS each with different source waters, treatment steps and disinfection residuals (see Table 4.2). AOC concentration was quantified at service reservoir (SR) inlet and outlets to evaluate changes in the AOC concentration with time spent in the network. The information gained in this chapter will determine if pipes or service reservoirs act as sources or sinks of AOC in operational networks. As piped areas of the DWDS are characterised by a high surface area to bulk water ratio, it is possible to reveal what impact interactions within the pipe wall (and potentially any attached biofilms) has on the AOC concentration.

In order to determine the impact of AOC concentration and other environmental parameters on bacterial growth within the DWDS, TCC and ICC and other general water quality parameters (including total chlorine and temperature) were sampled within the same four DWDS. Bacterial growth within DWDS is traditionally assessed using culture-based techniques such as plate counts, which are known to only detect <0.1 % of drinking water bacteria and so are not representative of the drinking water bacterial community (Section 2.2.3). Flow cytometry, on the other hand, enables the quick detection and counting of all bacterial cells in water, and will therefore be used to determine the relationship between AOC and (re)growth within DWDS. By undertaking in-depth sampling of AOC, cell counts and disinfection residual this thesis will provide a holistic understanding of the parameters affecting biological stability within operational DWDS.

6.2 AOC Concentration within DWDS

The AOC concentration was analysed at the inlet and outlet of three SR within each of the four DWDS (1-4) (Table 6.1).

Table 6.1: Treatment processes within the four supply systems.

WTW ID	WTW 4	WTW 12	WTW 16	WTW 20
Water Source	Surface: Reservoir	Surface: River	Surface: River	Borehole
Full Treatment Process	pH Adjustment	pH Adjustment	pH Adjustment	pH Adjustment
	Coagulation	Coagulation	Coagulation	Coagulation
	Clarification (DAF)	Clarification (DAF)	Ultrafiltration	Clarification
	Gravity Filtration	Gravity Filtration	Chlorine Gas Disinfection	Hollow Fibre Membrane
		pH adjustment	pH adjustment	
Disinfectant Residual	Chlorination	Chloramination	Chloramination	Chloramination
DWDS ID	DWDS 1	DWDS 2	DWDS 3	DWDS 4
Pipe Loop	A		B	C

WTW = water treatment works; DWDS = drinking water distribution system; DAF = dissolved air flotation

Each of the DWDS is characterised by different hydraulic retention times and SR configurations (see Figure 6.1 for SR layout within each DWDS).

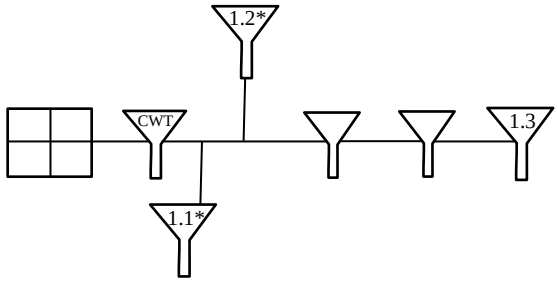

DWDS 1: reservoir; gravity filtration; chlorination

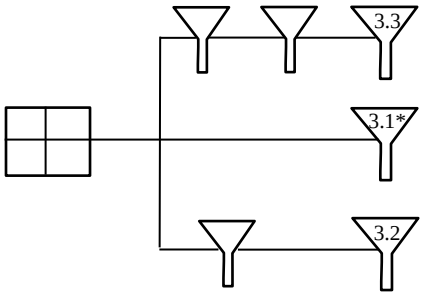

DWDS 3; river; membrane; chloramination

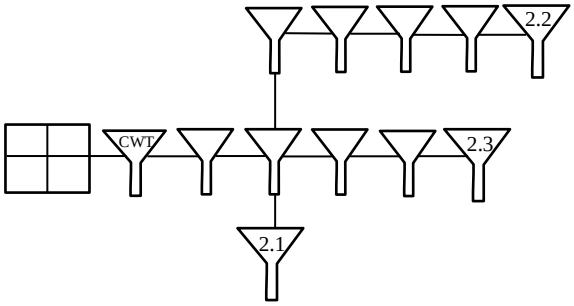

DWDS 2: river; gravity filtration; chloramination

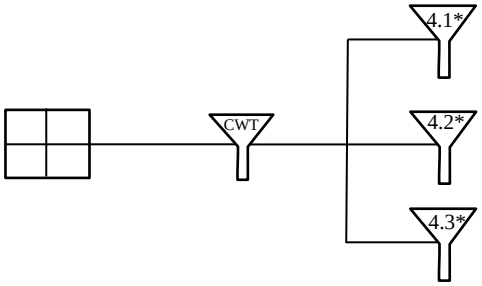

DWDS 4: groundwater; chloramination

Key:

= WTW **= SR** **= Pipeline** **= Clear Water Tank**

Figure 6.1: Schematic of the arrangement of service reservoirs (SR) within the four DWDS selected for further sampling (not to scale). The SRs sampled for AOC are numbered from one to three in each distribution system, as indicated by the second number in each case, with the first number denoting the DWDS to which the SR belongs. Unlabelled SRs are not sampled as part of this study and are only drawn to show the pathway of the water. SRs labelled with a * are subject to the pipe only effect, as water has not previously passed through a SR. Samples analysed included: WTW (raw): AOC, TCC & ICC; WTW (post-treatment): AOC, TCC, ICC & total chlorine; SR inlets: AOC; SR outlets: AOC, TCC, ICC & total chlorine.

The three SR sampled in each DWDS were selected on the basis of a) suitable location for an inlet tap installation b) situated at different distances within the network (different hydraulic retention times). The 12 SR sampled for AOC were located 3.35 to 53.26 km into the network. It was not possible to sample every SR within each DWDS within the scope of this thesis. The various pathways that the water travels to reach each of the 12 SR are shown in Figure 4.1. In some cases water passes through a series of pipes and SR to reach the sampled SR, and in some cases only pipes. The order of the 3 SR analysed for AOC within each DWDS are not in series, but some of the WTW-pipe-service reservoir layouts are comparable (this is taken into account in Figure 6.1).

6.2.1 AOC Concentration, DWDS Infrastructure and Seasonality

DWDS pipes and SR are characterised by different volume to surface areas. To ensure that pipe and SR effects on AOC could be clearly differentiated SR inlet and outlet points were sampled. As identified in Figure 4.1, the 12 DWDS consist of 6 DWDS which are pipe only (water does not pass through a SR before reaching the final sampled SR). Interestingly, when comparing AOC concentration in post-treated water to SR inlet values, the AOC concentration was found to increase within all of the pipe only sections during winter and 83% of pipe only sections during summer (Figure 6.2). In contrast, the AOC concentration was found to decrease within the majority of SRs sampled (75% in summer and 67% in winter) (Figure 6.1). In DWDS 2, the AOC concentration was found to increase from the WTW to the SR inlet within DWDS 1.1 and DWDS 1.2; the two DWDS which are dominated by pipe only effects. In contrast, the AOC concentration declined from the WTW to the SR inlet of SR 1.3. In DWDS 1.3 water passes through multiple SR before reaching the inlet, suggesting a decline in AOC concentration during SR residence time. This trend was also identified in DWDS 2 as AOC was found to decline from leaving the WTW to reaching SR 2.2. During this time the water passes through 6 SR before reaching the final sampled SR.

During winter, AOC was found to decline from leaving the WTW to reaching the inlet of both SR 3.2 and SR 3.3. However, in SR 3.1 AOC was found to increase before reaching the SR. Water reaching SR 3.1 does not pass through any other SRs before reaching the SR and is therefore dominated by pipe only effects.

6.2.2 AOC Concentration & Hydraulic Retention Time

Contrasting trends in the relationship between AOC concentration and hydraulic retention time (HRT) were observed within the sampled DWDS. The AOC concentration within DWDS 4 remained low in post-treated water and through the network (62-103 µg/L at all 3 SR inlet / outlets within DWDS 4) (Figure 6.2). DWDS 4 is supplied by ground water containing a low AOC concentration, and has a much shorter hydraulic retention time than the other three DWDS. In contrast, a slight increase in AOC was observed in DWDS 2 with HRT. When analysing the SR within the DWDS individually, a sharp increase of 41 µg/L was observed within SR 2.2.

The mean AOC concentration within DWDS 1 and 3 was found to decline significantly with increasing hydraulic retention time (34.40% in DWDS 1 and 34.97% in DWDS 3). DWDS 1 first exhibited an AOC increase suggesting chlorine was reacting with AOC prior to AOC consumption during (re)growth, hereafter causing a decline.

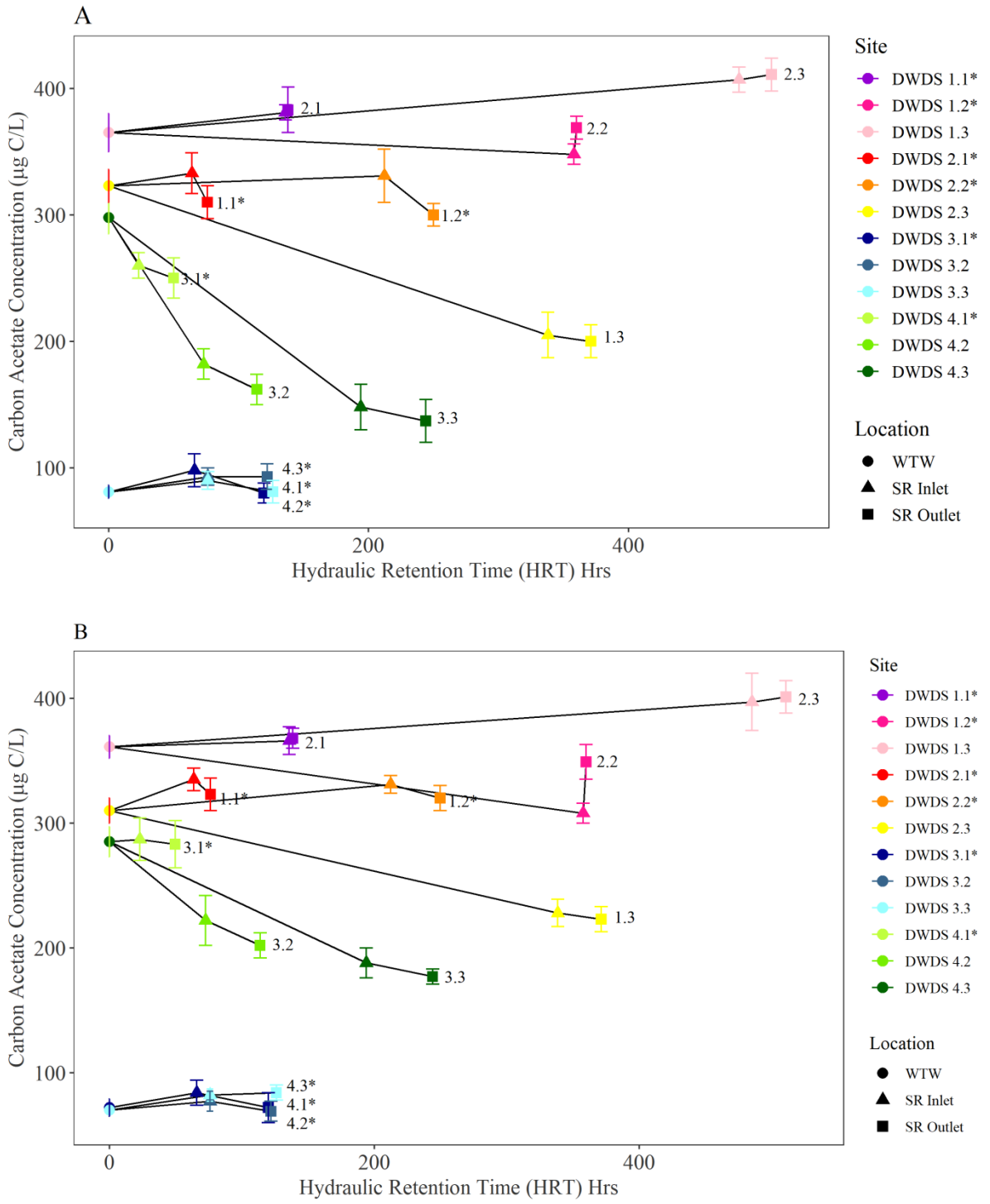

Figure 6.2: Variation in the AOC concentration along 4 DWDS (see Table 1 for DWDS details) with respect to the time that water has spent in the network, i.e. hydraulic retention time (HRT), during A) Summer and B) Winter. Hydraulic residence time is calculated from the pipe and/or SR volume divided by the flow rate (l/s). Locations of samples are indicated by the key and follow the sequence post-treatment (WTW outlet) and through 3 service reservoirs (SR), inlet and outlet. Data is the annual average ± standard deviation. A network schematic of the SRs within each system is provided in Figure 4.1. SR marked with a * are pipe only systems (water does not pass through an un-sampled SR).

6.3 AOC and Planktonic Cell Concentration In DWDS

To provide an insight into the relationship between AOC concentration, cell counts and disinfection residual within the bulk water, and assess the degree of biological stability, AOC results were compared with TCC, ICC, total chlorine and temperature data for DWDS 1 (Figure 6.3 & 6.4), DWDS 2 (Figure 6.5 & 6.6) and DWDS 3 (Figure 6.7 & 6.8). Due to sampling constraints, flow cytometry data was not unavailable for DWDS 4, therefore AOC and cell concentration comparisons were not possible. Three SR in each DWDS were analysed, as outlined previously (Figure 6.1). The relationship between AOC and microbial load was assessed over 12 months to firstly determine the impact of AOC concentration on cell growth, and secondly, to identify any seasonal trends in the AOC concentration and other water quality data.

The AOC concentration within DWDS 1 and DWDS 3 exhibited a seasonal trend, with AOC concentration being elevated in spring, before declining through summer and autumn (Figures 6.3 & 6.7). AOC concentrations also decreased from post treatment to final SR sampled in this study. In DWDS 1, TCC's were high in post-treated water before declining and continuing to stay low throughout the DWDS (TCC'S 98% lower in DWDS 1.3 than post-treated water). Summer (re)growth was evident within all SR in DWDS 1, with SR 1.1 exhibiting a sharp increase in ICC to 7240 cells/mL. This correlated with a decline in the AOC concentration. DWDS 1, a chlorinated system, exhibited a 55.32% decline in total chlorine concentration from post-treatment to SR 1.3.

Despite very low percentages of intact cells being found in the treated waters of all three DWDS, these percentages were seen to increase with HRT in the distribution systems. The most significant increase in the percentage of intact cells was found within DWDS 2 with the percentage of intact cells increasing from 2.40% to over 50%. A significant decline in AOC concentration was found in SR 2.2, which correlates with an increase in ICC, especially during

autumn. As with DWDS 1, some (re)growth was evident within DWDS 2, especially in SR 2.2. The chloraminated DWDS 2 exhibited a decline in total chlorine concentration of 30.56%.

The AOC concentration within DWDS 3 was lower than DWDS 1 and 2 at all points within the system. This correlated with lower TCC and ICC values within the DWDS. A small increase in ICC was observed within SR 3.1, 3.2 and 3.3 during spring and summer, in which the percentage of intact cells increased from 13.49 to 24.61%. DWDS 3 (chloraminated) exhibited the smallest decline (21.97%) in chlorine concentration from post treatment to SR 3.3 (21.97%).

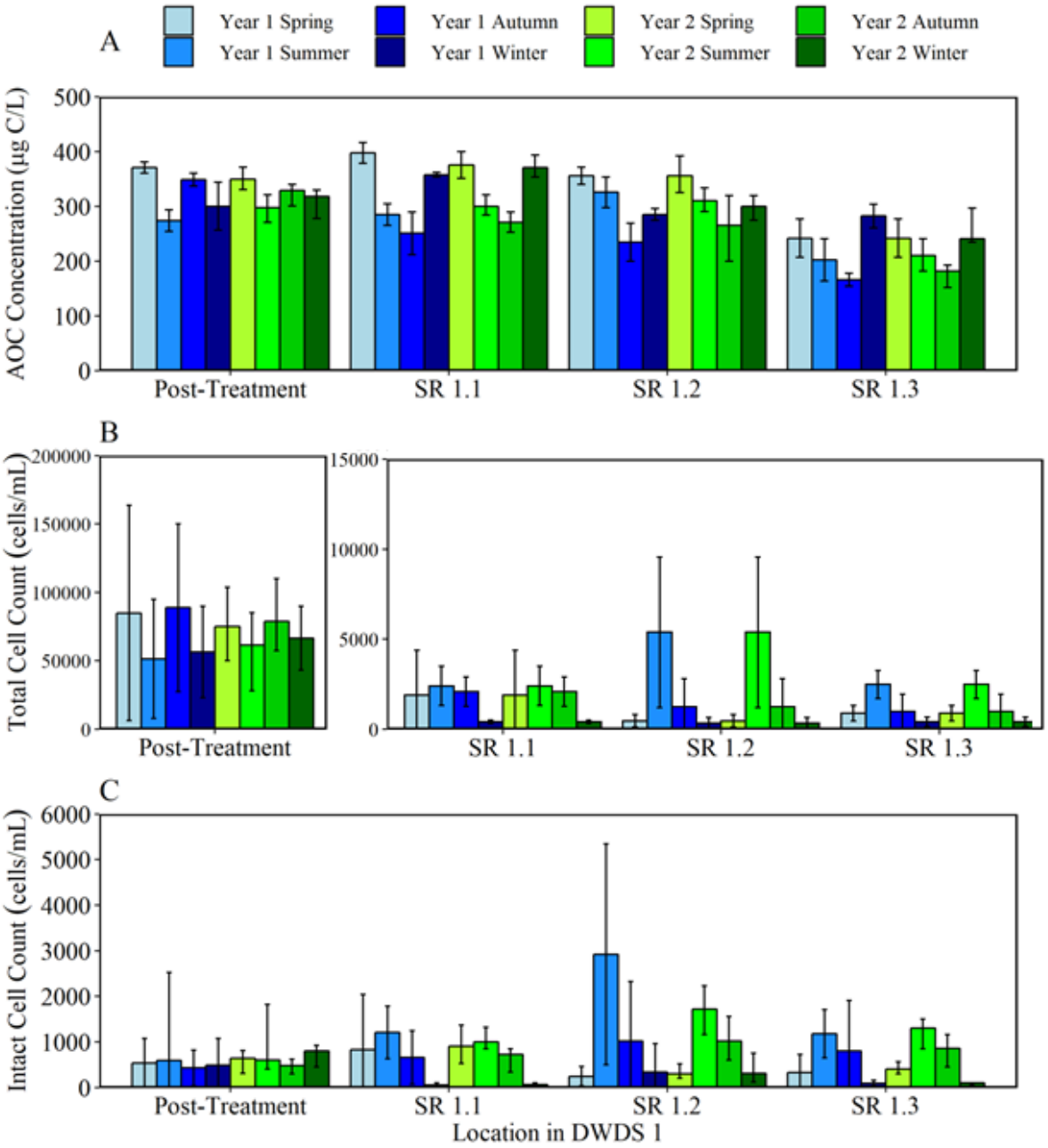

Figure 6.3: Seasonal water quality data for DWDS 1. Variation in the mean a) AOC concentration b) total cell counts (TCC) and c) intact cell counts (ICC) in post-treated water and three service reservoirs (SR) within DWDS 2 during the two year sampling programme. Nb different y-axis scale for each parameter and different y axis in Figures 6.2, 6.4 and 6.6. See Figure 4.1 for schematic of SR locations in each DWDS (the three SR are not in series).

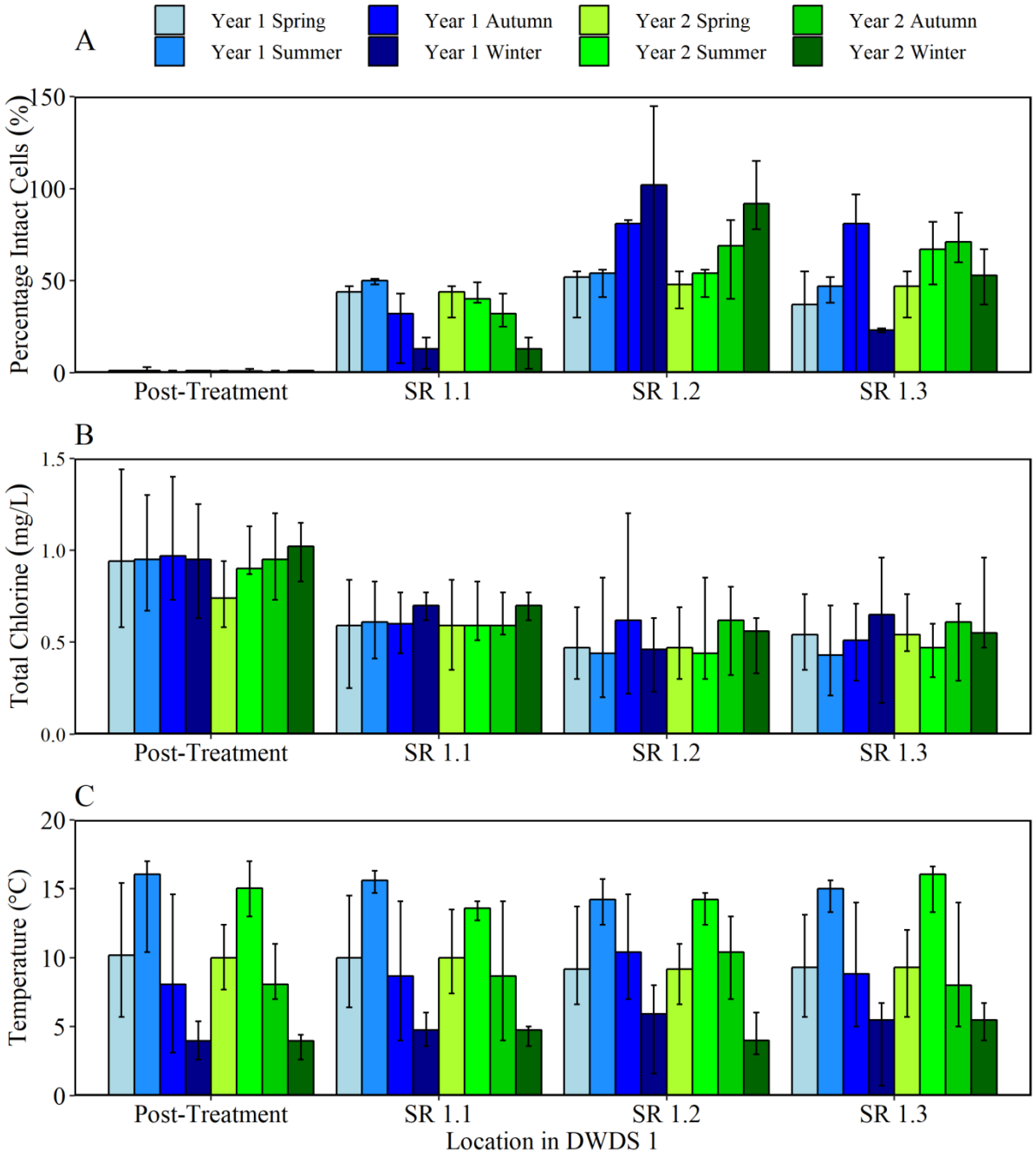

Figure 6.4: Seasonal water quality data for DWDS 1. Variation in the mean a) percentage of intact cells ((ICC/TCC)* 100) b) total chlorine and c) temperature in post-treated water and three service reservoirs (SR) within DWDS 2 during the two year sampling programme. Nb different y-axis scale for each parameter and different y axis in Figures 6.3, 6.5 and 6.7. See Figure 4.1 for schematic of SR locations in each DWDS (the three SR are not in series).

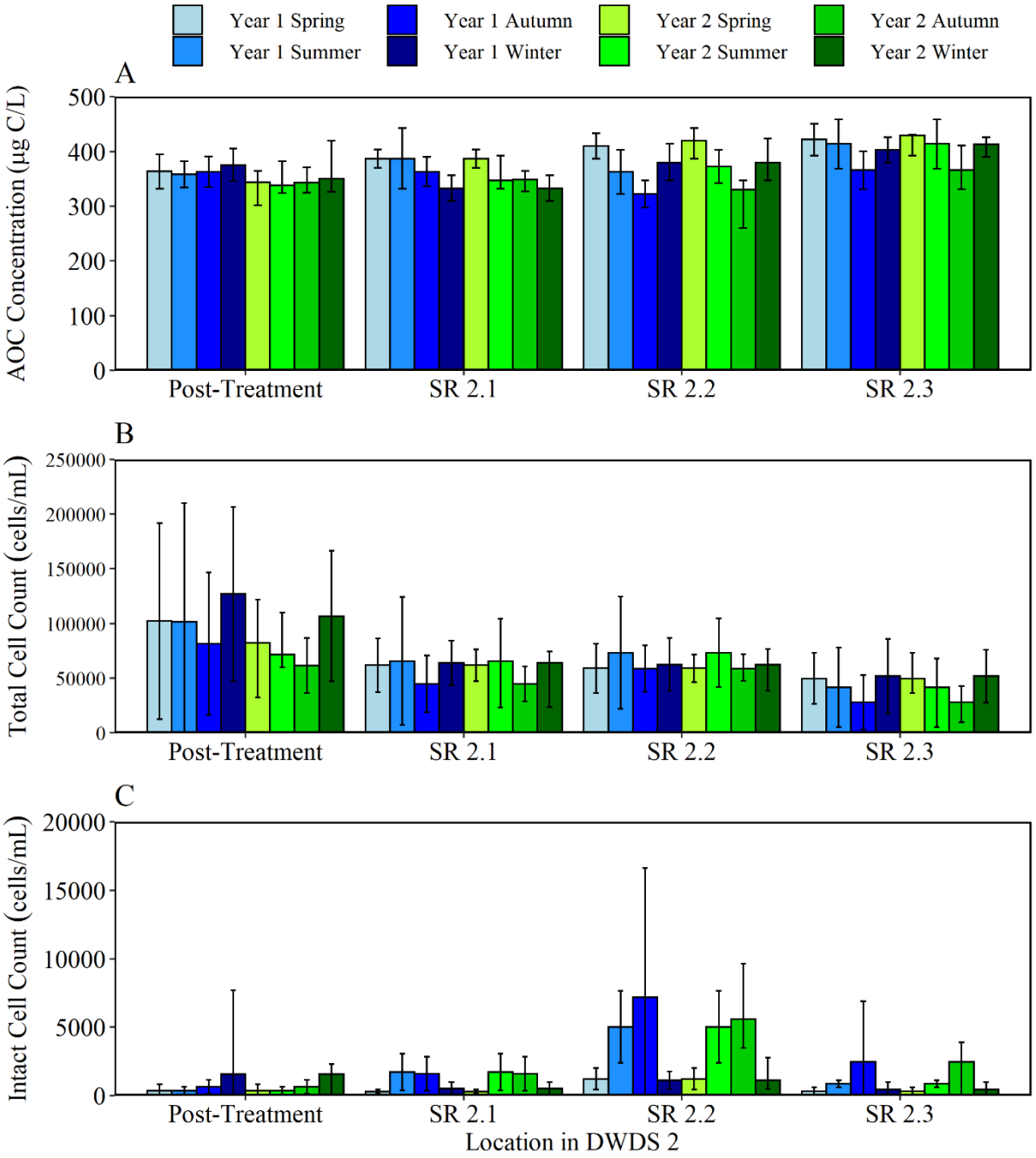

Figure 6.5: Seasonal water quality data for DWDS 2. Variation in the mean a) AOC concentration b) total cell counts (TCC) and c) intact cell counts (ICC) in post-treated water and three service reservoirs (SR) within DWDS 3 during the two year sampling programme. Nb different y-axis scale for each parameter and different y axis in Figures 6.2, 6.4 and 6.6. See Figure 4.1 for schematic of SR locations in each DWDS (the three SR are not in series).

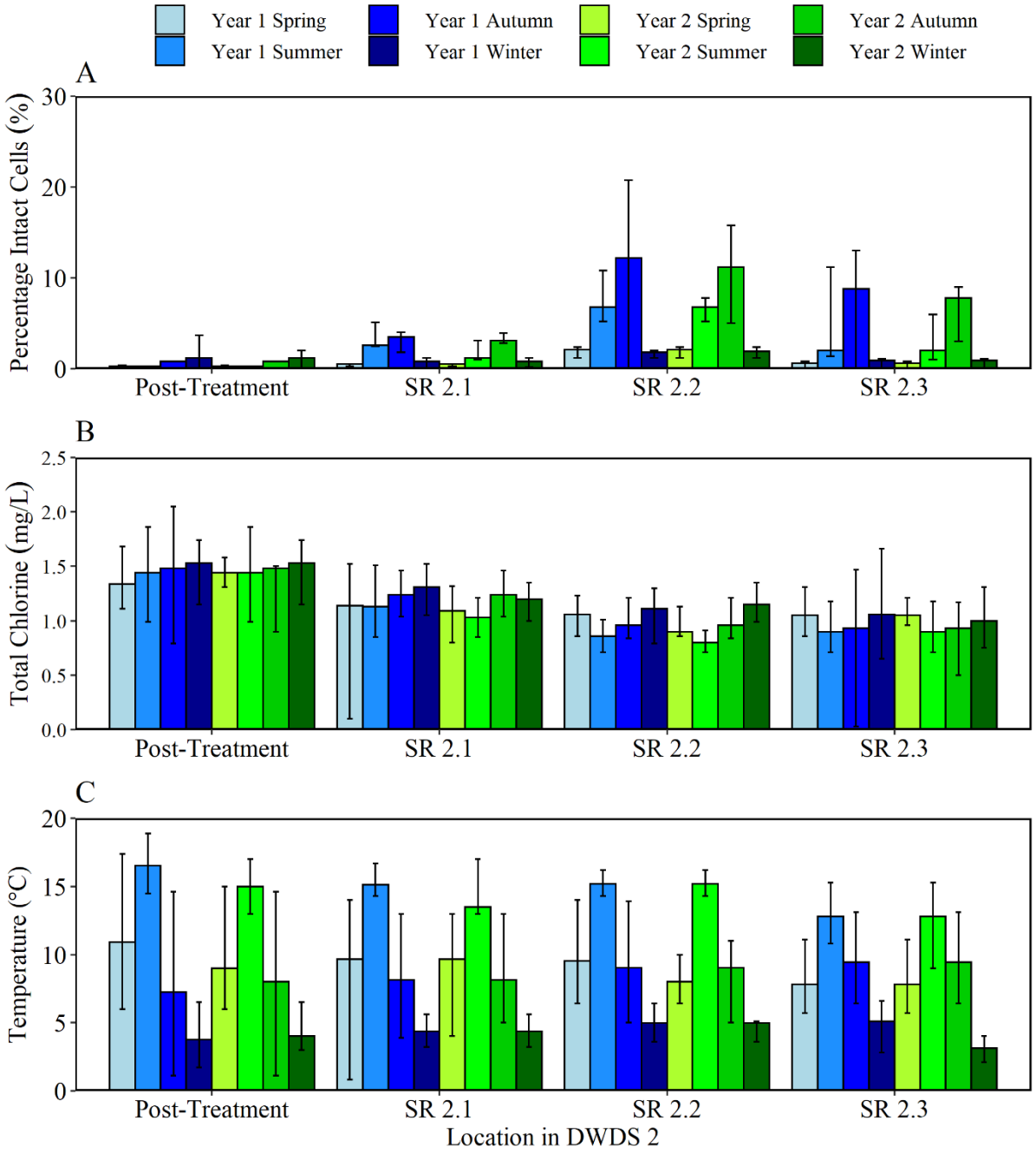

Figure 6.6: Seasonal water quality data for DWDS 2. Variation in the mean a) percentage of intact cells ((ICC/TCC)* 100) b) total chlorine and c) temperature in post-treated water and three service reservoirs (SR) within DWDS 2 during the two year sampling programme. Nb different y-axis scale for each parameter and different y axis in Figures 6.3, 6.5 and 6.7. See Figure 4.1 for schematic of SR locations in each DWDS (the three SR are not in series).

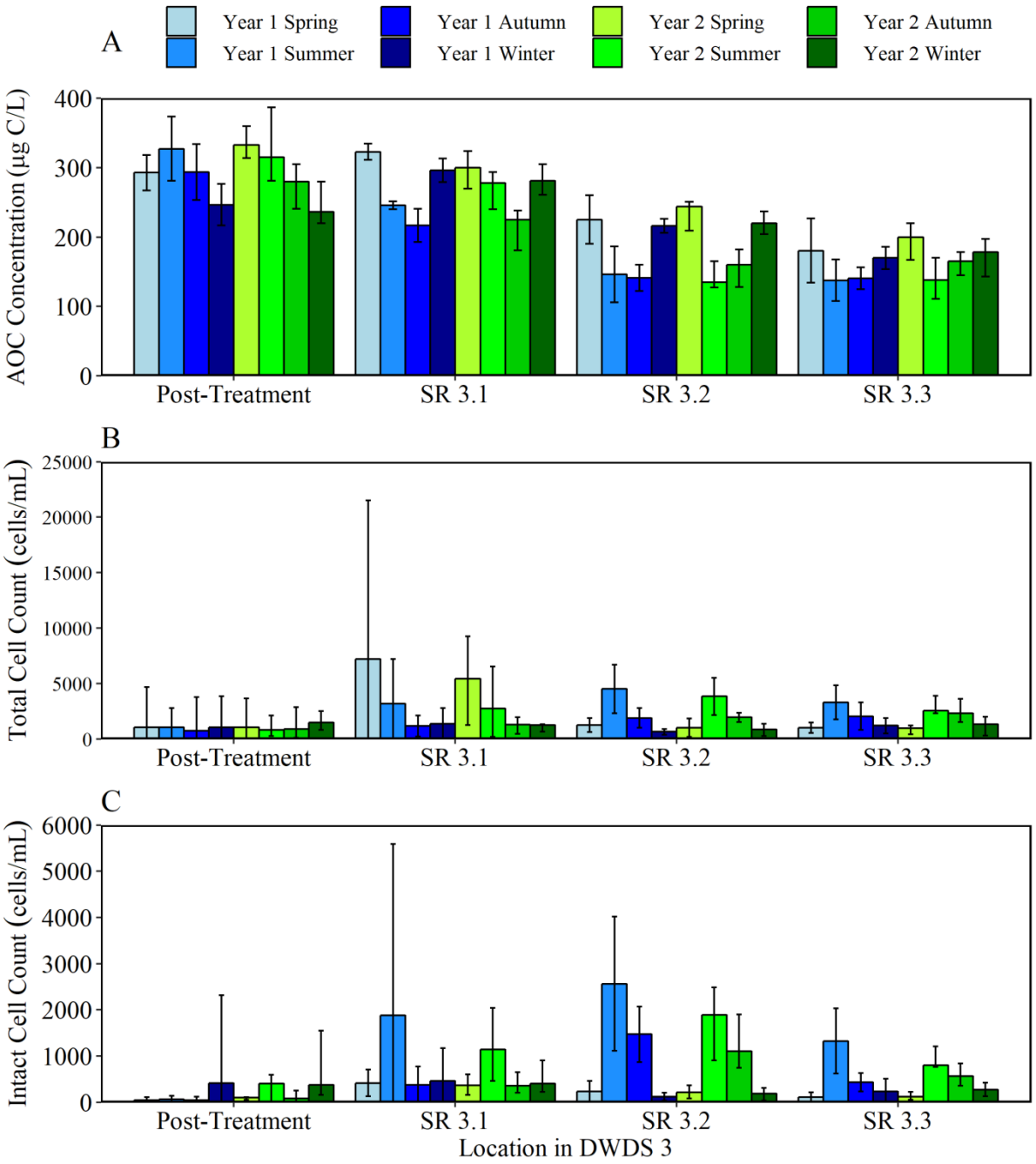

Figure 6.7: Seasonal water quality data for DWDS 3. Variation in the mean a) AOC concentration b) total cell counts (TCC) and c) intact cell counts (ICC) in post-treated water and three service reservoirs (SR) within DWDS 4 during the two year sampling programme. Nb different y-axis scale for each parameter and different y axis in Figures 6.2, 6.4 and 6.6. See Figure 4.1 for schematic of SR locations in each DWDS (the three SR are not in series).

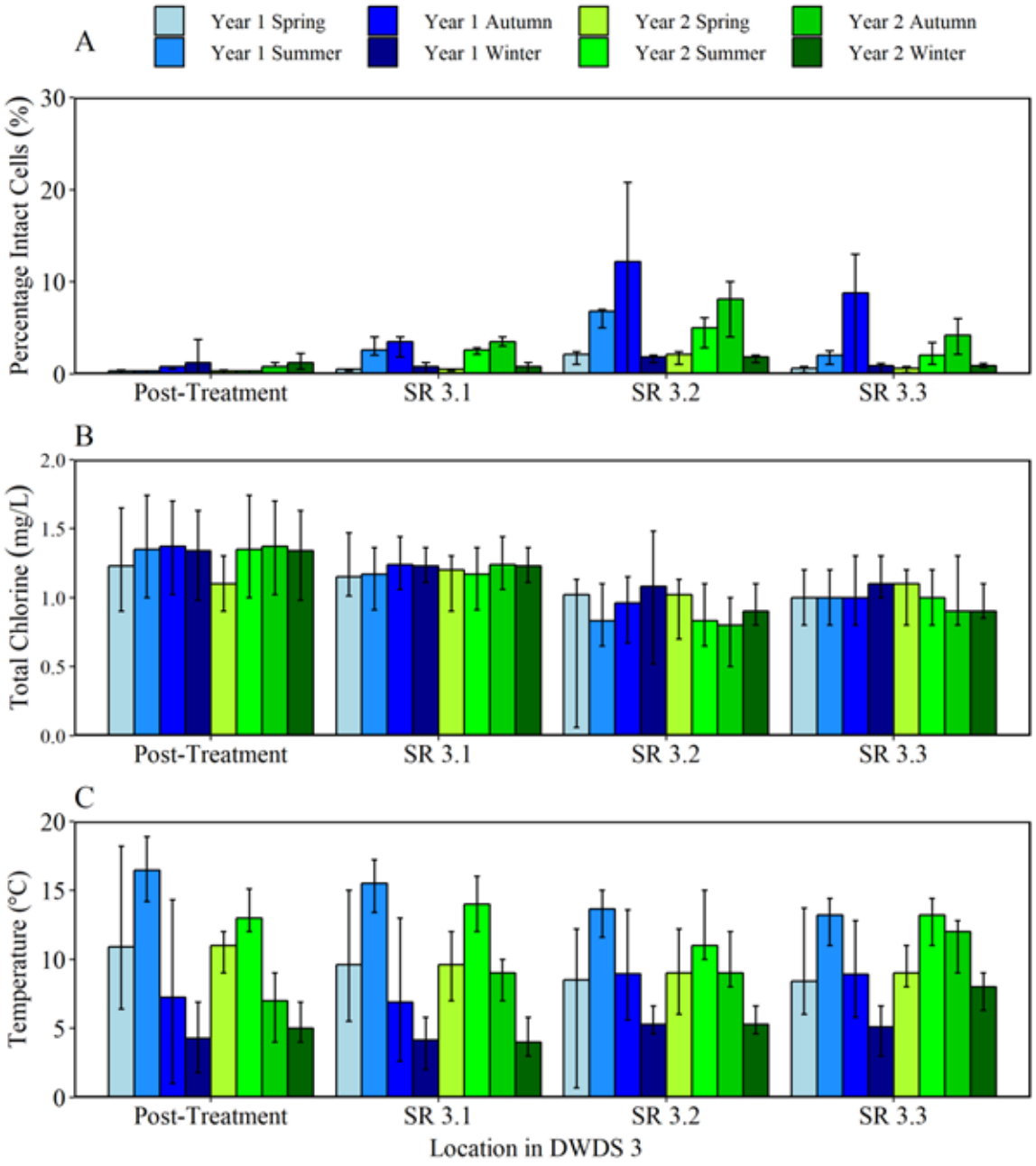

Figure 6.8: Seasonal water quality data for DWDS 3. Variation in the mean a) percentage of intact cells ((ICC/TCC)* 100) b) total chlorine and c) temperature in post-treated water and three service reservoirs (SR) within DWDS 2 during the two year sampling programme. Nb different y-axis scale for each parameter and different y axis in Figures 6.3, 6.5 and 6.7. See Figure 4.1 for schematic of SR locations in each DWDS (the three SR are not in series).

6.4 Self Organising Map Analysis

To help understand trends and relationships between the large numbers of water quality parameters sampled within the four DWDS in this study, a self organising map (SOM) was constructed to help visualise the data (Figure 6.9).The concentration of AOC was found to be highest when the TCC was high but the percentage of intact cells was low, thus suggesting limited AOC consumption. A clear trend can also be identified that when the total chlorine is low (illustrated by blue shading), the ICC is high. This confirms the ability of total chlorine to suppress cell growth when at higher concentrations.

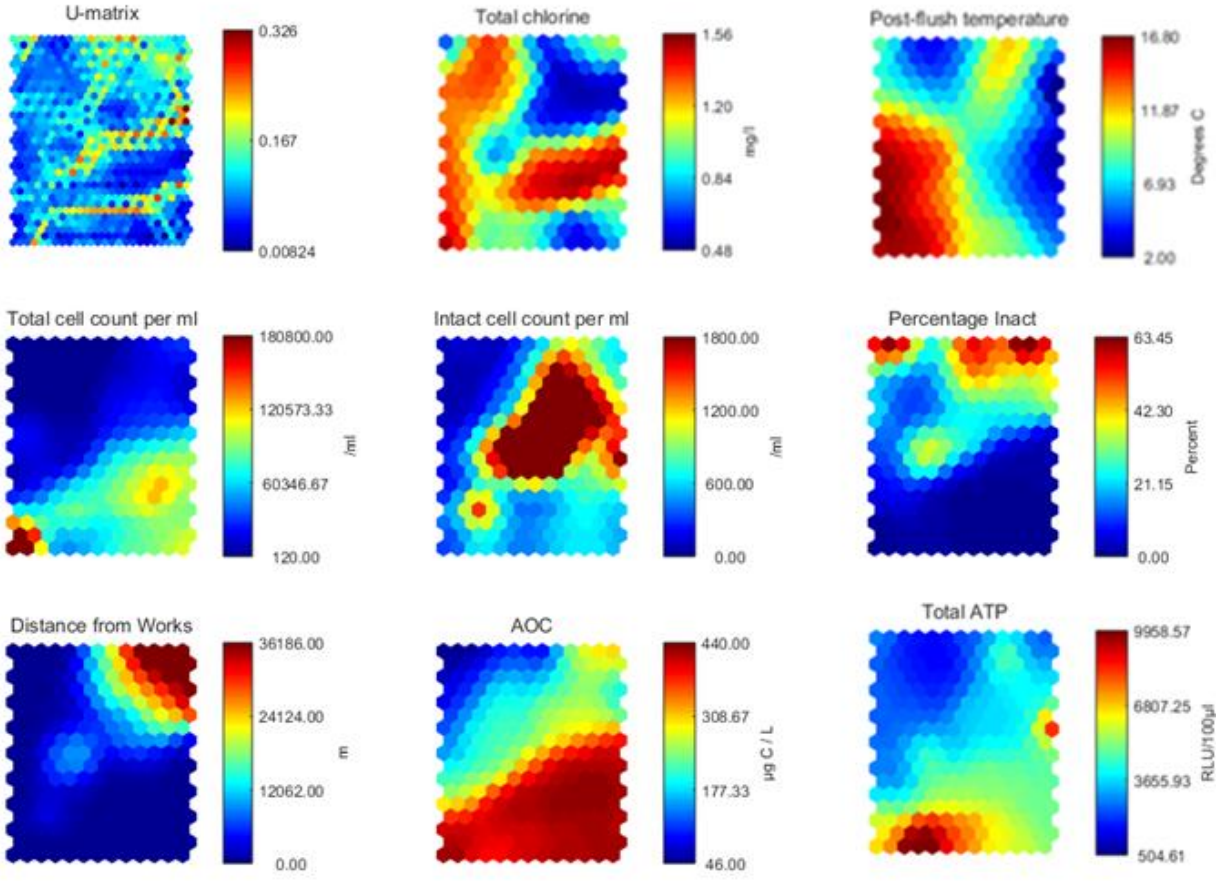

Figure 6.9: Self Organising Map (SOM) analysis of total chlorine (mg / l), water temperature, total cell count (cells / mL), intact cell count (cells / ml), percentage of intact cells, distance from water treatment works (km), AOC concentration (µg C / L) and total ATP (RLU). The cell shading denotes the numerical value of the vectors and a colour bar is presented to show the mapping between shading and numerical value. In this study, blue denotes low and red denotes high values.

6.4 Discussion

The AOC concentration within DWDS was found to be a function of several factors including source water quality, chlorine residue, seasonality, AOC concentration removal at the treatment works and bacterial activity. As this study employs both SR inlet and outlet sampling, it is possible to identify changes in AOC concentration with HRT within both piped sections and the SRs. The HRT is calculated from the pipe and/or SR volume, divided by the flow rate (l/s). When comparing the AOC concentration in post-treated water to SR outlet water, AOC was found to decline with increasing HRT within the majority (7 out of 12 in both summer and winter) of DWDS, indicating that these systems were acting as net sinks of AOC. The decline in AOC in DWDS 1 and 3 correlated with an increase in ICC. A decrease in AOC with distance in the distribution systems has been found to correlate with an increase in heterotrophic bacteria (LeChevallier *et al.* 1987; Van der Kooij *et al*. 1989; Han *et al.* 2012).

To determine if the reduction of AOC levels in distribution may be caused by planktonic bacteria or those growing on the walls of the mains or SRs as biofilms, the AOC concentration in post-treated water was compared to SR inlet water. The 12 DWDS consisted of 6 DWDS which are pipe only and 6 which pass through SR before reaching the final sampled SR (see Figure 4.1). The AOC concentration was found to increase within all of the pipe only sections during winter and 83% of pipe only sections during summer. In cases where organic matter is released from the biofilm, this can increase AOC and cell counts within the bulk water (Han *et al*. 2012). In contrast, the AOC concentration was found to decrease within 8 of the 12 SR sampled in both summer and winter. A reduction in AOC during elevated storage within a SR points to AOC consumption by heterotrophic bacteria.

The AOC concentration with DWDS is not only influenced by the degree of cell growth but also the disinfection residual. In DWDS 1, an initial increase in AOC concentration was observed before declining with distance in the network. The initial increase in AOC is a

potential result of organic matter reacting with chlorine. One reason for an increase in AOC concentration is the oxidation of organic matter macromolecules into small-molecule biodegradable organic compounds (such as carboxylic acids) by chlorine or chloramine (Lou *et al*. 2009; Liu *et al.* 2015). Hence, the trade-off between achieving effective disinfection and limiting unwanted by-product formation (in this case AOC) becomes a main operational goal for water utilities. Despite AOC increasing after leaving the works, the presence of chlorine resulted in a low number of intact cells a short distance from the WTW. However, as total chlorine declines in the system from 0.95 mg/L to 0.53 mg/L at the outlet of SR 2, there is an increase in the number of intact cells with the percentage of ICC rising from 2% in post-treated water to >63% in SR2.

A seasonal trend was identified in DWDS 1-3, in which the AOC concentration generally increased to a maximum in spring, before declining from in summer and autumn. Polanska *et al*. (2005) also observed an increasing trend in the AOC concentration during spring. Summer (re)growth was evident with DWDS 1 and 3, with an increase ICC within all SRs within DWDS 1 during summer. We conclude that a decrease in AOC from spring to summer is due to the consumption of AOC by heterotrophic organisms. This is demonstrated by an increase in the number of intact cells during summer. Similarly, there are fewest TCC and ICC within the winter months. The lower temperatures in winter would limit the bacterial (re)growth during distribution and therefore AOC consumption by bacteria would be lower. It would also be likely that the reaction between chlorine and organic matter would also slow down at lower temperatures (Liu *et al.* 2002). The combined effect of supressed microbial growth and slower oxidation of organic carbon, resulted in a continuous increase in AOC concentration during the winter season.

In DWDS 4 AOC values remained low (<125 µg/L) in post-treated water and within the DWDS. This site is supplied by borehole water containing low concentration of AOC. This

highlights the importance of good source water quality. Similarly, DWDS 3 was found to contain AOC concentrations lower than DWDS 1 and 2 throughout distribution. Intact cell counts remained relatively low within DWDS 4 most likely as the AOC in the system was unable to support any additional (re)growth. Organic carbon, especially AOC has been identified as a primary factor controlling microbial growth in drinking water distribution systems (Lehtola *et al.* 2001; LeChevallier *et al*. 1991). DWDS 3 and DWDS 4 are also the two systems with the shortest hydraulic residence time (105 hrs in DWDS 1, 268 hrs in DWDS 4, 371 hrs in DWDS 2, 510 hrs in DWDS 3) (Table 4.3).

In DWDS 2, supplied by chloraminated surface water, the AOC concentration was characterised by the highest AOC values and highest TCC. Despite having >40,000 TCC (cells/mL) within each SR, <9% of these were intact. It is likely that these cells attributed to the high AOC values with the system.

6.5 Summary

Application of the optimised AOC method developed in this thesis provided novel evidence of different pipe and service reservoir behaviour. This chapter presents first time data of the AOC concentration increasing within pipe only systems, and declining within SR. The results from this study highlight the complex cycling of AOC within DWDS, being a combination of both planktonic and biofilm processes within the pipes and SR. AOC was demonstrated to be a useful tool in assessing water quality and gaining understanding of DWDS behaviour, which would be otherwise not be observable.

Chapter 7: The Impact of AOC Concentration on Biofilm Growth and Mobilisation

7.1 Aims and Objectives

The novel AOC method outlined in Chapter 5 was previously applied to four DWDS to characterise spatial and temporal variations in AOC concentration, and determine the impact of AOC concentration on microbial (re)growth in the bulk water (Chapter 6). Elevated AOC concentrations were found to correlate with increased levels of microbial growth in the bulk water. Increased levels of (re)growth can lead to a loss of biological stability, defined as drinking water in which the microbial quality does not change as the water travels from WTW to the customers tap. However, it is unclear how the AOC concentration impacts biofilm growth and potential mobilisation within the DWDS. The majority of new microbial growth in DWDS occurs on the pipe wall, in comparison to the bulk water (Lehtola *et al.* 2004; Moritz *et al.* 2010).

This chapter aims to understand the impact of AOC concentration on both planktonic and attached microorganisms, in order to gain a holistic understanding of AOC within DWDS. Specifically, the information gained will help determine the impact of AOC concentration on biofilm accumulation, characteristics and mobilisation behaviour. This study aims to determine the impact of AOC concentration on biofilm cell growth and maturation for one year. In addition, by quantifying the community composition of both the biofilm and the bulk water, this work will quantify the impact of the AOC concentration on both planktonic and attached bacterial and fungal communities. Finally, this research will determine if an elevated AOC concentration in the bulk water will affect the microbial and discolouration risk of the biofilm.

7.2 Introduction

Using three novel, full-scale experimental pipe loops (Table 7.1) supplied with either high- (WTW 2; DWDS 1; Pipe Loop A), medium- (WTW 16; DWDS 3; Pipe Loop B) or low-AOC

(WTW 20; DWDS 3; Pipe Loop C) drinking water biofilm and bulk water samples were collected over a 12 month study period to determine the impact of AOC concentration on biofilm accumulation. Specifically, the number of cells (and the proportion that remained intact) in the biofilms were quantified and the bacterial and fungal communities were compared between the sites, to identify any selective pressures due to the AOC concentration. After 12 months growth, the flow rate was raised within each pipe loop to determine any differences in the mobilisation and discolouration response of biofilms that developed under different AOC concentrations.

Table 7.1: Source water quality, treatment stages and disinfectant types supplying the three novel, full-scale experimental pipe loops.

AOC Concentration	Source Water	Treatment Type	WTW ID	Disinfectant Type	DWDS ID	Pipe Loop ID
High	Reservoir	RGF	2	Cl_2	DWDS 1	A
Medium	River	Membrane	16	NH_2Cl	DWDS 3	B
Low	Groundwater		20	NH_2Cl	DWDS 4	C

WTW = water treatment works; DWDS = drinking water distribution system, ID = identification number / letter. RGF: rapid gravity filter, Cl_2: chlorine, and NH_2Cl: Monochloramine.

7.3 Bulk water Quality

In order to determine the impact of AOC concentration on bulk water quality, AOC was sampled both within raw water supply each WTW, and within post-treated water supplying each pipe loop.

7.3.1 The Impact of AOC Concentration on Raw Water Quality (upstream of pipe-loops)

To assess any changes in raw water quality supplying the three WTW, and compare this to the quality of post-treated water supplying the pipe loop test facilities, standard drinking water parameters were monitored (see section 4.6) along with AOC, TCC and ICC to assess the

biological stability of raw water. Additionally, bulk water sampling was conducted to monitor any changes in incoming water quality during the 12 month study period to determine any seasonal changes in bulk water quality. Routine raw water drinking water parameters sampled included turbidity, iron, manganese, total chlorine and TOC. It should be noted that turbidity, iron, manganese and TOC are not sampled at WTW 20 as this is a ground water source with historically low levels of background contaminants, therefore this data is unavailable.

The mean and range of each of the measured raw water quality parameters (excluding AOC, TCC and ICC which are plotted in Figure 7.1, Figure 7.2 and Figure 7.3), for each site, are shown in Table 7.2.

Table 7.2: Raw water quality (upstream of pipe loop) during the formation of biofilms over a 12 month period at Pipe Loop A and Pipe Loop B.

Water Quality Parameter	WTW 2 (Pipe Loop A) Mean (St. Dev)	WTW 16 (Pipe Loop B) Mean (St. Dev)
Turbidity (NTU)	2.27 (1.66)	0.68 (0.59)
Iron (µg / L)	152.07 (90.17)	116.93 (64.23)
Manganese (µg / L)	18.33 (14.17)	8.09 (3.70)
ATP (RLU/100µl)	207,246 (213,568)	25,975 (18,281)
Colony counts 22°C (CFU / mL)	202 (108)	239 (89.05)
Colony counts 37°C (CFU / mL)	47 (88)	31 (46)
TOC (mg / L)	4.3 (1.1)	3.6 (1.6)

Raw water supplying WTW 2 contained higher concentrations of turbidity, iron, manganese, ATP, colony counts at 37°C and TOC, in comparison to raw water supplying WTW 16 (Table 7.2). Notably, the ATP concentration within raw water supplying WTW 2 was approximately 8 fold greater (when using the mean) than the ATP concentration within raw water supplying WTW 16.

The AOC concentration (Figure 7.1) within raw water was measured in triplicate every two weeks for a 12 month period. On average, WTW 20 contained the lowest concentration of

AOC (91 ±12 µg C / L), when compared to WTW 2 (379 ±31 µg C / L) & WTW 16 (319 ±35 µg C / L) (data in text is expressed as the mean ± standard deviation). AOC concentration within the raw ground water supplying WTW 20 remained relatively consistent throughout the 12 month period, whereas AOC within WTW 2 and 16 was found to gradually increase during autumn / winter and gradually decline during summer (Figure 7.1).

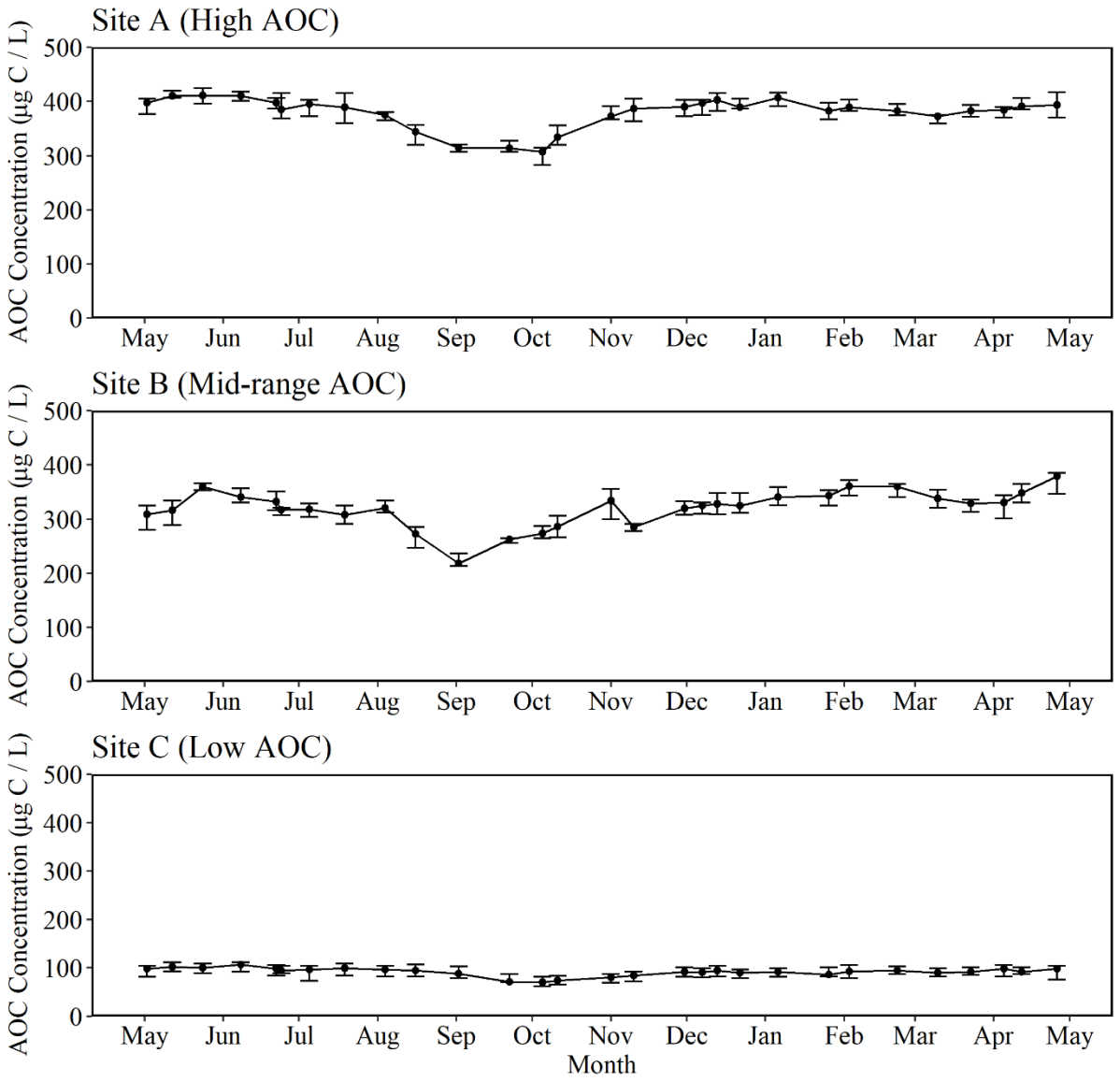

Figure 7.1: Assimilable organic carbon (AOC) concentration (n=3) in raw water at WTW 2 (A), WTW 16 (B) and WTW 20 (c), plotted against time. AOC concentration was sampled every 2 weeks for 1 year.

During the 12 month experimental programme, high TCC and ICC within raw water were found to correlate with highest TCC and ICC within the bulk water of each pipe loop. A high level of variability in TCC and ICC was exhibited within raw bulk water supplying WTW 2 and WTW 16. This is likely due to source water quality as WTW 2 is supplied by an upland reservoir, whereas WTW 16 is supplied by a river source. Raw water TCC and ICC were only sampled within WTW 2 & WTW 16 (see Section 4.5.1), and are presented in Figure 7.2. Mean TCC within raw reservoir water supplying WTW 2 ($2.51 \times 10^6 \pm 1.7 \times 10^6$ cells/mL) was much higher than the river water supplying WTW 16 ($1.08 \times 10^6 \pm 9.22 \times 10^5$ cells/mL; Figure 7.2). When split into monthly averages, the greatest TCC was found within June (early summer peak) at WTW 2, and September (late summer peak) at WTW 16.

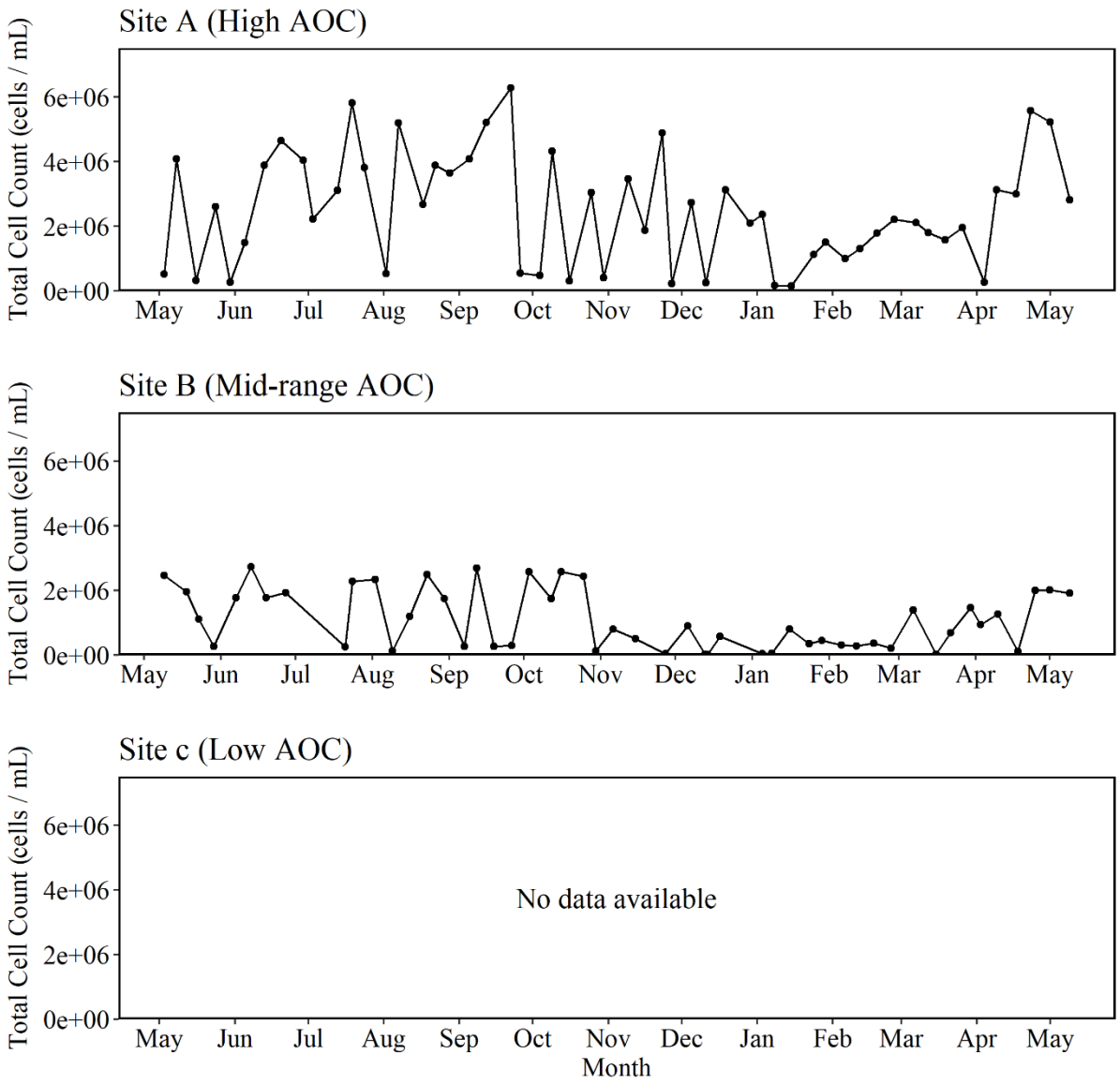

Figure 7.2: Total cell count (TCC) concentration (n=1)* in raw water at WTW 2 (A) and WTW 16 (B), plotted against time. TCC was sampled every 2 days for 1 year. TCC was not sampled within raw water at WTW 20 (C). *see Section 4.4.1 for details of samples collected by Scottish Water.

ICC exhibited the same trend as TCC; the average ICC within the raw water supplying WTW 6 contained more intact cells (mean=1,987,970, StDev=1,473,259 cells/mL) than raw water supplying WTW 20 (mean=865,171, StDev=801,794 cells/mL) (Figure 7.3). The percentage of cells found to be intact within raw water was on average 79% in WTW 2, and 80% in WTW 16. Consistent with TCC, maximum ICC within WTW 2 again peaked in September, whereas maximum ICC within WTW 16 peaked during October. Both TCC and ICC within raw water

exhibited a high degree of variability throughout the year (WTW 2 TCC range = =157,640 - 6,284,000, ICC range = 130,320 – 6,489,600; WTW 16 TCC range 3,200 – 2,737,200; WTW 16 TCC range = 0 – 2,504,400). This high level of variability was not reflected in the AOC concentration in the raw water (Figure 7.1)

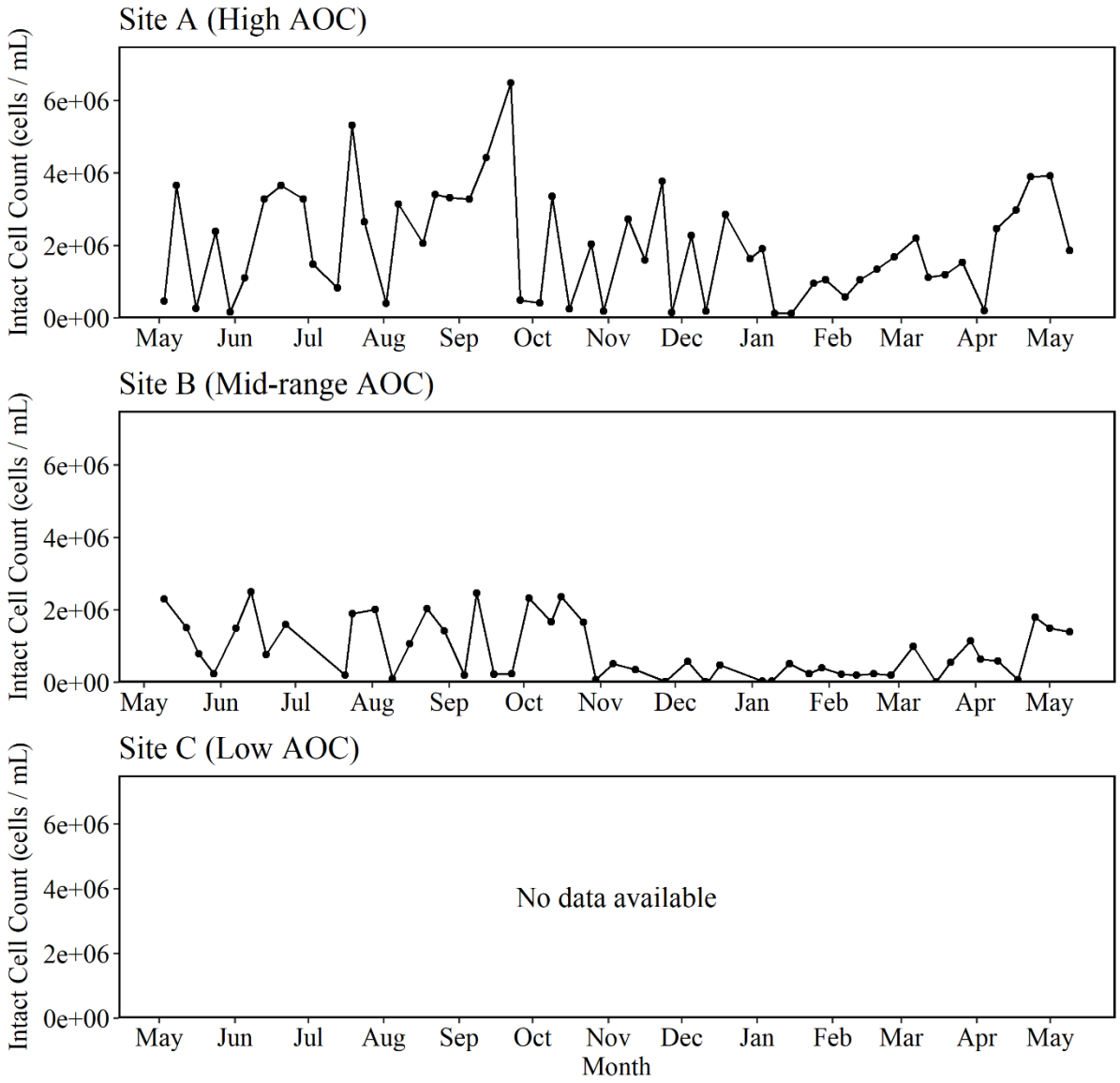

Figure 7.3: Intact cell count (ICC) concentration (n=1)* in raw water at WTW 2 and WTW 16, plotted against time. ICC was sampled every 2 days for 1 year. ICC was not sampled within raw water at WTW 20 (C). *see Section 4.4.1 for details of samples collected by Scottish Water.

7.3.2 The Impact of AOC on Post-Treated and Pipe Loop Bulk Water Quality

To determine the impact of the AOC concentration on bulk-water microbial water quality and biostability, post-treated bulk water quality was monitored at the WTW, in parallel with water

from each of the three pipe loops (PL): PL A (WTW 2), PL B (WTW 16) and PL C (WTW 20). Bulk water sampling ensured that the water in each of the pipe loops was representative of post-treated water entering each of the DWDS, and therefore any biofilm data is likely representative of the network. For all bulk water parameters, post-treated water and pipe loop water were of similar quality and exhibited the same trends (Figures 7.4 – 7.8). Total chlorine remained fairly constant throughout the 12 month period at all sample points, of each site (Figure 7.4). Mean total chlorine in post-treated water at WTW 2 was 0.89 ±0.11 mg/L; 1.34 ±0.15 mg/L at WTW 16 and 0.64 ±0.10 mg/L at WTW 20.

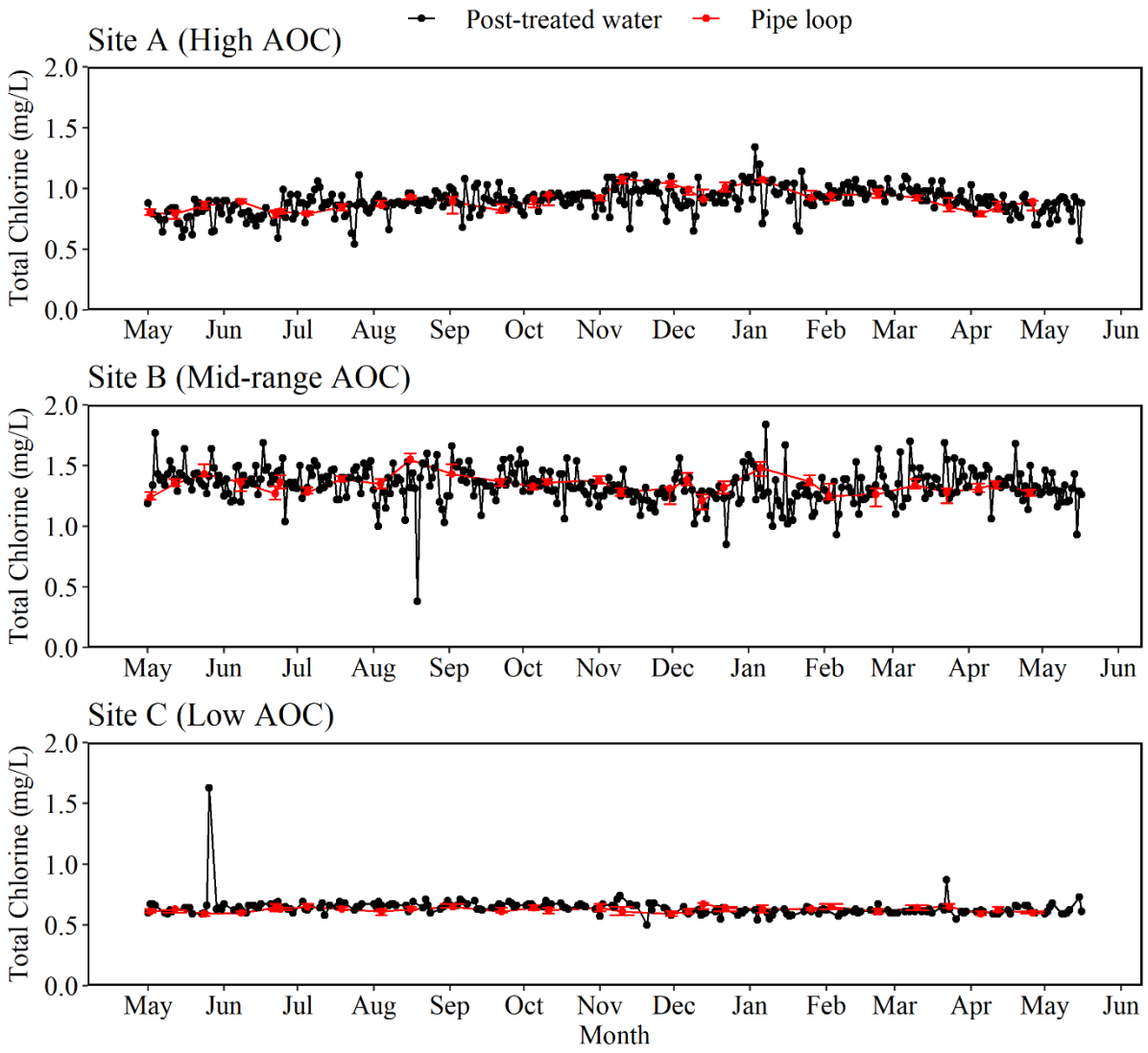

Figure 7.4: Total chlorine in post-treated water (n=1)* (black) and pipe loop (n=3) (red) at WTW 2 (Pipe loop A) (A), WTW 16 (Pipe loop B) (B) and WTW 20 (Pipe loop C) (C), plotted against time. Total chlorine in post-treated water was sampled every 2 weeks for 1 year. WTW 2: chlorine, WTW 16: chloramine; WTW 20: chloramine. Pipe loop data (red) is average ±StDev. *see Section 4.4.1 for details of samples collected by Scottish Water.

The mean water temperature within post-treated water supplying the three pipe loops showed little variation between sites; 9.1 ±5.3°C at WTW 2, 9.7 ±5.8°C at WTW 16 and 9.1 ±0.9°C at WTW 20 (Figure 7.5). Both post-treated water from WTW 2 (surface water reservoir source) and WTW 16 (a surface water river source) exhibited a seasonal variation, whilst the water temperature at WTW 20 remained relatively constant throughout the 12 month period, consistent with the behaviour of a ground water source. WTW 2 and WTW 16 exhibited an

18.0°C and 19.3°C difference in temperature, respectfully, during the study, whilst WTW 20 exhibited only a 6.9°C difference in temperature over the 12 months.

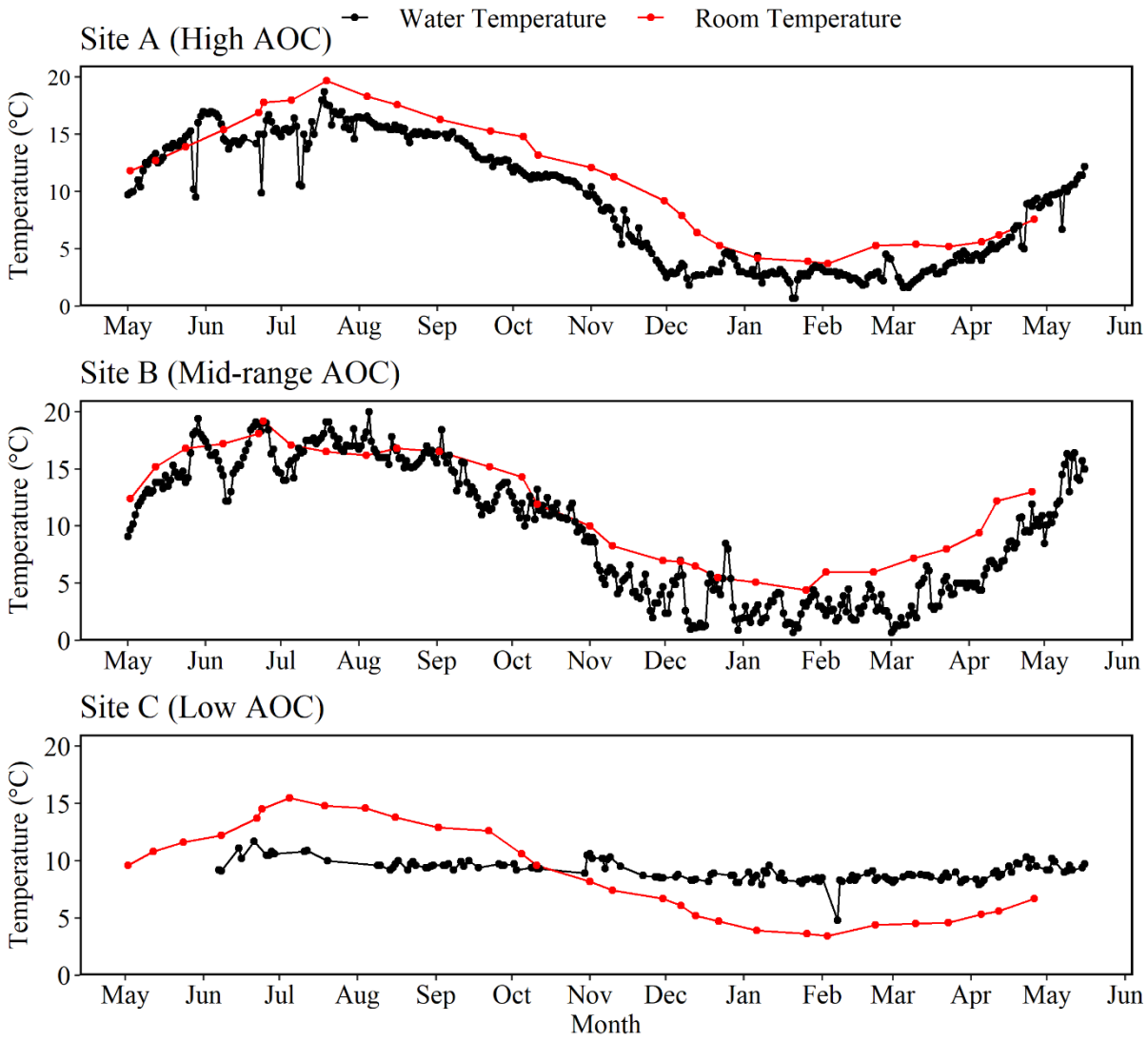

Figure 7.5: Temperature in post-treated water (n=1)* (black) and pipe loop sample tap (n=3) (red) at WTW 2 (Pipe loop A) (A), WTW 16 (Pipe loop B) (B) and WTW 20 (Pipe loop C) (C), plotted against time. Temperature in post-treated water was sampled every 2 weeks for 1 year. Pipe loop data (red) is average ±StDev. *see Section 4.4.1 for details of samples collected by Scottish Water.

Turbidity remained constantly low throughout the 12 months, containing a mean of 0.2 ±0.1 NTU within post-treated water at WTW 2 (0.2 ±0 NTU in PL A), 0.2 ±0.1 NTU within post-treated water at WTW 16 (0.2 ±0 NTU in PL B) and 0.2 ±0 at WTW 20 (0.2 ±0 NTU in PL

C). Iron remained below the limits of detection (<7 µg/l) in post-treated water leaving all three WTW throughout the 12 month sampling period. Manganese within post-treated water was highest at WTW 2 (mean=5.98 ±4.09 µg/l) and WTW 16 (4.96 ±3.01 µg/l) and lowest within WTW 20 (2.05 ±0.40 µg/l). All three WTW had low or no culturable colonies at 22°C; mean=0 ±1 CFU /mL at WTW 2, 0 ±1 CFU /mL at WTW 16, 0 ±1 CFU /mL at WTW 20, or 37°C; mean=0 ±0 CFU /mL at WTW 2, 0 ±0 CFU /mL at WTW 16, 0 ±0 CFU /mL at WTW 20.

The AOC concentration within post-treated water exhibited similar seasonal trends to raw water data, but at a lower level. The AOC concentration was highest within post-treated water leaving WTW 2 (mean=300 µg C / L), mid-range in WTW 16 (mean=245 µg C/ L) and lowest in WTW 20 (mean=73 µg C / L) (See Figure 7.6). The AOC concentration within post-treated water at WTW 20 showed least seasonal variation, consistent with behaviour of ground water source waters.

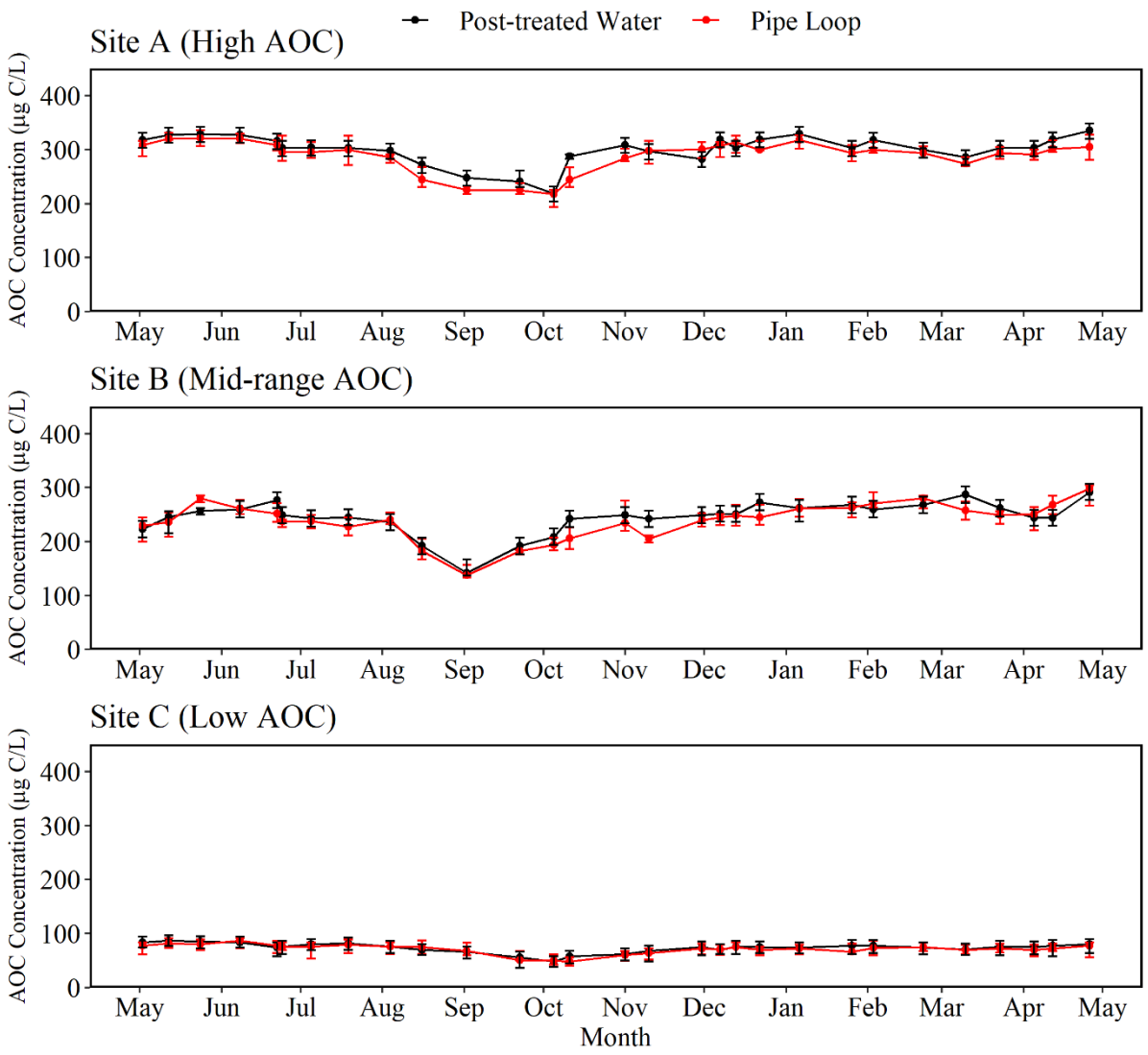

Figure 7.6: Assimilable organic carbon (AOC) concentration in post-treated water (n=3) (black) and pipe loop sample tap (n=3) (red) at WTW 2 (Pipe loop A) (A), WTW 16 (Pipe loop B) (B) and WTW 20 (Pipe loop C) (C), plotted against time. AOC concentration in post-treated water and pipe loop sample tap was sampled every 2 weeks for 1 year. Pipe loop data (red) is average ±StDev.

TCC and ICC were highest within Pipe loop A, the site supplied by post-treated water from WTW 2 which contained the highest AOC concentration. Mean TCC was 118,668 cells / mL within WTW 2, 1691 cells / mL within WTW 16 and 450 cells / mL within site 20 (Figure 7.7, *n.b.* the different y-axis in each plot A, B & C). The variability in TCC and ICC in the raw

water was also observed in post-treated water at WTW 2 and WTW 16, suggesting that the treatment process was not removing all cells.

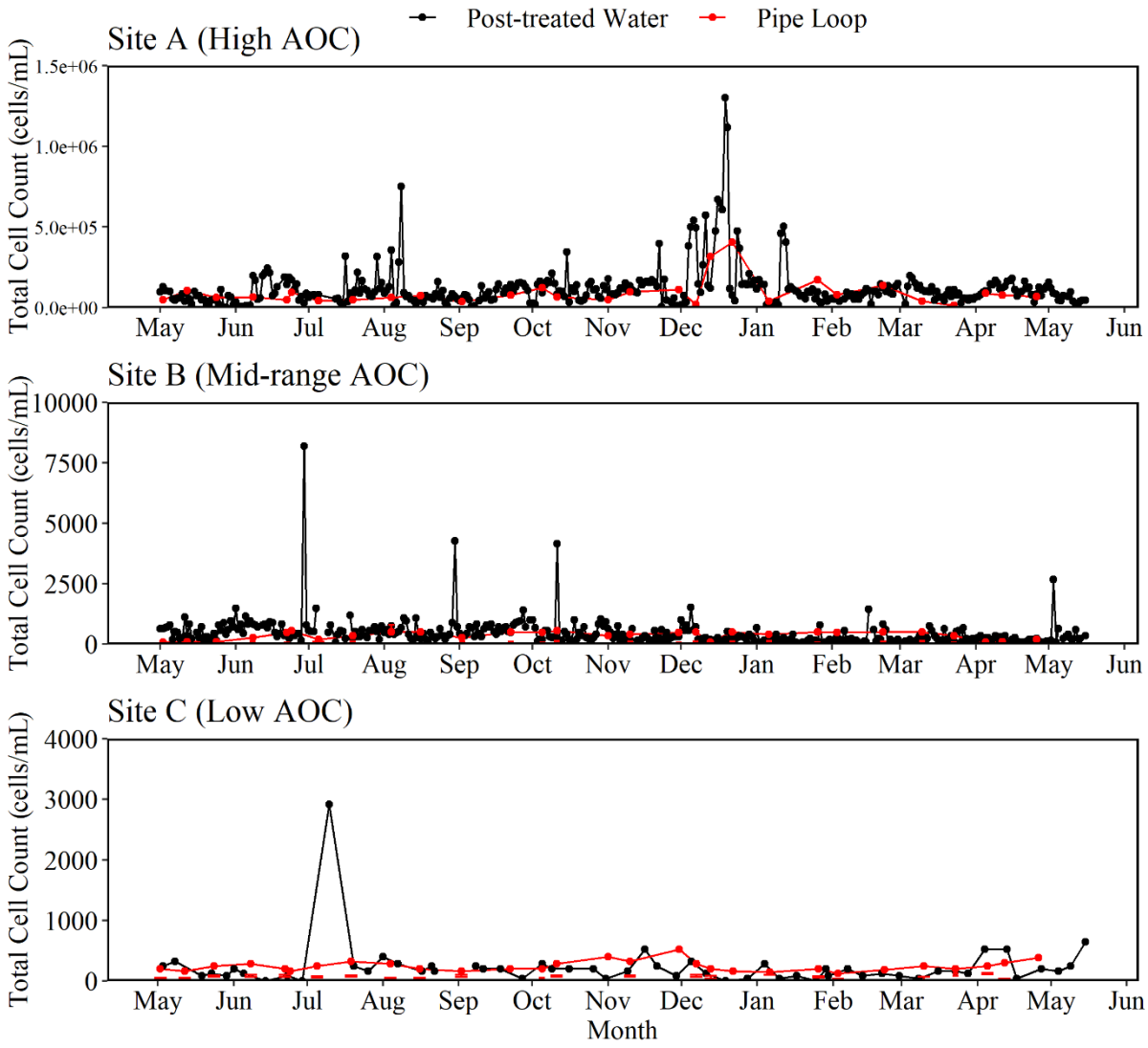

Figure 7.7: Total cell count (TCC) concentration in post-treated water (n=1)* and pipe loop sample tap (n=3) at WTW 2 (Pipe loop A) (A), WTW 16 (Pipe loop B) (B) and WTW 20 (Pipe loop C) (C), plotted against time. TCC was sampled every 2 days in post-treated water and every 2 weeks at the pipe loop sample tap for 1 year. Nb the different y-axis in each plot (A, B & C). Pipe loop data (red) is average ±StDev. Data point 12,800 cells/mL on 31/08/2017 within post-treated water leaving WTW 20 was removed as it was deemed to be an anonymous result. *see Section 4.4.1 for details of samples collected by Scottish Water.

ICC within post-treated water in WTW 2 were again considerably higher than the other two sites (Figure 7.8 (*n.b.* the different y-axis in each plot A, B & C)). Mean TCC was 569 (0 –

24,720) cells / mL within WTW 2, 206 (0 – 33,200) cells / mL within WTW 16 and 49 (0 – 160) cells / mL within WTW 20. The high level of variability in TCC and ICC within raw water (Figures 7.2 and 7.3) is also visible in post-treated water (Figures 7.7 and 7.8), suggesting that raw water variability is able to get through the treatment process at the WTW.

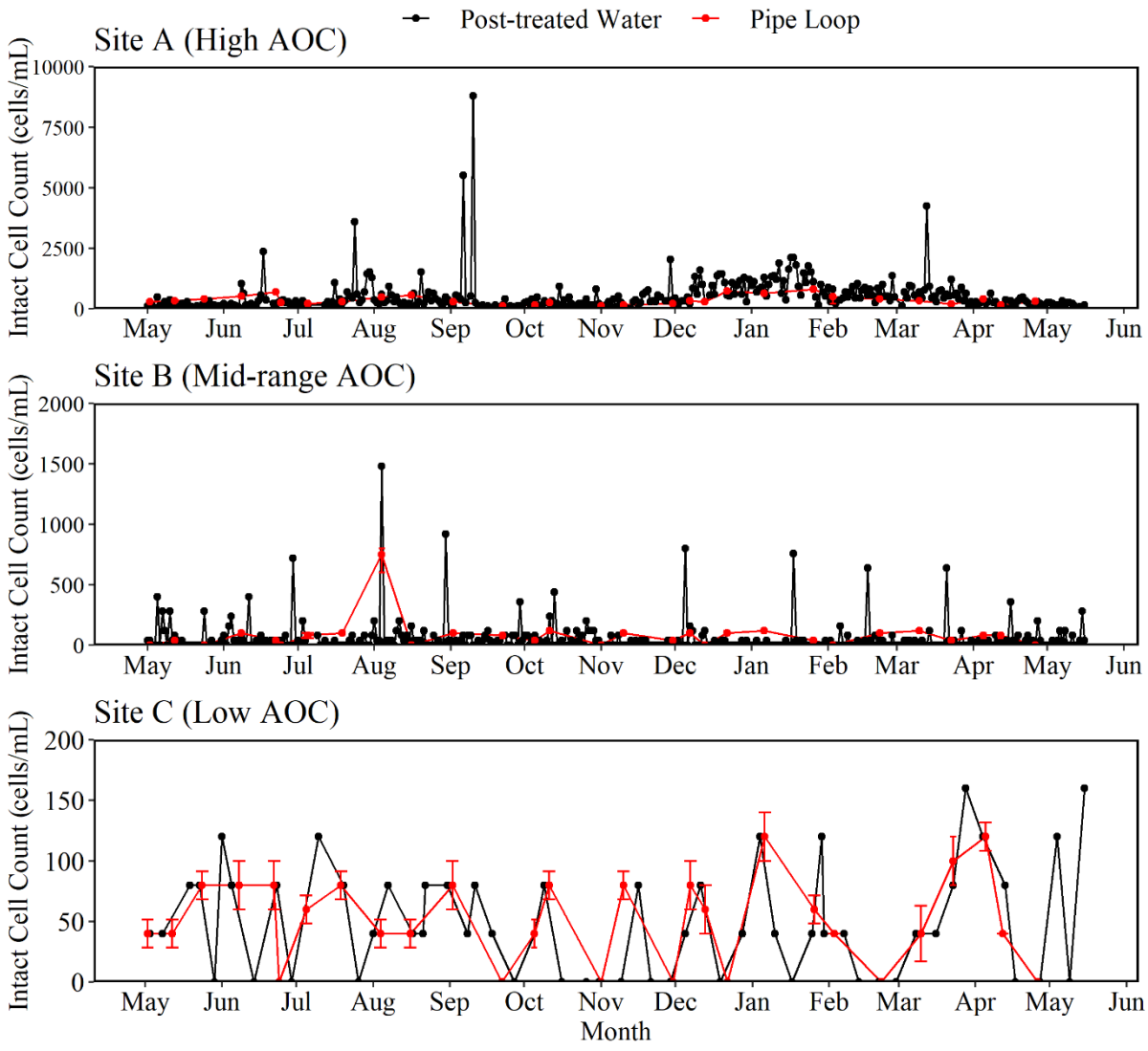

Figure 7.8: Intact cell count (ICC) concentration in post-treated water (n=1)* and pipe loop sample tap (n=3) at WTW 2 (Pipe loop A) (A), WTW 16 (Pipe loop B) (B) and WTW 20 (Pipe loop C) (C), plotted against time. ICC was sampled every 2 days in post-treated water and every 2 weeks at the pipe loop sample tap for 1 year. Nb the different y-axis in each plot (A, B & C). Pipe loop data (red) is average ±StDev. *see Section 4.4.1 for details of samples collected by Scottish Water.

7.3.3 The Impact of AOC Concentration on Bulk Water Community Composition

The impact of AOC concentration on the community composition of bacteria and fungi within the bulk water of Pipe Loops A, B and C. Water samples were collected at the beginning of the experiment growth phase (Day 0), after 6 months and at the end of the growth phase (Month 12). DNA was successfully extracted from all bulk water samples.

7.3.3.1 Bacterial and Fungal Community Analysis

The bacterial and fungal bulk water community composition was found to vary over time and between different sites. The dominant bacterial class within bulk water samples was *Proteobacteria.* The dominant genera within bacterial bulk water communities varied over time and location with *Herbaspirillum, Pseudomonas, Brucella, Acinetobacter, Staphylococcus* and *Gloeobacter* all being dominant at different times. *Pseudomonas* was particularly dominant at Site A, containing the highest AOC concentration. A similar trend was also shown with regards to fungal communities. More variation was evident over time and between sites in the bulk water than biofilms, with *Pezizaceae, Psathyrellaceae, Pleosporaceae, Cladosporiaceae, Aspergillaceae* and *Cladosporiaceae* all being abundant at different time points. *Pleosporaceae* was particularly dominant at Site A, containing the highest AOC concentration.

Figure 7.9 shows the similarities in bacterial community between all bulk water samples (Day 0, Month 6 and Month 12), analysed at the OTU level. The dendrogram was plotted using bacterial OTU relative abundance data. A clear site difference was identified between the three pipe loops, with samples clustering by AOC concentration (high, medium and low). Bulk water within Pipe Loop A (characterised by a high AOC concentration), was the only site to exhibit a change in bacterial community over time (Clusters 1, 2 & 3, Figure 7.9).

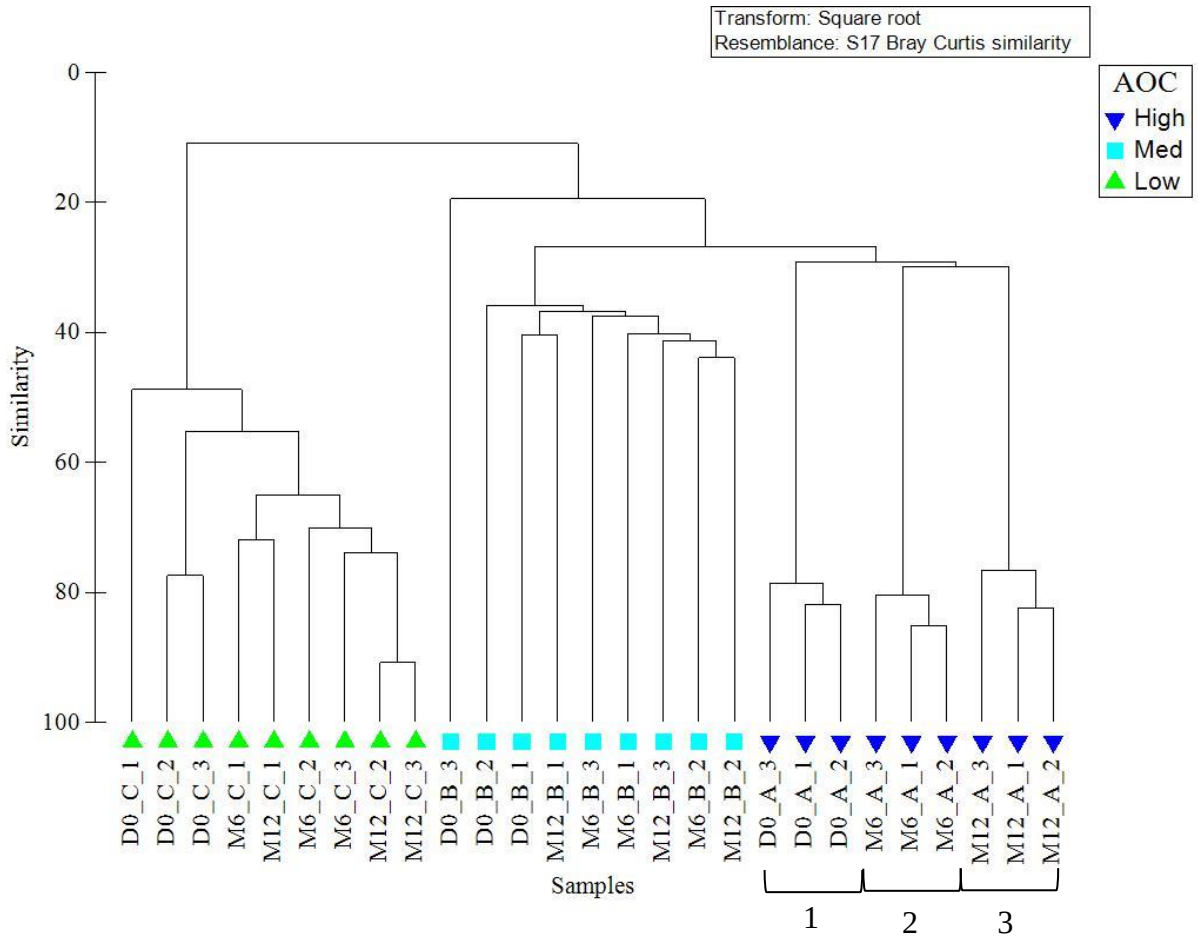

Figure 7.9: Dendrogram plotted using post-treated bulk water bacterial OTU relative abundance data from water supplying PL A (high AOC concentration), PL B (medium AOC concentration) and PL C (low AOC concentration). Data was square root transformed and a Bray Curtis similarity matrix was generated. Sample identification numbers are shown (first letter / number indicates time point, the second letter indicates the pipe loop, and the third number indicates the triplicate number). Samples are grouped by AOC concentration.

Bulk water samples were further compared visually (Figure 7.10) and statistically (Tables 7.3 and 7.4) to determine if the site difference in bacterial community composition was statistically significant. Figure 7.10 presents an nMDS plot of Day 0, Month 6 and Month 12 bacterial OTU relative abundance data. A clear site effect was being evident, with three distinct clusters at high, medium and low AOC concentration, being identified.

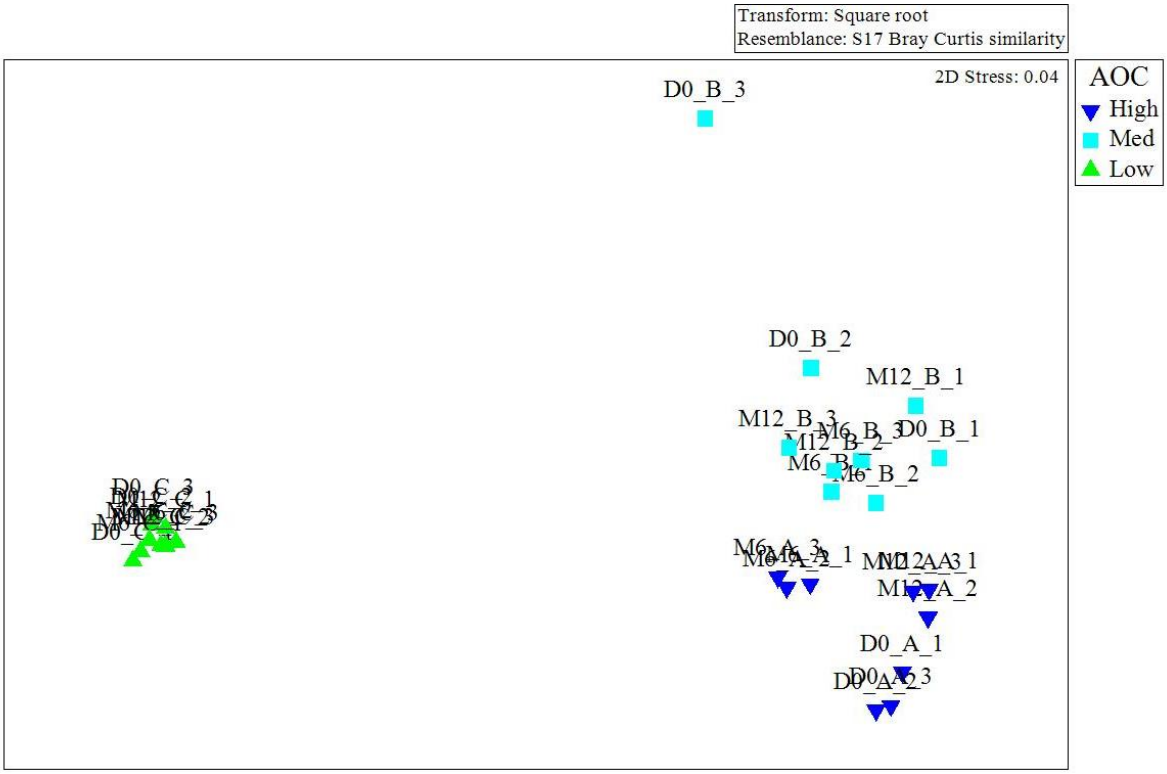

Figure 7.10: Visualisation of bacterial community similarities within post-treated bulk water. nMDS plotted using 12 month bacterial OTU relative abundance data. Data was square root transformed and a Bray Curtis similarity matrix was generated. Sample identification numbers are shown (first letter / number indicates time point, the second letter indicates the pipe loop, and the third number indicates the triplicate number).

ANOSIM values confirm that the site difference is statistically significant for all relative abundance data (see Table 7.3). ANOSIM data by site showed that presence / absence data had, on average, a higher global R value than relative abundance data. This indicated that similar community bacterial community members were present, but at different abundances. SIMPER analysis identified that average dissimilarity was higher for relative abundance data (84.95±5.53) than presence absence data (61.52±9.56). Bio-replicates at each sample point were found to be most similar within bulk water in Pipe Loop C (containing a low AOC concentration) (see SIMPER analysis, Table 7.4). 12 month bacterial samples from Pipe Loop A and Pipe Loop B showed more variation between replicates (see Table 7.4), suggesting that higher AOC values created a more variable community within the bulk water.

Table 7.3: ANOSIM values for bulk water bacteria OTU relative abundance and presence / absence data, including Day 0, Month 6 and Month 12.

Samples	Data	Global R Value	p-Value
Day 0 (ANOSIM by site)	Presence / absence	0.533	0.086
	Relative abundance	0.975	0.039
Month 6 (ANOSIM by site)	Presence / absence	0.441	0.050
	Relative abundance	1	0.041
Month 12 (ANOSIM by site)	Presence / absence	0.622	0.048
	Relative abundance	1	0.026
Site A: Day 0 and Month 12 (ANOSIM by date)	Presence / absence	0.432	0.236
	Relative abundance	0.521	0.186
Site B: Day 0 and Month 12 (ANOSIM by date)	Presence / absence	0.384	0.264
	Relative abundance	0.466	0.120
Site C: Day 0 and Month 12 (ANOSIM by date)	Presence / absence	0.111	0.200
	Relative abundance	0.362	0.200

Global R value: 0 = same, 1 = completely different. The significance level is the p value <0.05: significant; >0.05: weak evidence).

Table 7.4: SIMPER analysis Day 0 and Month 12 bulk water bacteria OTU presence / absence and relative abundance data.

Date	Data	Site	Average Similarity[A]	Site Group	Average Dissimilarity[B]
Presence/ absence	Day 0	A	28.21	Site A & Site B	52.56
		B	38.62	Site B & Site C	61.11
		C	42.05	Site A & Site C	77.27
	Month 12	A	21.36	Site A & Site B	51.36
		B	29.14	Site B & Site C	60.42
		C	43.22	Site A & Site C	66.38
Relative Abundance	Day 0	A	10.45	Site A & Site B	75.41
		B	16.63	Site B & Site C	84.23
		C	23.58	Site A & Site C	90.10
	Month 12	A	10.90	Site A & Site B	83.86
		B	14.83	Site B & Site C	85.33
		C	22.23	Site A & Site C	90.74

[A]Average similarity between samples taken at same time point, at the same site; [B]Average dissimilarity between different sites (A, B & C).

A dendrogram shows the similarities in fungal community between all bulk water samples (Day 0, Month 6 and Month 12), analysed at the OTU level (Figure 7.11). As found with bacterial OTU relative abundance bulk water data (Figure 7.9), samples were found to group by AOC concentration (high, medium and low). Site A exhibited also exhibited a change in community composition with time, with three distinct clusters at Day 0, Month 6 and Month 12 (Figure 7.11; clusters 2, 3 and 4) being identified. A distinct cluster was also identified at Day 0 within Pipe Loop C (Figure 7.11; cluster 1).

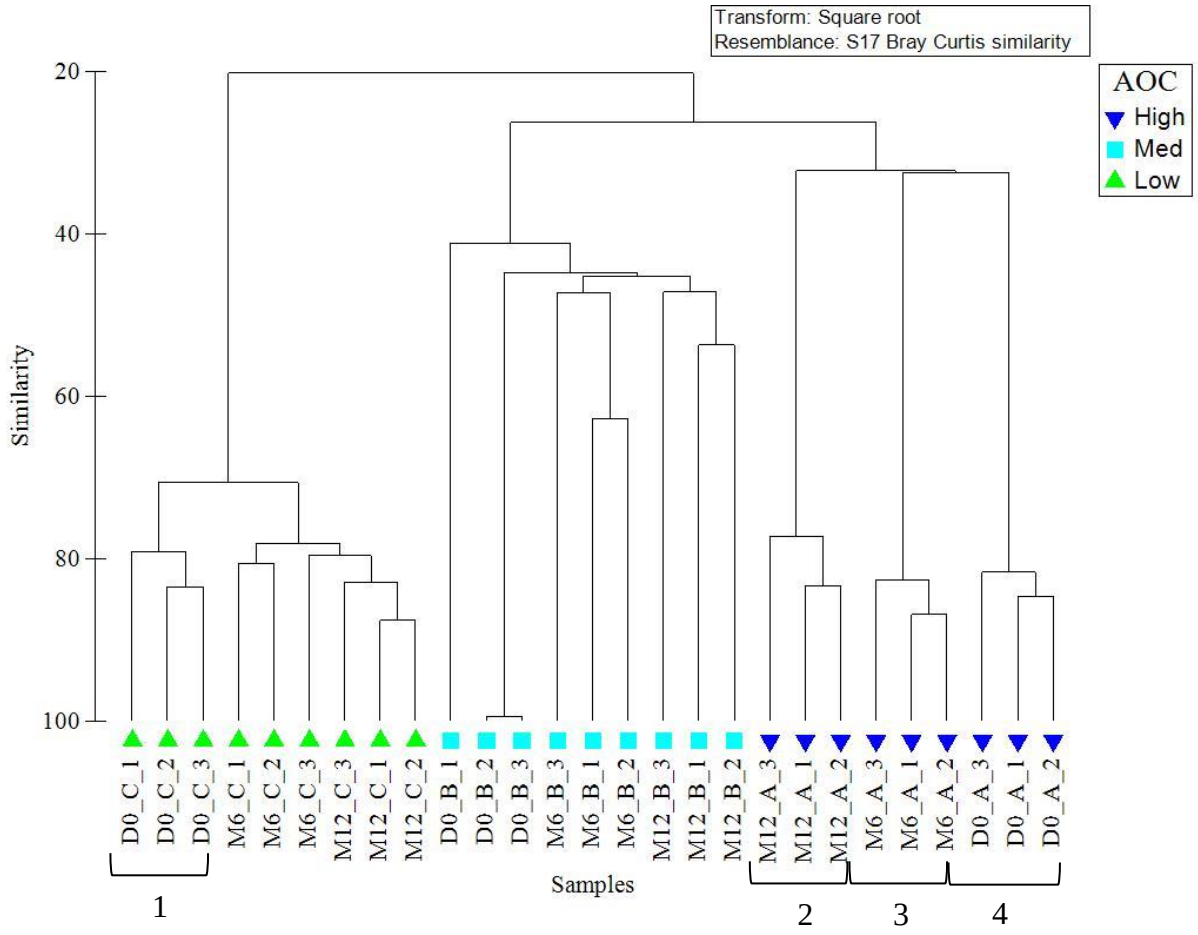

Figure 7.11: Dendrogram plotted using fungal OTU relative abundance data from post-treated bulk water quality supplying PL A (high AOC concentration), PL B (medium AOC concentration) and PL C (low AOC concentration). Data was square root transformed and a Bray Curtis similarity matrix was generated. Sample identification numbers are shown (first letter / number indicates time point, the second letter indicates the pipe loop, and the third number indicates the triplicate number). Samples are grouped by AOC concentration.

Figure 7.12 presents an nMDS plot of Day 0, Month 6 and Month 12 bacterial OTU relative abundance data. A clear site effect was again evident, with three distinct clusters by AOC concentration (high, medium and low). ANOSIM values confirm that the site difference in fungal relative abundance was statistically significant (Table 7.5). The community composition of fungi within bulk water in Pipe Loop A was also found to cluster by date (Figure 7.12), suggesting the community composition at this site is most subject to seasonal changes. Similar to bacterial relative abundance data, SIMPER analysis of relative abundance data identified that average dissimilarity was higher for relative abundance data (67.03±3.14) than presence absence data (59.78±2.45). Bio-replicates at each sample point were found to be most similar within bulk water within Pipe Loop C (containing a low AOC concentration), and most different within Pipe Loop A bulk water (containing a high AOC concentration (see SIMPER analysis, Table 7.6). This suggests that a higher AOC values created a more variable fungal community within the bulk water.

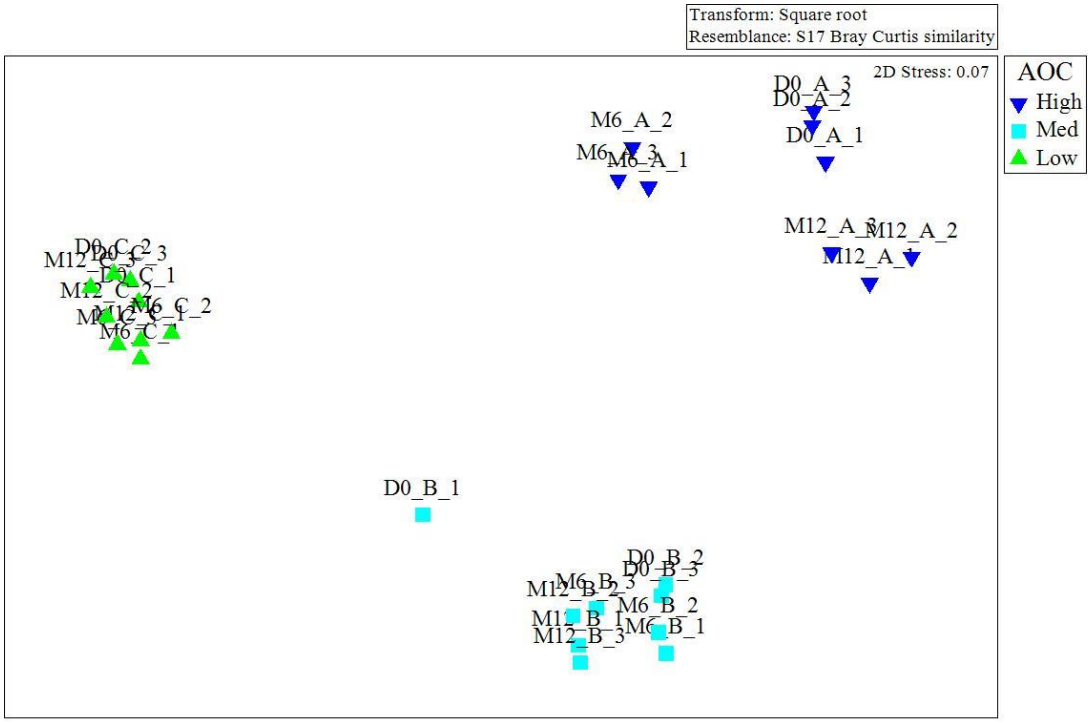

Figure 7.12: Visualisation of fungal community similarities within post-treated bulk water. nMDS plotted using 12 month fungal OTU relative abundance data. Data was square root transformed and a Bray Curtis similarity matrix was generated. Sample identification numbers are shown (first letter / number indicates time point, the second letter indicates the pipe loop, and the third number indicates the triplicate number).

Table 7.5: ANOSIM values for bulk water bacteria OTU relative abundance and presence / absence data, including Day 0, Month 6 and Month 12 data.

Samples	Data	Global R Value	p-Value
Day 0 (ANOSIM by site)	Presence / absence	0.642	0.010
	Relative abundance	0.912	0.050
Month 6 (ANOSIM by site)	Presence / absence	0.600	0.100
	Relative abundance	0.874	0.002
Month 12 (ANOSIM by site)	Presence / absence	0.542	0.032
	Relative abundance	0.911	0.010
Site A: Day 0 and Month 12 (ANOSIM by date)	Presence / absence	0.425	0.120
	Relative abundance	0.524	0.320
Site B: Day 0 and Month 12 (ANOSIM by date)	Presence / absence	0.345	0.122
	Relative abundance	0.311	0.060
Site C: Day 0 and Month 12 (ANOSIM by date)	Presence / absence	0.255	0.091
	Relative abundance	0.321	0.045

Global R value: 0 = same, 1 = completely different. The significance level is the p value <0.05: significant; >0.05: weak evidence).

Table 7.6: SIMPER analysis Day 0 and Month 12 bulk water bacteria OTU presence / absence and relative abundance data.

Date	Data	Site	Average Similarity[A]	Site Group	Average Dissimilarity[B]
Presence/ absence	Day 0	A	32.76	Site A & Site B	61.07
		B	42.91	Site B & Site C	60.17
		C	39.91	Site A & Site C	61.96
	Month 12	A	45.00	Site A & Site B	55.05
		B	63.10	Site B & Site C	59.64
		C	33.77	Site A & Site C	60.79
Relative Abundance	Day 0	A	34.55	Site A & Site B	65.96
		B	40.49	Site B & Site C	67.89
		C	28.23	Site A & Site C	69.83
	Month 12	A	39.46	Site A & Site B	61.41
		B	40.69	Site B & Site C	67.27
		C	24.95	Site A & Site C	69.84

[A]Average similarity between samples taken at same time point, at the same site; [B]Average dissimilarity between different sites (A, B & C).

7.3.3.2 The Impact of AOC on the Diversity Indices of Bacterial and Fungal Bulk Water Communities

Diversity indices tests, including relative richness, relative evenness and relative diversity were undertaken for bacterial (Table 7.7) and fungal communities (Table 7.8) from bulk water samples taken from Pipe Loops A, B & C to understand the impact of AOC concentration on the relative richness, relative evenness and relative diversity of biofilm samples. The relative richness, evenness and diversity of bacterial (Table 7.7) and fungal communities (Table 7.8) within bulk water at Day 0, Month 6 and Month 12 were found exhibit a clear site effect. No statistically significant changes were found over time for either taxa (see ANOSIM analysis Tables 7.3 and 7.5).

Table 7.7: Ecological indices of bacterial planktonic communities from drinking water bulk water samples supplying Pipe Loops A, B & C (n=3) at Day 0, Month 6 and Month 12. A) Relative richness, B) relative evenness, and C) relative diversity.

Pipe Loop	Time	Relative Richness (Chao)		Relative Evenness (Simpson)		Relative Diversity (Shannons Index)	
		Mean	Range	Mean	Range	Mean	Range
A	Day 0	1362.00	85.98	0.89	0.01	5.82	0.52
	6 Month	1251.33	184.32	0.88	0.04	5.85	0.71
	12 Month	1569.67	97.90	0.86	0.04	5.26	1.00
B	Day 0	911.00	30.27	0.94	0.01	3.89	0.55
	6 Month	796.00	61.51	0.93	0.01	4.27	0.28
	12 Month	914.67	57.83	0.94	0.01	4.51	0.13
C	Day 0	622.67	127.01	0.98	0.02	3.20	0.17
	6 Month	566.00	110.57	0.98	0.01	3.73	0.44
	12 Month	710.33	83.63	0.99	0.01	3.63	0.45

Table 7.8: Ecological indices of fungal planktonic communities from drinking water bulk water samples supplying Pipe Loops A, B & C (n=3) at Day 0, Month 6 and Month 12 . A) Relative richness, B) relative evenness, and C) relative diversity.

Pipe Loop	Time	Relative Richness (Chao)		Relative Evenness (Simpson)		Relative Diversity (Shannons Index)	
		Mean	Range	Mean	Range	Mean	Range
A	Day 0	1005.67	15.82	0.89	0.03	4.84	0.68
	6 Month	1013.67	31.63	0.86	0.01	5.21	0.35
	12 Month	994.67	54.15	0.90	0.02	4.69	0.71
B	Day 0	755.67	116.32	0.94	0.01	3.87	0.41
	6 Month	871.67	53.78	0.95	0.02	4.15	0.28
	12 Month	783.33	49.00	0.94	0.01	3.96	0.42
C	Day 0	651.67	72.25	0.97	0.00	3.30	0.28
	6 Month	686.67	75.08	0.99	0.01	3.51	0.29
	12 Month	646.33	61.08	0.99	0.01	3.13	0.10

7.3.4 The Impact of AOC Concentration on the Bulk water Response within Pipe Loops Test Facilities during Flushing

The effect of AOC concentration on how easily material was mobilised into the bulk water under elevated shear stress (flushing) was determined. Following on from the 12 month growth phase, the bulk quality of each of the pipe loops (A, B & C) was assessed at each of the flushing steps implemented during the mobilisation phase (see Section 4.6.4.1, Table 4.6). The turbidity, iron, manganese, TCC, ICC, TOC and AOC concentration within the bulk water were plotted at each flow rate / shear stress (Figure 7.13 – Figure 7.19). The calculations used to generate the shear stress are listed in Appendix 5.

7.3.4.1 Turbidity, Iron and Manganese Bulk water Response to Increased Shear Stress

The bulk water turbidity response during flushing is shown in Figure 7.13. Pipe Loops B and C exhibited a positive, linear turbidity response as the shear stress was raised. Pipe loop A, the site supplied by post-treated water containing the highest AOC concentration, exhibited the greatest turbidity response following mobilisation, increasing from 0.27 to 4.75 NTU. Pipe

Loop A therefore posed the greatest discoloration risk. Conversely, Pipe Loop C supplied by post-treated ground water containing the lowest AOC concentration experienced the smallest turbidity response increasing from 0.2 to 2.15 NTU. The turbidity response during flushing of Pipe Loop A did plateau slightly during the final flushing step, suggesting that material most material had been mobilised during the first flushing steps.

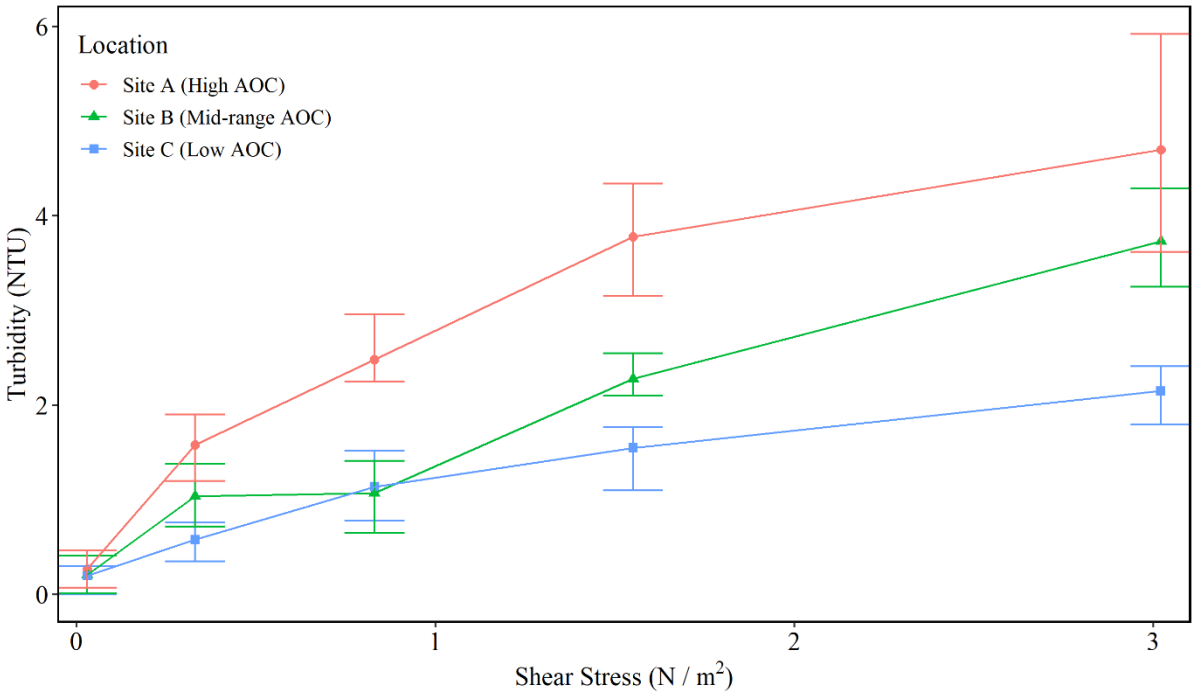

Figure 7.13: Turbidity in bulk water within pipe loop test facilities at Pipe loop A (WTW 2), Pipe loop B (WTW 16) and Pipe loop C (WTW 20), during the mobilisation phase. Turbidity was monitored using an online turbidity logger (averages are presented ± StDev).

Similar to the turbidity response in each of the pipe loops, the concentration of iron (Figure 7.14) and manganese (Figure 7.15) in the bulk water following flushing was highest in Pipe Loop A, and lowest in Pipe Loop C. All three sites contained relatively low iron (mean=12.53 µg/L in Pipe Loop A, mean=10.07 µg/L in Pipe Loop B and mean=6.83 µg/L in Pipe Loop C) and manganese (mean=8.67 µg/L in Pipe Loop A, mean=5.10 µg/L in Pipe Loop B and mean=3.10 µg/L in Pipe Loop C) concentration prior to flushing. Despite this, Pipe loop A exhibited the greatest increase in iron (increase of 225.00 µg/L) and manganese (increase of

33.90 µg/L) following flushing, as indicated by the gradient in Table 7.9. These results demonstrate that sufficient iron can accumulate over the course of a year to generate an iron failure (over 200 µg/l DWI, 2017) when flushing.

The gradient, R^2 and P values for turbidity, iron and manganese concentration in bulk water within each of the three pipe loop test facilities during the mobilisation phase are listed in Table 7.9. Pipe Loop A can be seen to have consistently the highest gradient value, confirming the greatest turbidity, iron and manganese was experienced within Pipe loop A. In contrast, the smallest gradient can consistently be found within Pipe Loop A. R^2 values are consistently high for turbidity, iron and manganese parameters within Pipe Loops A, B and C, indicating a linear response to the increase in shear stress during flushing.

Table 7.9: Gradient (G), R^2 and P values for turbidity, iron and manganese in bulk water within pipe loop test facilities at PL A (WTW 2), PL B (WTW 16) and PL C (WTW 20), during the mobilisation phase.

Pipe Loop ID	Turbidity			Iron			Manganese		
	Gradient[A]	R^{2B}	P value[C]	Gradient[A]	R^{2B}	P value[C]	Gradient[A]	R^{2B}	P value[C]
A	1.39	0.8902	0.0160	72.58	0.8947	0.0150	11.58	0.9110	0.0116
B	1.13	0.9720	0.0020	54.43	0.9300	0.0080	9.55	0.9447	0.0056
C	0.63	0.9374	0.0068	36.06	0.8948	0.0150	4.30	0.9564	0.0039

[A]The gradient defines the rate of change along the regression line; [B]R^2 value indicates the goodness of fit of the linear regression model to the data, nearer to 1 the better the fit; [C] A significant p value indicates that the gradient is significantly different from 0.

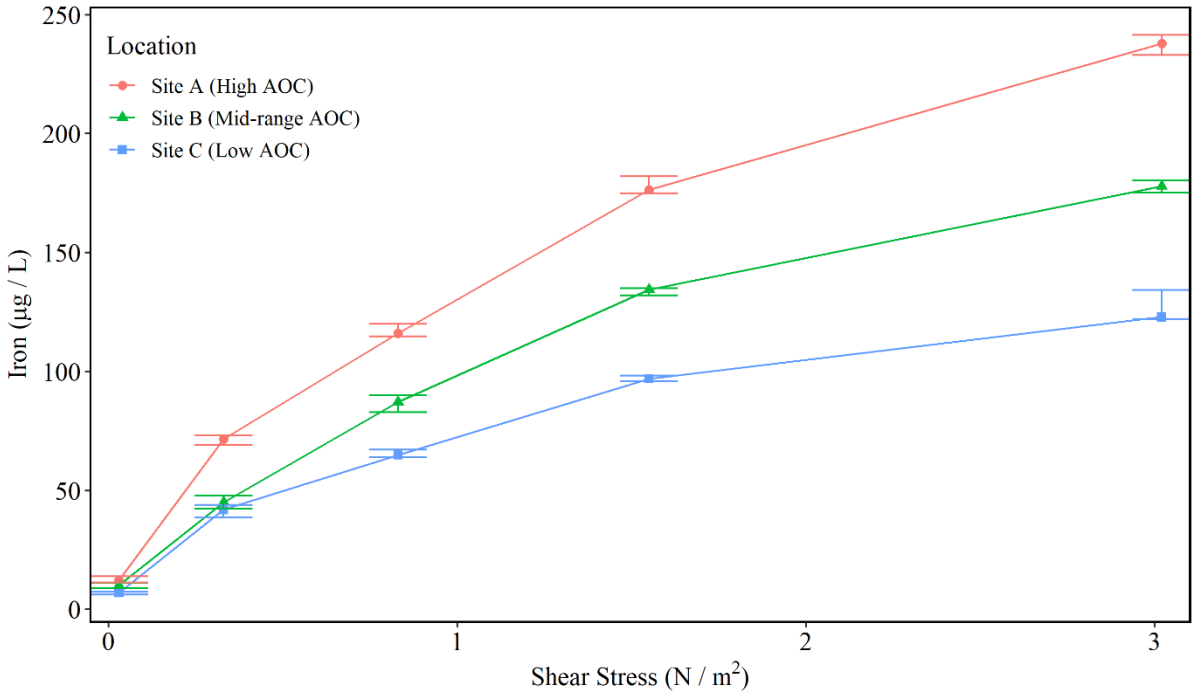

Figure 7.14: Iron (Fe) (n=3) in bulk water within pipe loop test facilities at Pipe loop A (WTW 2), Pipe loop B (WTW 16) and Pipe loop C (WTW 20), during the mobilisation phase.

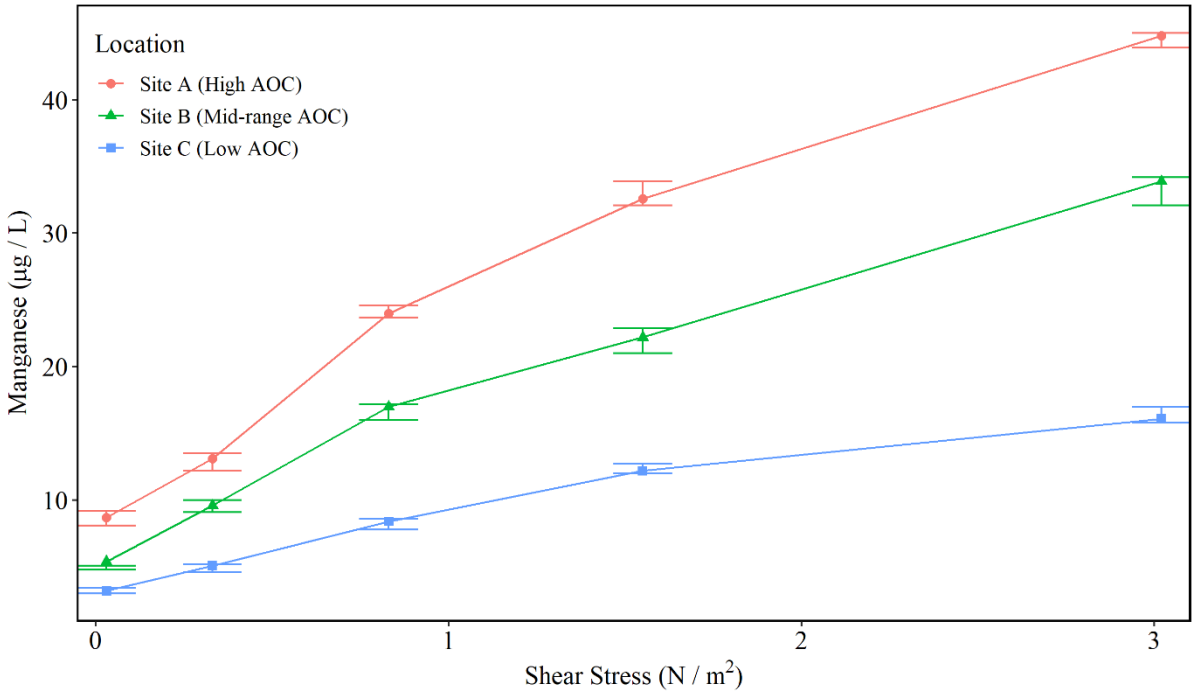

Figure 7.15: Manganese (Mn) (n=3) in bulk water within pipe loop test facilities at Pipe loop A (WTW 2), Pipe loop B (WTW 16) and Pipe loop C (WTW 20), during the mobilisation phase.

7.3.4.2 Cell Count Bulk Water Response to Increased Shear Stress

Prior to the commencement of flushing, post-treated water in Pipe loop A contained a higher concentration of TCC in the bulk water (mean=31,551 cells/mL) in comparison to Pipe loop B (mean=2039 cells/mL) and Pipe loop C (mean=250 cells/mL). Following flushing, all three pipe loops exhibited an increase of both TCC (Figure 7.16) and ICC (Figure 7.17) within bulk water. The TCC increased by the greatest extent within Pipe Loop A and Pipe Loop B, increasing by 21,229 cells/mL within Pipe Loop A, and 20,595 cells/mL within Pipe Loop. The bulk water within Pipe Loop C had the smallest increase in TCC during flushing, with the TCC increasing by 6376 cells/mL from the mixing phase to the final flushing step. Despite Pipe Loop A containing the highest TCC within bulk water at the end of the growth phase, the rate of change in TCC during mobilisation was highest in Pipe Loop B (see gradient values in Table 7.10).

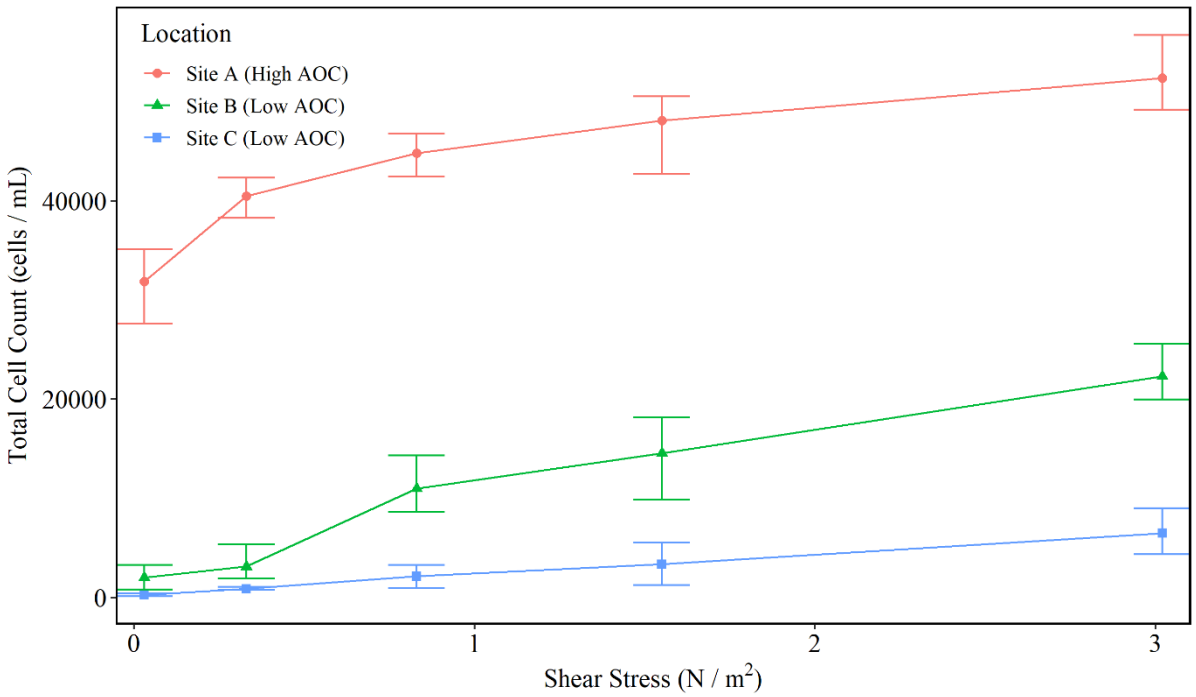

Figure 7.16: Total cell count (TCC) (n=3) in bulk water within pipe loop test facilities at Pipe loop A (WTW 2), Pipe loop B (WTW 16) and Pipe loop C (WTW 20), during the mobilisation phase.

In contrast to TCC, ICC within bulk water prior to mobilisation was relatively similar between sites, with 1,504 cells/mL within Pipe Loop A, 552 cells/mL within Pipe Loop B and 71 cells/mL within Pipe Loop C. The greatest increase in ICC following flushing occurred within Pipe Loop A (increase of 16,972 cells/mL), followed by Pipe Loop B (increase of 10,687 cells/mL) and finally the smallest increase in ICC within Pipe Loop C (4,816 cells/mL). During the mobilisation phase, TCC and ICC within bulk water in Pipe Loop A had the least linear response to shear stress, in comparison to Pipe Loop B and C.

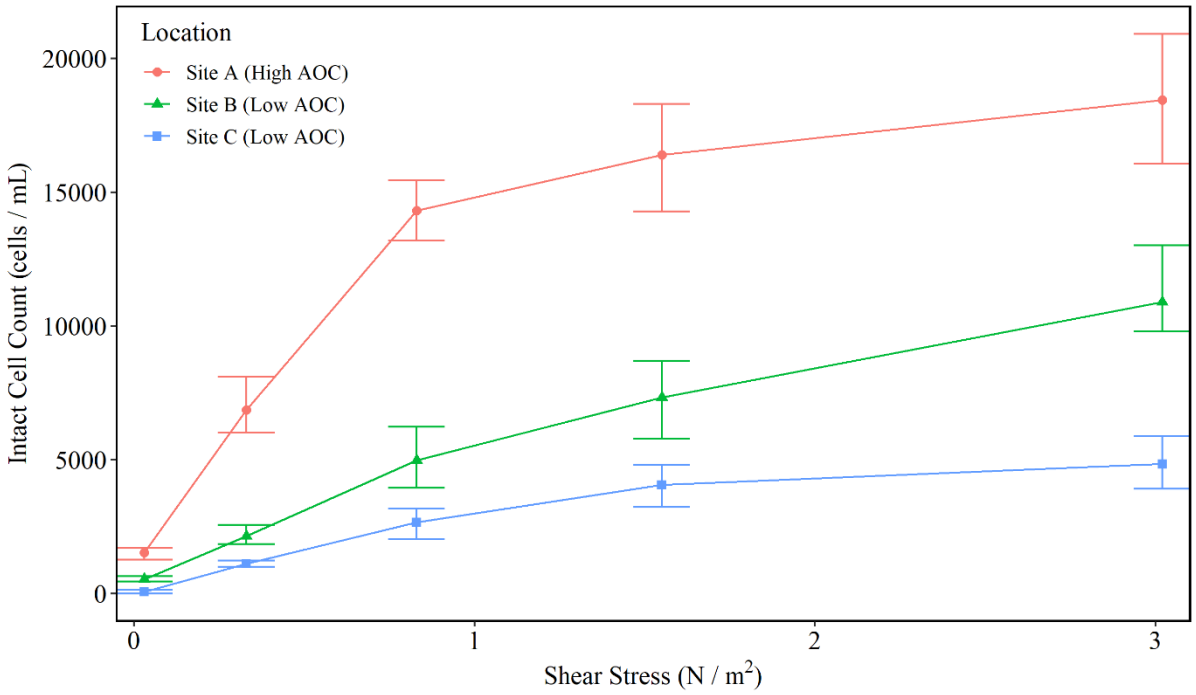

Figure 7.17: Intact cell count (ICC) (n=3) in bulk water within pipe loop test facilities at Pipe loop A (WTW 2), Pipe loop B (WTW 16) and Pipe loop C (WTW 20) during the mobilisation phase.

The gradient, R^2 and P values for TCC and ICC in bulk water within each of the three pipe loop test facilities during the mobilisation phase are listed in Table 7.10. Despite the largest turbidity, iron manganese and ICC response being observed in Pipe Loop A, the largest TCC gradient was found in Pipe Loop B.

Table 7.10: Gradient (G), R2 and P values for total cell count (TCC) and intact cell count (ICC) in bulk water within pipe loop test facilities at PL A (WTW 2), PL B (WTW 16) and PL C (WTW 20), during the mobilisation phase.

Pipe Loop ID	TCC			ICC		
	Gradient[A]	R^{2B}	P value[C]	Gradient[A]	R^{2B}	P value[C]
A	5902	0.8029	0.0396	5100	0.7362	0.0629
B	6870	0.9514	0.0046	3394	0.9621	0.0032
C	2072	0.9982	0.0000	1551	0.8656	0.0218

[A]The gradient defines the rate of change along the regression line; [B]R^2 value indicates the goodness of fit of the linear regression model to the data, nearer to 1 the better the fit; [C]A significant p value indicates that the gradient is significantly different from 0.

7.3.4.3 Organic Carbon Response

The response of TOC within bulk water in Pipe Loops A, B and C is plotted in Figure 7.18. The behaviour of TOC within bulk water during flushing mirrored all other water quality parameters (turbidity, iron, manganese, TCC and ICC), excluding AOC. TOC concentration was consistently highest within Pipe Loop A throughout the flushing phase. The greatest increase in TOC within bulk water was experienced within Pipe Loop A (increase of 9.50 mg/L), followed by Pipe Loop B (increase of 6.53 mg/L) and finally Pipe Loop C (4.53 mg/L).

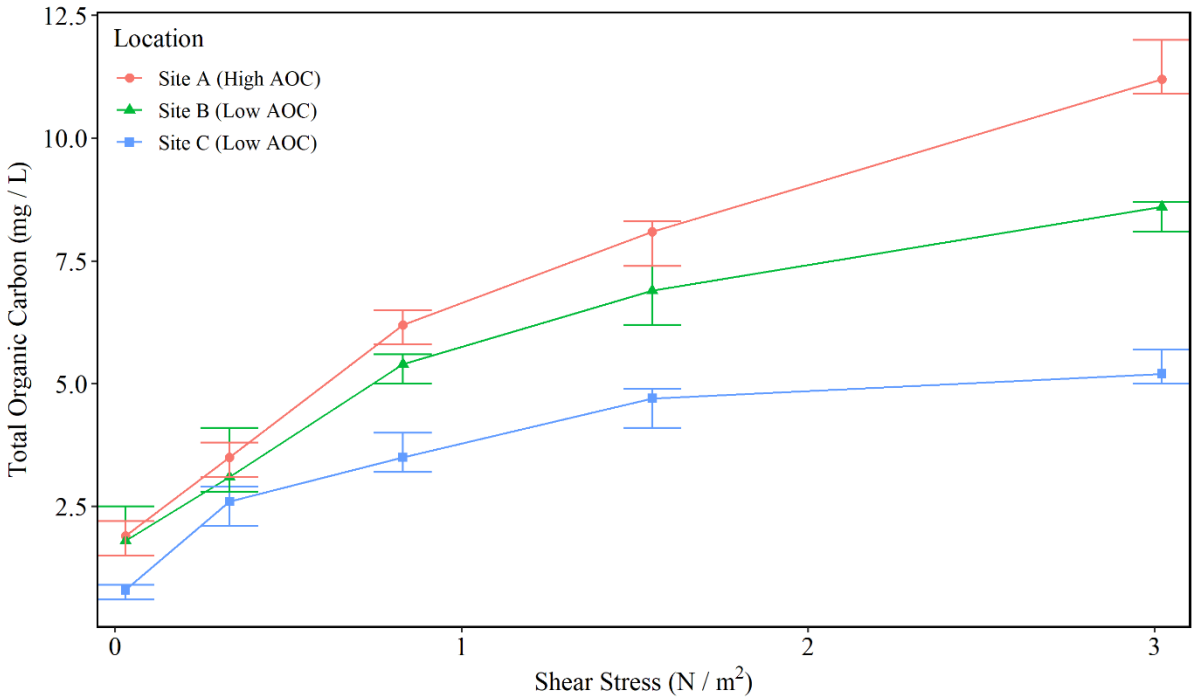

Figure 7.18: Total organic carbon (TOC) (n=3) in bulk water within pipe loop test facilities at Pipe loop A (WTW 2), Pipe loop B (WTW 16) and Pipe loop C (WTW 20), during the mobilisation phase.

In summary, all bulk water samples collected during mobilisation, including turbidity, iron, manganese, TCC, ICC and TOC exhibited a clear site effect. The largest response in each of these parameters during flushing was consistently observed within Pipe Loop A, with the smallest response being observed within Pipe Loop C. Pipe Loop A was fed within post-treated drinking water containing the highest AOC concentration during both the growth and mobilisation phase, whilst Pipe Loop C was supplied by bulk water containing the consistently the lowest AOC concentration.

In contrast to all of the other bulk water samples collected during mobilisation, the rate of AOC mobilisation from the biofilm was surprisingly similar between all three sites, independent of the background AOC concentration (Figure 7.19). The AOC response to an increase in shear stress was not linear, with all three pipe loops almost reaching a plateau in AOC concentration during the final flushing step. A clear site different in AOC concentration was exhibited within each pipe loop pre-flush (during the mixing step), with the highest AOC

concentration within Pipe Loop A (mean=284 µg/L), followed by Pipe Loop B (mean=202 µg C/L) and the lowest AOC concentration within Pipe Loop C (mean=43 µg C/L). However, the increase in AOC concentration from pre- to post-flush was unexpectedly the same or similar between sites, with a 115 µg C/L increase in AOC within Pipe Loop A, 120 µg C/L increase in AOC within Pipe Loop B, and a 115 µg C/L increase in AOC within Pipe Loop C.

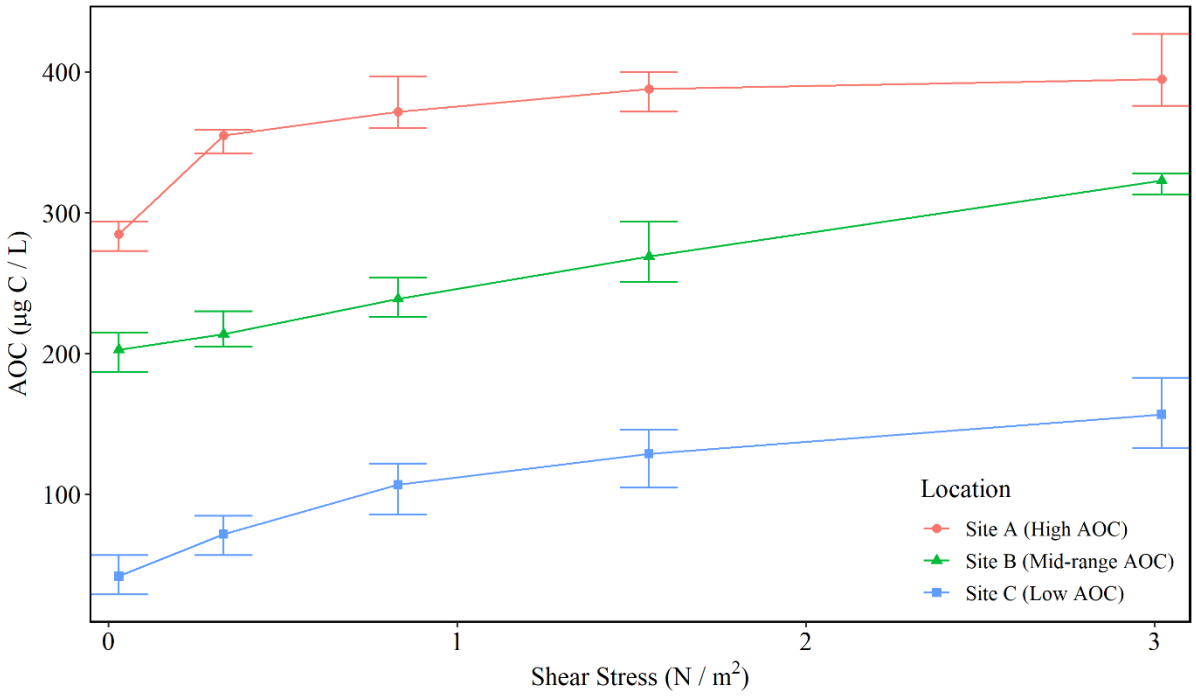

Figure 7.19: Assimilable organic carbon (AOC) (n=3) in bulk water within pipe loop test facilities at Pipe loop A (WTW 2), Pipe loop B (WTW 16) and Pipe loop C (WTW 20), during the mobilisation phase.

The gradient, R^2 and P values for TOC and AOC in bulk water within each of the three pipe loop test facilities during the mobilisation phase are listed in Table 7.11. Despite the largest TOC gradient being experienced within Pipe Loop A, the smallest AOC gradient was also experienced within Pipe Loop A. The R^2 value for AOC concentration within Pipe Loop A was considerably lower than other pipe loops, suggesting the AOC response during mobilisation within Pipe Loop A was non-linear.

Table 7.11: Gradient (G), R2 and P values for total organic carbon (TOC) and assimilable organic carbon (AOC) in bulk water within pipe loop test facilities at PL A (WTW 2), PL B (WTW 16) and PL C (WTW 20), during the mobilisation phase.

Pipe Loop ID	TOC			AOC		
	Gradient[A]	R^{2B}	P value[C]	Gradient[A]	R^{2B}	P value[C]
A	3.01	0.9500	0.0048	28	0.5840	0.1325
B	2.20	0.9030	0.0132	40	0.9969	0.0001
C	1.31	0.7857	0.0452	36	0.8830	0.0176

[A]The gradient defines the rate of change along the regression line; [B]R^2 value indicates the goodness of fit of the linear regression model to the data, nearer to 1 the better the fit; [C]A significant p value indicates that the gradient is significantly different from 0.

7.4 Biofilm Accumulation and Post-flush Biofilms Subsequent Mobilisation

Biofilm samples from coupons within Pipe loops A, B and C were analysed to determine the total volume (biofilms cells, EPS and (in)organics) (Section 4.7.5.2), cell count and community composition of the biofilm and how this varied with AOC concentration. The total biofilm volume was assessed at Day 0 and Month 12, whilst both the cell count concentration and community composition were sampled at Day 0, Month 3, Month 6, Month 9, Month 12 and post-flush.

7.4.1 Biofilm SEM Images

SEM imaging was used to enable qualitative visual comparisons of biofilms following the 12 month growth phase, to determine any differences between each of the pipe loops supplied by post-treated water with different AOC concentrations. The SEM images show that the biofilms which accumulated in each pipe loop exhibited a significant difference in both quantity and structure of biofilm (Figures 7.20 and 7.21). The biofilm developed on coupons in Pipe Loop A, supplied by the highest AOC concentration, had more extensive biofilm coverage, with a dense EPS matrix, compared to Pipe Loop B or Pipe Loop C. The EPS also looked to have a filament type structure. It is possible that the biofilm structure affected how easily the biofilm accumulated on the pipe surface and how easily it was mobilised during flushing. In contrast,

the biofilms that accumulated at Pipe Loop B and C had granular or patchy EPS coverage. Inorganic particles were visualised within SEM images of biofilms from all three pipe loops. As most inorganic material was released from biofilms grown in high AOC conditions (Pipe Loop A). The biofilm structure could also impact the rate at which inorganics are incorporated into the biofilm, and the rate at which they are released.

In contrast, cells were difficult to visualise in the SEM images potentially due to the large amount of EPS accumulated after 12 months biofilm growth obstructing the view of the cells. A previous study of drinking water biofilms found that proteins and carbohydrates appeared above cells in the biofilm (Fish *et al.* 2015). In addition to SEM images, more detailed biofilm analysis was conducted to determine a) the cell count (total and intact) and b) the bacterial and fungal community composition of the biofilms to quantitatively characterise and compare biofilm from different sites.

A)

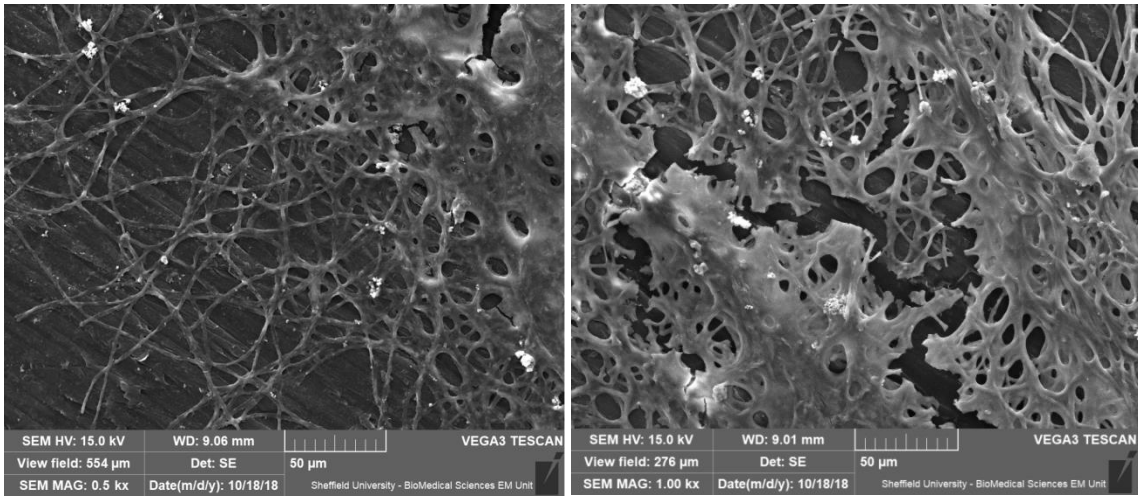

B)

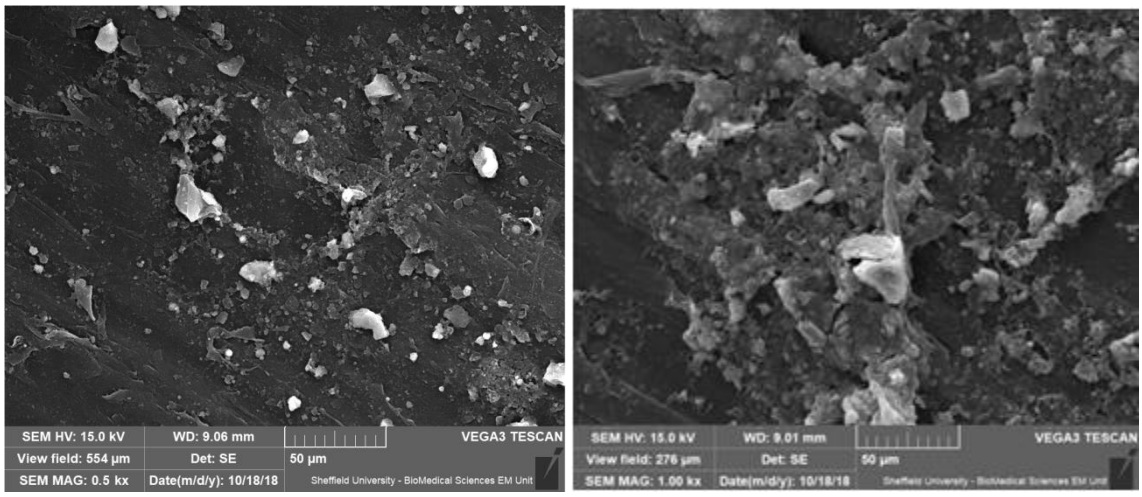

C)

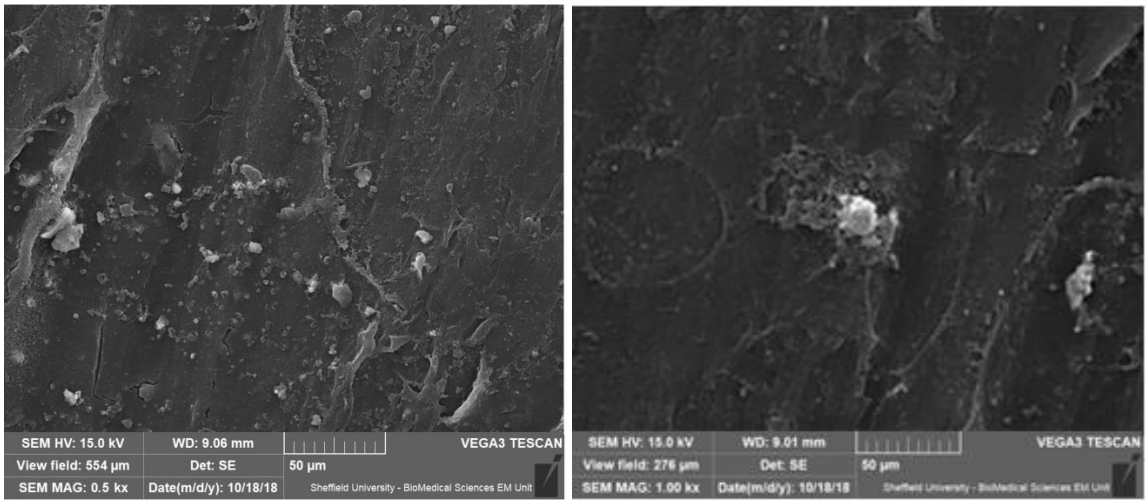

Figure 7.20: Representative SEM images of 12 month biofilm samples from A) Pipe loop A and B) Pipe loop B and C) Pipe loop C, imaged at the magnification indicated by the scale bar on each image. Images on left magnification = 500 x, images on right magnifaction = 1000 x.

A)

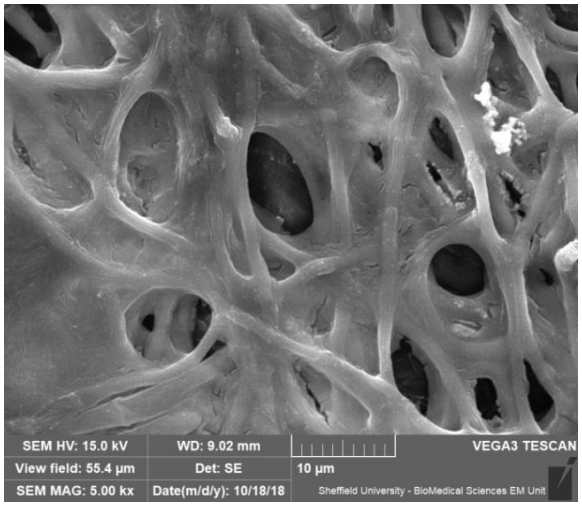

B)

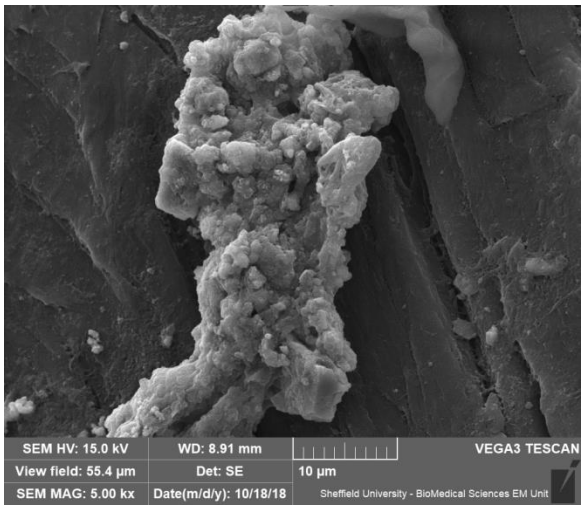

C)

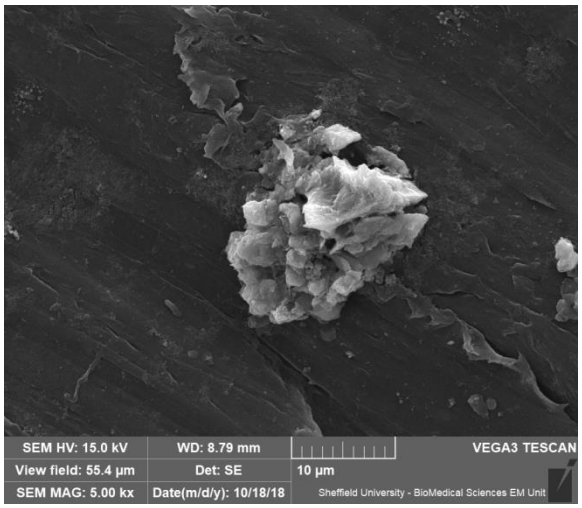

Figure 7.21: Representative SEM images of 12 month biofilm samples from A) Pipe loop A and B) Pipe loop B and C) Pipe loop C, imaged at the magnification indicated by the scale bar on each image. Magnification = 5000 x.

7.4.2 Cell Concentration during the Growth Phase and Post-flush

In order to assess the number of cells within biofilms accumulating on coupons in each pipe loop, the TCC and ICC of the biofilms were measured every three months during the experiment growth phase, and once following the mobilisation (post-flush) phase to determine the biofilm response to an increase in shear stress (Figures 7.22 & 7.23) In all cases, both the TCC and the ICC of the biofilm increased during the growth-phase and decreased following flushing. The greatest increase in both TCC and ICC following the 12 month growth phase was seen in Pipe Loop A; the pipe loop supplied with post-treated water containing the highest concentration of AOC. Biofilms within pipe loop A were found to have a dense, filament type structure (Figures 7.20 and 7.21), suggesting that the physical structure of the biofilm may affect how easily cells accumulate within the biofilm and how easily they become mobilised into the water column. The rate of biofilm growth was different at each site, with a greater rate in Pipe Loop A and slowest rate at Pipe Loop C. However, biofilm growth within Pipe Loop A appeared to slow, perhaps indicating that growth had reached a plateau, whereas biofilm growth within the other two pipe loops was still increasing. Following on from flushing, the greatest loss of TCC from the biofilm was experienced within Pipe Loop A (60% decline in TCC), as compared to 28% loss TCC within Pipe Loop B and 23% loss TCC within Pipe Loop C. The greatest loss of ICC occurred within Pipe Loop B (30% loss of ICC) in comparison to a 24% decline within Pipe Loop A and 18% within Pipe Loop C.

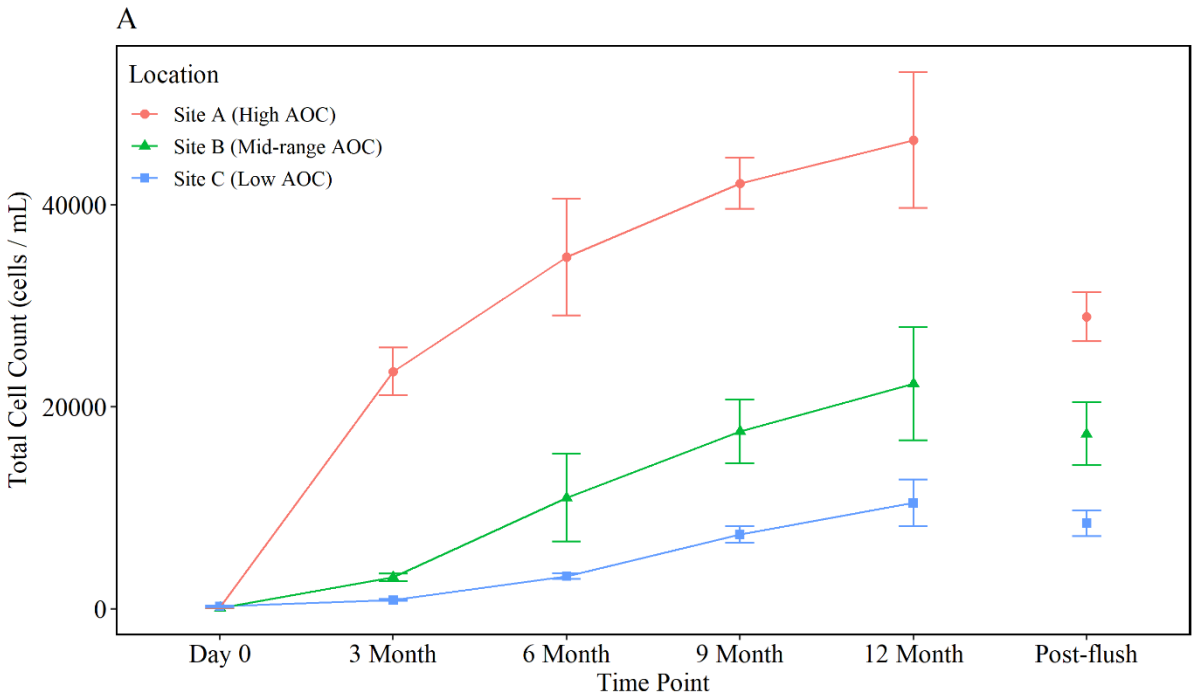

Figure 7.22: Total cell count (TCC) within drinking water biofilms within pipe loop test facilities at Pipe loop A (WTW 2), Pipe loop B (WTW 16) and Pipe loop C (WTW 20), during the growth (Day 0 -12 month) and mobilisation (post-flush) phase. Average (n=3) ±StDev plotted.

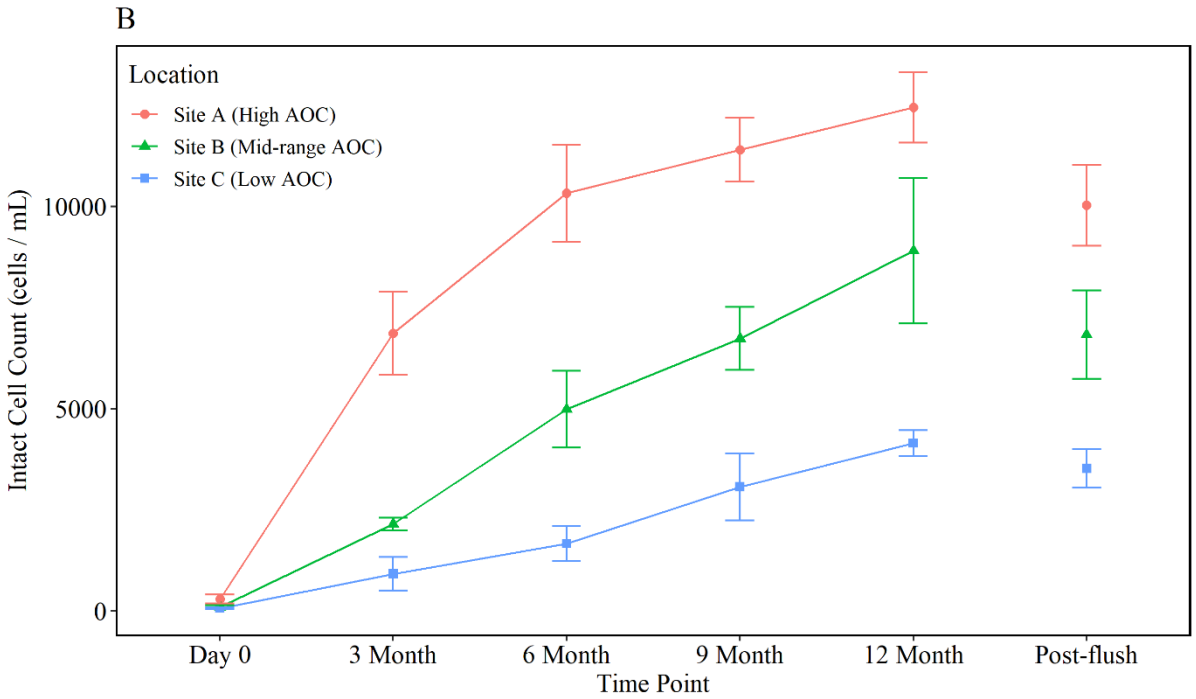

Figure 7.23: Intact cell count (TCC) within drinking water biofilms within pipe loop test facilities at Pipe loop A (WTW 2), Pipe loop B (WTW 16) and Pipe loop C (WTW 20), during the growth (Day 0 -12 month) and mobilisation (post-flush) phase. Average (n=3) ±StDev plotted.

7.4.3 Biofilm Community Composition

The community composition of the biofilms within Pipe Loops A, B and C were characterised every three months during the experiment growth phase and once following the mobilisation (post-flush) phase (see Section 4.7.2.2 and 4.7.3 for methods). Only two of the three Day 0 Pipe Loop B, and two of the three Day 0 Pipe Loop C biofilms contained quantities of bacterial or fungal DNA detectable via the methods used in this study. DNA was successfully extracted from three Day 0 samples from Pipe Loop A.

7.4.3.1 Bacterial and Fungal Community Analysis

The bacterial and community composition of biofilms from Pipe Loops A, B and C exhibited less variation than their bulk water counterparts, The dominant bacterial class within biofilm samples was *Proteobacteria* and within it *Betaproteobacteria* (representing a 60% of the total community). At genus level *Pseudomonas*, *Herbaspirillum* and *Brucella* were most were most abundant, with little change over time. The fungal community was dominated by *Ascomycota* (15–40%) and *Corticiaceae (*10–31%). The most abundant fungal genera post-flush was *Pezizaccea*, which were in much lower abundance during growth.

Figure 7.24 shows the similarities in bacterial community between all biofilm samples (Day 0, Month 3, 6, 9, 12 and Post-Flush), analysed at the OTU level. The dendrogram was plotted using bacterial OTU relative abundance data and presents evidence of a community shift from initial colonisers to biofilm maturation (Figure 7.24). Day 0 samples were found to be independent from all other samples and exhibited no site effect (Day 0 ANOSIM by site: Global R value = 0.25; p-value = 0.143) (Cluster 1, Figure 7.24). Month 3 samples were found to again cluster independently from all the other samples, but a significant site effect was observed (Month 3 ANOSIM by site: Global R value = 1; p-value = 0.004) (Clusters 2-4, Figure 7.24). After 3 months, some variation in samples was observed but site specific clusters were less obvious. Bacterial post-flush samples were found to cluster together (Post-Flush ANOSIM

by site: Global R value = 0.226; p-value = 0.029) (Cluster 5, Figure 7.24), suggesting that flushing has a homogenisation effect.

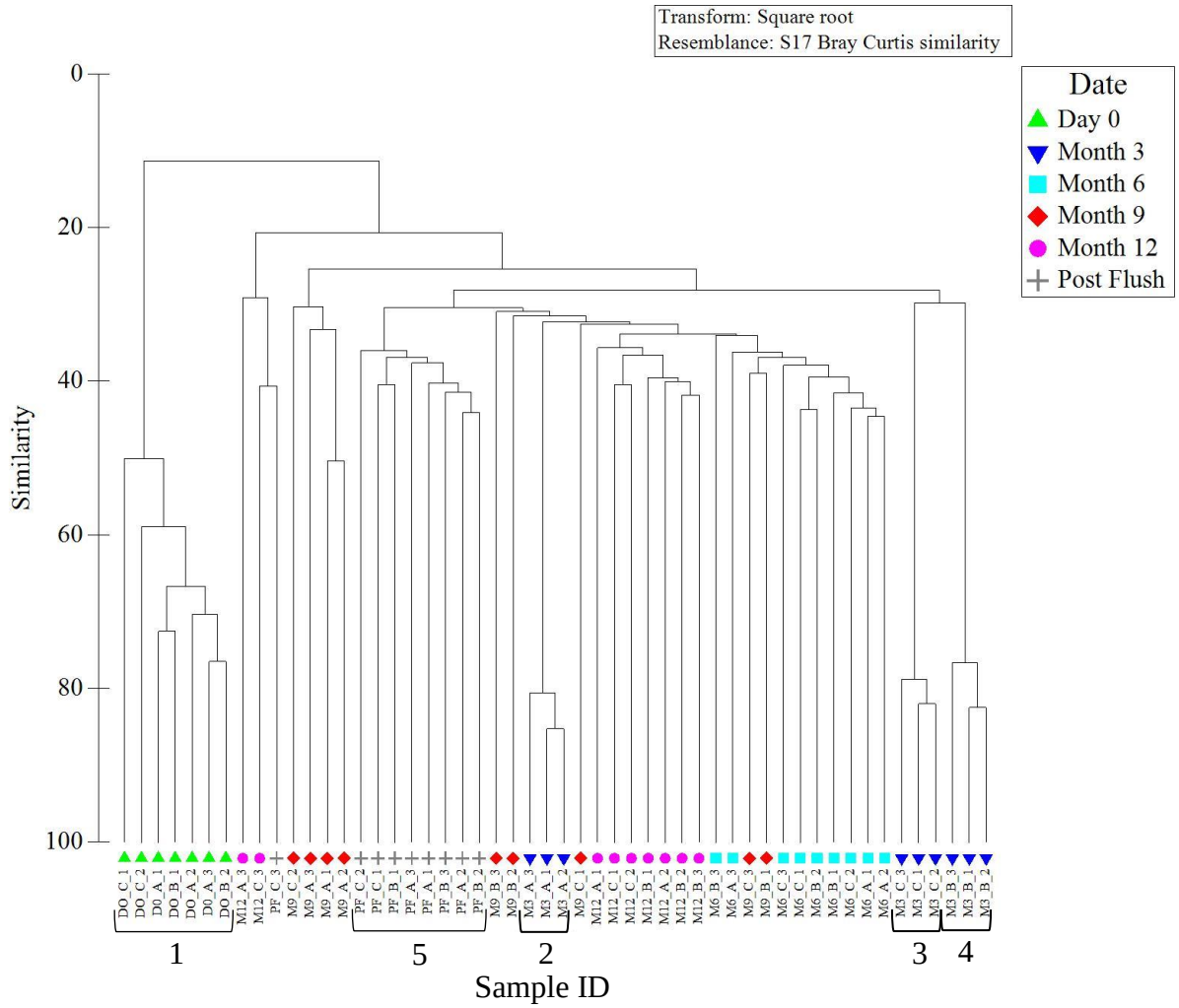

Figure 7.24: Dendrogram plotted using biofilm bacterial OTU relative abundance data from both the mobilisation (Day 0 – 12 month) and the mobilisation phase (post-flush). Data was square root transformed and a Bray Curtis similarity matrix was generated. Sample identification numbers are shown (first letter / number indicates time point, the second letter indicates the pipe loop, and the third number indicates the triplicate number).

To determine if site difference were evident in more mature biofilms, rather than just at initial biofilm development, bacterial communities within 12 month biofilm samples were compared visually (Figure 7.25 A) and statistically (Tables 7.12 and 7.13). Some clustering of 12 month samples was observed (similarity of 40%), with a site effect being evident (Figure 7.25 A). ANOSIM of 12 months samples showed that there were some differences in relative abundance

(R = 0.284, p-value = 0.032) (Table 7.12)). ANOSIM data for Month 12, showed high levels of similarity for both presence / absence and relative abundance data, however only the similarity in relative abundance data was significant. This indicated that similar community bacterial community members were present, but at different abundances.

Month 12 and Post-Flush sampled were analysed in an nMDS plot to identify if there was a community shift following flushing (Figure 7.25 B). See Table 7.12 for ANOSIM of 12 month and post-flush samples analysed by date. Bio-replicates at each sample point were found to fairly similar within Site B (supplied by post-treated water containing a mid AOC concentration) (see SIMPER analysis, Table 7.13). 12 month samples from Site A and Site C showed more variation between replicates (see Table 7.13), suggesting that extreme AOC values (either high or low) created a more variable community. Similarly, 12 month and post flush samples showed some grouping of samples (similarity of 40%), with some clustering by site and time point (Figure 7.25 A). There was also a clear clustering of Month 12 and Post-flush samples, with the exception of sample point PF_C_3. Post-flush samples again showed that samples from Site B were most similar (see SIMPER analysis, Table 7.13).

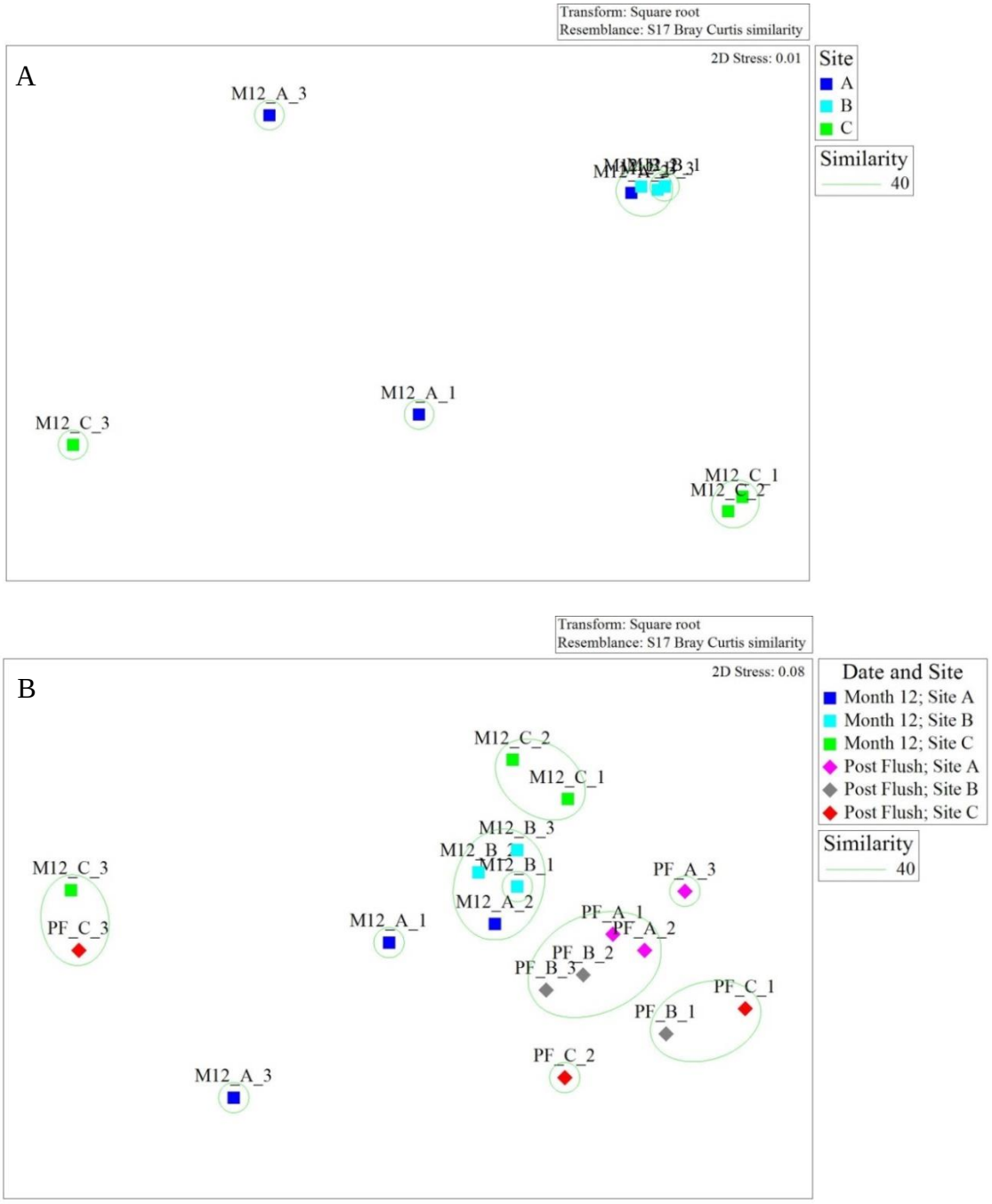

Figure 7.25: Visualisation of biofilm bacterial community similarities. A) nMDS plotted using 12 month bacterial OTU relative abundance data. B) nMDS plotted using bacterial OTU relative abundance data including samples from the growth (12 month samples only) and the mobilisation phase (post-flush (PF)). Data was square root transformed and a Bray Curtis similarity matrix was generated. Sample identification numbers are shown (first letter / number indicates time point, the second letter indicates the pipe loop, and the third number indicates the triplicate number). Similarity cluster lines were based on the similarity levels found in the hierarchical analysis (see Figure 7.28).

Table 7.12: ANOSIM values for biofilm bacteria OTU relative abundance and presence / absence data, including Month 12 & Post-Flush data.

Samples	Data	Global R Value	p-Value
Month 12 (ANOSIM by site)	Presence / absence	0.218	0.096
	Relative abundance	0.284	0.032
Site A: Month 12 and Post-flush (ANOSIM by date)	Presence / absence	0.593	0.100
	Relative abundance	0.778	0.100
Site B: Month 12 and Post-flush (ANOSIM by date)	Presence / absence	0.704	0.100
	Relative abundance	1	0.100
Site C: Month 12 and Post-flush (ANOSIM by date)	Presence / absence	0.111	0.500
	Relative abundance	-0.148	0.600

Global R value: 0 = same, 1 = completely different. The significance level is the p value <0.05: significant; >0.05: weak evidence).

Table 7.13: SIMPER analysis Month 12 and Post-flush biofilm bacteria OTU presence / absence and relative abundance data.

Date	Data	Site	Average Similarity[A]	Site Group	Average Dissimilarity[B]
Presence/ absence	Month 12	A	37.76	Site A & Site B	61.07
		B	42.91	Site B & Site C	60.17
		C	39.91	Site A & Site C	61.96
	Post-Flush	A	45.00	Site A & Site B	55.05
		B	63.10	Site B & Site C	59.64
		C	33.77	Site A & Site C	60.79
Relative Abundance	Month 12	A	34.55	Site A & Site B	65.96
		B	40.49	Site B & Site C	67.89
		C	28.23	Site A & Site C	69.83
	Post-Flush	A	39.46	Site A & Site B	61.41
		B	40.69	Site B & Site C	67.27
		C	24.95	Site A & Site C	69.84

[A]Average similarity between samples taken at same time point, at the same site; [B]Average dissimilarity between different sites (A, B & C).

The dendrogram in Figure 7.26 shows the similarities in fungal community between all biofilm samples (Day 0, Month 3, 6, 9, 12 and post-flush), analysed at the OTU level. Fungi OTU

relative abundance data exhibited a similar trend to bacterial OTU data, with Day 0 samples clustering independently from all other samples (Cluster 1, Figure 7.26) and exhibiting no site effect (Day 0 ANOSIM by site: Global R value = 0.55; p-value = 0.086). As observed with Month 3 bacteria samples (Figure 7.26), Month 3 fungi samples were found to cluster independently from all the other samples, and a site effect was observed (Month 3 ANOSIM by site: Global R value = 1; p-value = 0.004). Following the same trend as bacteria data, all samples after Month 3 showed some variation but site specific clusters were less obvious. Unlike post-flush bacterial OTU relative abundance data, clustering of post-flush fungal data was not evident.

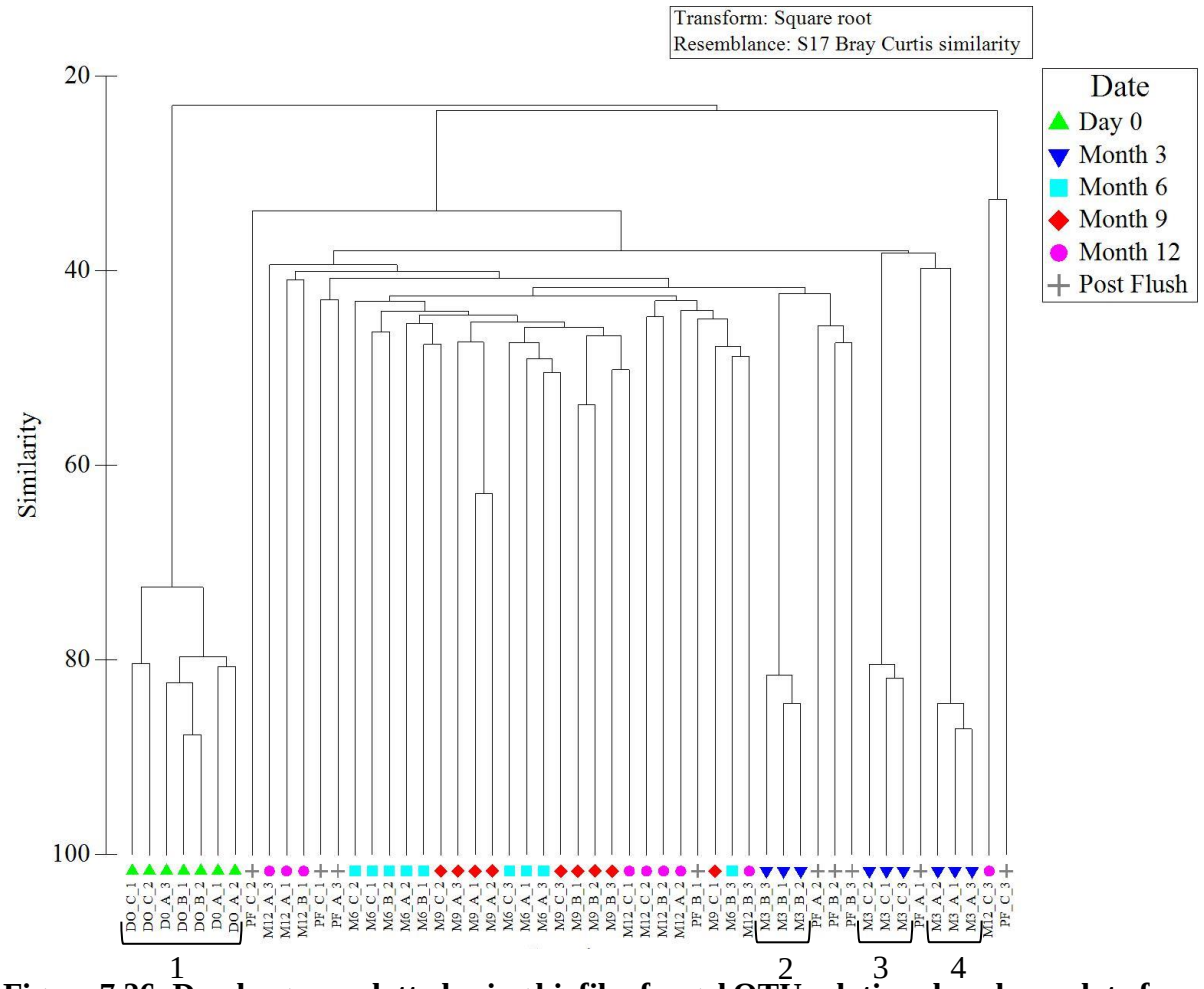

Figure 7.26: Dendrogram plotted using biofilm fungal OTU relative abundance data from both the growth (Day 0 – 12 month) and the mobilisation phase (post-flush (PF)). Data was square root transformed and a Bray Curtis similarity matrix was generated. Sample identification numbers are shown (first letter / number indicates time point, the second letter indicates the pipe loop, and the third number indicates the triplicate number).

An nMDS plot of 12 month fungal OTU relative abundance data shows some clustering of samples was observed (similarity of 40%) (Figure 7.27). Sample M12_C_3 was removed from Figure 7.27 A, and all subsequent analysis as it was an outlier. ANOSIM analysis of 12 month samples only global R = 0.062 p-value = 0.286 (see Table 7.14 for ANOSIM of 12 month and post-flush samples analysed by date). Similarity between replicates of 12 month fungal OTU relative abundance data was again highest at Site B (Site B Month 12 SIMPER: 43.89 similarity (Table 7.15). Similarly, 12 Month and post flush samples showed some grouping of samples (similarity of 40%), with some clustering by site and time point, with the exclusion of samples M12_C_3 and PF_C_3 (Figure 7.27 B). ANOSIM values for Month 12 and post-flush fungi OTU relative abundance and presence / absence data again showed high levels of similarity (as indicated by the low global R value), however none of the values were found to be significantly significant (Table 7.14).

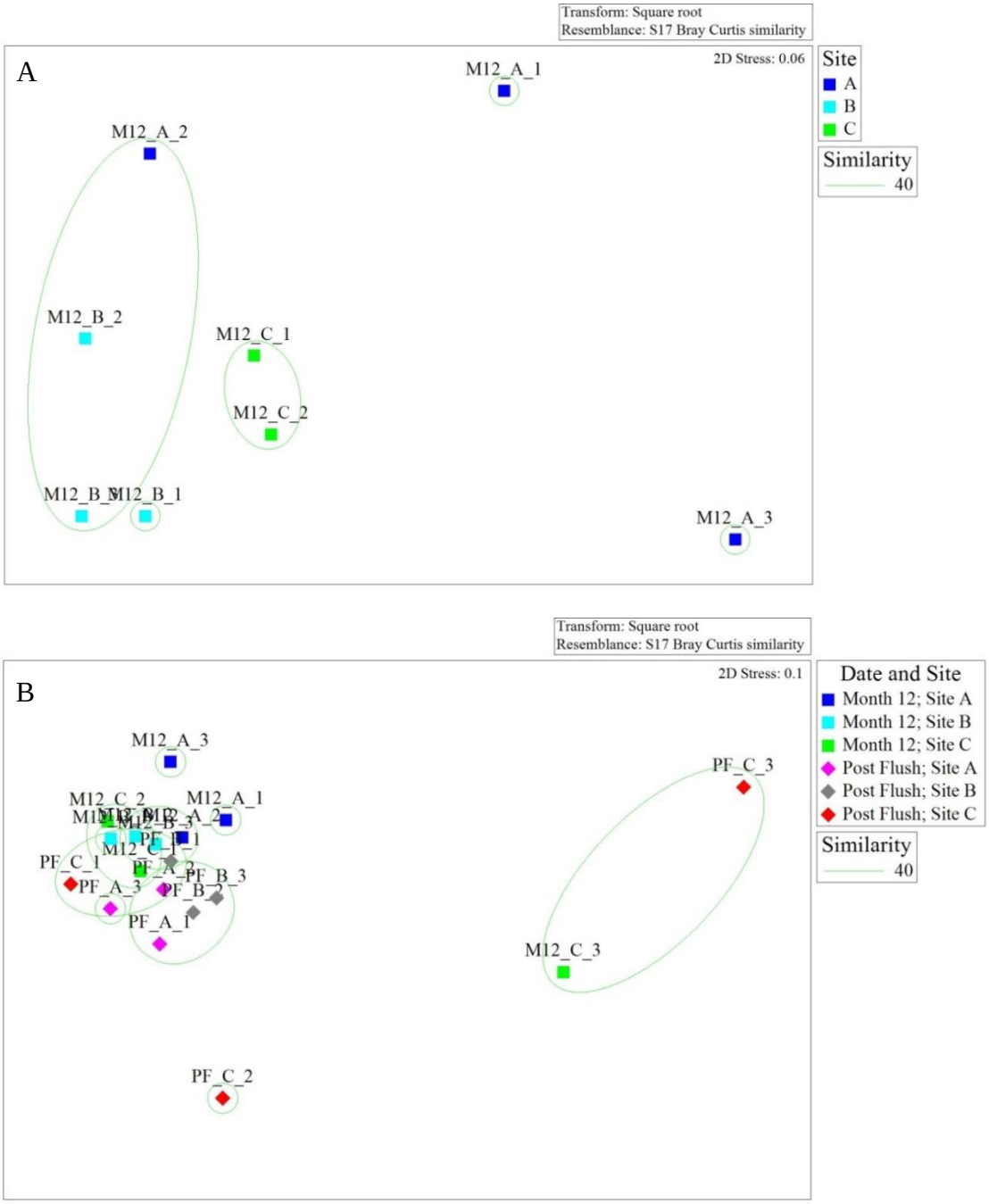

Figure 7.27: Visualisation of biofilm fungal community similarities. A) nMDS plotted using 12 month fungal OTU relative abundance data with data point M12_C_3 removed. B) nMDS plotted using fungal OTU relative abundance data from both the growth (12 month samples only) and the mobilisation phase (post-flush (PF)). Data was square root transformed and a Bray Curtis similarity matrix was generated. Sample identification numbers are shown (first letter / number indicates time point, the second letter indicates the pipe loop, and the third number indicates the triplicate number). Similarity cluster lines were based on the similarity levels found in the hierarchical analysis (see Figure 7.30).

Table 7.14: ANOSIM values for biofilm fungi OTU relative abundance and presence / absence data, including Month 12 & Post-Flush data.

Samples	Data	Global R Value	P-Value
Month 12 (ANOSIM by site)	Presence / absence	0.021	0.470
	Relative abundance	0.062	0.286
Site A: Month 12 and Post-flush (ANOSIM by date)	Presence / absence	0.259	0.200
	Relative abundance	0.296	0.300
Site B: Month 12 and Post-flush (ANOSIM by date)	Presence / absence	0.111	0.300
	Relative abundance	0.444	0.200
Site C: Month 12 and Post-flush (ANOSIM by date)	Presence / absence	-0.074	0.500
	Relative abundance	-0.185	0.800

Global R value: 0 = same, 1 = completely different. The significance level is the p value <0.05: significant; >0.05: weak evidence).

Table 7.15: SIMPER analysis Month 12 and Post-flush biofilm fungi OTU presence / absence and relative abundance data.

Date	Data	Site	Average Similarity	Site Group	Average Dissimilarity
Presence/ absence	Month 12	A	63.88	Site A & Site B	39.18
		B	59.52	Site B & Site C	39.93
		C	60.54	Site A & Site C	37.61
	Post-Flush	A	63.85	Site A & Site B	37.19
		B	62.68	Site B & Site C	40.71
		C	55.29	Site A & Site C	40.95
Relative Abundance	Month 12	A	39.56	Site A & Site B	59.71
		B	43.89	Site B & Site C	61.52
		C	32.55	Site A & Site C	62.67
	Post-Flush	A	40.32	Site A & Site B	58.37
		B	43.35	Site B & Site C	66.55
		C	24.33	Site A & Site C	67.83

[A]Average similarity between samples taken at same time point, at the same site; [B]Average dissimilarity between different sites (A, B & C).

7.4.3.2 Diversity Indices of Bacterial and Fungal Biofilm Data

Diversity indices tests were undertaken for bacterial and fungal communities from drinking water biofilm samples taken from Pipe Loops A, B & C to determine if the AOC concentration had an impact on the relative richness, relative evenness and relative diversity of biofilm samples. The relative richness, evenness and diversity of bacterial communities at Day 0, Month 3, Month 6, Month 9, Month 12 and Post-flush were found to exhibit little variation between sites but some change with time (Table 7.16). The relative richness, evenness and diversity of bacterial communities increased from Day 0 to Month 3, as would be expected for a maturing biofilm.

Table 7.16: Ecological indices of biofilm bacterial communities from drinking water biofilm samples taken from Pipe Loops A, B & C (n=3) at Day 0, Month 3, Month 6, Month 9, Month 12 and Post-Flush. A) Relative richness, B) relative evenness, and C) relative diversity.

Pipe Loop	Time	Relative Richness (Chao)		Relative Evenness (Simpson)		Relative Diversity (Shannons Index)	
		Mean	StDev	Mean	Range	Mean	Range
A	Day 0	54.33	8.02	52.50	0.71	57.50	3.54
	3 Month	805.33	44.00	1111.00	71.53	1122.67	131.64
	6 Month	1017.67	163.37	929.33	239.83	1032.67	118.57
	9 Month	1687.67	390.76	881.33	205.05	1043.67	431.62
	12 Month	894.33	145.11	826.00	154.92	940.33	486.46
	Post-flush	642.33	167.66	818.33	55.43	785.67	217.12
B	Day 0	0.93	0.00	0.94	0.01	0.93	0.00
	3 Month	0.98	0.00	0.99	0.00	0.99	0.00
	6 Month	0.87	0.14	0.96	0.02	0.98	0.02
	9 Month	0.99	0.01	0.99	0.00	0.97	0.02
	12 Month	0.93	0.03	0.96	0.01	0.95	0.02
	Post-flush	0.96	0.01	0.94	0.01	0.90	0.03
C	Day 0	3.09	0.07	3.15	0.20	3.16	0.00
	3 Month	4.98	0.10	5.48	0.12	5.40	0.04
	6 Month	3.76	0.98	4.65	0.28	4.99	0.33
	9 Month	5.98	0.47	5.15	0.09	4.91	0.69
	12 Month	3.95	0.47	4.36	0.20	4.12	0.56
	Post-flush	4.47	0.10	4.13	0.05	3.37	0.30

The relative richness, relative evenness and relative diversity of fungal communities within drinking water biofilm samples taken from Pipe Loops A, B & C, are plotted in listed in Table 7.17. Similar to bacterial data, the diversity indices of fungal biofilm communities showed little variation from Day 0 to Post-flush, within only a statistically significant increase in the relative richness, evenness and diversity increase from Day 0 to Month 3.

Table 7.17: Ecological indices of biofilm fungal communities from drinking water biofilm samples taken from Pipe Loops A, B & C (n=3) at Day 0, Month 3, Month 6, Month 9, Month 12 and Post-Flush. A) Relative richness, B) relative evenness, and C) relative diversity.

Pipe Loop	Time	Relative Richness (Chao)		Relative Evenness (Simpson)		Relative Diversity (Shannons Index)	
		Mean	StDev	Mean	Range	Mean	Range
A	Day 0	58.25	0.25	53.90	0.99	62.25	5.30
	3 Month	1024.69	20.02	926.78	88.68	1105.10	56.74
	6 Month	1012.69	125.69	1157.67	141.21	1004.24	128.21
	9 Month	1058.30	127.50	1073.04	28.50	998.61	172.61
	12 Month	1004.78	145.33	862.13	85.65	997.77	185.10
	Post-flush	994.60	87.15	900.03	39.60	851.28	247.54
B	Day 0	0.90	0.03	0.90	0.04	0.92	0.01
	3 Month	0.97	0.00	0.97	0.00	0.96	0.02
	6 Month	0.98	0.01	0.90	0.11	0.97	0.01
	9 Month	0.97	0.00	0.96	0.01	0.93	0.02
	12 Month	0.95	0.00	0.96	0.01	0.90	0.12
	Post-flush	0.96	0.01	0.85	0.20	0.81	0.25
C	Day 0	2.88	0.23	2.86	0.30	3.11	0.09
	3 Month	4.43	0.05	4.21	0.09	4.02	0.16
	6 Month	4.22	0.25	3.72	0.59	4.26	0.41
	9 Month	4.20	0.11	3.99	0.21	3.66	0.22
	12 Month	3.49	0.01	3.83	0.18	3.44	1.39
	Post-flush	3.90	0.28	3.23	0.98	2.81	1.63

7.4.3.3 Comparison of Bulk water and Biofilm Bacterial and Fungal Biofilm Data

The community composition of bacteria and fungi found within the bulk water and biofilms in Pipe Loops A, B and C were compared to identify any differences in the planktonic and attached microbiome. Figure 7.28 presents an nMDS plot comparing bulk water (post-treated

water supplying Pipe Loop A, B and C) and biofilm (Pipe Loop A, B and C) bacterial OTU relative abundance data. The biofilm samples were found to cluster together, independent of site location. Interestingly, AOC release from the biofilm was also very similar in each pipe loop (Figure 7.19). Therefore, similar levels of AOC storage within the biofilm could lead to the development of similar community compositions within the biofilm. In contrast, bulk water samples were found to clearly cluster by site. ANOSIM data by site showed that presence / absence data had, on average, a higher global R value than relative abundance data (Table 7.18). This indicated that similar community bacterial community members were present in the bulk water and within the biofilm, but that they were present at different abundances.

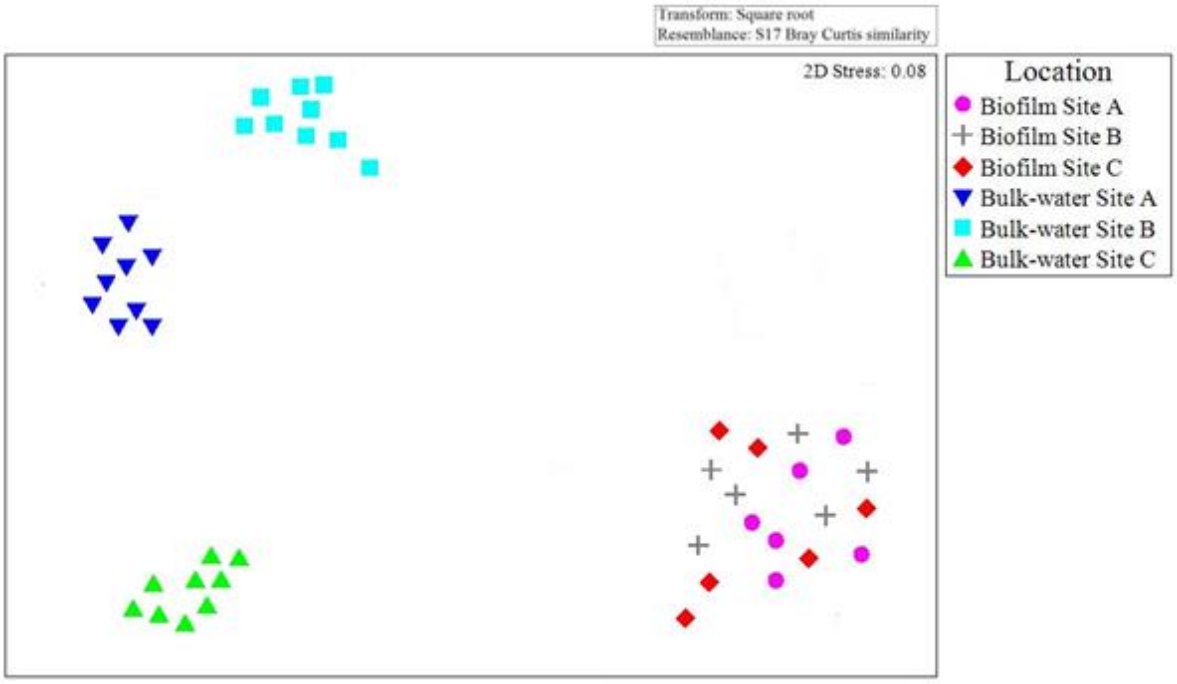

Figure 7.28: nMDS plotted using bulk water bacterial OTU relative abundance data (post-treated water supplying Pipe Loop A, B and C) from Day 0, Month 6 and Month 12, and biofilm (Pipe Loop A, B and C) bacterial OTU relative abundance data from 6 and 12 months. Data was square root transformed and a Bray Curtis similarity matrix was generated.

Table 7.18: ANOSIM values for Month 12 bulk water and Month 12 biofilm bacterial OTU relative abundance and presence / absence data.

Samples	Data	Global R Value	P-Value
Site A: Month 12 bulk water & Month 12 biofilm	Presence / absence	0.545	0.010
	Relative abundance	0.912	0.050
Site B: Month 12 bulk water & Month 12 biofilm	Presence / absence	0.478	0.020
	Relative abundance	0.842	0.025
Site C: Month 12 bulk water & Month 12 biofilm	Presence / absence	0.511	0.090
	Relative abundance	0.745	0.100

Global R value: 0 = same, 1 = completely different. The significance level is the p value <0.05: significant; >0.05: weak evidence).

An nMDS plot comparing bulk water (post-treated water supplying Pipe Loop A, B and C) and biofilm (Pipe Loop A, B and C) fungal OTU relative abundance data is presented in Figure 7.29. Similar to bacterial relative abundance data, fungal biofilm samples were found to cluster together, independent of site location, whereas bulk water samples were found to clearly cluster by site. ANOSIM analysis of fungal OTU data by site showed higher that presence / absence data had, on average, a higher global R value than relative abundance data (Table 7.19). This indicated that similar community bacterial community members were present in the bulk water and within the biofilm, but that they were present at different abundances.

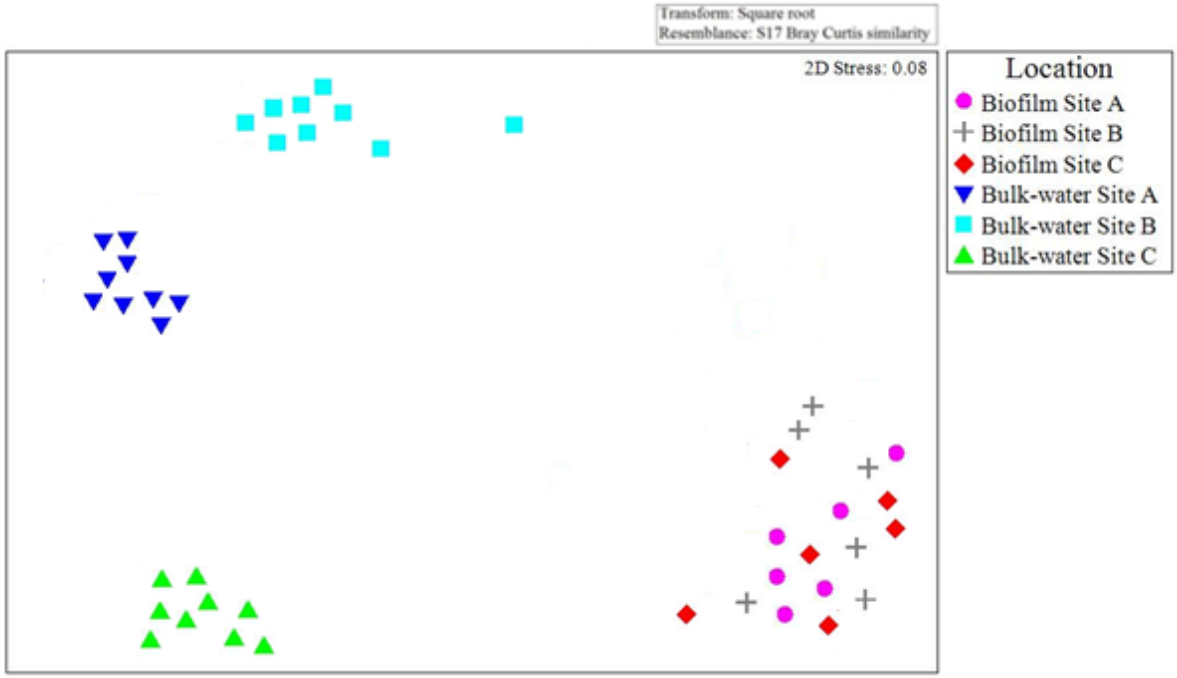

Figure 7.29: nMDS plotted using bulk water fungal OTU relative abundance data (post-treated water supplying Pipe Loop A, B and C) from Day 0, Month 6 and Month 12, and biofilm (Pipe Loop A, B and C) fungal OTU relative abundance data from 6 and 12 months. Data was square root transformed and a Bray Curtis similarity matrix was generated.

Table 7.19: ANOSIM values for Month 12 bulk water and Month 12 fungal OTU relative abundance and presence / absence data.

Samples	Data	Global R Value	P-Value
Site A: Month 12 bulk water & Month 12 biofilm	Presence / absence	0.358	0.026
	Relative abundance	0.822	0.050
Site B: Month 12 bulk water & Month 12 biofilm	Presence / absence	0.515	0.090
	Relative abundance	0.845	0.900
Site C: Month 12 bulk water & Month 12 biofilm	Presence / absence	0.311	0.050
	Relative abundance	0.915	0.100

Global R value: 0 = same, 1 = completely different. The significance level is the p value <0.05: significant; >0.05: weak evidence).

7.5 Discussion

7.5.1 Growth Phase: Bulk water

This results of this chapter confirm that microbial regrowth is limited in drinking water systems where the AOC concentration is limited. Water quality within Pipe Loop A (supplied by post-treated water from WTW 2) was characterised by the highest AOC, TCC and ICC concentration, suggesting this site was the least biologically stable. In contrast, Pipe Loop C (supplied by post-treated water from WTW 20) consistently had the lowest concentration and least variability, of AOC, TCC and ICC. Pipe Loop C is therefore the most biologically stable based on values cited in the literature (≤10 – 120 µg/L) (Van der Kooij, 1992; LeChevallier *et al*. 1996; Ohkouchi *et al.* 2013; Wang, Tao & Xin, 2014; LeChevallier *et al.* 2015). Pipe Loop A was supplied by chlorinated water, whereas Pipe Loop B and Pipe Loop C were supplied with chloraminated post-treated water. Compared to chloramine, chlorine tended to cause higher AOC concentrations within drinking water, as a result of chlorine creating smaller molecules within TOC which might contribute to a higher AOC concentration. As TCC and ICC were not available for raw water supplying WTW 20, it is not clear if this is due to source water quality or the treatment process. Cheswick *et al*. 2019 analysed TCC and ICC within raw and post-treated water across 213 drinking Scottish Water WTW over three years (n = 39,340). Cell counts within post-treated were found to be mostly driven by individual treatment processes, with membrane treatment having the highest removal efficiency of TCC and ICC (Cheswick *et al.* 2019).

The AOC concentration within post-treated drinking water was confirmed to be a function of source water quality and the type of treatment processes applied. Pipe Loop A (WTW 2) and Pipe Loop B (WTW 16), which are both supplied by surface water sources, exhibited a seasonal trend in post-treated water quality over the 12 month study period. These sites exhibited an increase in AOC concentration during spring, before declining during the

summer months (Figure 7.6), which correlated with an increase in intact cell counts (Figure 7.8). This is likely due to AOC being used by heterotrophic organisms for growth. Polanska *et al*. 2005 also observed an increasing trend in the AOC concentration during spring. This trend was also identified during bulk water sampling from service reservoirs in operational DWDS (Chapter 6). In contrast, Pipe Loop C exhibited little variation in water quality during the 12 month experimental programme. Liu *et al.* (2012) found that better source water quality resulted in lower AOC concentrations in post-treated water. It is therefore important to consider how source water and seasonal variation impacts the AOC concentration, and how this impacts the rate of (re)growth and degree of biostability within the drinking water.

This thesis has compared for first time the impact of AOC concentration on both bulk water and biofilm bacterial and fungal community composition and structure within operational DWDS. The community composition and structure of bulk water within each of the three pipe loops was found to be a function of the AOC concentration. This is potentially a result of different microorganisms having different catabolic capabilities for certain substrates (Newton *et al.* 2011). The exact composition of AOC within drinking water is not constant, and will depend on source water quality, the treatment process and the disinfection residual applied. The rate at which organisms can utilise the AOC will depend on which organic molecules make up the AOC (Escobar *et al.* 2000).The community composition and structure of microorganisms and its relation to carbon concentration has been assessed in terms on indigenous microorganisms that colonise the surfaces of filter materials used at WTW (Section 2.3.2.8). Liao *et al.* (2013), for example, theorised that the AOC concentration could impact microbial community composition (at class level) in biofilters.

7.5.2 Growth Phase: Biofilm

AOC concentration was found to not only impact microbial growth within the bulk water, but also influence the volume, cell count and community composition of biofilms residing at the

pipe wall. AOC had a significant effect on the degree of biofilm accumulation during the twelve month study period. SEM images (Figures 7.20 & 7.21) and cell counts (Figures 7.22 and 7.23) confirmed the accumulation of biofilm over time, with site specific differences in accumulation being observed. SEM images indicated that the greatest volume of biofilm material had accumulated on 12 month coupons taken from Pipe Loop A, supplied by post-treated water containing the highest AOC concentration. Similarly, the number of cells incorporated into the biofilm was greatest within the pipe loop supplied by post-treated water containing the consistent highest AOC concentration. This research shows for the first time that the AOC concentration not only affects microbial growth and biological stability in the bulk-water, but also microbial growth within the biofilm, with greatest growth of cells in the biofilm will occur when AOC is not limited The AOC concentration was found to not only affect the final cell number of cells within the biofilm, but also the growth rate of cells within the biofilm The increase in TCC and ICC within the biofilm was slowing between Month 9 and Month 12 (Figures 7.22 & 7.23), suggesting that biofilms will mature faster at high AOC concentration.

SEM images showed that the biofilms within each of the pipe loops accumulated different amounts of biofilm and the biofilm structure was very different (Figures 7.20 and 7.21). Within Pipe Loop A (supplied by post-treated water containing the highest AOC concentration), the largest amount of biofilm could be visualised using SEM and the biofilm has a much more dense, filamentous structure. Stoodley *et al.* (2001a) suggested that carbon (and nitrogen) affected the biofilm physical structure with higher carbon creating a thicker a thicker structure supporting "mushroom" cell clusters. The results of this thesis suggest that the AOC concentration will not only influence the amount of biofilm that accumulates, but also affect the structure and density of the biofilm.

The AOC concentration was found to have a smaller effect on the community structure and composition of the bacterial or fungi residing in the biofilm (in comparison to bacteria and fungi within

the bulk water). As the biofilm analysed in this thesis were still maturing, it is likely that time was the dominant effect on the community composition. The community composition of bacteria and fungi within the biofilm was found to change over time. Both the bacterial and fungal community composition became more stable over time (Figures 7.24 and 7.26), with a clear shift from initial colonisers (Day 0 and Month 3) to a more stable 'core community' after the 12 month growth period. Similarly, the community structure changed over time, with an increased in the relative richness and diversity from Day 0 to Month 3. AOC release from the biofilm was also very similar in each pipe loop (Figure 7.19). Therefore, similar levels of AOC storage within the biofilm could lead to the development of similar community compositions within the biofilm.

7.5.3 Mobilisation phase: Bulk water

During the mobilisation phase, the rate of AOC release from the biofilm to the water column was the same within each pipe loop, independent of the AOC concentration within the bulk water. All other measured drinking water parameters, including TOC, exhibited a site effect during mobilisation. This suggests that complex cycling of AOC occurs in DWDS, in which biofilms likely play a major role. During flushing, the pipe loop supplied by post-treated water containing the highest AOC concentration experienced greatest and most consistent increase in discoloration, as indicated by turbidity (Figure 7.13) and largest increase in bulk water iron (Figure 7.14) and manganese (Figure 7.15) concentration. The pipe loop supplied by bulk water containing the highest concentration of AOC exhibited an iron response sufficient to generate an iron failure (over 200 µg/l DWI, 2017). This is in the absence of any prior material being present on the pipes prior to the start of the experiment and material only being able to accumulate for one year. This could be a result of the biofilm within Pipe Loop A having accumulated more inorganic material during the growth phase, or the biofilm at Pipe Loop A being less resistant to mobilisation.

The TCC/ICC concentration increased within the bulk water during flushing, suggesting that cells were being mobilised from the biofilm with increasing shear stress. The

greatest increase in both TCC and ICC within the bulk water occurred within Pipe Loop A, supplied by post-treated water containing the highest AOC concentration. Highest TCC/ ICC response within the bulk water therefore correlated with the highest turbidity response. Pipe loop A exhibited the least linear response to flushing, especially with regards to TCC and ICC within the bulk water. This suggests that the AOC concentration not only affects the number of cells that will be released from the biofilm during flushing, but also the stability of the biofilms and how easily it will detach from the pipe wall.

7.5.4 Biofilm

Following flushing, biofilm samples within all three pipe loop samples exhibited a loss of cells (both total and intact), confirming that cells were being mobilised into the bulk water. The greatest loss of TCC from biofilm samples was experienced within Pipe Loop A, characterised by bulk water containing the highest AOC concentration. This suggests that a greater AOC concentration led to increased growth and replication within the biofilm during the growth phase, or that the stability of the biofilm was lower hence more cells were released during flushing. The presence of an elevated AOC concentration therefore promotes microbial mobilisation and planktonic contamination. The observed trends in TCC/ICC and AOC concentration were the same as relationship between in turbidity and metals data, with the largest TCC/ICC, turbidity and metals response occurring within Pipe Loop A, containing highest AOC concentration within the bulk water. This suggests that mobilisation of a greater concentration of microbial cells could cause an increased discolouration response. This is in contrast to Fish *et al.* 2018, in which TCC and ICC inversely correlated with turbidity and metals (iron and manganese) data during flushing trials within an experimental DWDS. This study, however, used three different chlorine concentrations (chlorine-boost 0.80-0.82 mg/L, no Dosing 0.35-0.45 m/g and dechlorinated 0.03-0.05 mg/L) which could explain the differences in trend between TCC/ICC and the turbidity response. Community composition

data identified independent clustering of Month 12 and Post-flush samples, suggesting a shift in both bacterial and fungal community composition following flushing. Bacterial and fungal ecological indices were also found to change after flushing, with a decline in OTU richness and diversity post-flush.

7.5.5 Bulk water vs. Biofilm Comparisons

After 12 months accumulation, the community composition of bacteria developed biofilm at each site were found to be remarkably similar, despite the community composition of incoming post-treated water exhibiting a clear site effect. The AOC concentration was found to impact the planktonic (bulk water) microbiome to a greater extent than microorganisms residing in the biofilm. The AOC concentration within bulk water has been found to impact the rate and amount of biofilm growth but another parameter other than AOC is likely governing the community composition of bacteria and fungi within biofilms. Furthermore, the bacterial and fungal richness and diversity was found to be higher within biofilms than in bulk water, a trend also identified by Douterelo *et al.* (2013). It is widely accepted that a very small fraction (<5%) of bacteria in DWDS is present in the bulk water (Lehtola *et al.* 2004; Simoes *et al*. 2010; Liu *et al.* 2014), which could result in differences in community composition between planktonic and attached microbial community compositions. Previous studies have found that the bacterial community composition differed between biofilms and bulk water drinking water samples (Martiny *et al.* 2005; Douterelo *et al.* 2011). A number of explanations for this difference between bulk water and biofilm community composition have been suggested including; particular bacterial species are able to express cell surface polymers that can increase cell hydrophobicity and promote processes such as co-aggregation (Rickard et al. 2003; 2004), different bacterial groups have greater sensitivity to chlorine (McCoy et al. 2012) and so are better adapted to biofilm environments, and certain organisms are better suited to the biofilm environment as the availability of nutrients is higher at the pipe wall (Emtiazi *et al.* 2004),

7.6 Summary

The AOC concentration within post-treated water was found to dictate both the rate of biofilm growth, and the discoloration risk the biofilms posed when they are mobilised. It was found that under elevated AOC concentrations, the highest number of cells (total and intact) were incorporated into the biofilm. The rate of biofilm maturation was also subject to AOC concentration, with biofilms within Site A (supplied by post-treated water containing the highest AOC concentration) having the fastest growth rate before approaching a plateau in growth at 12 months. An elevated AOC concentration within the bulk water also increased the discoloration risk posed by the biofilm, with the greatest NTU and metals responses observed at Pipe Loop A during flushing. However, the rate of AOC release from the biofilm into the water column was found to be independent from bulk water AOC concentration. This suggests the need to consider how AOC is used or incorporated into the biofilm, and further understand processes that govern AOC accumulation and subsequent release into the bulk water. The bacterial and fungal community composition was found to differ between biofilms and bulk water samples, with bulk water community composition being found to be dependent of bulk water AOC concentration. The bacterial and fungal community composition within the biofilm was not found to be a function of AOC concentration or the community composition within the bulk water.

Chapter 8: Discussion and Further Work

8.1 Discussion

8.1.1 The Importance of the AOC Method in Determining Planktonic (re)growth and Drinking Water Biostability

The first aim of this thesis was to develop a rapid, robust AOC method that can be routinely applied to operational WTW to gain an insight into AOC removal efficiencies during treatment. The fast, standardised AOC method developed in this study enabled an in-depth study of AOC variation in the DWDS, previously limited due to the time and resource intensive nature of existing AOC assays. The speed and reproducibility of the assay enabled this study to analyse the AOC concentration in drinking water (32 sample points throughout four operational DWDS (including WTW, SR inlet and outlets), over a period of two years. Such an in-depth study, providing an insight into the effect of microbial growth, seasonality, disinfection, DWDS infrastructure and hydraulic retention time on the AOC concentration, would not be possible without the development of a quick, reproducible AOC method. Previous studies that analyse distribution effects are often limited by being spatially unrepresentative (having only a few sample locations in the network) (Lautenschlager *et al.* 2013, Liu *et al*. 2014) or being on a short-term basis looking at weekly or monthly variations (Hu *et al.* 1999). This is therefore the first study of its kind to analyse long-term changes in AOC within both pipes and service reservoirs in DWDS.

The AOC method developed in this study was successfully validated within raw and post-treated water at twenty WTW, confirming AOC removal during conventional water treatment. Although an average of 40% of AOC was removed from the drinking water during treatment, microbial (re)growth was still evident downstream within all four DWDS sampled. The second aim of this thesis was to quantify the degree of 'biological stability' within DWDS by comparing the AOC concentration with routine bulk water quality parameters to provide a

greater insight the relationship between AOC concentration, microbial cell counts and disinfectant within DWDS. AOC has previously been demonstrated to limit microbial growth at concentrations <100 µg/L (Van der Kooij, 1992, LeChevallier *et al*. 1996; Wang, Tao & Xin, 2014; Ohkouchi *et al.* 2013) (Section 2.3.2.7; Table 2.6). Although the degree of microbial (re)growth was reduced in DWDS 1 which was supplied by drinking water containing <100 µg/L, (re)growth was not prevented. This suggests that there is not one universal AOC concentration that represents the threshold for biological stability. Rather, the AOC concentration that will limit (re)growth is dependent on the conditions in each individual WTW or DWDS, and is likely governed by various chemical and microbial interactions that occur as the water passes from source to tap.

The term (re)growth has previously been used to describe the recovery of disinfectant injured cells, whereas aftergrowth has been used to describe microbial growth in a distribution system (Characklis, 1988; van der Kooij, 2003). In this thesis, (re)growth is used to describe microorganisms that survive the treatment process and the multiplication of organisms within the DWDS itself. It is important to consider if (re)growth only refers to planktonic cell growth within the DWDS (as it is often defined), or if the term also includes the growth of cells within biofilms attached to DWDS pipe walls. Often the main focus of (re)growth or biostability research is on the impact of AOC concentration on planktonic bio-stability, despite knowledge that biofilms interactions also impact drinking water quality (Section 1.1). The majority of microbial growth in DWDS occurs on the pipe wall, in comparison to the bulk water (Lehtola *et al*. 2004; Moritz *et al.* 2010), and therefore biofilm formation, activity and subsequent mobilisation is thought to be one of the main causes of a loss in drinking water biostability in DWDS (Manuel *et al*. 2010).

By utilising the AOC method developed in this thesis, along with flow cytometric assessments of planktonic (re)growth, it was possible to identify spatial and seasonal trends in

microbial (re)growth and drinking water biostability within DWDS. This study found evidence of microbial summer (re)growth and subsequent AOC depletion (Figure 6.2, Figure 6.4 and Figure 6.6); a trend that would have been previously undetectable without the development of a fast, reproducible AOC method, and flow cytometric analysis of cell concentrations (total and intact). When making assessments of drinking water biostability, it is also important to accurately quantify the microbial content of drinking water post-treatment and throughout the DWDS. The relationship between AOC and microbial enumeration within drinking water has previously only been assessed in terms of coliforms (LeChevallier *et al.* 1996) and HPC (Van der Kooij, 1992), which only take into account the culturable proportion of bacteria (Allen *et al*. 2004; Hammes *et al*. 2008). In this thesis, the AOC concentration was found to influence both bacterial and fungal communities differently within the bulk water and the biofilm, highlighting the importance of looking across different taxa.

8.1.2 Factors Affecting AOC and Biological Stability in DWDS

8.1.2.1 Disinfection

This thesis aimed to quantify AOC concentrations from DWDS supplied by different source waters and WTW, determine if and how AOC varies within and between different systems, and how AOC is impacted upon by the choice and concentration of disinfection residual. The relationship between AOC, microbial (re)growth and disinfection was analysed within both chlorinated and chloraminated DWDS. The AOC concentration within DWDS was found to be influenced by the degree of cell growth and the presence, type and concentration of disinfection residual (see Figure 6.1 A & B; Section 6.5). An initial increase in AOC in chlorinated water was identified at short distances from the WTW. This increase in AOC was potentially a result of organic matter reacting with chlorine. One reason for an increase in AOC concentration is the oxidation of organic matter macromolecules into small-molecule biodegradable organic

compounds (such as carboxylic acids) by chlorine or chloramine (Lou *et al.* 2009; Liu *et al.* 2015). Hence, the trade-off between achieving effective disinfection and limiting unwanted by-product formation (in this case AOC) becomes a main operational goal for water utilities.

8.1.2.2 Seasonality

One aim of this thesis was to understand temporal and spatial fluctuations in AOC within DWDS by conducting service reservoir (SR) inlet and outlet sampling. This piece of work aimed to identify which areas of the DWDS (pipes or service reservoirs) were acting as sources and sinks of AOC. The long-term timescale of analyses undertaken in this thesis enabled seasonal trends in AOC concentration (and other water quality parameters) to be identified. AOC concentration within DWDS was found to generally increase to a maximum in spring, before declining in summer and autumn. This trend in AOC concentration coincided with an increase in the rate of planktonic microbial (re)growth during summer. Seasonality is therefore able to influence the AOC concentration and rate of (re)growth within drinking water, thereby impacting the degree of water biostability. It is therefore important to consider seasonality when managing the microbial bulk water quality in DWDS. Polanska *et al.* (2005) also observed an increasing trend in the AOC concentration within WTW and DWDS during spring, reaching a maximum in summer; however the rate of (re)growth was not monitored. A decrease in AOC from spring to summer is likely due to the consumption of AOC by heterotrophic organisms. This is demonstrated by an increase in the number of intact cells during summer. A number of studies have demonstrated that at temperatures above 15°C, microbial activity (ICC) will increase (Ndiongue *et al.* 2005; Li *et al*. 2018). The chemical reaction between chlorine and organic matter has also been shown to slow down at lower temperatures (Liu *et al.* 2002). The combined effect of supressed microbial growth and slower oxidation of organic carbon resulted in a continuous increase in AOC concentration during the winter season.

Although a seasonal trend in AOC and planktonic (re)growth was identified during DWDS bulk water sampling, the same trend was not identified in biofilm growth within the pipe loop test facilities. The biofilms that accumulated at the pipe loop were establishing and maturing during the 12 month study period (Figures 7.26 and 7.27), and therefore biofilm maturation was the greatest ecological influence on the biofilms. Once biofilms are established it is possible that seasonal variation might be exhibited within the biofilm. It is also possible that organisms residing in the biofilm are able to exhibit greater resilience to changes in the bulk water conditions, such as higher disinfection concentrations (Wingender *et al.* 1999; Hageskal *et al*. 2012).

8.1.2.3 Hydraulic Retention Time & DWDS Infrastructure

During DWDS bulk water sampling, a general decrease in AOC with increasing hydraulic retention time was found to correlate with an increase in planktonic intact cells. However, AOC concentration is not only a function of hydraulic retention time, but is instead a function of more complex cycling between bulk water and biofilm. By undertaking both SR inlet and outlet sampling, this study identified, for the first-time evidence of pipe vs. SR behaviour, with pipe only sections of the network acting as sources of AOC and SR dominated DWDS acting as sinks of AOC. Pipe only areas of the network have a higher surface to bulk water ratio, and therefore it is likely that interactions with biofilms on the pipe wall are the dominant factors affecting the AOC concentration. In contrast, water within SR has less contact time with the infrastructure surface, and therefore planktonic processes are the dominant factors affecting the AOC concentration. The AOC concentration was found to increase within all of the pipe only sections during winter and 83% of pipe only sections during summer (Figures 6.1 A and B). In cases where organic matter is released from the biofilm, this can increase AOC and cell counts within the bulk water (Han *et al.* 2012). Pipe loop test facility data confirmed the ability of biofilms to contribute to AOC in bulk water during mobilisation events, irrespective of the

background AOC concentration (Figure 7.23). In contrast, the AOC concentration was found to decrease within 67% of SR sampled in both summer and winter (Figures 6.1 A and B). A reduction in AOC during elevated storage within a SR points to AOC consumption by heterotrophic bacteria. This evidence confirms the importance of surface to water volume ratios in the DWDS in determining final water quality, and highlights that the location of the sampling point in the DWDS is critical to interpreting the biostability of drinking water.

8.1.3 The impact of AOC Concentration on Biofilm Mobilisation and Potential Discoloration Risk

This thesis aimed to characterise the effect of elevated shear stress (flushing) upon the biofilms that has accumulated under different AOC concentrations, and to quantify how easily the material mobilised into the bulk water (in terms of AOC concentration, cell counts, turbidity and inorganic material.) Ultimately this research will determine if an elevated AOC concentration in the bulk water will affect the microbial and discolouration risk of the biofilm. a high AOC concentration during biofilm development resulted in the greatest, and most consistent, increase in discoloration (indicated by turbidity and largest increase in bulk water iron and manganese concentration) during mobilisation compared to other AOC concentrations (Figures 7.17, 7.18 and 7.19). This could be a result of the high AOC biofilm having accumulated more inorganic material during the growth phase, or the biofilm being less resistant to mobilisation. Therefore, elevated AOC concentrations may contribute to forming biofilms which pose a greater discoloration risk. Similarly, the smallest discolouration response following mobilisation was exhibited by biofilms accumulated under low AOC conditions. Further research is needed to understand if, or how, the AOC concentration influences biofilm structure and stability. The rate of biofilm detachment is also dependent on hydraulic conditions (Abe *et al.* 2012; Douterelo *et al*. 2013; Fish *et al*. 2017), disinfection residual and

temperature (Ginige *et al.* 2011) within the DWDS, all of which can also influence the AOC concentration within the bulk water.

In addition to turbidity, (in)organics are also released into the bulk water during flushing, as a result of EPS and cells in the biofilm being mobilised. As identified in Figures 7.26 and 7.27, the site containing the highest concentration of AOC also had the greatest TCC and ICC released from the biofilm into the bulk water during mobilisation tests. A greater AOC concentration led to increased cell incorporation into the biofilm during the growth phase, and a lower degree of biofilm stability so that more cells were released during flushing.

8.1.4 The Impact of AOC on Biofilm Growth

An aim of this research was to determine the relationship between AOC concentration and biofilm volume, community composition and stability within a DWDS. AOC was found to have a significant effect on both the degree of biofilm accumulation and the cell content of the biofilm, during the twelve month study period. SEM images and cell counts confirm the accumulation of biofilm over time (Figures 7.24 and 7.25). The AOC concentration significantly impacted the number of cells within biofilm, with a higher AOC concentration in the bulk water leading to greater number of cells (total and intact) within the biofilm and the bulk water. This suggests greatest growth of cells in the biofilm will occur when AOC is not limited; a trend identified for the first time within a full scale pipe loop system. DWDS sampling revealed pipe only areas of the network acted as net sources of AOC, suggesting biofilms generally contribute towards AOC in the bulk water. The rate of exchange of AOC between the bulk water and biofilm will dependent on other environmental conditions within the DWDS. Fish *et al.* (2017) suggested that high varied flow rates might lead to increased nutrient uptake by the biofilm, causing the biofilm to act as a net sink of nutrients.

The AOC concentration was found to have a significant impact on biofilm community composition, with bacterial and fungal community compositions exhibiting a clear site effect.

The AOC concentration was also found to impact the biofilm bacterial and fungal community composition, but to a lesser extent. AOC impacted initial colonisation, with three distinct communities being identified. The biofilm community composition became more similar by 12 months, although the communities were still distinct. A clear shift was observed from initial colonisers (Day 0 and Month 3) to a more stable 'core community' after 12 months.

8.1.5 AOC Behaviour

The AOC concentration within post-treated drinking water is a function of source water quality and the type of treatment processes applied. However, the AOC concentration is not constant throughout the DWDS, and will be affected by environmental conditions (physical, chemical and microbial) in the DWDS, including the degree of (re)growth (within the bulk water and within biofilms), DWDS infrastructure (the surface-area-to-water-volume ratio of pipes vs SR), hydraulic retention time, type and concentration of disinfectant, and seasonality. Bulk water AOC is utilised by heterotrophic, planktonic microorganisms for growth, subsequently leading to a net depletion of AOC. The rate of planktonic microbial (re)growth is not only dependent on the carbon concentration, but also nutrient availability, disinfectant, and seasonality (temperature). Although the application of a disinfection residual is able to limit planktonic cell growth within DWDS (Gillespie *et al.* 2014), disinfectant can oxidise the natural organic matter in drinking water to produce AOC that can support the growth of heterotrophic bacteria (Liu *et al*. 2002; Ramseier *et al*. 2011). The rate of this reaction is also influenced by water temperature. Data presented in Figures 6.2, 6.4 and 6.6, confirms that elevated water temperature is associated with increased bacterial abundance in DWDS, as also found by Francisque *et al.* (2009) and Liu *et al.* (2013).

This thesis established spatial and temporal variations in AOC concentration with distance into the network or hydraulic retention time. Hydraulic retention time is a function of distance from WTW, water velocity (caused by water consumption) and storage time within

SR (Prest *et al*. 2016). A higher hydraulic retention time in the network has been associated with higher bacterial numbers (Nescerecka *et al.* 2014), decay of a disinfection residual (Servais *at al*. 1995) and depletion of AOC (Han *et al*. 2012). However, this study found that the AOC concentration in drinking water was not only a function of hydraulic retention time but was also dependant on the surface-area-to-water-volume ratio within DWDS. It is this ratio that effects the time that water spends in contact with either the surface of pipes or SR, and any biofilm that may be attached.

Crucially, the AOC concentration in drinking water is impacted by interactions occurring in the bulk water, and those taking place in biofilms. During DWDS sampling. pipe dominated areas of the network exhibited a net decrease in the AOC concentration (Figures 6.1 A and B), suggesting that AOC in the bulk water was being used to support microbial growth within the biofilm attached to the pipe wall. The rate of this exchange between the bulk water and biofilm is dependent on the time in which water is able to come into contact with the pipe or SR surface. Carbon and nutrients follow a gradient towards the pipe wall, a process which is driven by the turbulence of the water (Fish *et al.* 2016). It is only when the biofilm is mobilised that AOC, and potentially cells, will be supplied back into the bulk water. Biofilm mobilisation is either generated through daily background release or larger mobilisation events occurring after a change in environmental conditions, such as an increase in the hydraulic shear stress. AOC release from the biofilm was examined herein for the first time and unexpectedly demonstrated that the rate of AOC release from the biofilm was the same within each site, independent of the AOC concentration within the bulk water. This suggests that complex cycling of AOC occurs in the biofilm, in which excess AOC is potentially stored within the biofilm at times of elevated AOC concentration in the bulk water. The storage of AOC within the biofilm is likely limited by ecological processes occurring within the biofilm, providing a threshold to AOC storage. A conceptual model is presented in Figure 8.1, illustrating the

complex cycling of AOC in DWDS, based on the interpretations of data presented throughout this thesis. The comprehensive model provides a greater understanding of AOC cycling within drinking water, essential in the management and maintenance of biological stability within DWDS environments.

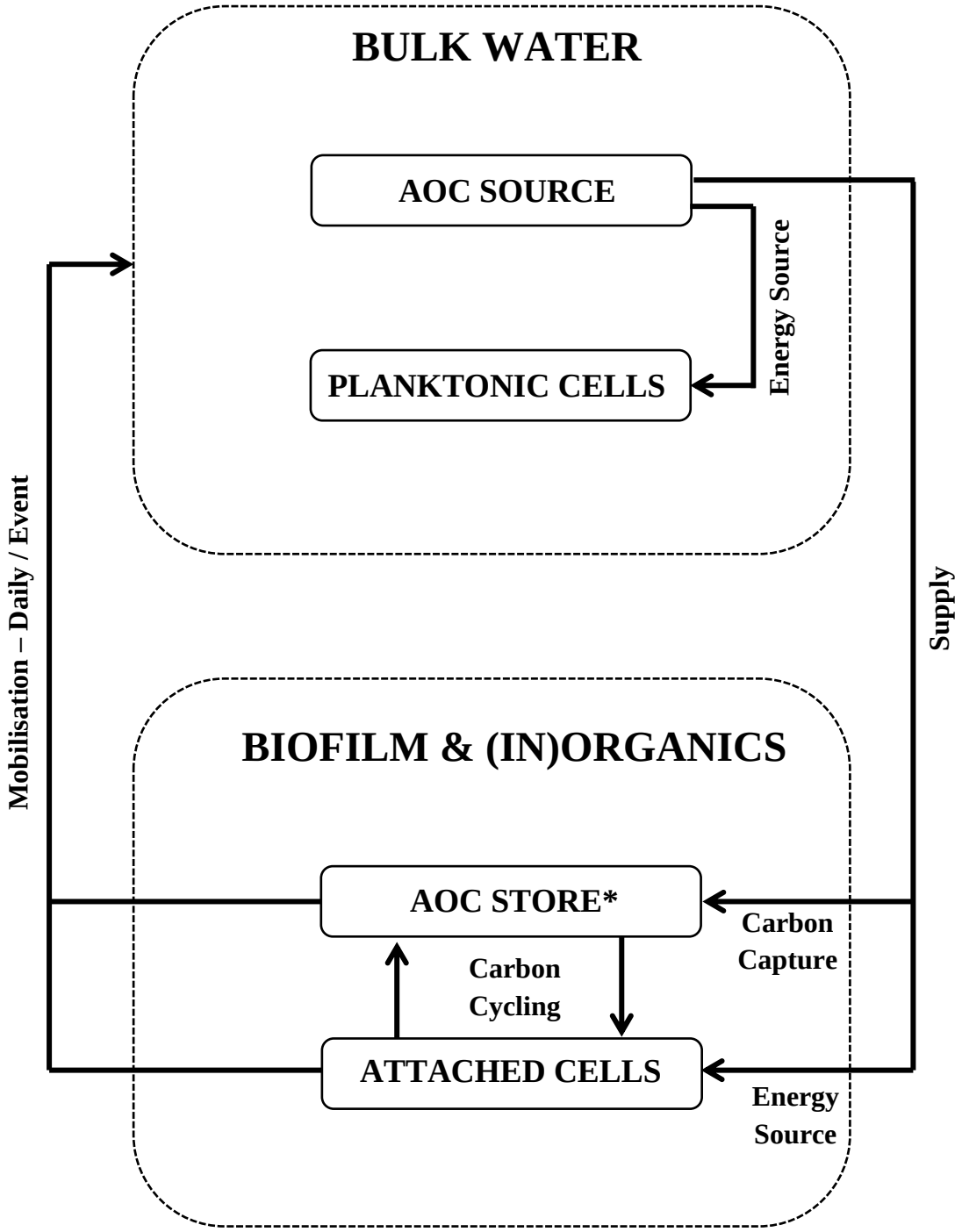

Figure 8.1: Conceptual model of assimilable organic carbon (AOC) cycling within DWDS. *AOC store within biofilm: biofilm includes EPS, cells and associated particles.

8.2 Further Work

This project has provided a novel insight into characterising AOC within operational drinking water supply systems and the effect of AOC concentration on drinking water microbiology within both the bulk water and attached in biofilms. Furthermore, this research led to the development of thee state-of-the-art pipe loop test facilities, which provide a unique opportunity to investigate biofilm–water quality interactions in future research projects. Two potential future project which would provide a continuation to this EngD would be a) further analysis of nutrients b) the impact of disinfection on drinking water biostability.

8.2.1 Further analysis of Nutrients

Drinking water supplies are often dosed with phosphate to either reduce the formation of iron and manganese precipitates, or to increase the water pH and thereby reduce the extent to which lead dissolves in water. Microorganisms not only require carbon for growth but other nutrients including nitrogen and phosphorus (Mietinen *et al.* 1997). To gain a holistic understanding of biostability within drinking water, it is important to monitor the impact of other nutrients, such as phosphorous, on accumulation and mobilisation of biofilm within drinking water. It is not known if a change in a limiting nutrient can occur during the DWDS due to changes in pipe material, mixing of waters from different treatment facilities or due to biofilm formation (Prest, 2015). Secondly, it is also important to determine the importance of autotrophic microbial growth within DWDS. Although the extent of autotrophic growth within DWDS is much smaller in comparison to heterotrophic growth, their occurrence has been reported in various DWDSs, and have often been related to aesthetic or operational problems (e.g. bio-corrosion). A greater understanding of the behaviour of physical structure of biofilms would be required in order to accurately predict biofilm response to changing nutrient availability.

8.2.2 The Impact of Disinfection on Drinking Water Biostability

A disinfection residual is often added to final water to limit microbial (re)growth during distribution. The type and concentration of disinfection affects the abundance and community composition of microorganisms in the bulk water and within drinking water biofilms; and affect discoloration response of biofilms should they become mobilised (Fish *et al*. 2018). Chloramination has been shown to be more effective than chlorine at being able to penetrate biofilms (De Beer, Srinivasan & Stewart 1994, Chandy & Angles 2001, LeChevallier *et al.* 2007). However, monochloramines can act as a source of ammonia, providing a nutrient source for AOB. Although studies have analysed the impact of different chlorine concentrations on biofilm accumulation and subsequent mobilisation, it is not clear what effect switching between different disinfection residual types (chlorine and chloramines) has on biofilms within drinking water. A range of interesting research questions include the effect of switching disinfection types on: the growth and release effects of material trapped at the wall, biofilm community composition and nitrification rates. A second experiment would be to explore the effects of pulse dosing, both with the same and/or changing disinfectant type. This research would assess if it is possible to develop the equivalent to 'flow conditioning' for disinfection *i.e.* periodic stressing of the system to limit build-up of material and hence manage risk. This could potentially represent a very low cost management option if effective. It would also be possible to explore the effects of pulse dosing a high chlorine concentration into chloraminated systems (as performed in US practice).

Chapter 9: Business Case

9.1 Introduction

Modern water treatment systems produce high-quality, safe drinking water. However, microorganisms are able to survive the treatment process, such as inactivation by chlorine disinfection, and persist within DWDS. As heterotrophic microorganisms require organic carbon for growth, the concentration of AOC within water is thought to govern the degree of microbial growth and determine the microbiological 'stability' of drinking water during its distribution. This project aims to '*Understand the Impact of Assimilable Organic Carbon on Biological Stability and Biofilm Development within Drinking Water'*. The project is conducted in collaboration with the University of Sheffield and Scottish Water (Scottish Water). Ultimately this project offers the development of a more rapid, reproducible AOC method that can be used for regular industry based sampling and provides an insight into how AOC concentration can influence biofilm accumulation, composition and detachment within fully operational DWDS. This business case will consider the knowledge transfer and cost effectiveness of the project, the current (and future) benefits of the project to Scottish Water and suggest a business case for exploiting the outcomes of the research.

9.2. Project Overview

The EngD project was conducted in collaboration with Scottish Water (Scottish Water) and the University of Sheffield to develop a quick and reproducible AOC method that could be used for routine drinking water analyses. The AOC method was applied to a number of WTW and DWDS to validate the method and to understand the impact of AOC fluctuations on microbial growth. AOC sampling at both service reservoir (SR) inlet and outlet sample taps provided the ability to distinguish pipe or SR effects on AOC within the DWDS. In addition, the impact of

AOC on biofilms was analysed through the installation of pipe loop test facilities at three WTW, each characterised by drinking water containing different AOC concentrations.

9.3 Project Overview & Aims

This research aimed to analyse AOC removal efficiencies at the WTW and determine the impact of spatial and temporal variation in AOC concentration on the biostability of post-treated water and biofilm growth within the DWDS.

The objectives of this research were:

i) To develop a rapid, robust AOC method that can be used for routine drinking water analyses, and validate the developed method through application at WTW.

ii) To quantify AOC concentrations from DWDS supplied by different source waters and WTW, ranging from clean borehole to surface water site and different disinfection residuals (chlorinated and chloraminated).

iii) To quantify the degree of 'biological stability' within DWDS by comparing the AOC concentration with routine bulk water quality parameters to provide a greater insight the relationship between AOC concentration, microbial cell counts and disinfectant within DWDS.

iv) To understand spatial and temporal fluctuations in AOC within DWDS, and identify which areas were acting as sources and sinks of AOC.

v) To determine the relationship between AOC concentration and biofilm volume, community composition and stability within a DWDS.

vi) To characterise the effect of elevated shear stress (flushing) upon the biofilms that remain attached, and to quantify the material mobilised into the bulk water.

9.4 Problem definition and specifying of research needs

Despite drinking water utilities in the UK consistently achieving a very high degree of water quality compliance, regulatory failures do still occur. Although high quality water is produced at WTW, the microbial quality of water can deteriorate in the DWDS. There are numerous pathways by which contaminants, including micro-organisms, can enter and colonise the DWDS. Microorganisms require carbon, nitrogen and phosphorus in the ratio of 100C:10N:1P for growth (LeChevallier *et al*. 1991; Chandy & Angles 2001), inferring that in most systems carbon will be the limiting nutrient. As AOC refers to the fraction of total organic carbon (TOC) that is most easily assimilated by aquatic organisms for growth, it is expected that by limiting the AOC concentration in a system this should result in reduced bacterial (re)growth. However, AOC is not currently sampled by water utilities due the time and resources required to complete the method.

9.5 Scottish Water

Scottish Water is a publically owned combined water and sewerage company, operating 252 drinking WTW (The Scottish Government, 2014), providing 1.3 billion litres of drinking water every day (Scottish Water, 2018). Scottish Water undertakes over 300,000 scientific tests each year, of which over 90,000 are conducted for microbial analysis. Regulatory sampling by Scottish Water is conducted to detect organisms who's presence is indicative of faecal or environmental contamination; including coliform bacteria, Escherichia coli (E.coli), Enterococci and Clostridium perfringens (Scottish Water 2013)). Like most water utilities in the UK, Scottish Water is able to achieve a high level of with 99.91% of all drinking water tests meeting statutory microbiological standards (Scottish Water 2013).Specifically, with regards to samples taken for coliform bacteria and E. coli analysis only, the majority of samples are taken in the service reservoir (approximately 55% of samples taken), with 30% at the exit of the treatment works and 15% at the consumers tap. Taking this into account, the highest

number of bacteriological failures for coliform bacteria, per samples taken, occurs at the customers tap (Scottish Water 2014). This same trend was identified at in Severn Trent systems (Ellis *et al.* 2013). This suggests that the quality of drinking water degrades considerably as it passes through the length of the distribution network

Microbiological assessments traditionally conducted during treatment and distribution generally include bacteria enumeration of bulk water samples using conventional plating methods such as heterotrophic plate counts (HPC) (Sartory 2004). HPC enumeration techniques greatly underestimate the real numbers of microorganisms within drinking water as the majority of the planktonic and bacteria detached from biofilms are unable to grow on the media (Allen *et al.* 2004, Berney *et al.* 2008). Furthermore, the majority of microbiological biomass within a DWDS exists attached to the walls, with only a small amount existing within the water itself, thus highlighting the unrepresentative nature of using bulk water samples alone (Zacheus *et al*. 2001; Flemming *et al.* 2002). It was therefore important that this study explored the impact of AOC not only on microorganisms residing in the bulk water, but also those within biofilms. To explore these impacts it was clear from an early stage that the majority of research for this project should consist of *in-situ* assessments at Scottish Water.

9.6 Project Benefits to Scottish Water

To date, this research project has provided Scottish Water with a number of benefits including;

- The development of a novel and advanced AOC method that can be used in Scottish Water.
- Enhanced knowledge of treatment works performance including AOC removal efficiency.

- Previously unknown information regarding the impact of AOC on microbiology with DWDS, including different behaviour of AOC in different infrastructure (pipe vs service reservoir effects).
- Investment made on state of the art pilot biofilm sampling pipe loop facilities.
- Investment into SR inlet sample tap installations to provide insights into pipe vs SR behaviour.

9.7 The cost effectiveness of the project for Scottish Water

The STREAM EngD is jointly funded by the Engineering and Physical Sciences Research Council (EPSRC) and Scottish Water. EPSRC provided a stipend £15,226 / year, plus £3900 / year in tuition fees. On top of that EPSRC pays ~£11,000 per year for training and support. This funding is used to fund the costs associated with the Transferable Skills, Education and Learning (TSEL) weeks, the induction semester, accommodation and travel. The remainder of this funding is used to support project expenses, accumulating to ~£3500 / year in 'direct' project support.

When the project commenced, Scottish Water committed to providing top-up funding of (minimum) £48,000 over four years for an EngD project. This budget was initially divided into:

- Out-source gene sequencing and associated taxonomy analysis - £25,000
- Preparation of DNA (deoxyribonucleic acid) samples for sequencing – £10,000 (all other analysis costs internal to Scottish Water laboratories – including flow cytometry (FCM), adenosine triphosphate (ATP) and AOC)
- Allowance for consumables for sampling equipment and facilities including coupons and/or pipe loop test system - £5000 (this is subject to review and revision, for example if coupons are to be installed this will incur substantial enabling works but potentially this would be internal cost to Scottish Water)

- Travel and subsistence for accessing a range of field sites across Scottish Water region – £5,000 (in addition to the sums available via the normal STREAM funding)

After the project plan was developed, additional funding was provided by Scottish Water for:

- Construction of the three pipe loop test facilities (£13,000 per loop)
- Installation of two service reservoir inlet taps

The additional cost of the pipe loops test facilities provided Scottish Water with state of the art pipe loops that can provide Scottish Water with analysis of biofilms grown in situ. Scottish Water also have plans to use these test loop facilities for additional research projects in the future.

This project has benefited Scottish Water though the development of an AOC method and knowledge of AOC variations throughout drinking water treatment and distribution. There is a potential to offer AOC protocol training internally at Scottish Water and potentially offer training to other water companies. This project also hopes to provide Scottish Water with an indirect economic benefit through reducing the number of microbial investigations that Scottish Water have to undertake. The majority of samples taken for coliform bacteria and *Escherichia coli* (*E. coli)* analysis are taken in the service reservoir (approximately 55% of samples taken), with 30% at the exit of the treatment works and 15% at the consumers tap. Taking this into account, the highest number of bacteriological failures for coliform bacteria, per samples taken, occurs at the customers tap (biollWater, 2014). This same trend was identified at Severn Trent systems (Ellis *et al.* 2013). Water companies are subjected to financial implications when investigating coliform and *E. coli* failures during routine water quality monitoring. Ellis *et al.* (2018) analysed the cost associated with investigations for 737 coliform and *E. coli* failures across five UK water companies (including Scottish Water). The average investigation costs ranged from £575 for a customer tap failure to £4,775 for a water

treatment works finished water failure. These costs can be divided into labour costs, re-sampling and transportation. It is hoped that knowledge gained from this project will provide Scottish Water with additional knowledge regarding AOC and microbial growth to help efficiently manage the biological stability of these systems. Furthermore, this project will equip Scottish Water with a holistic understanding of microbiology within DWDS, gaining knowledge of the role of biofilms within DWDS and their impact on bulk water quality. As an estimated 95% of the overall biomass is attached to pipe walls, while only 5% resides in the water itself (Flemming *et al*. 2002) is essential to understand attached communities within these environments.

9.8 A business case for exploiting the outcomes from the research

9.8.1 Rationale for research exploitation

As a result of this project, Scottish Water now have access to three pilot loop systems installed within their WTW. This project utilised the pipe loops to analyse the relationship between *in-situ* biofilm growth, mobilisation and AOC concentration. However, DWDS are very complex systems and microbial growth is not only impacted upon by carbon concentration. There is therefore potential to explore the impact of a range of variables on water quality and biofilms.

9.8.2 Exploitation options

The pipe loops can easily be utilised to analyse the impact of other nutrients such as nitrogen and phosphorous on microbial growth. The concentrations of biologically available nitrogen and phosphorus are well known to play a key role in determining the ecological status of aquatic systems (Wetzel, 1983). However, it is not clear how the ratio of these organic nutrients influences the type of microorganisms which occur and whether or not individual species or whole communities are likely to be N- or P-limited within DWDS. At present, the monitoring strategies for drinking water involve detecting microorganisms in water from taps using culture

methods, which only analyse the planktonic, culturable fraction of bacteria. 95% of the overall biomass of DWDS microbiology exists attached to pipe walls, while only 5% resides in the water itself (Flemming *et al.* 2002). In this research proposal, culture-dependent methods would be combined with advanced techniques such as flow cytometry and DNA sequencing to monitor microbial abundance and diversity. Exploitation options include ambitious field trials to determine the degree of carbon, nitrogen and phosphorus limitation within operational drinking water systems, and its impact on bulk water microbiology. This would include sampling drinking water at a number of water utilities, including within raw water, treated water and distributed water (both from pipe lines and service reservoirs).

9.8.3 Benefits

The proposed future project could combine the representative nature of fieldwork studies with the controlled environment of a pipe loop test facility which allows environmental manipulation, experimental replication and biofilm sampling.

9.8.4 Risks

The risks associated with the proposed research are limited as no upfront costs are required to construct the pipe loop test facilities. Furthermore, service reservoir inlet taps are already in place for bulk water sampling.

9.8.5 Costs

The infrastructure needed for this work including existing pipe loop test facilities and service reservoir inlet and outlet sampling taps are already installed. This would therefore mean that the majority of the cost required for this project would be in the form of a researcher salary, sequencing costs and laboratory consumables.

The requirements for this investigation would be:

- Researcher salary: £20,000 per annum

- Out-source gene sequencing and associated taxonomy analysis - £25,000
- Preparation of DNA samples for sequencing – £10,000
- Travel and subsistence for accessing field sites across Scottish Water region – £5,000

9.8.6 Timescales

The timescale of the proposal would be dependent on the length of the sampling regime. This work would either be completed as part of a PhD/EngD project or as a post-doctoral research project. It is anticipated that this research could be completed within three years.

9.8.7 Evaluation

The overriding objective of the proposed project is to use the information and understanding from this thesis to inform proactive management and the prevention of microbiological failures in drinking water. Microbial (re)growth within the DWDS has the potential to generate bacterial regulatory failures, create taste, odour, colour, nitrification and turbidity in the drinking water and increase the occurrence of operational issues such as biofouling and bio-corrosion. In addition, biofilms can support the multiplication of potentially pathogenic bacteria detrimental to human health (Wingender & Flemming, 2011). Therefore, the monitoring and control of nutrients entering and being distributed within the DWDS is critical to limiting (re)growth of microorganisms within these systems.

9.9 Knowledge transfer and exploitation of the project outcomes within Scottish Water

Results from this thesis have been shared with operators, Process Scientists and industrial supervisors at quarterly Process Science meetings. F Pick also delivered an oral presentation at both Scottish Water NOM Conference and Juniper House Science Meeting, and a poster presentation at Scottish Water Working Towards Zero Microbial Failures Conference. F. Pick

shared results and information regarding the project with interested parties within Scottish Water.

9.10 How the research will benefit the Scottish Water, the water sector, and society

9.10.1 Benefits to Scottish Water

Understanding the relationship between AOC and drinking water microbiology will allow Scottish Water to develop a greater understanding of managing biological stability source to tap, which can be used to proactively maintain microbiological compliance. The overriding objective of the EngD project will be a means to identify the root cause of microbial growth and ultimately prevent microbiological failures. The fast and reproducible AOC test developed in this study will enable routine AOC analysis to be conducted in DWDS. By monitoring the AOC concentration within bulk water, it is possible to manage the rate of microbial (re)growth within both the bulk water and in biofilms.

9.10.2 Benefits to the water sector

Once the AOC methodology developed in this study has been published, the AOC method has the potential to utilised by other water companies in the UK. AOC is not currently widely sampled as it is a time consuming and resource intensive method. The use of a consistent method across the water sector would enable comparisons between datasets. As the water sector is largely focused around five year Asset Management Plan (AMP) cycles, it is vital that the industry works together with researchers, to enable them to consider the impacts of long-term pressures and possible management strategies.

9.10.3 Benefits to society

Improved management of the microbial quality drinking water will benefit wider society, safeguarding the continued provision of high quality water and protecting against water-borne

disease, with the emerging pressures of increased urbanisation and climate change. Although water-borne outbreaks are uncommon, they do still occur. The recent *Cryptosporidium* outbreak during August 2015, affected 300,000 homes in Lancashire costing United Utilities approximately £25 million as listed in their trading update for the six months ending 30 September 2015 (Water Briefing, 2015). Furthermore, better management of the microbial quality of drinking water can potentially lead to a reduced risk of discoloration; the main cause of customer complaints in England and Wales (Husband & Boxall, 2011). It is important the abiotic and biotic factors influencing microbial growth within the DWDS are fully understood to protect water quality and hence public health and well-being.

Chapter 10 Conclusion

This thesis aimed to provide a greater understanding of the relationship between AOC and drinking water quality, in particular the impact of AOC on microbiology within both the bulk water and biofilms attached to the pipe walls of drinking water distribution systems (DWDS) infrastructure. In order to enable routine AOC sampling within drinking water supply systems, an AOC assay was developed which incorporates the standardisation of using known strains of bacteria (*Pseudomonas fluorescens* strain P-17 and *Spirillum* strain NOX), with the increased speed of using a higher inoculum volume and enumeration using flow cytometry. By utilising known bacterial strains it is possible to use standardised yield curves to convert the cell count to AOC concentration. Validation of the developed assay has confirmed its suitability for use in the field, capturing an extensive range of AOC loading in raw and post-treated water across 20 WTW. The AOC concentration was found to decline during the treatment process within all WTW, with an average 40% decrease in AOC concentration. However, although the quality of post-treated water is high, microbial growth still occurred in DWDS, leading to a loss of biological stability.

Application of the new AOC method within service reservoir (SR) inlet and outlets demonstrated, for the first time, complex cycling of AOC within DWDS. The AOC concentration was found to increase within the majority of pipe only sections of the DWDS but decreased within SR. This indicates that the concentration of AOC is a function of both planktonic and biofilm processes within DWDS and that these process are different (net use vs. net release). A comparison of AOC concentration to cell counts within the DWDS highlighted the relationship between AOC and (re)growth was dependent upon the disinfection residual and seasonality. Within chlorinated DWDS, an initial increase in AOC was identified at short distances from the WTW. The use of chloramination within DWDS was able to suppress the presence of intact cells more efficiently than free chlorine, but not completely

prevent (re)growth. Seasonality influenced the AOC concentration and rate of (re)growth within drinking water, thereby impacting the degree of water biostability.

Using state-of-the-art pipe loop test facilities, an increased AOC concentration was found to result in a greater concentration of cells (total and intact) within the biofilm. This suggests greatest growth of cells in the biofilm will occur when AOC is not limited. After 12 months accumulation, the community composition of bacteria developed biofilm at each site were found to be remarkably similar, despite the community composition of incoming post-treated water exhibiting a clear site effect. The AOC concentration was found to impact the planktonic (bulk water) microbiome to a greater extent than microorganisms residing in the biofilm.

A higher AOC concentration led to biofilms developing that posed the greatest discolouration risk if they should detach. Surprisingly, during mobilisation, the rate of AOC release from the biofilm was the same in all three pipe loops, despite the bulk water containing different AOC concentrations. As AOC generally increased within pipe only section during DWDS sampling, this suggests that drinking water biofilms are a net source of AOC. This study proposed a comprehensive conceptual model that captures the complex cycling of AOC that occurs in the biofilm, in which the AOC concentration is subject to internal storage, consumption by attached cells and different mobilisation rates due to daily release or hydraulic events.

This thesis highlighted the importance of monitoring AOC regularly within DWDS, at different locations in the network, to identify areas in a network where (re)growth is likely to occur and therefore impact drinking water biostability. The AOC concentration was found to impact planktonic and biofilm microorganisms differently, confirming that planktonic samples provide a limited insight into biofilm behaviour within DWDS. This thesis provided greater understanding of AOC behaviour and demonstrated for the first time that the AOC

concentration,, together with biofilm processes, play a key role in governing microbial ecology and bio-stability within DWDS environments. The comprehensive model provided in this study provided a useful tool to understand complex AOC cycling within drinking water, essential in the future management of DWDS systems.

Chapter 11: References

Abe, Y., Skali-Lami, S., Block, J. C. & Francius, G. (2012), `Cohesiveness and hydrodynamic properties of young drinking water biofilms', *Water Research* 46(4), 1155-1166.

Aggarwal, S., Jeon, Y. & Hozalski, R. M. (2015), `Feasibility of using a particle counter or flow-cytometer for bacterial enumeration in the assimilable organic carbon (AOC) analysis method', *Biodegradation*. 1-11.

Alhamlan, F. S., Al-Qahtani, A. A., & Al-Ahdal, M. N. A. (2015). Recommended advanced techniques for waterborne pathogen detection in developing countries. *The Journal of Infection in Developing Countries*, 9(02), 128-135.

Allen, M., Edberg, S. & Reasoner, D. (2004), `Heterotrophic plate count bacteria - what is their significance in drinking water?', *International Journal of Food Microbiology* 92, 265-274.

Alowitz, Michael J., and Michelle M. Scherer. "Kinetics of nitrate, nitrite, and Cr (VI) reduction by iron metal." *Environmental Science & Technology* 36.3 (2002): 299-306.

APHA (2005), *Standard Methods for the Examination of Water and Wastewater*, 21st Edition, American Public Health Association, New York.

Ashbolt, N. J. (2015). Microbial contamination of drinking water and human health from community water systems. *Current environmental health reports*, 2(1), 95-106.

Bazri, M. M. & Mohseni, M. (2013), `A rapid technique for assessing assimilable organic carbon of UV/H2O2-treated water. ', *Journal of Environmental Science and Health. Part A.* 48(9), 1086-1093.

Beal, C., Stewart, R. A., Huang, T. & Rey, E. (2011), `SEQ residential end use study', *Journal of the Australian Water Association* 38(1), 80-84.

Beech, I. B. & Sunner, J. (2004), `Biocorrosion: towards understanding interactions between biofilms and metals.', *Current opinion in Biotechnology* 15(3), 181-186.

Berney, M., Vital, M., Hülshoff, I., Weilenmann, H. U., Egli, T., & Hammes, F. (2008). Rapid, cultivation-independent assessment of microbial viability in drinking water. *Water research*, 42(14), 4010-4018.

Bougeard, C. M., Goslan, E. H., Jefferson, B. & Parsons, S. A. (2010), `Comparison of the disinfection by-product formation potential of treated waters exposed to chlorine and monochloramine', *Water Research* 44(3), 729-740.

Boxall, J. B., Skipworth, P. J. & Saul, A. J. (2001), `A novel approach to modelling sediment movement in distribution mains based on particle characteristics', *Water software systems 1*, 263-273.

Boxall, J., Skipworth, P. & Saul, A. (2003), `Aggressive ushing for discolouration event mitigation in water distribution networks', *Water Supply* 3(1-2), 179-186.

Boxall, J. B., & Saul, A. J. (2005). Modeling discoloration in potable water distribution systems. *Journal of Environmental Engineering*, 131(5), 716-725.

Brazos, B. J. & O'Connor, J. T. (1996), `Seasonal effects on generation of particle-associated bacteria during distribution', *Journal of environmental engineering* 122(12), 1050-57.

Brettar, I. & Höfle, M. G. (2008), `Molecular assessment of bacterial pathogensa contribution to drinking water safety', *Current opinion in biotechnology* 19(3), 274-280.

Butterfield, P. W., Camper, A. K., Ellis, B. D. & Jones, W. L. (2002), `Chlorination of model drinking water biofilm: implications for growth and organic carbon removal', *Water Research* 36(17), 4391-4405.

Cabaniss, S. E., Madey, G., Maurice, P., Zhou, Y., Leff, L., Wetzel, B., Leenheer, J., and Wershaw, B. (2007). Stochastic Synthesis of Natural Organic Matter, *UNM, ND, KSU, UNC, USGS*, 22 Apr, 2007.

Camper, A. (1996), `Factors limiting microbial growth in the distribution system laboratory, pilot-scale experiments', *Denver, Colo: American Water Works Association Research Foundation, American Water Works Association.*

Camper, A., Brastrup, K., Sandvig, A., Clement, J., Spencer, C. & Capuzzi, A. S. (2003), `Effect of distribution system material on bacterial growth', *Jour. AWWA* 95(7), 107-121.

Capellier, M., Picoche, C. & Deguin, A. (1996), `Evolution of BDOC in distribution networks. Two examples', *Journal of water science* 5, 51-67.

Carter, J. T., Rice, E. W., Buchberger, S. G., & Lee, Y. (2000). Relationships between levels of heterotrophic bacteria and water quality parameters in a drinking water distribution system. *Water Research*, 34(5), 1495-1502.

Chandy, J. P. & Angles, M. L. (2001), `Determination of nutrients limiting biofilm formation and the subsequent impact on disinfectant decay', *Water Research* 35(11), 2677-2682.

Chang, Y. C., Le Puil, M., Biggersta_, J., Randall, A. A., Schulte, A. & Taylor, J. S. (2003), `Direct estimation of biofilm density on different pipe material coupons using a specific DNA-probe', *Molecular and cellular probes* 17(5), 237-243.

Characklis, W.G. (1988). *Bacterial (re)growth in distribution systems,* Project Report, American Water Works Association, USA.

Charnock, C., & Kjønnø, O. (2000). Assimilable organic carbon and biodegradable dissolved organic carbon in Norwegian raw and drinking waters. *Water Research*, 34(10), 2629-2642.

Chen, C., Zhang, X., He, W., Lu, W., & Han, H. (2007). Comparison of seven kinds of drinking water treatment processes to enhance organic material removal: a pilot test. *Science of the Total Environment,* 382(1), 93-102.

Cheswick, R., Cartmell, E., Lee, S., Upton, A., Weir, P., Moore, G., Nocker, A., Jefferson, B., & Jarvis, P. (2019). Comparing flow cytometry with culture-based methods for microbial monitoring and as a diagnostic tool for assessing drinking water treatment processes. *Environment international*, 130, 104893.

Chu, C., Lu, C. & Lee, C. (2005), `Effects of inorganic nutrients on the (re)growth of heterotrophic bacteria in drinking water distribution systems', *Journal of environmental management* 74(3), 255-263.

CIWEM. (2012). Lead in Drinking Water. Available online: http://www.ciwem.org/policy-and- international/policy-position -statements/lead-in-drinking-water.aspx (accessed October 2016).

Cloete, T. E., Westaard, D. & Van Vuuren, S. J. (2003), `Dynamic response of biofilm to pipe surface and uid velocity', *Water Science and Technology* 47(5), 57-59.

Cook, D. M., & Boxall, J. B. (2011). Discoloration material accumulation in water distribution systems. *Journal of Pipeline Systems Engineering and Practice*, 2(4), 113-122.

Costerton, J. W., Geesey, G. G. and Cheng, K. J. (1978), `How bacteria stick', *Scientific American* 238, 86-95.

Costerton, J. W., Lewandowski, Z., Caldwell, D. E., Korber, D. R. & Lappin- Scott, H. M. (1995), `Microbial biofilms', *Annual Reviews in Microbiology* 49(1), 711-745.

Craun, G. F. & Calderon, R. (2001), `Waterborne disease outbreaks caused by distribution system deficiencies', *W J. Am. Water Works Ass* 93(9), 6475.

Craun, G. F., Brunkard, J. M., Yoder, J. S., Roberts, V. A., Carpenter, J., Wade, T., Calderon, R. L., Roberts, J. M., Beach, M. J. & Roy, S. L. (2010), `Causes of outbreaks associated with drinking water in the United States from 1971 to 2006.', *Clinical Microbiology Reviews* 23(3), 507-528.

Crittenden J.C, Trussel R.R, Hand D.W, Howe K.J, Tchobanoglous G. (2005) *Water treatment: principles and design.* 2nd edition. John Wiley & sons.

De Beer, D., Srinivasan, R. & Stewart, P. S. (1994), `Direct measurement of chlorine penetration into biofilms during disinfection', *Applied and Environmental Microbiology* 60(12), 4339-4344.

De Beer, D., Stoodley, P., Roe, F. & Lewandowski, Z. (1994), `Effects of biofilm structures on oxygen distribution and mass transport', *Biotechnology and bioengineering* 43(11), 1131-1138.

De Beer, D. & Stoodley, P. (1995), `Relation between the structure of an aerobic biofilm and transport phenomena', *Water Science and Technology* 32(8), 11-18.

De Beer, D., Stoodley, P. & Lewandowski, Z. (1996), `Liquid flow and mass transport in heterogeneous biofilms', *Water Research* 30(11), 2761-2765.

Deines, P., Sekar, R., Husband, P. S., Boxall, J. B., Osborn, A. M. & Biggs, C. A. (2010), `A new coupon design for simultaneous analysis of in situ microbial biofilm formation and community structure in drinking water distribution systems.', *Applied microbiology and biotechnology* 87(2), 749-756.

Denkhaus, E., Meisen, S., Telgheder, U., & Wingender, J. (2007). Chemical and physical methods for characterisation of biofilms. *Microchimica Acta*, 158(1-2), 1-27.

Douterelo, I., Sharpe, R. L. & Boxall, J. B. (2013), `Influence of hydraulic regimes on bacterial community structure and composition in an experimental drinking water distribution system', *Water research* 47(2), 503-516.

Douterelo, I., Jackson, M., Solomon, C., & Boxall, J. (2016). Microbial analysis of in situ biofilm formation in drinking water distribution systems: implications for monitoring and control of drinking water quality. *Applied microbiology and biotechnology*, 100(7), 3301-3311.

Douterelo, I., Fish, K. E., & Boxall, J. B. (2018). Succession of bacterial and fungal communities within biofilms of a chlorinated drinking water distribution system. *Water research*, 141, 74-85.

Dunne, W. M. (2002), `Bacterial adhesion: seen any good biofilms lately?', *Clinical microbiology reviews* 15(2), 155-166.

Drinking Water Inspectorate (DWI) (2017), *What are the drinking water standards?, Technical report,* Drinking Water Inspectorate, London.

Drinking Water Inspectorate (DWI). (2016). D*rinking water, 2015. Summary of the Chief Inspector's report for drinking water in England.* Drinking Water Inspectorate, London.

Drinking Water Inspectorate (DWI), (2015). *Drinking water quality in England The position after 25 years of regulation. A report by the Chief Inspector of Drinking Water*. London, England.

Drinking Water Inspectorate (DWI). (2017) Chief Inspector's Letter to Ministers (for England and Wales). Available online: http://dwi.defra.gov.uk/about/annual-report/2017/Letter-Eng.pdf (accessed January 2019).

Drinking Water Inspectorate (DWI). (2018). Consolidated review of the widespread loss of supplies arising from the freeze/thaw event affecting England and Wales in March 2018. Available online: http://www.dwi.gov.uk/press-media/press-releases/2018winter_event.pdf (accessed July 2018),

Drinking Water Inspectorate (DWI). (2019). List of Approved Products for use in Public Water Supply in the United Kingdom. Available online: http://www.dwi.gov.uk/drinking-water-products/approved-products/soslistcurrent.pdf (accessed June 2019).

Edgar, R. C. (2013). UPARSE: highly accurate OTU sequences from microbial amplicon reads. Nature methods, 10(10), 996–998.

Elhadidy, A. M., Van Dyke, M. I., Peldszus, S., & Huck, P. M. (2016). Application of flow cytometry to monitor assimilable organic carbon (AOC) and microbial community changes in water. *Journal of microbiological methods*, 130, 154-163.

Ellis, K., Ryan, B., Templeton, M. R. & Biggs, C. A. (2013), `Bacteriological water quality compliance and root cause analysis: an industry case study.', *Water Science and Technology: Water Supply* 13(4), 1034-1045.

Ellis, K., Gowdy, C., Jakomis, N., Ryan, B., Thom, C., Biggs, C. A., & Speight, V. (2018). Understanding the costs of investigating coliform and E. coli detections during routine drinking water quality monitoring. *Urban Water Journal*, 15(2), 101-108.

Emtiazi, F., Schwartz, T., Marten, S.M., Krolla-Sidenstein, P., Obst, U., 2004. Investigation of natural biofilms formed during the production of drinking water from surface water embankment filtration. Water Research, 38 (5), 1197-1206

Escobar, I. C. & Randall., A. A. (1999), `Influence of NF on distribution system biostability', *American Water Works Association* 91(6), 76-89.

Escobar, I. C. & Randall, A. A. (2000), `Sample storage impact on the assimilable organic carbon (AOC) bioassay', *Water Research* 34(5), 1680-168.

Escobar, I. C. & Randall, A. A. (2001), `Assimilable organic carbon (AOC) and biodegradable dissolved organic carbon (BDOC): complementary measurements.', *Water Research* 35(18), 4444-4454.

Escobar, I. C., Randall, A. A. & Taylor, J. S. (2001), `Bacterial growth in distribution systems: effect of assimilable organic carbon and biodegradable dissolved organic carbon', *Environmental science and technology* 35(17), 3442-3447.

European Council (1998) Directive 98/83/EC of 3 November 1998 relating to the quality of water intended for human consumption. *Official Journal of the European Communities* (No 1. 330/321.

Fang, W., Hu, J. Y. & Ong, S. L. (2009), `Influence of phosphorus on biofilm formation in model drinking water distribution systems', *Journal of applied microbiology* 106(4), 1328-1335.

Fish, K.E. (2013). The Impact of Hydraulic Regime Upon Biofilms in Drinking Water Distribution Systems. PhD Thesis, University of Sheffield.

Fish, K. E., Collins, R., Green, N. H., Sharpe, R. L., Douterelo, I., Osborn, A. M., & Boxall, J. B. (2015). Characterisation of the physical composition and microbial community structure of biofilms within a model full-scale drinking water distribution system. *PLoS One*, 10(2), e0115824.

Fish, K. E., Osborn, A. M., & Boxall, J. (2016). Characterising and understanding the impact of microbial biofilms and the extracellular polymeric substance (EPS) matrix in drinking water distribution systems. *Environmental science: water research & technology*, 2(4), 614-630.

Fish, K., Osborn, A. M., & Boxall, J. B. (2017). Biofilm structures (EPS and bacterial communities) in drinking water distribution systems are conditioned by hydraulics and influence discolouration. *Science of the Total Environment*, 593, 571-580.

Fish, K. E., Husband, S. P., & Boxall, J. B. (2018, July). The impact of chlorine concentration on the discolouration response of biofilms in drinking water distribution systems. *In WDSA/CCWI Joint Conference Proceedings* (Vol. 1).

Flemming, H. C., Neu, T. R. & Wozniak, D. J. (2007), `The EPS matrix: the house of biofilm cells', *Journal of bacteriology*, 189(22), 7945-7947.

Flemming, H., Percival, S. & Walker, J. (2002), `Contamination potential of biofilms in water distribution systems.', *Water Supply*, 2(1), 271-280.

Flemming, H. C. & Wingender, J. (2010), `The biofilm matrix', Nature Reviews Microbiology 8(9), 623-633.

Francisque, A., Rodriguez, M. J., Miranda-Moreno, L. F., Sadiq, R., & Proulx, F. (2009). Modeling of heterotrophic bacteria counts in a water distribution system. *Water research*, 43(4), 1075-1087.

Gagnon, G. A., O'Leary, K. C., Volk, C. J., Chauret, C., Stover, L. & Andrews, R. C. (2004), `Comparative analysis of chlorine dioxide, free chlorine and chloramines on bacterial water quality in model distribution systems', *Journal of environmental engineering* 130(11), 1269-1279.

Gall, A. M., Mariñas, B. J., Lu, Y., & Shisler, J. L. (2015). Waterborne viruses: a barrier to safe drinking water. *PLoS pathogens,* 11(6), e1004867.

Gauthier, V., Gérard, B., Portal, J. M., Block, J. C., & Gatel, D. (1999). Organic matter as loose deposits in a drinking water distribution system. *Water Research*, 33(4), 1014-1026.

Gauthier, V., Barbeau, B., Millette, R., Block, J. C., & Prevost, M. (2001). Suspended particles in the drinking water of two distribution systems. *Water Science and Technology: Water Supply*, 1(4), 237-245.

Gibbs, R. A., Scutt, J. E., & Croll, B. T. (1993). Assimilable organic carbon concentrations and bacterial numbers in a water distribution system. *Water Science and Technology*, 27(3-4), 159-166.

Gillespie, S., Lipphaus, P., Green, J., Parsons, S., Weir, P., Juskowiak, K., Jefferson, B., Jarvis, P., & Nocker, A. (2014). Assessing microbiological water quality in drinking water distribution systems with disinfectant residual using flow cytometry. *Water Research*, 65, 224-234.

Ginige, M. P., Wylie, J. & Plumb, J. (2011), `Influence of biofilms on iron and manganese deposition in drinking water distribution systems', *Biofouling* 27(2), 151-163.

Haddix, P. L., Shaw, N. J. & LeChevallier, M. W. (2004), `Characterization of bioluminescent derivatives of assimilable organic carbon test bacteria.', *Applied and environmental microbiology* 70(2), 850-854.

Hageskal, G., Tryland, I., Liltved, H. & Skaar, I. (2012), `No simple solution to waterborne fungi: various responses to water disinfection methods', *Water Science and Technology: Water Supply* 12(2), 220-226.

Hallam, N. B., West, J. R., Forster, C. F. & Simms, J. (2001), `The potential for biofilm growth in water distribution systems', *Water Research* 35(17), 4063-4071.

Hambsch, B. and Werner, P. (1990), Automated measurement of bacterial growth curves for the characterization of organic substances in water., Technical report, *In Proc. of the AWWA Technology Conference Advances in Water Analysis and Treatment*, November, 11-15.

Hammes, F. A. & Egli, T. (2005), `New method for assimilable organic carbon determination using ow-cytometric enumeration and a natural microbial consortium as inoculum.', *Environmental science and technology* 39(9), 3289-3294.

Hammes, F. A. & Egli, T. (2007). A flow cytometric method for AOC determination. Deliverable 3.3.1. Techneu.

Hammes, F., Berger, C., Koster, O. & Egli, T. (2010), `Assessing biological stability of drinking water without disinfectant residuals in a full-scale water supply system.', *Journal of Water Supply: Research and Technology AQUA* 59(1), 31-40.

Hammes, F., Berney, M., Wang, Y., Vital, M., Köster, O., & Egli, T. (2008). Flow-cytometric total bacterial cell counts as a descriptive microbiological parameter for drinking water treatment processes. *Water Research*, 42(1-2), 269-277.

Hammes, F., Meylan, S., Salhi, E., Köster, O., Egli, T., & Von Gunten, U. (2007). Formation of assimilable organic carbon (AOC) and specific natural organic matter (NOM) fractions during ozonation of phytoplankton. *Water research*, 41(7), 1447-1454.

Hammes, F., Salhi, E., Köster, O., Kaiser, H. P., Egli, T. & Von Gunten, U. (2006), `Mechanistic and kinetic evaluation of organic disinfection byproduct and assimilable organic carbon (AOC) formation during the ozonation of drinking water.', *Water research* 40(12), pp. 2275-2286.

Han, J. Y., Kai-Lin, H., Chung-Yi, L., Lou, J. C., & Wu, M. C. (2012). Control of assimilable organic carbon (AOC) concentrations in a water distribution system. *Desalination and Water Treatment*, 47(1-3), 11-16.

Henne, K., Kahlisch, L., Brettar, I., & Höfle, M. G. (2012). Comparison of structure and composition of bacterial core communities in mature drinking water biofilms and bulk water of a local network. *Applied and environmental microbiology*, AEM-06373.

Hijnen, W. A. M., Schurer, R., Bahlman, J. A., Ketelaars, H. A. M., Italiaander, R., van der Wal, A., & van der Wielen, P. W. J. J. (2018). Slowly biodegradable organic compounds impact the biostability of non-chlorinated drinking water produced from surface water. *Water research*, 129, 240-251.

Horn, H., Reiff, H. & Morgenroth, E. (2003), `Simulation of growth and detachment in biofilm systems under de_ned hydrodynamic conditions', *Biotechnology and Bioengineering* 81(5), 607-617.

Hu, J. Y., Wang, Z. S., Ng, W. J. & Ong, S. L. (1999), `The effect of water treatment processes on the biological stability of potable water.', *Water Research* 33(11), 2587-2592.

Husband, P. S. & Boxall, J. B. (2011), `Asset deterioration and discolouration in water distribution systems', *Water Research* 45(1), 113-124.

Husband, S., & Boxall, J. (2016). Understanding and managing discolouration risk in trunk mains. *Water research*, 107, 127-140.

Husband, P. S., Boxall, J. B. & Saul, A. J. (2008), `Laboratory studies investigating the processes leading to discolouration in water distribution networks', *Water research* 42(16), 4309-4318.

Husband, S. & Boxall, J. B. (2010), `Field studies of discoloration in water distribution systems: Model verification and practical implications', *Journal of Environmental Engineering* 136(1), 86-94.

Hydraulics Research Station (Great Britain). (1983). *Charts for the hydraulic design of channels and pipes*. Thomas Telford Ltd, London.

Ihssen, J., & Egli, T. (2004). Specific growth rate and not cell density controls the general stress response in Escherichia coli. *Microbiology*, 150(6), 1637-1648.

International Agency for Research on Cancer (1991). *IARC monographs on the evaluation of carcinogenic risks to humans, Volume 52. Chlorinated drinking-water; chlorination by-products; some other halogenated compounds; cobalt and cobalt compounds*. Lyon.

Japan Water Works Association (JWWA). (2001). *Standard Methods for the Examination of Water*, JWWA, Tokyo.

Juhna, T., Birzniece, D. & Rubulis, J. (2007), `Effect of phosphorus on survival of Escherichia coli in drinking water biofilms', *Applied and environmental microbiology* 73(11), 3755-3758.

Karthikeyan, S., Korber, D. R., Wolfaardt, G. M., & Caldwell, D. E. (2001). Adaptation of bacterial communities to environmental transitions from labile to refractory substrates. *International Microbiology*, 4(2), 73-80.

Keinänen, M. M., Korhonen, L. K., Lehtola, M. J., Miettinen, I. T., Martikainen, P. J., Vartiainen, T. & Suutari, M. H. (2002), `The microbial community structure of drinking water biofilms can be affected by phosphorus availability', *Applied and Environmental Microbiology* 68(1), 434-439.

Kerr, C. J., Osborn, K. S., Robson, G. D. & Handley, P. S. (1998), `The relationship between pipe material and biofilm formation in a laboratory model system', *Journal of applied microbiology* 85, 29S-38S.

Kim, B. R., Anderson, J. E., Mueller, S. A., Gaines, W. A. & Kendall, A. M. (2002), `Literature review efficacy of various disinfectants against Legionella in water systems', *Water Research* 36(18), 4433-4444.

Kohl, P. M., & Medlar, S. J. (2006). Occurrence of manganese in drinking water and manganese control. *American Water Works Association.*

Kokare, C. R., Chakraborty, S., Khopade, A. N. & Mahadik, K. R. (2009), `Biofilm: Importance and applications', *Indian Journal of Biotechnology* 8(2), 159-168.

Laspidou, C. S. & Rittmann, B. E. (2004), `Modeling the development of biofilm density including active bacteria, inert biomass, and extracellular polymeric substances', *Water Research* 38(14), 3349-3361.

Lautenschlager, K., Hwang, C., Liu, W. T., Boon, N., Köster O., Vrouwenvelder, H., Egli, T. & Hammes, F. (2013), `A microbiology-based multiparametric approach towards assessing biological stability in drinking water distribution networks.', *Water Research,* 47(9), 3015-3025.

LeChevallier, M. W., Babcock, R. M. & Lee, R. G. (1987), `Examination and characterization of distribution system biofilms.', *Applied and Environmental Microbiology* 54, 2714-2724.

LeChevallier, M. W., Schulz, W., & Lee, R. G. (1991). Bacterial nutrients in drinking water. *Appl. Environ. Microbiol.*, 57(3), 857-862.

LeChevallier, M. W., Lowry, C. D., Lee, R. G. & Gibbon, D. L. (1993), `Examining the relationship between iron corrosion and the disinfection of biofilm bacteria', *Journal (American Water Works Association)* 85(7), 111-123.

LeChevallier, M. W., Schulz, W. & Lee, R. G. (1991), `Bacterial nutrients in drinking water.', *Applied and Environmental Microbiology* 57(3), 857-862.

LeChevallier, M. W., Lowry, C. D., Lee, R. G., & Gibbon, D. L. (1993b). Examining the relationship between iron corrosion and the disinfection of biofilm bacteria. *Journal-American Water Works Association*, 85(7), 111-123.

LeChevallier, M. W., Shaw, N. E., Kaplan, L. A. & Bott, T. L. (1993a), `Development of a rapid assimilable organic carbon method for water.', *Applied and environmental microbiology* 59(5), 1526-1531.

LeChevallier, M. W., Welch, N. J. & Smith, D. B. (1996), `Full-scale studies of factors related to coliform (re)growth in drinking water.', *Applied and Environmental Microbiology* 62(7), 2201-2211.

LeChevallier, M. W. (2003). *Conditions favouring coliform and HPC bacterial growth in drinking water and on water contact surfaces. Heterotrophic Plate Count Measurement in Drinking Water Safety Management*. Geneva, World Health Organization, 177-198.

LeChevallier, M. W., Cawthon, C. D. & Lee, R. G. (2007), `Inactivation of biofilm bacteria', *Applied and environmental Microbiology* 54(10), 2492-2499.

LeChevallier, M. W., Schneider, O. D., Weinrich, L. A., Jjemba, P. K., Evans, P. J., Hooper, J. L., & Chappell, R. W. (2015). *An operational definition of biostability in drinking water.* Water Research Foundation, Denver.

Lehtola, M. J., Miettinen, I. T., Keinänen, M. M., Kekki, T. K., Laine, O., Hirvonen, A., Vartiainenb, T. & Martikainen, P. J. (2004), `Microbiology, chemistry and biofilm development in a pilot drinking water distribution system with copper and plastic pipes', *Water Research* 38(17), 3769-3779.

Lehtola, M. J., Miettinen, I. T., Lampola, T., Hirvonen, A., Vartiainen, T. & Martikainen, P. J. (2005), `Pipeline materials modify the effectiveness of disinfectants in drinking water distribution systems.', *Water Research* 39(10), 1962-1971.

Lehtola, M. J., Miettinen, I. T., Vartiainen, T., Myllykangas, T. & Martikainen, P. J. (2001), `Microbially available organic carbon, phosphorus, and microbial growth in ozonated drinking water.', *Water research* 35(7), 1635-1640.

Lehtola, M., Miettinen, I. & Martikainen, P. (2002), `Biofilm formation in drinking water affected by low concentrations of phosphorus.', *Can. J. Microbiol*. 48(6), 494-499.

Lehtola, M. J., Laxander, M., Miettinen, I. T., Hirvonen, A., Vartiainen, T. & Martikainen, P. J. (2006), `The effects of changing water ow velocity on the formation of biofilms and water quality in pilot distribution system consisting of copper or polyethylene pipes', Water research 40(11), 2151-2160.

Lehtola, M. J., Torvinen, E., Kusnetsov, J., Pitkänen, T., Maunula, L., von Bonsdorff, C. H., Martikainen, P. J., Wilks, S A., Keevil, C. W., & Miettinen, I. T. (2007). Survival of Mycobacterium avium, Legionella pneumophila, Escherichia coli, and caliciviruses in drinking water-associated biofilms grown under high-shear turbulent flow. *Appl. Environ. Microbiol.*, *73*(9), 2854-2859.

Li, D., Li, Z., Yu, J., Cao, N., Liu, R. & Yang, M. (2010), `Characterization of bacterial community structure in a drinking water distribution system during an occurrence of Red Water.', *Appl. Environ. Microbiol.* 76(21), 7171- 7180.

Li, W., Zhang, J., Wang, F., Qian, L., Zhou, Y., Qi, W., & Chen, J. (2018). Effect of disinfectant residual on the interaction between bacterial growth and assimilable organic carbon in a drinking water distribution system. *Chemosphere*, *202*, 586-597.

Liao, X., Chen, C., Wang, Z., Wan, R., Chang, C. H., Zhang, X., & Xie, S. (2013). Changes of biomass and bacterial communities in biological activated carbon filters for drinking water treatment. Process Biochemistry, 48(2), 312-316.

Liu, R., Zhu, J., Yu, Z., Joshi, D., Zhang, H., Lin, W. & Yang, M. (2010), `Molecular analysis of long-term biofilm formation on PVC and cast iron surfaces in drinking water distribution system', *Journal of Environmental Sciences* 26(4), 865-874.

Liu, G., Van der Mark, E. J., Verberk, J. Q. J. C., & Van Dijk, J. C. (2013). Flow cytometry total cell counts: a field study assessing microbiological water quality and growth in unchlorinated drinking water distribution systems. *BioMed research international*, 2013.

Liu, G., Bakker, G. L., Li, S., Vreeburg, J. H. G., Verberk, J. Q. J. C., Medema, G. J., Liu W. T., & Van Dijk, J. C. (2014). Pyrosequencing reveals bacterial communities in unchlorinated drinking water distribution system: an integral study of bulk water, suspended solids, loose deposits, and pipe wall biofilm. *Environmental science & technology*, 48(10), 5467-5476.

Liu, W., Wu, H., Wang, Z., Ong, S. L., Hu, J. Y. & Ng, W. J. (2002), `Investigation of assimilable organic carbon (AOC) and bacterial (re)growth in drinking water distribution system.', *Water research* 36(4), 891-898.

Liu, X., Wang, J., Liu, T., Kong, W., He, X., Jin, Y. & Zhang, B. (2015), `Effects of Assimilable Organic Carbon and Free Chlorine on Bacterial Growth in Drinking Water', *PloS one* 10(6), e0128825.

Liu, Y. & Tay, J. H. (2002), `The essential role of hydrodynamic shear force in the formation of biofilm and granular sludge', *Water Research* 36(7), 1653-1665.

Lou, J. C., Chang, T. W., & Huang, C. E. (2009). Effective removal of disinfection by-products and assimilable organic carbon: An advanced water treatment system. *Journal of hazardous materials*, *172*(2-3), 1365-1371.

Lou, J. C., Chen, B. H., Chang, T. W., Yang, H. W., & Han, J. Y. (2011). Variation and removal efficiency of assimilable organic carbon (AOC) in an advanced water treatment system. *Environmental monitoring and assessment*, 178(1-4), 73-83.

Lou, J. C., Yang, C. Y., Chang, C. J., Chen, W. H., Tseng, W. B., & Han, J. Y. (2014). Analysis and removal of assimilable organic carbon (AOC) from treated drinking water using a biological activated carbon filter system. *Journal of Environmental Chemical Engineering*, 2(3), 1684-1690.

Lu, P., Zhang, X., Zhang, C., Niu, Z., Xie, S., & Chen, C. (2014). Biostability in distribution systems in one city in southern China: characteristics, modeling and control strategy. *Journal of Environmental Sciences*, 26(2), 323-331.

Lührig, K., Canbäck, B., Paul, C. J., Johansson, T., Persson, K. M., & Rådström, P. (2015). Bacterial community analysis of drinking water biofilms in southern Sweden. *Microbes and environments*, 30(1), 99-107.

Machell, J., Boxall, J., Saul, A. & Bramley, D. (2009), `Improved representation of water age in distribution networks to inform water quality', *Journal of Water Resources Planning and Management*. 135(5), 382-391.

Mah, T. F. C. & O'Toole, G. A. (2001), `Mechanisms of biofilm resistance to antimicrobial agents', *Trends in microbiology* 9(1), 34-39.

Manuel, C. M., Nunes, O. C. & Melo, L. F. (2007), `Dynamics of drinking water biofilm in flow/non-flow conditions', *Water Research* 41(3), 551-562.

Manuel C.M., Nunes O.C., and Melo L.F. (2010). “Unsteady state flow and stagnation in distribution systems affect the biological stability of drinking water.” *Biofouling: The Journal of Bioadhesion and Biofilm*. 26: 129-139.

Mathieu, L., Bertrand, I., Abe, Y., Angel, E., Block, J. C., Skali-Lami, S., & Francius, G. (2014). Drinking water biofilm cohesiveness changes under chlorination or hydrodynamic stress. W*ater Research*, 55, 175-184.

Martiny, A. C., Jørgensen, T. M., Albrechtsen, H. J., Arvin, E., & Molin, S. (2003). Long-term succession of structure and diversity of a biofilm formed in a model drinking water distribution system. *Applied and Environmental Microbiology,* 69(11), 6899-6907.

Martiny, A. C., Albrechtsen, H. J., Arvin, E., & Molin, S. (2005). Identification of bacteria in biofilm and bulk water samples from a nonchlorinated model drinking water distribution system: detection of a large nitrite-oxidizing population associated with Nitrospira spp. *Appl. Environ. Microbiol.*, 71(12), 8611-8617.

Matilainen, A., Vepsäläinen, M., & Sillanpää, M. (2010). Natural organic matter removal by coagulation during drinking water treatment: a review. Advances in colloid and interface science, 159(2), 189-197.

McCoy, S. T., & VanBriesen, J. M. (2012). Temporal variability of bacterial diversity in a chlorinated drinking water distribution system. Journal of Environmental Engineering, 138(7), 786-795.

Medema, G. J., Payment, P., Dufour, A., Robertson, Waite, M., Hunter, P., Kirby, R. & Andersson, Y. (2003), `Safe drinking water: an ongoing challenge', *Assessing Microbial Safety of Drinking Water* 11, 11- 45.

Menaia, J. & Mesquita, E. (2004), `Drinking water pipe biofilm: present knowledge, concepts and significance', *Water Supply* 4(2), 115-124.

Mi, Z., Dai, Y., Xie, S., Chen, C., & Zhang, X. (2015). Impact of disinfection on drinking water biofilm bacterial community. *Journal of Environmental Sciences*, 37, 200-205.

Miettinen, I. T., Vartiainen, T., & Martikainen, P. J. (1997). Phosphorus and bacterial growth in drinking water. *Applied and environmental microbiology*, 63(8), 3242-3245.

Miettinen, I. T., Vartiainen, T., & Martikainen, P. J. (1999). Determination of assimilable organic carbon in humus-rich drinking waters. *Water Research*, 33(10), 2277-2282.

Minnesota Rural Water Association (MRWA), (2009*). Iron and Manganese*. [online]. Available from: https://www.mrwa.com/WaterWorksMnl/Chapter%2014%20Iron%20and%20Manganese.pdf (Viewed 05 October 2018).

Moritz, M. M., Flemming, H. C., & Wingender, J. (2010). Integration of Pseudomonas aeruginosa and Legionella pneumophila in drinking water biofilms grown on domestic plumbing materials. *International journal of hygiene and environmental health*, 213(3), 190-197.

Morton, S. C., Zhang, Y. & Edwards, M. A. (2005), `Implications of nutrient release from iron metal for microbial (re)growth in water distribution systems', *Water Research* 39(13), 2883-2892.

Müller, K. C., Forster, R., Gammeter, S., & Hambsch, B. (2003). Influence of ozonated cyanobacteria on bacterial growth in rapid sand filters. *Journal of Water Supply: Research and Technology-AQUA,* 52(5), 333-340.

Murga, R., Forster, T. S., Brown, E., Pruckler, J. M., Fields, B. S., & Donlan, R. M. (2001). Role of biofilms in the survival of Legionella pneumophila in a model potable-water system. *Microbiology*, 147(11), 3121-3126.

Ndiongue, S., Huck, P. M., & Slawson, R. M. (2005). Effects of temperature and biodegradable organic matter on control of biofilms by free chlorine in a model drinking water distribution system. Water Research, 39(6), 953-964.

Nescerecka, A., Rubulis, J., Vital, M., Juhna, T. & Hammes, F. (2014), `Biological instability in a chlorinated drinking water distribution network', *PloS one* 9(5), e96354.

Neu, T. R. & Lawrence, J. R. (2009), `Extracellular polymeric substances in microbial biofilms', Microbial glycobiology: structures, relevance and applications. *Elsevier, San Diego,* 735-758.

Nieuwenhuijsen, M. J., Smith, R., Golfinopoulos, S., Best, N., Bennett, J., Aggazzotti, G., Righi, E., Fantuzzi, G., Bucchini, L., Cordier, S., Moreno, V., Vecchia, C.L., Bosetti, C.,

Vartiainen,T., Rautiu, R., Toledano, M., Iszatt, N., Grazuleviciene, R., Kogevinas, M., & Villanueva, C. M. (2009). Health impacts of long-term exposure to disinfection by-products in drinking water in Europe: HIWATE. *Journal of water and health*, 7(2), 185-207.

Niquette, P., Servais, P. & Savoir, R. (2000), `Impacts of pipe materials on densities of fixed bacterial biomass in a drinking water distribution system', *Water Research* 34(6), 1952-1956.

Norton, C. D. & LeChevallier, M. W. (2000), `A pilot study of bacteriological population changes through potable water treatment and distribution', *Applied and Environmental Microbiology* 66(1), 268-276.

Ohashi, A., de Silva, D. V., Mobarry, B., Manem, J. A., Stahl, D. A., & Rittmann, B. E. (1995). Influence of substrate C/N ratio on the structure of multi-species biofilms consisting of nitrifiers and heterotrophs. *Water Science and Technology*, 32(8), 75-84.

Ohkouchi, Y., Ly, B. T., Ishikawa, S., Aokid, Y., Echigoa, S. & Itch, S. (2011), `A survey on levels and seasonal changes of assimilable organic carbon (AOC) and its precursors in drinking water.', *Environmental Technology* 32(13-14), 1605-1613.

Ohkouchi, Y., Ly, B. T., Ishikawa, S., Kawano, Y. & Itoh, S. (2013), `Determination of an acceptable assimilable organic carbon (AOC) level for biological stability in water distribution systems with minimized chlorine residual.', *Environmental monitoring and assessment*, 185(2), 1427-1436.

Okabe, S., Kokazi, T., & Watanabe, Y. (2002). Biofilm formation potentials in drinking waters treated by different advanced treatment processes. *Water Science and Technology: Water Supply*, 2(4), 97-104.

Okabe, S., Kindaichi, T., Ito, T., & Satoh, H. (2004). Analysis of size distribution and areal cell density of ammonia-oxidizing bacterial microcolonies in relation to substrate microprofiles in biofilms. *Biotechnology and bioengineering*, 85(1), 86-95.

Ollos, P. J., Huck, P. M. & Slawson, R. M. (2003), `Factors affecting biofilm accumulation in model distribution systems', *Journal (American Water Works Association)*, 87-97.

Pang, C. M., & Liu, W. T. (2006). Biological filtration limits carbon availability and affects downstream biofilm formation and community structure. *Appl. Environ. Microbiol.*, 72(9), 5702-5712.

Park, S. K., Choi, J. H. & Hu, J. Y. (2002), `Assessing bacterial growth potential in a model distribution system receiving nanofiltration membrane treated water', *Desalination* 296, 7-15.

Paul, E., Ochoa, J. C., Pechaud, Y., Liu, Y., & Liné, A. (2012). Effect of shear stress and growth conditions on detachment and physical properties of biofilms. *Water Research*, 46(17), 5499-5508.

Payment, P. (1997), `Epidemiology of endemic gastrointestinal and respiratory diseases: Incidence, fraction attributable to tap water and costs to society', *Water Science and Technology* 35(11), 7-10.

Peng, C. Y., & Korshin, G. V. (2011). Speciation of trace inorganic contaminants in corrosion scales and deposits formed in drinking water distribution systems. *Water Research*, 45(17), 5553-5563.

Pepper, I. L., Rusin, P., Quintanar, D. R., Haney, C., Josephson, K. L., & Gerba, C. P. (2004). Tracking the concentration of heterotrophic plate count bacteria from the source to the consumer's tap. *International journal of food microbiology*, 92(3), 289-295.

Polanska, M., Huysman, K., & Van Keer, C. (2005), `Investigation of assimilable organic carbon (AOC) in Flemish drinking water', *Water Research* 39, 2259-2266.

Prasad, T. D., & Danso-Amoako, E. (2014). Influence of chemical and biological parameters on iron and manganese accumulation in water distribution networks. *Procedia Engineering*, 70, 1353-1361.

Prest, E. (2015). Biological stability in drinking water distribution systems: a novel approach for systematic mciorbial water quality monitoring. Doctoral dissertation. Delft University of Technology.

Prest, E. I., Hammes, F., van Loosdrecht, M., & Vrouwenvelder, J. S. (2016). Biological stability of drinking water: controlling factors, methods, and challenges. *Frontiers in microbiology*, 7, 45.

Prince, R., Goulter, I., and Ryan, G. (2003). "What causes customer complaints about discoloured water." *Journal of American Water Works Association.* 302, 62–68.

Pryor, M., Springthorpe, S., Ri_ard, S., Brooks, T., Huo, Y., Davis, G. & Sattar, S. A. (2004), `Investigation of opportunistic pathogens in municipal drinking water under different supply and treatment regimes', *Water Science and Technology* 50(1), 83-90.

R Foundation for Statistical Computing Platform, (2018*). The R Project for Statistical Computing*. Available online: https://www.r-project.org/ (accessed January 2018).

Ramseier, M. K., Peter, A., Traber, J., & von Gunten, U. (2011). Formation of assimilable organic carbon during oxidation of natural waters with ozone, chlorine dioxide, chlorine, permanganate, and ferrate. *Water Research*, 45(5), 2002-2010.

Ragazzo, P. & Nardo, M. (2002), `Biofilm formation in surface distribution systems', In Conference Proceedings of the NSF International/WHO Symposium on HPC, Bacteria in Drinking water, *Public Health Implications*, 22-24.

Revetta, R. P., Santo Domingo, J. W., Kelty, C., Humrighouse, B., Oerther, D., Lamendella, R., Keinanen-Toivola, M. & Williams, M. (2007), `Molecular diversity of drinking water microbial communities: a phylogenetic approach', *Proceedings of the Water Environment Federation* 1, 629-645.

Richardson, S. D., Plewa, M. J., Wagner, E. D., Schoeny, R. & DeMarini, D. M. (2007), `Occurrence, genotoxicity, and carcinogenicity of regulated and emerging disinfection by-products in drinking water: a review and roadmap for research', *Mutation Research/Reviews in Mutation Research*, 636(1), 178-242.

Rickard, A.H., Gilbert, P., High, N.J., Kolenbrander, P.E., Handley, P.S., 2003. Bacterial 668 coaggregation: an integral process in the development of multi-species biofilms. *Trends in Microbiology*, 11 (2), 94-100. 670

Rickard, A.H., Gilbert, P., Handley, P.S., 2004. Influence of growth environment on 674 coaggregation between freshwater biofilm bacteria. *Journal of Applied Microbiology*, 96 (6), 1367-1373

Rittmann, B. E., & Snoeyink, V. L. (1984). Achieving biologically stable drinking water. *Journal-American Water Works Association*, 76(10), 106-114.

Roccaro, P., Chang, H. S. & Vagliasindi, F. G.and Korshin, G. V. (2008), `Differential absorbance study of effects of temperature on chlorine consumption and formation of disinfection by-products in chlorinated water', *Water Research* 42(8), 1879-1888.

Rochex, A., Godon, J. J., Bernet, N. & Escudi_e, R. (2008), `Role of shear stress on composition, diversity and dynamics of biofilm bacterial communities', *Water Research* 42(20), 4915-4922.

Ross, P. S., Hammes, F., Dignum, M., Magic-Knezev, A. & Hambsch, B. Rietveld, L. C. (2013), `A comparative study of three different assimilable organic carbon (AOC) methods: results of a round-robin test', *Water Science and Technology: Water Supply* 13(4), 1024-1033.

Sack, E. L., Van der Wielen, P. W., & van der Kooij, D. (2011). *Flavobacterium johnsoniae* as a model organism for characterizing biopolymer utilization in oligotrophic freshwater environments. *Applied Environmental Microbiology*. 77(19), 6931-6938.

Sadiq, R., & Rodriguez, M. J. (2004). Disinfection by-products (DBPs) in drinking water and predictive models for their occurrence: a review. *Science of the Total Environment, 321*(1-3), 21-46.

Safe Drinking Water Foundation (SDWF) (2016). *What is chlorination?* Available online: https://www.safewater.org/fact-sheets-1/2017/1/23/what-is-chlorination. Saskatoon, Canada (accessed January 2018).

Sartory, D. (2004), `Heterotrophic plate count monitoring of treated drinking water in the UK: a useful operational tool', *International Journal of Food Microbiology* 92, 297-306.

Sathasivan, A., & Ohgaki, S. (1999). Application of new bacterial (re)growth potential method for water distribution system–a clear evidence of phosphorus limitation. *Water Research*, 33(1), 137-144.

Schwering, M., Song, J., Louie, M., Turner, R. J., & Ceri, H. (2013). Multi-species biofilms defined from drinking water microorganisms provide increased protection against chlorine disinfection. *Biofouling*, 29(8), 917-928.

Scottish Water (2013). Annual Water Quality Report (2013). Available online: https://www.scottishwater.co.uk/assets/about%20us/files/key%20publications/annualwaterqualityreport2013.pdf (accessed January 2017).

Scottish Water (2014), Annual report and accounts 2013/14, Technical report, Scottish Water.

Scottish Water (2018). Annual Report Highlights Strong Performance for Customers. Available online: https://www.scottishwater.co.uk/About-Us/News-and-Views/250618-Annual-Report (accessed online July 2018).

Servais, P., Laurent, P., & Randon, G. (1995). Comparison of the bacterial dynamics in various French distribution systems. *AQUA-London then Oxford-journal of the International Water Supply Association,* 44, 10-10.

Seth, A., Bachmann, R., Boxall, J., Saul, A., & Edyvean, R. (2004). Characterisation of materials causing discolouration in potable water systems. *Water Science and Technology,* 49(2), 27-32.

Sharp, E. L., Parsons, S. A. & Jefferson, B. (2006), `Seasonal variations in natural organic matter and its impact on coagulation in water treatment', *Science of the Total Environment* 363(1), 183-194.

Sharp, R. R., Camper, A. K., Crippen, J. J., Schneider, O. D. & Leggiero, S. (2001), `Evaluation of drinking water biostability using biofilm methods.', *Journal of environmental engineering* 127(5), 403-410.

Sharpe, R. L., Smith, C. J., Biggs, C. A., & Boxall, J. B. (2010). Pilot scale laboratory investigations into the impact of steady state conditioning flow on potable water discolouration. *Water Distribution System Analysis*, 12-15.

Sharpe, R. (2012). Laboratory investigations into processes causing discoloured potable water (Doctoral dissertation, University of Sheffield).

Siebel, E., Wang, Y., Egli, T., Hammes, F., 2008. Correlations between total cell concentration, total adenosine tri-phosphate concentration and heterotrophic plate counts during microbial monitoring of drinking water. *Drink. Water Eng. Sci*. 1, 1 e 6.

Silhan, J., Corfitzen, C. B., & Albrechtsen, H. J. (2006). Effect of temperature and pipe material on biofilm formation and survival of Escherichia coli in used drinking water pipes: a laboratory-based study. *Water Science and Technology*, 54(3), 49-56.

Simoes, M., Pereira, M. O., & Vieira, M. J. (2005). Effect of mechanical stress on biofilms challenged by different chemicals. *Water Research*, 39(20), 5142-5152.

Simoes, L. C., Simoes, M., & Vieira, M. J. (2010). Influence of the diversity of bacterial isolates from drinking water on resistance of biofilms to disinfection. Appl. Environ. Microbiol., 76(19), 6673-6679.

Smeets, P. W. M. H., Medema, G. J. & Van Dijk, J. C. (2009), `The Dutch secret: how to provide safe drinking water without chlorine in the Netherlands', Drinking Water Engineering and Science 2(1), 1-14.

Smith, A., Reacher, M., Smerdon, W., Adak, G. K., Nichols, G. & Chalmers, R. M. (2006), `Outbreaks of waterborne infectious intestinal disease in England and Wales, 1992-2003', *Epidemiology and infection* 134(6), 1141-1149.

Soonglerdsongpha, S., Kasuga, I., Kurisu, F., & Furumai, H. (2011). Comparison of Assimilable Organic Carbon Removal and Bacterial Community Structures in Biological Activated Carbon Process for Advances Drinking Water Treatment Plants. *Sustainable Environment Research*, *21*(1), 59-64.

Stanfield, G., & Jago, P. H. (1989). *Application of ATP determinations to measure the concentration of assimilable organic carbon in water*. Blackwell Scientific Publications, Oxford.

Stanier, R. Y., Palleroni, N. J., & Doudoroff, M. (1966), `The aerobic pseudomonads a taxonomic study', *Journal of general microbiology* 43(2), 159- 271.

Stoianov, I. & Aisopou, A. (2014), `Chlorine decay under steady and unsteadystate hydraulic conditions', *Procedia Engineering* 70, 1592-1601.

Stoodley, P., Cargo, R., Rupp, C. J., Wilson, S. & Klapper, I. (2002), `Biofilm material properties as related to shear-induced deformation and detachment phenomena', *Journal of Industrial Microbiology and Biotechnology* 29(6), 361-367.

Stoodley, P., Dodds, I., Boyle, J. D. & Lappin-Scott, H. M. (1999), `Influence of hydrodynamics and nutrients on biofilm structure', *Journal of applied microbiology* 85, 19S-28S.

Stoodley, P., Hall-Stoodley, L., & Lappin-Scott, H. M. (2001a). Growth Biofilms Pt B, vol. 337, pp. 306–318.

Stoodley, P., Wilson, S., Hall-Stoodley, L., Boyle, J. D., Lappin-Scott, H. M. & Costerton, J. W. (2001b), `Growth and detachment of cell clusters from mature mixed-species biofilms', *Applied and Environmental Microbiology* 67(12), 5608-5613.

Sunny, I., Husband, S., Drake, N., & Boxall, J. B. (2017). Quantity and quality benefits of in-service invasive cleaning of trunk mains. *In Drinking Water Engineering and Science*, 10, 45-52.

Sunny, I., Husband, S. P., & Boxall, J. B. (2018, July). Seasonal Temperature and Turbidity Behaviour in Trunk Mains. In *WDSA/CCWI Joint Conference Proceedings* (Vol. 1).

Teitzel, G. M., & Parsek, M. R. (2003). Heavy metal resistance of biofilm and planktonic Pseudomonas aeruginosa. *Appl. Environ. Microbiol*., 69(4), 2313-2320.

Thayanukul, P., Kurisu, F., Kasuga, I. & Furumai, H. (2013), `Evaluation of microbial (re)growth potential by assimilable organic carbon in various reclaimed water and distribution systems', *Water Research* 47(1), 225-232.

The Scottish Government (2014), *Drinking water quality in Scotland 2013*, Technical report, The Scottish Government.

Toroz, I. & Uyak, V. (2005), `Seasonal variations of trihalomethanes (THMs) in water distribution networks of Istanbul City', *Desalination* 176(1), 127-141.

Torvinen, E., Lehtola, M. J., Martikainen, P. J. & Miettinen, I. T. (2007), `Survival of Mycobacterium avium in drinking water biofilms as affected by water ow velocity, availability of phosphorus, and temperature', *Applied and environmental microbiology* 73(19), 6201-6207.

Uhl, W. & Schaule, G. (2004), `Establishment of HPC (R2A) for (re)growth control in non-chlorinated distribution systems', *International journal of food microbiology* 92(3), 317-325.

UNICEF and World Health Organization (2015). *Progress on sanitation and drinking water – 2015 update and MDG assessment*. WHO Press, World Health Organization, Switzerland.

US Environmental Protection Agency (EPA) (2017). *Drinking Water Contaminant Candidate List (CCL) ('CCL 3 Universe' list*. Available online: http://www.epa.gov/safewater/ccl/pdfs/report_ccl3_microbes_universe.pdf (accessed November 2018).

US Environmental Protection Agency (EPA). (2018). *Why do water systems add phosphate to drinking water? What are the health effects of drinking water containing phosphates.* Available online:

https://safewater.zendesk.com/hc/en-us/articles/211406008-Why-do-water-systems-add-phosphate-to-drinking-water-What-are-the-health-effects-of-drinking-water-containing-phosphates- (accessed on June 2018).

Vaerewijck, M. J., Huys, G., Palomino, J. C., Swings, J. & Portaels, F. (2005), `Mycobacteria in drinking water distribution systems: ecology and significance for human health', *FEMS Microbiology Reviews* 29(5), 911-934.

Van Den Boomen, M., Van Mazijk, A., & Beuken, R. H. S. (2004). First evaluation of new design concepts for self-cleaning distribution networks. *Journal of Water Supply: Research and Technology-Aqua*, 53(1), 43-50.

Van der Kooij, D. (1990), `Assimilable organic carbon (AOC) in drinking water', *Drinking water microbiology*. Springer New York, 55-87.

Van der Kooij, D. (1992), `Assimilable organic carbon as an indicator of bacterial (re)growth.', *American Water Works Association*, 57-65.

Van der Kooij, D. (2002), Assimilable organic carbon (AOC) in treated water: determination and significance, *Encyclopedia of environmental microbiology*.

Van der Kooij, D. (2003), *Managing (re)growth in drinking water distribution systems. Heterotrophic plate counts and drinking-water safety*. IWA Publishing, London, United Kingdom.

Van der Kooij D., Vrouwenvelder H. S. and Veenendaa H. R. (1999). Tools for assessing water quality characteristics related with biofouling of membranes for nanofiltration or reverse osmosis in water treatment. *Proceedings of the AWWA Membrane Conference Long Beach*, CA, 28–3 March 1999.

Van der Kooij, D., & Hijnen, W. A. M. (1984). Substrate utilization by an oxalate-consuming Spirillum species in relation to its growth in ozonated water. *Applied Environmental Microbiology*. 47(3), 551-559.

Van der Kooij, D., Hijnen, W. A. M., & Kruithof, J. C. (1989). The effects of ozonation, biological filtration and distribution on the concentration of easily assimilable organic carbon (AOC) in drinking water. *Ozone: science & engineering*, 11(3), 297-311.

Van der Kooij, D., Visser, A. & Hijnen, W. (1982), `Determining the concentration of easily assimilable organic carbon in drinking water.', *American Water Works Association* 74(10), 540-543.

Van der Kooij, D., Veenendaal, H. R., Baars-Lorist, C., van der Klift, D. W., & Drost, Y. C. (1995). Biofilm formation on surfaces of glass and teflon exposed to treated water. *Water Research*, 29(7), 1655-1662.

Van der Wende, E., Characklis, W. G. & Smith, D. B. (2006), `Biofilms and bacterial drinking water quality', *Water Research* 23(10), 1313-1322.

Van der Wielen, P. W., Voost, S. & van der Kooij, D. (2009), `Ammonia oxidizing bacteria and archaea in groundwater treatment and drinking water distribution systems', *Applied and environmental microbiology* 75(14), 4687-4695.

Van Thienen, P., Vreeburg, J. H. G., & Blokker, E. J. M. (2011). Radial transport processes as a precursor to particle deposition in drinking water distribution systems. *Water Research*, 45(4), 1807-1817.

Verberk, J. Q. J. C., Hamilton, L. A., O'halloran, K. J., Van Der Horst, W., & Vreeburg, J. (2006). Analysis of particle numbers, size and composition in drinking water transportation pipelines: results of online measurements. *Water Science and Technology: water supply*, 6(4), 35-43.

Vikesland, P. J., Ozekin, K., & Valentine, R. L. (2001). Monochloramine decay in model and distribution system waters. *Water Research*, 35(7), 1766-1776.

Vital, M., Füchslin, H. P., Hammes, F., & Egli, T. (2007). Growth of Vibrio cholerae O1 Ogawa Eltor in freshwater. *Microbiology*, 153(7), 1993-2001.

Vital, M., Dignum, M., Magic-Knezev, A., Ross, P., Rietveld, L. & Hammes, F. (2012), `Flow cytometry and adenosine tri-phosphate analysis: Alternative possibilities to evaluate major bacteriological changes in drinking water treatment and distribution systems.', *Water Research* 46(15), 4665-4676.

Volk, C., Dundore, E., Schiermann, J. & Lechevallier, M. (2000), `Practical evaluation of iron corrosion control in a drinking water distribution system', *Water Research* 34(6), 1967-1974.

Volk, C. J. & LeChevallier, M. W. (1999), `Impacts of the reduction of nutrient levels on bacterial water quality in distribution systems.', *Applied and environmental microbiology* 65(11), 4957-4966.

Volk, C. J. & LeChevallier, M. W. (2002), `Effects of conventional treatment on AOC and BDOC levels.', *Journal American Water Works Association*, 112-123.

Vreeburg, I. J. & Boxall, J. B. (2007), `Discolouration in potable water distribution systems: A review', *Water Research* 41(3), 519-529.

Vreeburg, J. H. G., Schippers, D., Verberk, J. Q. J. C., & Van Dijk, J. C. (2008). Impact of particles on sediment accumulation in a drinking water distribution system. *Water Research*, 42(16), 4233-4242.

Wang, H., Masters, S., Hong, Y., Stallings, J., Falkinham III, J. O., Edwards, M. A. & Pruden, A. (2012), `Effect of disinfectant, water age, and pipe material on occurrence and persistence of Legionella, mycobacteria, Pseudomonas aeruginosa, and two amoebas', *Environmental science and technology* 46(21), 11566-11574.

Wang, Q., Tao, T. & Xin, K. (2014), `The Relationship between Water Biostability and Initial Bacterial Growth Variations to Different Organic Carbon Concentrations', *Procedia Engineering* 89, 160-167.

Water Briefing (2015), `*Cryptosporidium incident costs united utilities 25 million'*, Available online: wwww.waterbrie_ng.org (accessed January 2019).

Wei, J., Ye, B., Wang, W., Yang, L., Tao, J., & Hang, Z. (2010). Spatial and temporal evaluations of disinfection by-products in drinking water distribution systems in Beijing, China. *Science of the Total Environment*, 408(20), 4600-4606.

Weinrich, L. A., Giraldo, E. & LeChevallier, M. W. (2009), `Development and application of a bioluminescence-based test for assimilable organic carbon in reclaimed waters.', *Applied and environmental microbiology* 75(23), 7385-7390.

Weinrich, L. A., Jjemba, P. K., Giraldo, E. & LeChevallier, M. W. (2010), `Implications of organic carbon in the deterioration of water quality in reclaimed water distribution systems', *Water Research* 44(18), 5367-5375.

Weinrich, L. A., Schneider, O. D. & LeChevallier, M. W. (2011), `Bioluminescence-based method for measuring assimilable organic carbon in pre-treatment water for reverse osmosis membrane desalination.', *Applied and environmental microbiology* 77(3), 1148-1150.

Wen, G., Zhu, H., Wei, Y., Huang, T., & Ma, J. (2017). Formation of assimilable organic carbon during the oxidation of water containing Microcystis aeruginosa by ozone and an advanced oxidation process using ozone/hydrogen peroxide. *Chemical Engineering Journal*, 307, 364-371.

Werner, P. & Hambsch, B. (1986), `Investigations on the growth of bacteria in drinking water', *Water Supply*. 4(3), 227-232.

Wetzel, R. G. (1983). *Limnology* (2nd edn.) Saunders College Publ.

White, C., Tancos, M., & Lytle, D. A. (2011). Microbial community profile of a lead service line removed from a drinking water distribution system. *Applied Environmental microbiology. 77*(15), 5557-5561.

Wilczak, A., Jacangelo, J. G., Marcinko, J. P., Odell, L. H., & Kirmeyer, G. J. (1996). Occurrence of nitrification in chloraminated distribution systems. *Journal-American Water Works Association*, 88(7), 74-85.

Williams, M. M., Santo Domingo, J. W. & Meckes, M. C. (2005), `Population diversity in model potable water biofilms receiving chlorine or chloramine residual', *Biofouling* 21(5-6), 279-288.

Wingender, J., Grobe, S., Fiedler, S. & Flemming, H. C. (1999), `The effect of extracellular polysaccharides on the resistance of Pseudomonas aeruginosa to chlorine and hydrogen peroxide', *Special Publications of the Royal Society of Chemistry* 242, 93-100.

Wingender, J., & Flemming, H. C. (2011). Biofilms in drinking water and their role as reservoir for pathogens. *International journal of hygiene and environmental health*, 214(6), 417-423.

World Health Organisation (WHO), (1993). *Guidelines for Drinking-water Quality*. In: Recommendations, second ed., vol. 1. World Health Organization, Geneva.

World Health Organization (WHO), (1996). *Guidelines for drinking water quality*, vol. 2. Health Criteria and Other Supporting Information. World Health Organization, Geneva.

World Health Organisation (WHO), (1997). *Guidelines for Drinking-water Quality*. In: Surveillance and Control of Community Supplies, second ed., vol. 3. World Health Organization, Geneva.

World Health Organisation (WHO) (2003), *Assessing microbial safety of drinking water: Improving approaches and methods, Technical report*, London: World Health Organization. Organization for Economic Co-operation and Development. IWA Publishing.

World Health Organization (WHO) (2006). *Guidelines for Drinking Water Quality: Incorporating First Addendum.* Geneva: World Health Organisation.

World Health Organisation (WHO) (2008), *Guidelines for Drinking-water Quality 3rd edition*. Incorporating the first and second agenda. Volume 1 recommendations., Technical report, World Health Organisation Geneva.

WHO (2011) Guidelines for drinking-water quality -4th ed. Geneva, Switzerland: WHO Press.

World Health Organisation (WHO) (2015) *Water Sanitation and Health*. Available online: http://www.who.int/water_sanitation_health/diseases (accessed on June 2018).

World Health Organization (WHO) and the United Nations Children's Fund (UNICEF), (2017*). Progress on drinking water, sanitation and hygiene: 2017 update and SDG baselines.* Geneva. Licence: CC BY-NC-SA 3.0 IGO.

Wu, Z. Y., Walski, T., Mankowski, R., Herrin, G., Gurrieri, R., & Tryby, M. (2002). Calibrating water distribution model via genetic algorithms. *Proc. AWWA IMTech, Kansas City, Mo*.

Yang, B. M., Liu, J. K., Chien, C. C., Surampalli, R. Y., & Kao, C. M. (2011). Variations in AOC and microbial diversity in an advanced water treatment plant. *Journal of Hydrology*, 409(1-2), 225-235.

Yu, J., Kim, D. & Lee, T. (2010), `Microbial diversity in biofilms on water distribution pipes of different materials', *Water Science and Technology*, 163-171.

Zacheus, O. M., Lehtola, M. J., Korhonen, L. K. & Martikainen, P. J. (2001), `Soft deposits, the key site for microbial growth in drinking water distribution networks.', *Water Research* 35(7), 1757-1765.

Zhang, W., & DiGiano, F. A. (2002). Comparison of bacterial regrowth in distribution systems using free chlorine and chloramine: a statistical study of causative factors. *Water Research*, *36*(6), 1469-1482.

Zhang, M., Semmens, M. J., Schuler, D., & Hozalski, R. M. (2002). Biostability and microbiological quality in a chloraminated distribution system. *Journal-American Water Works Association*, *94*(9), 112-122.

Zhang, J., Li, W. Y., Wang, F., Qian, L., Xu, C., Liu, Y., & Qi, W. (2016). Exploring the biological stability situation of a full scale water distribution system in south China by three biological stability evaluation methods. *Chemosphere*, *161*, 43-52.

Zhao, X., Hu, H., Liu, S., Jiang, F., Shi, X., Li, M., & Xu, X. (2013). Improvement of the assimilable organic carbon (AOC) analytical method for reclaimed water. *Frontiers of Environmental Science & Engineering*, 7(4), 483-491.

Chapter 12: Appendices

Appendix 1: Literature Review

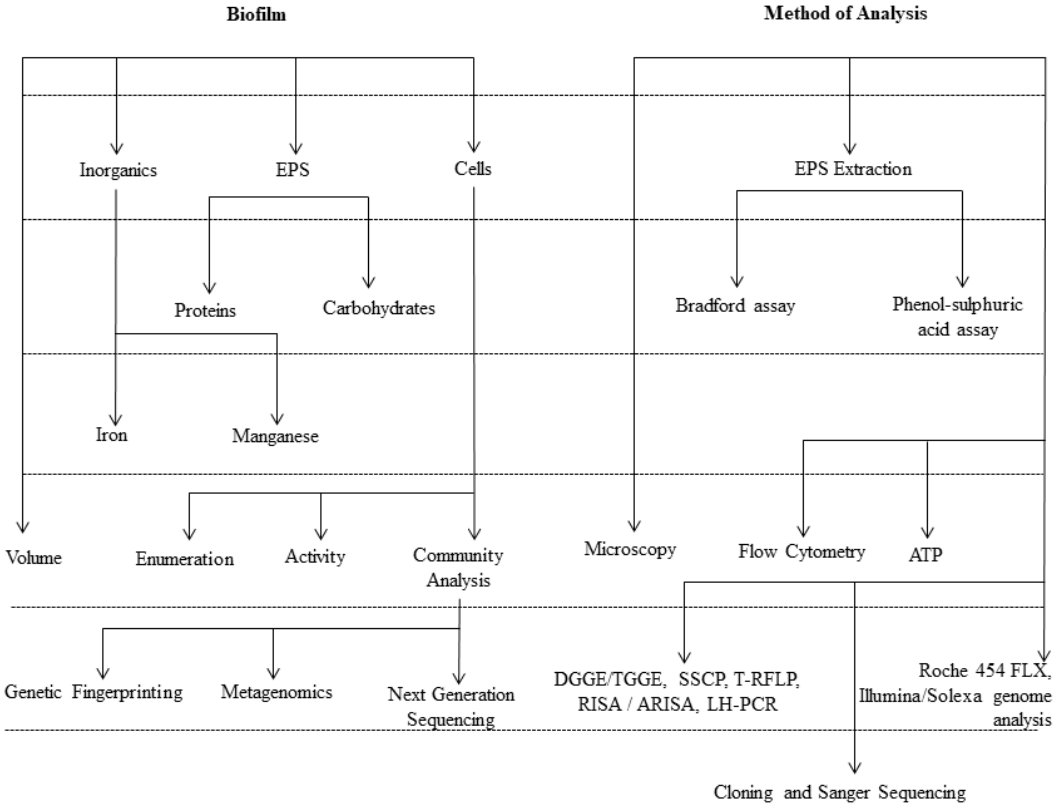

Figure A1.1: Biofilm components and associated analytical methods. EPS: extracellular polymeric substances; ATP: Adenosine triphosphate; DGGE: Denaturing gradient gel electrophoresis; TGGE: temperature gradient gel electrophoresis; SSCP: single-strand conformation polymorphism; T-RFLP: terminal restriction fragment length polymorphism; (A)RISA: (automated) ribosomal intergenic space analysis; LH-PCR: length heterogeneity PCR.

Table A1.1: Flushing steps, including shear stress and flow rate values, used in previous DWDS studies.

Study	Flushing Step	Shear Stress (Nm2)	Flow Rate (l/s)
Douterelo et al. 2014; Fish et al. 2017	1	0.42	0.80
	2	1.75	3.20
	3	2.91	4.50
Sharpe et al. 2017	1	0.8	0.5
	2	1.2	0.73
	3	1.75	1.07
	4	3.2	2
	5	4.0	2.5
	6	4.5	3
Furnass et al. 2014	0	0.09	0.72
	1	1.12	3.06
	2	2.31	4.35
	3	3.42	5.37
	4	4.54	6.23
	5	5.65	7.00
Husband et al. 2008	1	0.20	0.25
	2	0.50	0.33
	3	1.95	0.93
	4	4.90	3.32
	5	7.35	6.52
	6	8.90	9.10

Appendix 2: Coupon Preparation and Biofilm Removal

A2.1 Cleaning Coupons and Toothbrushes

Preparation:

- Make up 2% SDS (Sodium dodecyl sulphate). Weigh SDS out in a fume cupboard as very light powder. Add s.d.H2O and a flea, stir until dissolved (may require heating in a water bath set at 65oC if making a higher percentage SDS solution). Store at room temperature, do not autoclave.
- For a 500ml volume of a 2% solution:10g SDS, 500ml s.d.H2O.

Procedure

1. Place coupons (or toothbrushes) in SDS buffer in the sonicating water bath
2. Sonicate for 45mins
3. Remove and place coupons (or toothbrushes) in ultrapure s.d.H_2O
4. Sonicate for 10minutes
5. Air dry coupons (or toothbrushes) in laminar flow
6. Wrap in aluminium foil and autoclave

References

Backhaus *et al.* 1997 - SDS

Buss *et al.* 2003 – use of SDS as a detergent

Fish *et al.* 2013

A2.2 Biofilm Suspension Protocol

Procedure

1. Open sample bag and remove insert from outer coupon
2. Place in a 50ml falcon tube with 25ml of sterile PBS keep cool
3. Pour off the phosphate buffer – this acts as a wash to remove any unbound material
4. Add 30ml of phosphate buffer to the coupon and pour into a petri dish
5. Remove the microscope insert if present – use forceps
6. Brush the coupon using a toothbrush, standardise the brushing and tooth brush rinsing. To avoid bias brush 30 times in each direction indicated by the arrows while holding the coupon with the sterile forceps at the point marked by the red dot. After every 10 brushes rinse the toothbrush in the phosphate buffer.

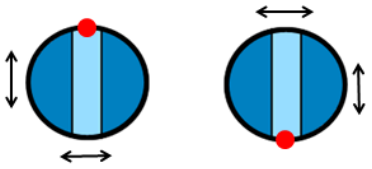

Fish *et al*. 2013

7. Return solution to the falcon tube – this 30ml is now the biofilm suspension
8. Keep the biofilm suspension cold and ensure it is processed the same day
9. Transfer 30 ml volume of biofilm suspension to a sterile falcon tube and store at 4 °C for ≤ 30 minutes before filtering through a 47 mm diameter, 0.22 µm pore nitrocellulose filter (Millipore, MA, USA) using a Microstat membrane filtration unit (Sartorius, UK)
10. Store filters in sterile bags at -80 °C ready for DNA extraction

Appendix 3: Buffers and Solutions

A3.1 Phosphate Buffer Saline (PBS)

- 2 mM Na3PO4 (tri sodium phosphate)
- 4 mM NaH2PO4 (mono sodium phosphate)
- 9 mM NaCl (sodium chloride)
- 1 mM KCl (potassium chloride)
- Autoclaved and stored at room temperature

Make stocks of each solution which are 100x the concentration required in the final buffer:

<u>200mM (0.2M) Na_3PO_4</u>

1: Work out the Molar Mass of the compound by adding the atomic weights:

Molar Mass = [(22.99x3) + (30.974) + (15.999x4)] x constant (1g mol^{-1})

Molar Mass = 163.94 x 1

Molar Mass = 163.94 g mol^{-1}

2: Rearrange the equation N^{o} Moles = Mass/Molar Mass to determine the mass of the compound needed to create the desired molar solution.

N^{o} Moles X Molar Mass = Mass

0.2 = Mass/163.94

Mass = 32.788 g l^{-1}

To make a 250ml 0.2M solution, use 8.197g in 250ml of s.d.H_2O

3: Use stock solution 200mM (0.2M) and $M_1V_1=M_2V_2$ equation to make a 500ml 2mM solution:

2mM x 500ml = 200mM x V_2

5ml = V_2

Therefore 5ml of 0.2M stock solution made up to 500ml will make a 2mM .solution

400mM (0.4M) NaH_2PO_4

1: Molar Mass = [(22.99) + (2 X 1.0079) + (30.974) + (15.999x4)] x constant (1g mol^{-1})

Molar Mass = 119.9752g mol^{-1}

2: N^{o} Moles X Molar Mass = Mass

0.4 x 119.9752= Mass

47.99 g l^{-1} = Mass

To make a 250ml 0.4M solution, use 11.9975g in 250ml of s.d.H_2O

3: Use stock solution 400mM (0.4M) and $M_1V_1=M_2V_2$ equation to make a 500ml 4mM solution:

4mM x 500ml = 400mM x V_2

5ml = V_2

Therefore 5ml of 0.4M stock solution made up to 500ml will make a 4mM solution.

900mM (0.9M) NaCl

1: Molar Mass = [(22.99) + (35.453)] x constant (1g mol^{-1})

Molar Mass = 58.443g mol^{-1}

2: Nº Moles X Molar Mass = Mass

0.9 x 58.443= Mass

52.599 g l^{-1} = Mass

To make a 250ml 0.9M solution, use 13.1498g in 250ml of s.d.H_2O

3: Use stock solution 900mM (0.9M) and $M_1V_1=M_2V_2$ equation to make a 500ml 9mM solution:

9mM x 500ml = 900mM x V_2

5ml = V_2

Therefore 5ml of 0.9M stock solution made up to 500ml will make a 9mM solution.

100mM (0.1M) KCl

1: Molar Mass = [(39.098) + (35.453)] x constant (1g mol^{-1})

Molar Mass = 74.551g mol^{-1}

2: Nº Moles X Molar Mass = Mass

0.1 x 74.551= Mass

7.455 g l^{-1} = Mass

To make a 250ml 0.1M solution, use 1.8634g in 250ml of s.d.H_2O

3: Use stock solution 100mM (0.1M) and $M_1V_1=M_2V_2$ equation to make a 500ml 1mM solution:

1mM x 500ml = 100mM x V_2

5ml = V_2

Therefore 5ml of 0.1M stock solution made up to 500ml will make a 1mM solution.

Phosphate Buffer Recipe using stock solutions:

- 5ml of 0.2M Na_3PO_4
- 5ml of 0.4M NaH_2PO_4
- 5ml of 0.9M NaCl
- 5ml of 0.1M KCl

A3.2 5% Formaldehyde Solution

- 70ml 37.5% formaldehyde
- 411ml s.d.H_2O

Mix in fume cupboard as formaldehyde is toxic, make sure label with toxic sticker.

Formaldehyde Solutions

5% solution of formaldehyde (formalin). As the formaldehyde supplied is 35-38% a dilution will need to be made.

For a 36.5% solution:

100ml = 36.5ml formaldehyde + 63.5ml H_2O

10ml = 3.65ml formaldehyde + 6.35ml H_2O

For 3.65ml to be equal to 5%:

3.65 x 20 = 73ml

(5%) (5 x 20 =100%) (total volume that 3.65ml formaldehyde needs to be in)

Therefore 10ml of 36.5% formaldehyde + 63ml of s.d. H_2O = 73ml 5% formaldehyde

As 50ml of a 5% solution is needed to fix samples for DAPI make up enough total volume for all samples; for example for 10 samples a 500ml volume is required:

70ml of 36.5% formaldehyde (7 x 10ml) in 441ml s.d.H_2O (7 x 63ml) = 511ml of 5% formaldehyde solution, aliquot into 50ml volumes

Appendix 4: Raw and Post-Treated Water Quality Data

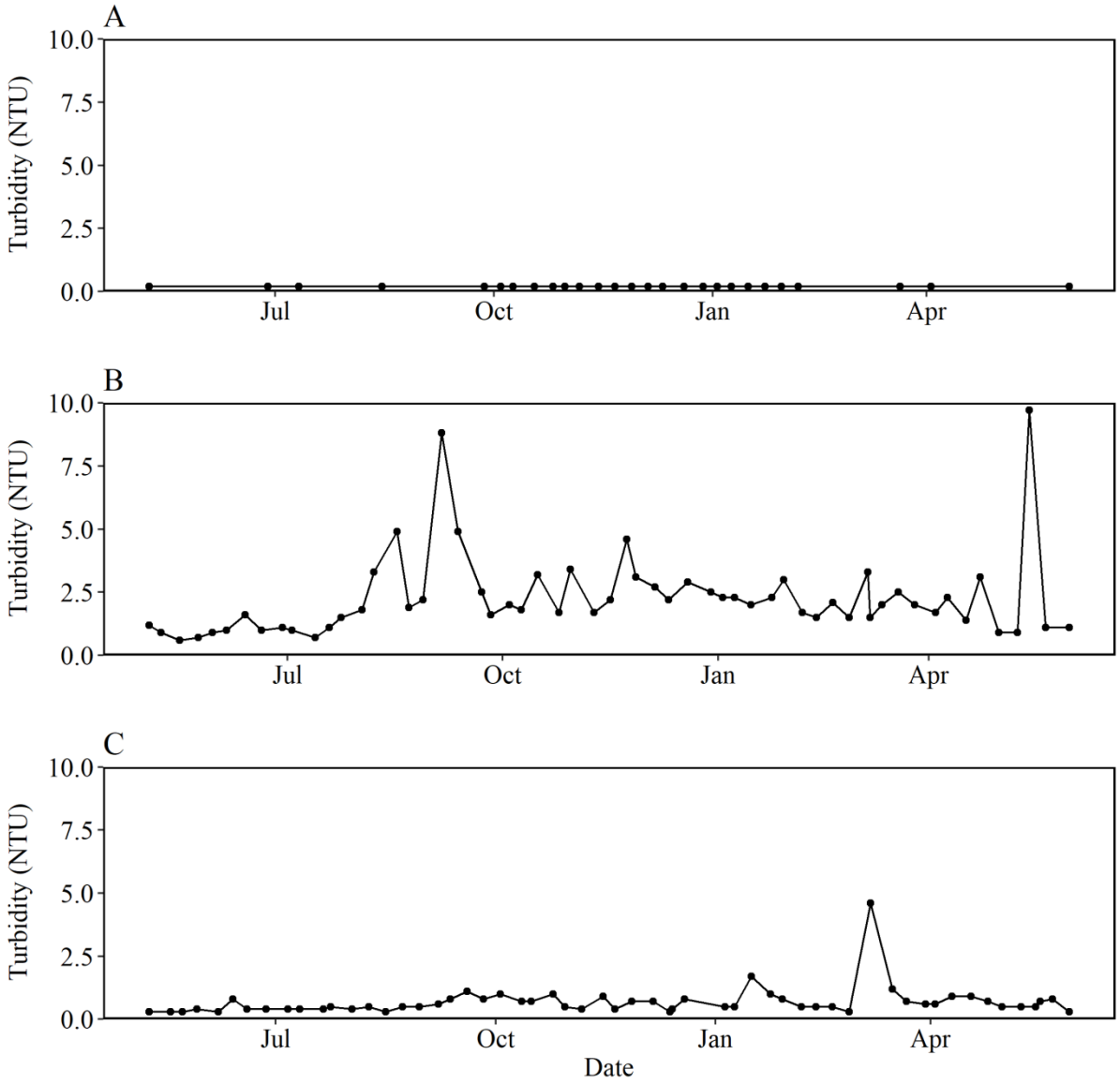

Figure A4.1: Turbidity (NTU) (n=1) in raw water at WTW 4, WTW 6 and WTW 20, plotted against time. Turbidity was sampled every week for 1 year.

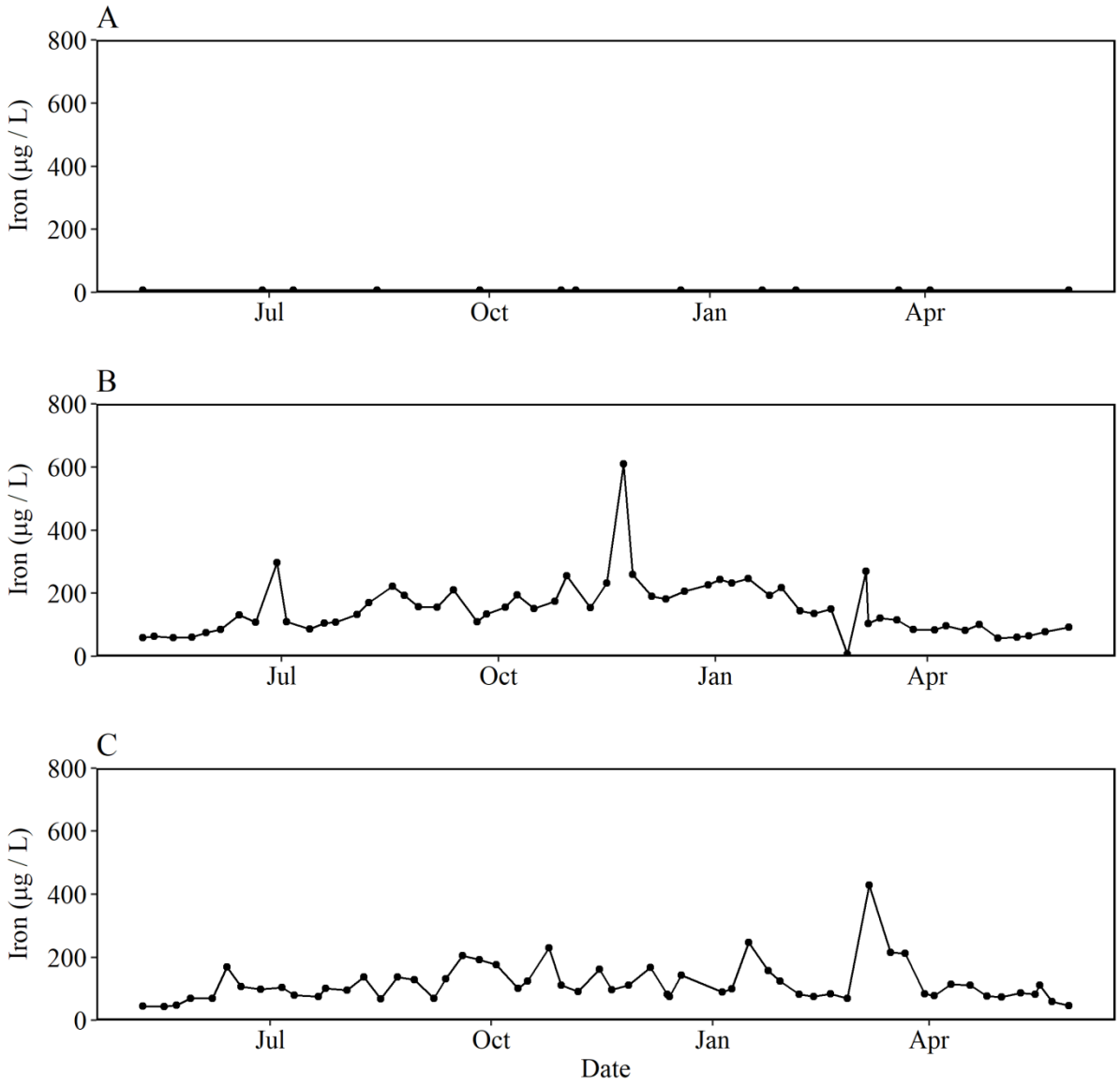

Figure A4.2: Iron (n=1) in raw water at WTW 4, WTW 6 and WTW 20, plotted against time. Iron was sampled every week for 1 year.

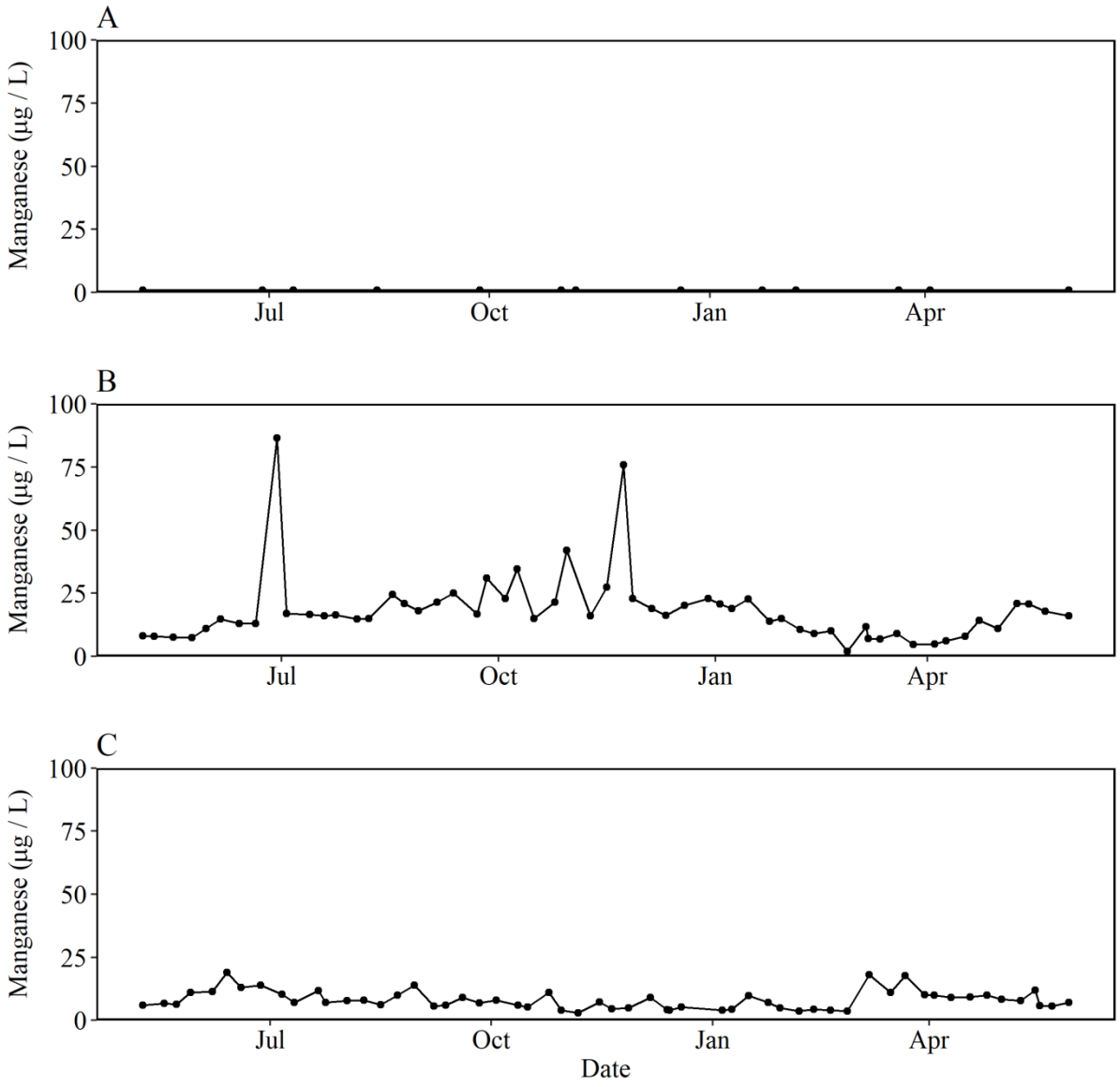

Figure A4.3: Manganese (n=1) in raw water at WTW 4, WTW 6 and WTW 20, plotted against time. Manganese was sampled every week for 1 year.

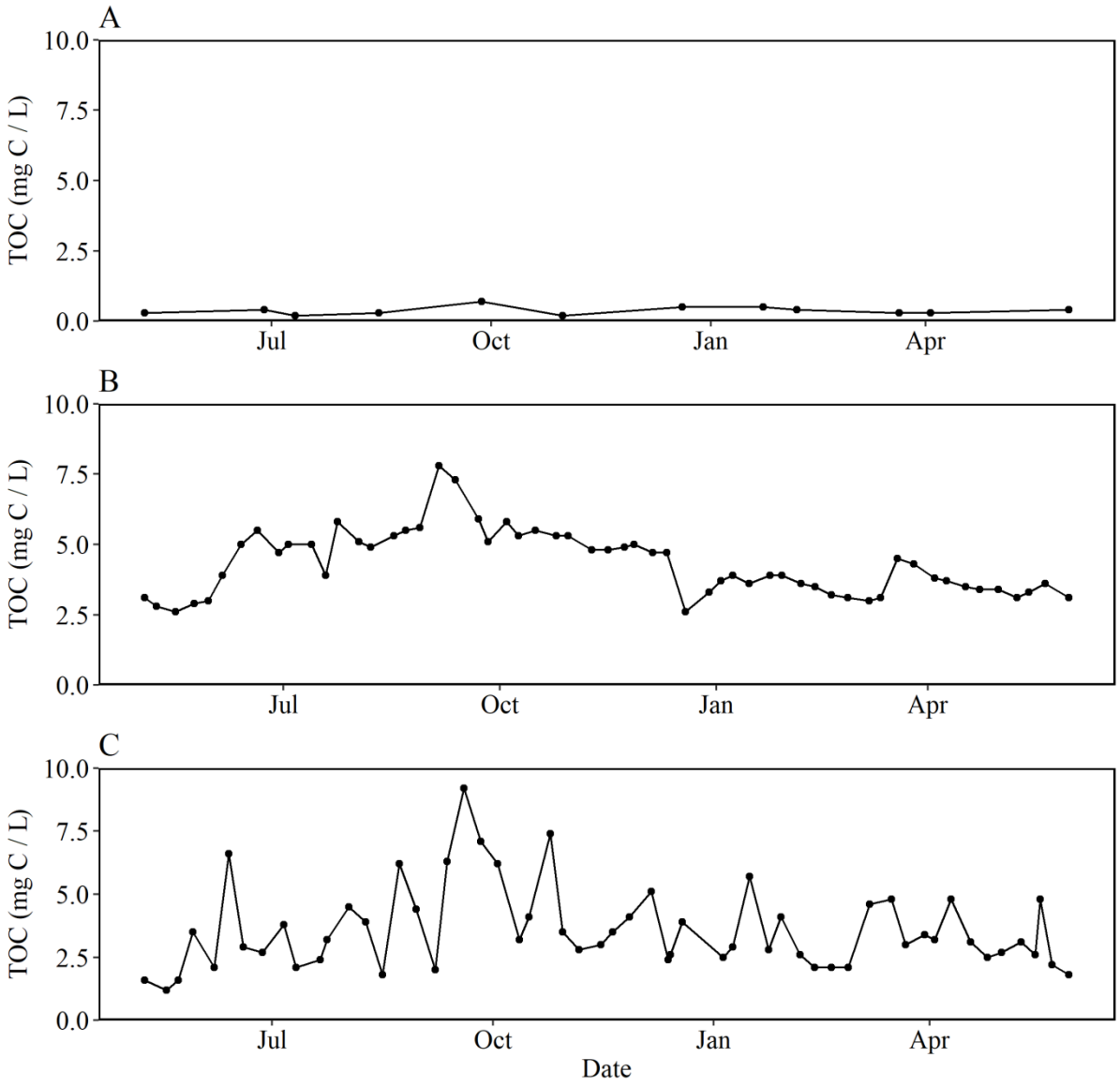

Figure A4.4: Total organic carbon (TOC) (black) and dissolved organic carbon (DOC) (red) (n=1) in raw water at WTW 4, WTW 6 and WTW 20, plotted against time. TOC was sampled every week for 1 year.

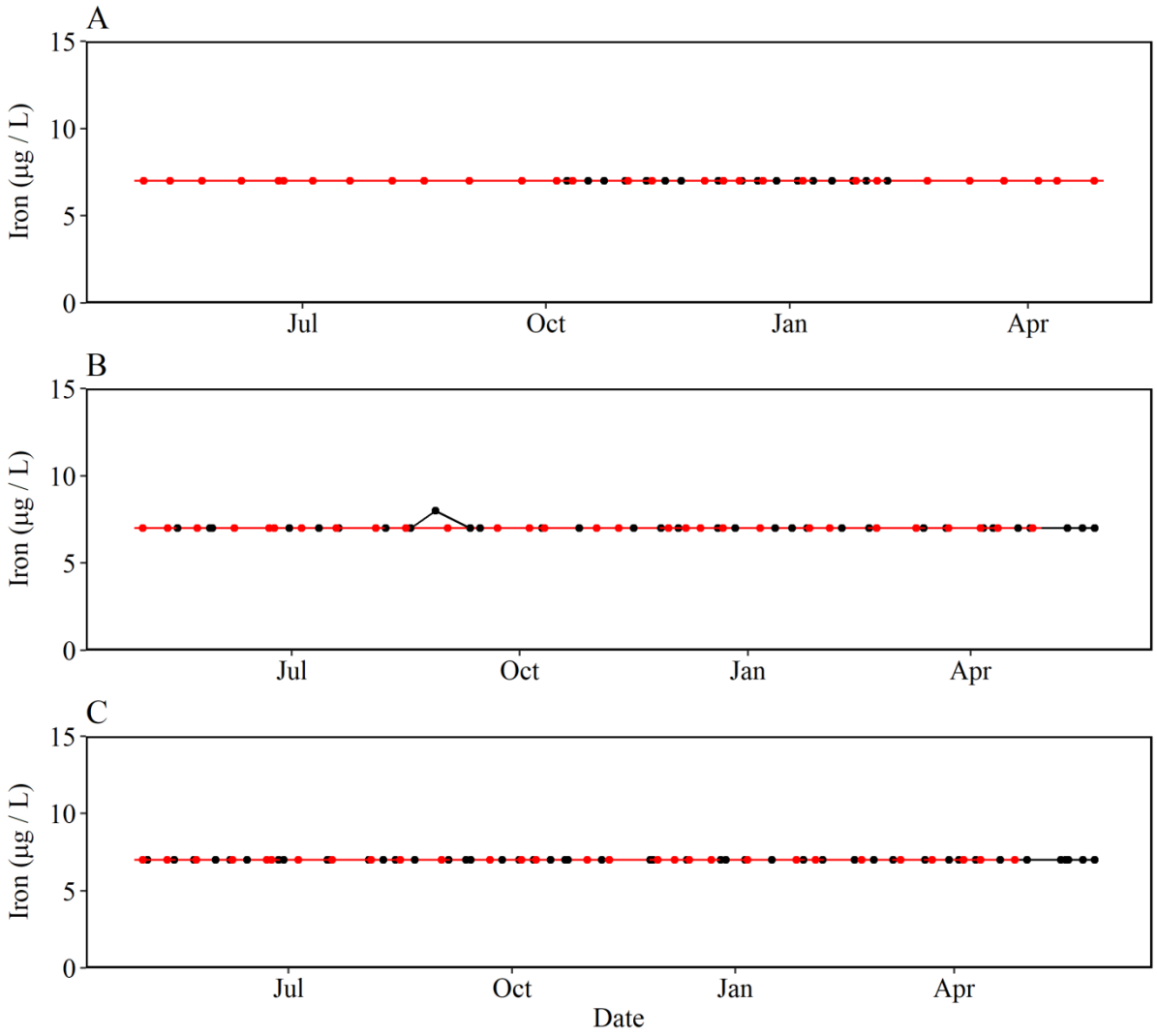

Figure A4.5: Iron in post-treated water (n=1) (black) and pipe loop sample tap (red) (n=3) at WTW 4 (PLA), WTW 6 (PL B) and WTW 20 (PL C), plotted against time. Iron in post-treated water was sampled every 2 weeks for 1 year.

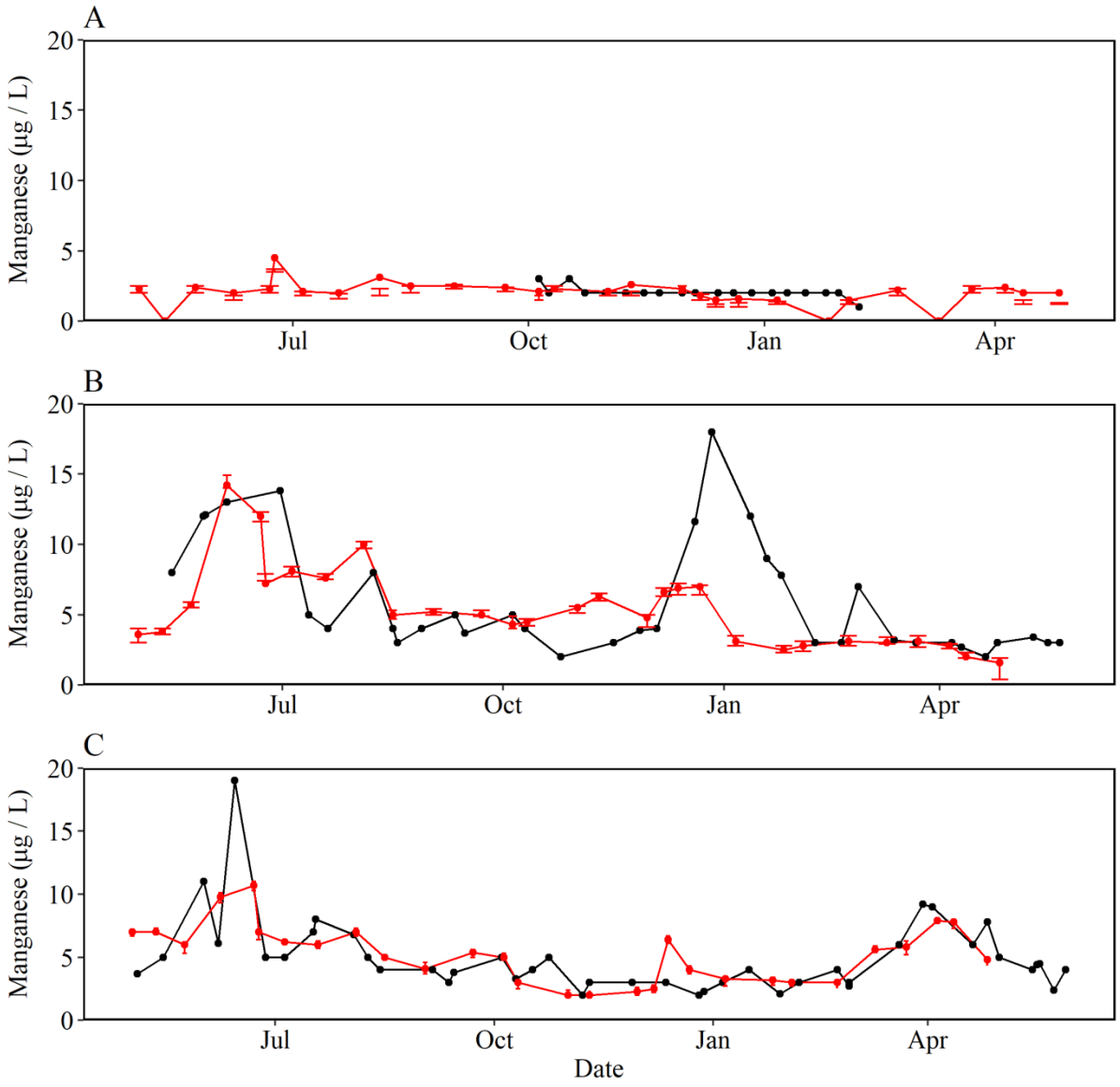

Figure A4.6: Manganese in post-treated water (n=1) (black) and pipe loop sample tap (red) (n=3) at PLA, WTW 6 (PL B) and WTW 20 (PL C), plotted against time. Manganese in post-treated water was sampled every 2 weeks for 1 year.

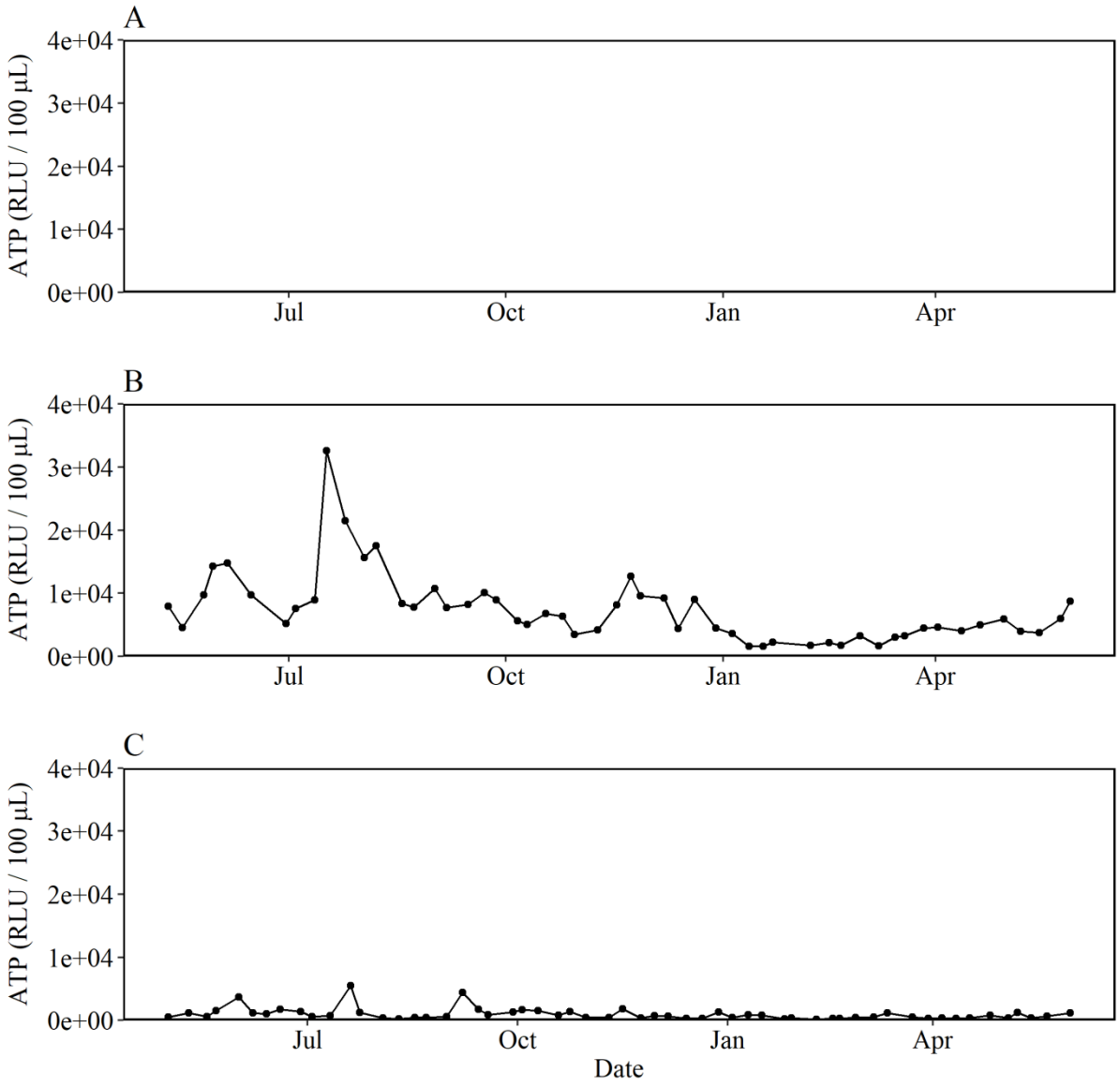

Figure A4.7: ATP in post-treated water (n=1) at WTW 6 and WTW 20, plotted against time. ATP in post-treated water was sampled every 2 weeks for 1 year.

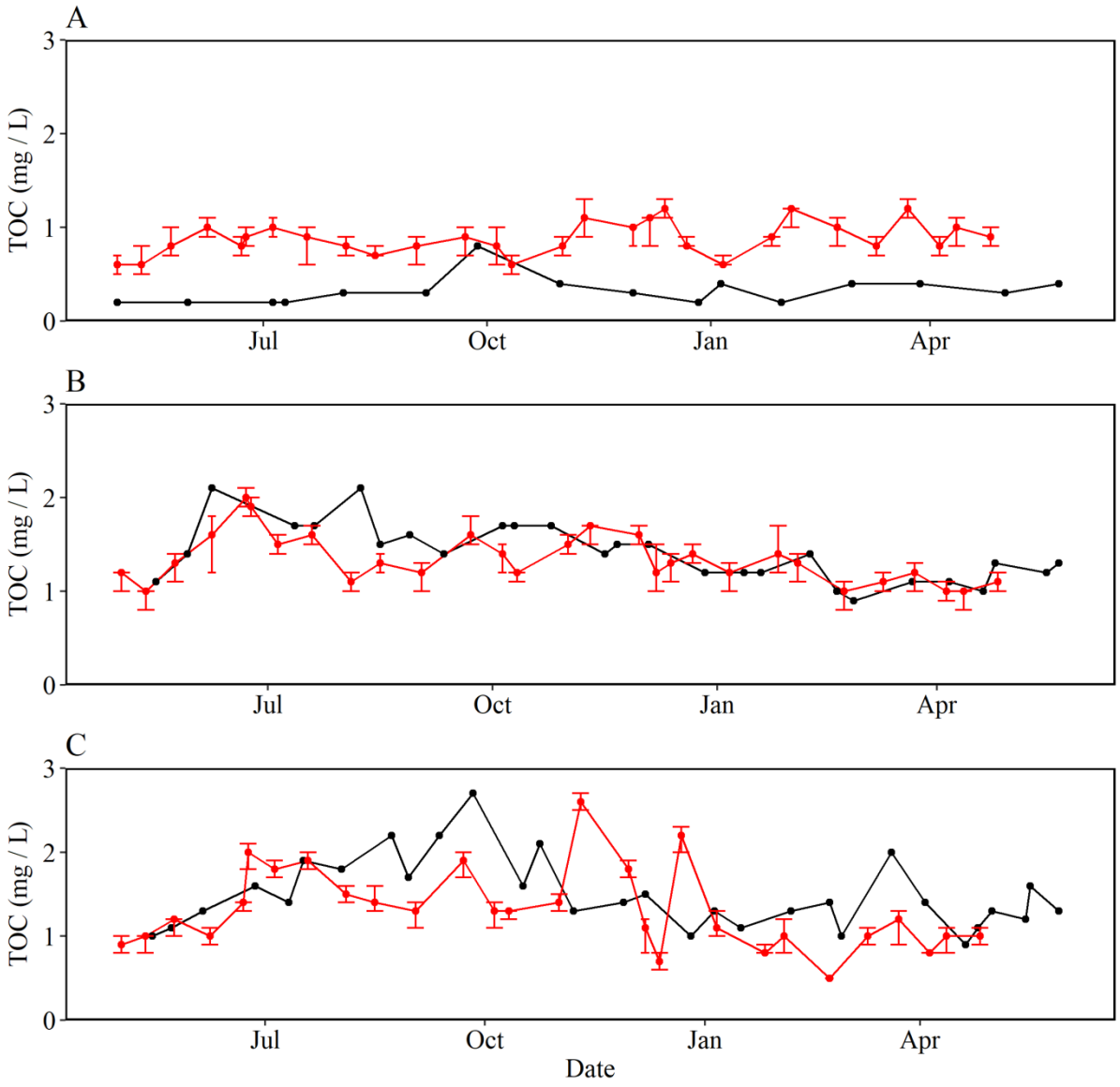

Figure A4.8: Total organic carbon (TOC) in in post-treated water (n=1) at WTW 4, WTW 6 and WTW 20, plotted against time. TOC in post-treated water was sampled every 2 weeks for 1 year.

A4.9: The concentration of trihalomethanes (THM) was also measured in post-treated water at WTW 6 and WTW 20. WTW 6 contained an average 18.5 (11 - 19.7) µg / L and WTW 20 contained 30.2 (5 – 98) µg / L.

Appendix 5: Shear Stress Calculations

In order to determine the shear stress at each of the flushing steps applied during the mobilisation phase of this experiment, shear stress was calculated theoretically using:

$$\tau = \rho g R S$$ (see Table 4.7 for definitions and units).

The hydraulic gradient (S) was calculated using the Colebrook-White and Darcy-Weisbach equations (see Section 4.5.4.1 for full details). It was not possible to manually measure frictional losses within the pipe loop as the length of the pipe loop in total is 10m. Due to the short length, and the relatively smooth surface of the HDPE pipe, it would be difficult to measure such a small change in head loss due to primary losses (caused by boundary shear stress). Furthermore, the pipe loop incorporates a series of 90° bends which would be the main contributor to frictional losses. In the Colebrook-White equation (Section 4.5.4.1; Equation 2), a k_s value is required to represent the roughness of the internal surface of the pipe. In this thesis, a k_s value of 0.075 mm was used as this is representative of the roughness of HDPE pipe (Husband *et al.* 2008) used in the three pipe loops.

To highlight the importance of using an appropriate ks pipe roughness value, a wide range of ks values (0.010, 0.075, 0.100 and 0.200 mm) were used to generate a shear stress value for each of the flushing steps used during the mobilisation phase of the pipe loop test facility investigation. A high ks value of 0.200 is more representative of a cast iron pipe than a plastic pipe (Hydraulics Research Station, 1983). When a different ks value is applied (Figure A5.1), a non-linear relationship between shear stress to flow rate is exhibited, highlighting the importance of using a representative k_s value when calculating shear stress.

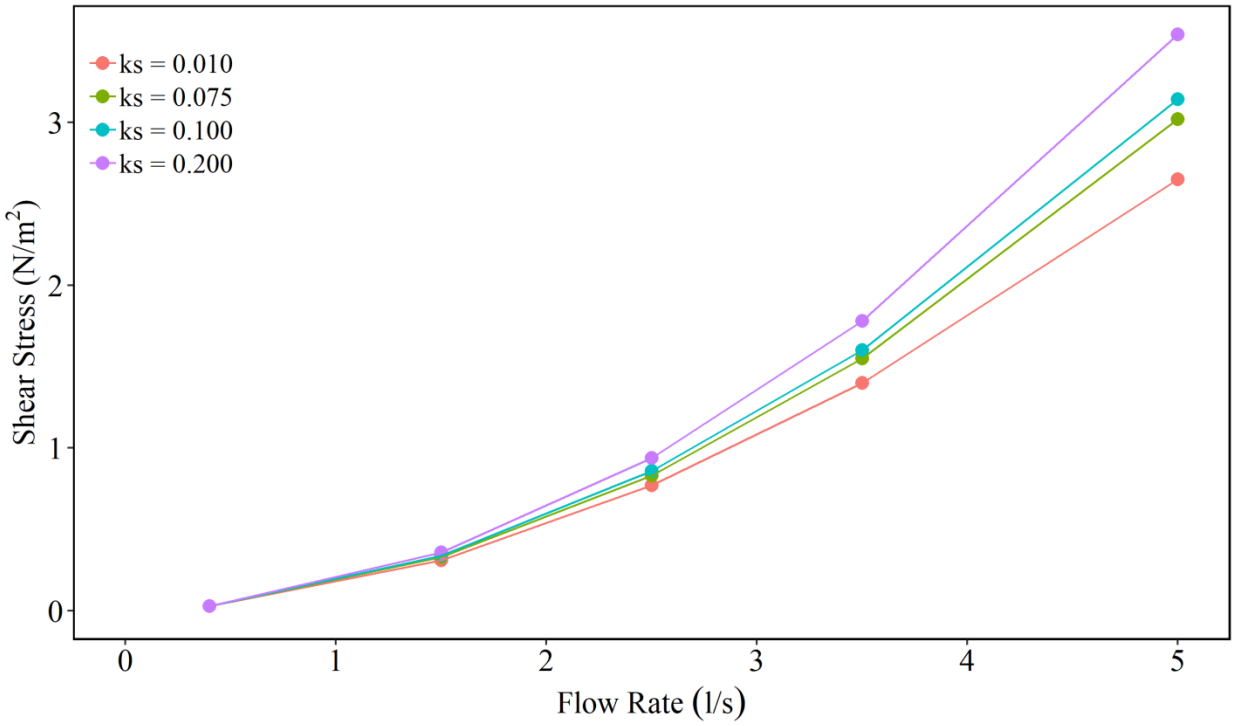

Figure A5.1: Shear stress (N/m^2) plotted at each flow rate (l/s) and k_s value (0.010, 0.075, 0.100 and 0.200 mm).

As an example, turbidity results were plotted against each set of shear stress values (using k_s values of 0.010, 0.075 and 0.100 and 0.200 mm) (Figure A5.2). The gradient (G), R^2 and P-values for turbidity in bulk water at each set of stress values are listed in Table A5.1. The gradient within in each pipe loop showed a some variation as a result of increasing the ks value from 0.010 to 0.200 mm. Increasing the ks value from 0.010 to 0.200 resulted in a 0.41 decrease in the gradient within Pipe Loop A, 0.34 gradient decrease within Pipe Loop B and 0.19 decrease in the gradient in Pipe Loop C. A literature approved k_s value of 0.075 mm for HDPE pipes was used for all subsequent plots.

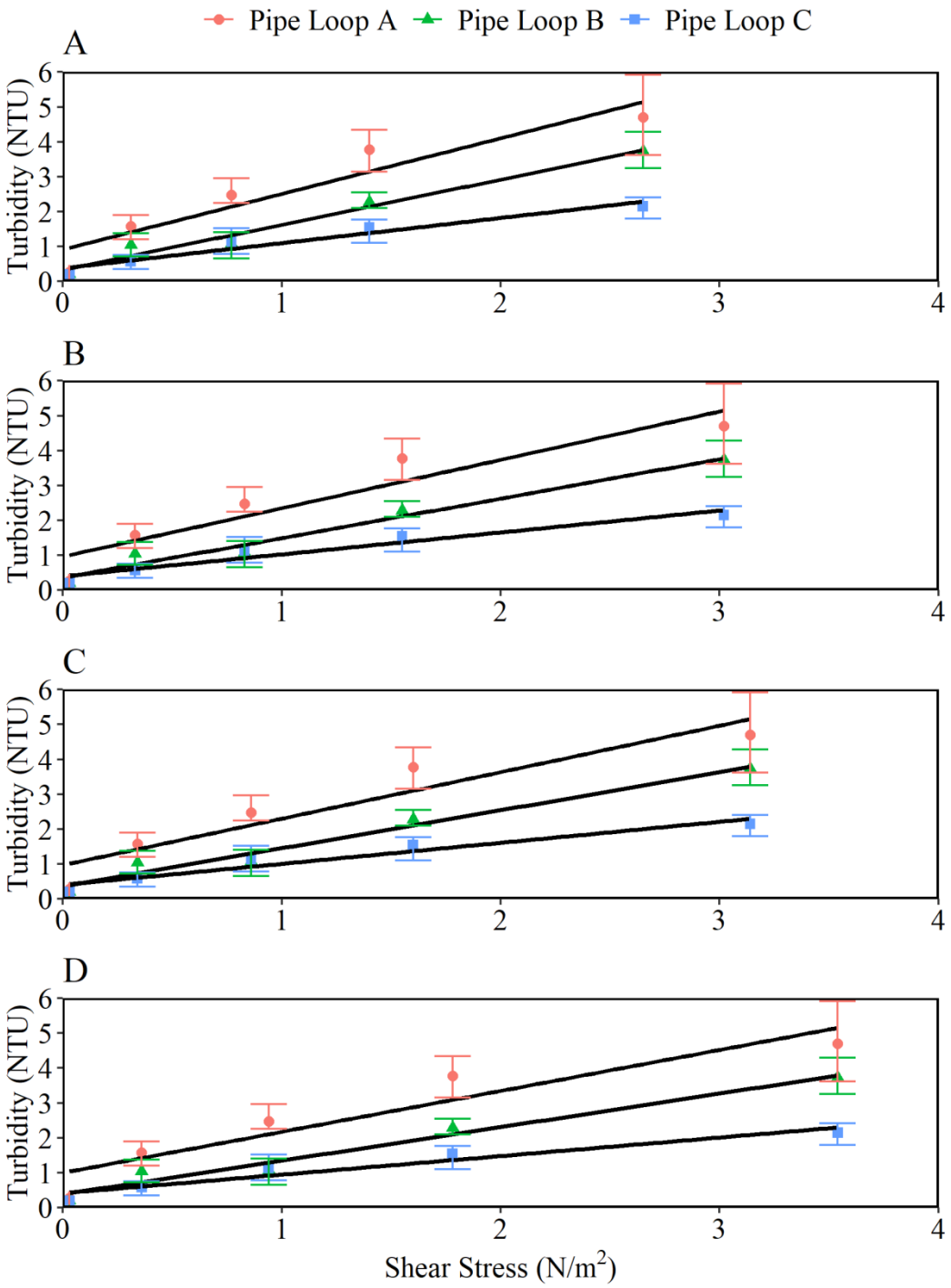

Figure A5.2: Turbidity plotted against each set of shear stress values using a k_s values of A) 0.010; B) 0.075; C) 0.100 and D) 0.200.

Table A5.1: Gradient (G), R^2 and P values for turbidity in bulk water within pipe loop test facilities at PL A (WTW 2), PL B (WTW 16) and PL C (WTW 20) during the mobilisation phase, at each set of shear stress values using a ks values of A) 0.010; B) 0.075; C) 0.100 and D) 0.200.

Pipe Loop ID	k_s Value	Turbidity		
		Gradient[A]	R^{2B}	P value[C]
A	**0.010**	1.59	0.8997	0.0139
	0.075	1.39	0.8902	0.0159
	0.100	1.33	0.8886	0.0163
	0.200	1.18	0.8837	0.0175
B	**0.010**	1.30	0.9726	0.0019
	0.075	1.13	0.9720	0.0020
	0.100	1.09	0.9714	0.0020
	0.200	0.96	0.9706	0.0023
C	**0.010**	0.72	0.9450	0.0056
	0.075	0.63	0.9374	0.0068
	0.100	0.60	0.9364	0.0069
	0.200	0.53	0.9325	0.0076

[A]The gradient defines the rate of change along the regression line; [B]R^2 value indicates the goodness of fit of the linear regression model to the data, nearer to 1 the better the fit; [C] A significant p value indicates that the gradient is significantly different from 0.

Appendix 6: Scientific Dissemination

A6.1 International Conferences

CCWI / WDSA Joint Conference, Kingston, Canada. Conference paper: Pick, F. C., Fish, K. E., Biggs, C. A., Moses, J., Moore, G., & Boxall, J.B. Application of enhanced assimilable organic carbon method across operational drinking water systems.

A6.2 Research Symposiums and Meetings

The findings of this project have been shared internally both at the University of Sheffield and Scottish Water, and externally at national and international conferences.

Oral Presentations at:

- Water Network Meeting: Chemical Free Treatment (Sheffield) 20th Oct 2016

- Water Network Meeting: Microbial Diagnostics and Monitoring (Cranfield) 27th April 2017
- University of Sheffield Research Symposium (Sheffield) July 2017
- Process Science meetings (Scottish Water)
- STREAM industrial doctoral centre (IDC) Challenge Week

Poster presentations at:

- Scottish Water Working Towards Zero Microbial Failures Conference, Glasgow 2016
- Redeveloping, implementing and managing innovative solutions and interventions for the protection of the environment and public (ReNUWIt) Conference, Sept 2016
- Scottish Water NOM Conference (Edinburgh) 10th May 2017
- Institute of Water (Manchester) June 2017

Other Significant Deliverables

- Presentation of thesis summary to Drinking Water Quality Regulator for Scotland (DWQR), 2019.
- Winner best grant proposal Newcastle University TSEL 2018
- Winner of best group presentation Newcastle University Challenge Week, 2018
- Completion of Induction semester (Cranfield): Modules studied included Asset Management Policy & Strategy, Water & Wastewater Treatment Principles, Process Science & Engineering, Hydraulics & Pumping Systems, Risk Management & Reliability Engineering and the Group Design Project
- TSEL 1 (Cranfield): Selling ideas in research, writing for & presenting to different audiences, project management for research, creativity & design
- TSEL II (Imperial): Research ethics, presentation skills, meeting and negotiating, innovation processes in the water sector

- TSEL III (Sheffield): Time management, collaboration, personal impact / effectiveness, writing a business case for investment, business and financial risk, knowledge transfer and research exploitation
- TSEL IV (Exeter): Supervision skills, patenting and intellectual Property (IP), PR and commercialisation, negotiating & influencing skills, generating a business model and developing a business case, public engagement, overseas collaborations, science communication
- TSEL V (Newcastle): Grant writing, interview and CV skills